New Responsive Surfactants for Aqueous Dispersion of CNTs and Graphene

O'DRISCOLL, LUKE,JAMES

New Responsive Surfactants for Aqueous Dispersion of CNTs and Graphene

Luke James O'Driscoll
Collingwood College

Department of Chemistry
Durham University

A thesis submitted for the degree of Doctor of Philosophy at Durham University

April 2014

Abstract

We have developed a flexible approach to the synthesis of surfactants with an 'Anchor-Linker-Head' (ALH) architecture. These ALH surfactants are designed for the dispersion of multi-walled carbon nanotubes (MWNTs) and exfoliation of graphite in water. Four series of surfactants have been synthesised, all with a pyrene anchor group, which binds strongly to graphitic surfaces through π-π interactions, and hydrophilic head groups based on a carboxylate moiety, carboxylate dendron, crown ether or podand. These are joined by oligoethylene glycol (OEG) linker groups.

The anionic surfactants **PyrB-PEGn-CH_2COONa** (n = 2, 4, 6, 12) **PyrB-PEGn-CH_2COG1(ONa)$_3$** (n = 2, 4, 6) all disperse MWNTs at least as well as commercial surfactants in Millipore water and achieve higher dispersion levels than comparable amide linker surfactants. Non-ionic surfactants are more effective, dispersing up to 61% of the MWNT feedstock. Exfoliation of graphite has been achieved using anionic and non-ionic surfactants. We examined the effect of salts, including NaCl, KCl and $CaCl_2$, on the ability of surfactants to disperse MWNTs and found the choice of linker and head group to be significant. MWNT dispersing ability in 0.6 M NaCl increases with OEG linker length. Structural variation gives surfactants which show improved, reduced, or comparable dispersion levels in 0.6 M NaCl *vs.* Millipore water, due to the effects of ionic screening and cation coordination.

MWNTs dispersed using anionic surfactants can be precipitated by addition of acid, and re-dispersed by addition of base. Eleven non-ionic surfactants have a lower critical solution temperature (LCST), which is tuned by structural changes. We demonstrate using **PyrB-PEG4-CH_2CO(15-c-5)** that LCST surfactants with a pyrene anchor can be used to repeatedly and reversibly precipitate dispersed MWNTs without harsh re-processing. We believe this to be the first report of such behaviour using a small molecule dispersant.

Statement of Copyright

Declaration

The work in this thesis was carried out in the Department of Chemistry at Durham University between October 2010 and March 2014. All of the work was carried out by the author unless otherwise stated and has not previously been submitted for a degree at this or any other university.

Acknowledgements

I would like to thank Martin Bryce for his supervision and guidance throughout my PhD. I would also like to thank Dan Welsh and Kara Howes, who I have worked alongside on this project, for their contributions and helpful discussions. Dan's effort in developing graphite exfoliation conditions will not be forgotten. I would also like to thank all other members of the Bryce group for making the lab an enjoyable place to work and for their input to discussions of problems, and at group meetings.

Funding for this research was provided by BP, and Harry Frampton, Dave Chappell and colleagues, together with Colin Lambert, Steve Bailey and David Visontai of the Department of Physics at Lancaster University, have provided useful feedback at our quarterly meetings. Ben Robinson and colleagues at Lancaster must also be thanked for conducting DLS measurements and their ongoing AFM study.

I would like to thank the staff of the chemistry department's analytical services, including NMR spectroscopy and mass spectrometry, the staff at the stores and the lab attendants, who have all helped my research to progress smoothly.

I would like to thank my friends and family for their continued support. You have all helped to take my mind off work when things weren't going as planned!

Finally I would like to thank Catherine for her patience while I have been writing and her support throughout my PhD.

Table of Contents

List of Abbreviations

ALH	Anchor-Linker-Head
APD	(±)-3-Amino-1,2-propanediol
ASAP	Atmospheric Solids Analysis Probe
A_{surf}	Surface Area Coverage per Surfactant Molecule
Bn	Benzyl-
BnBr	Benzyl Bromide
Boc	*tert*-Butoxycarbonyl
C_{EG}	Concentration of Exfoliated Graphite
C_h	Chiral Vector (of a SWNT)
C_{MWNT}	Concentration of MWNTs
CNTs	Carbon Nanotubes
CTAB	Cetyltrimethylammonium Bromide
CVD	Chemical Vapour Deposition
DLS	Dynamic Light Scattering
DSC	Differential Scanning Calorimetry
EG	Exfoliated Graphite
ESI	Electrospray Ionisation
Et	Ethyl
FLG	Few Layer Graphene
G0	"Zeroth Generation" (Dendron)
G1	First Generation (Dendron)
G2	Second Generation (Dendron)
GO	Graphene Oxide
HiPco	High Pressure Carbon Monoxide
HLB	Hydrophilic-Lipophilic Balance
HRMS	High Resolution Mass Spectrometry
LCMS	Liquid Chromatography Mass Spectrometry
LCST	Lower Critical Solution Temperature
Me	Methyl
MLG	Multi-Layer Graphene
Ms	Mesyl
MS	Mass Spectrometry
MWNTs	Multi-Walled Carbon Nanotubes
^{n}Bu	*n*-Butyl
NMR	Nuclear Magnetic Resonance
OEG	Oligoethylene Glycol
OTAB	Octadecyltrimethylammonium Bromide
PAMAM	Poly(amidoamine)
PBA	1-Pyrenebutyric Acid
PBS	Phosphate Buffered Saline
PEG	Polyethylene Glycol

PMB	*para*-Methoxybenzyl-
PyrB	Pyrenebutyl-
PyrBOH	1-Pyrenebutanol
PyrM	Pyrenemethyl-
PyrMBr	1-Bromomethyl Pyrene
PyrMOH	1-Pyrenemethanol
RGO	Reduced Graphene Oxide
RT	Room Temperature
SC	Sodium Cholate
SDBS	Sodium Dodecylbenzenesulphonate
SDOC	Sodium Deoxycholate
SDS	Sodium Dodecyl Sulphate
SPB	Sodium Pyrenebutyrate
STDOC	Sodium Taurodeoxycholate
SWNTs	Single-Walled Carbon Nanotubes
TBAF	Tetrabutylammonium Fluoride
TBDMS	*tert*-Butyldimethylsilyl
TBTU	*N*,*N*,*N'*,*N'*-Tetramethyl-*O*-(benzotriazol-1-yl)uronium Tetrafluoroborate
^{t}Bu	*tert*-Butyl
TEM	Transmission Electron Microscopy
THP	Tetrahydropyran
TMS	Trimethylsilyl
Tr	Trityl-
TRIS	Tris(hydroxymethyl)aminomethane
Ts	Tosyl-

Chapter 1: Introduction to Aqueous Dispersion of CNTs and Graphene

Carbon nanotubes (CNTs) and graphene are relatively recently discovered materials which possess a host of remarkable and useful properties. This section will discuss the discovery of these materials, summarise the properties and potential applications which make them so interesting and examine some of the difficulties in exploiting them on a commercial scale. This will be followed by a more in-depth analysis of materials and methods which have been used to disperse CNTs and exfoliate graphene in aqueous media, to provide a means of processing these materials industrially. Responsive dispersions of CNTs and graphene will also be reviewed. We will then outline our strategy for the design of surfactants which we have used to prepare responsive CNT or graphene dispersions.

1.1: Carbon Allotropes: An Overview

CNTs and graphene are amongst several "new" allotropes of carbon which have become the subject of considerable research over the last 30 years. Since the discovery of C_{60} (and C_{70}), the first of the fullerenes, in 1985,[1] multi-walled carbon nanotubes (MWNTs),[2] single-walled carbon nanotubes (SWNTs),[3,4] and graphene[5] have all been reported and developed into rich fields of study. Related species[6] including nano-onions,[7,8] endohedral fullerenes[9,10] and nanohorns[11] have also been described. The existence of further carbon allotropes such as carbyne (an extended linear poly-yne containing only *sp*-hybridised carbons) and graphyne (an expanded graphene structure with alternating benzene rings and alkynes) has also been postulated.[12] Figure 1.01 shows the structures of a selection of these allotropes. The smaller fullerenes, CNTs and graphene remain the most widely studied of these materials, and are beginning to be exploited in commercial applications.

1.2: Properties of CNTs

1.2.1: Discovery and Structure

Although Ijima's work published in 1991[2] is commonly referred to as the discovery of CNTs it has been noted that this is not necessarily correct,[15] and that material which at least closely resembled MWNTs had been reported previously. What is clearer is that the study of CNTs

began in earnest following Ijima's publication, which described "helical microtubules of graphitic carbon" produced *via* an arc-discharge method. These MWNTs ranged from 4-30 nm in diameter with lengths of up to 1 μm, and had between 2 and 50 walls.[2] In 1993 the discovery of SWNTs was reported simultaneously by Ijima and Ichihashi[3] and Bethune *et al.*[4] who both produced CNTs with diameters of around 1 nm which clearly consisted of only one graphitic wall. This was again accomplished using an arc-discharge method, in the presence of iron and cobalt respectively. Transmission electron microscopy (TEM) images from these early works are shown in Figure 1.02.

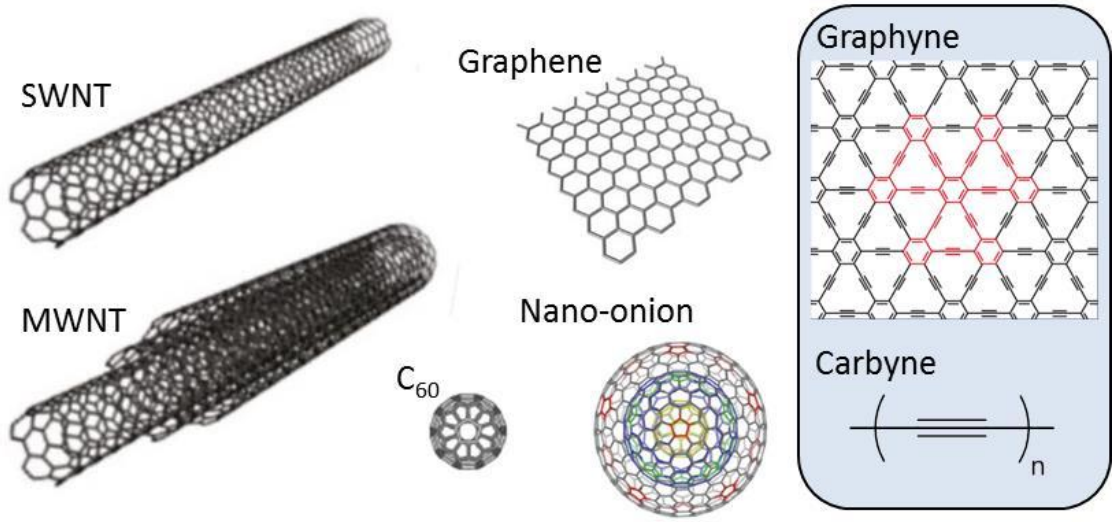

Figure 1.01: Structures of carbon allotropes, including hypothesised species (blue background). Adapted from images in references 6, 12, 13 and 14.

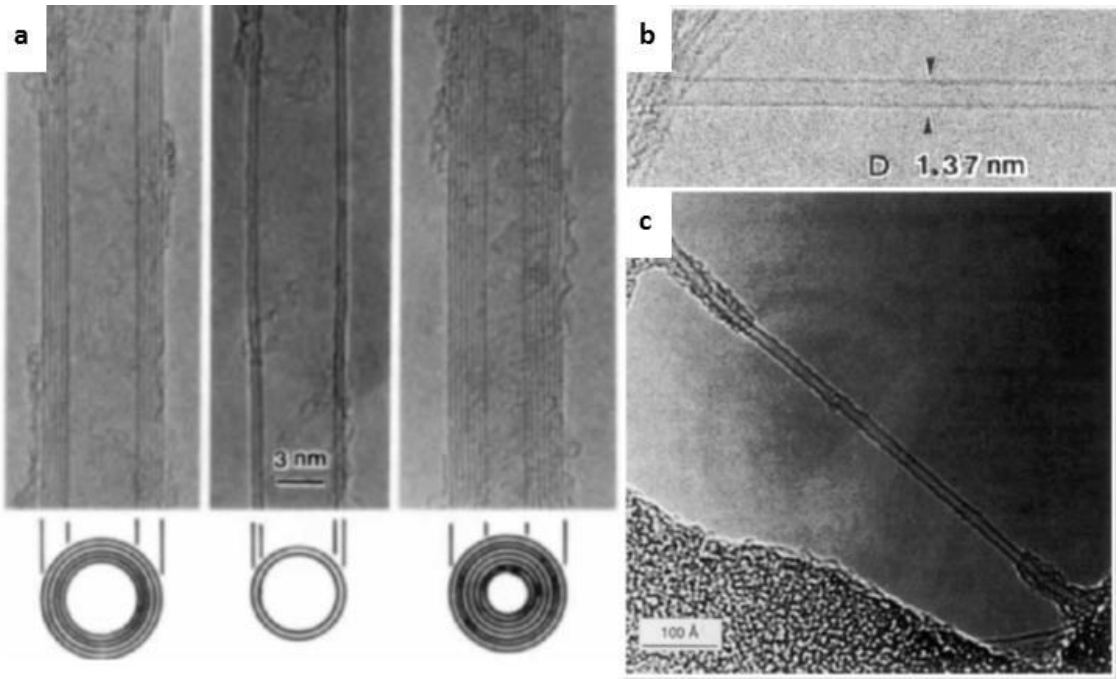

Figure 1.02: Early TEM images of CNTs: a) MWNTs from reference 2; b) A SWNT from reference 3; c) A SWNT from reference 4.

As shown in Figure 1.01 above, a SWNT consists of a hexagonal lattice of sp^2-bonded carbon atoms in a cylindrical arrangement. The ends of the cylinder are usually capped with fullerene hemispheres.[13] Another way to describe a SWNT is a sheet of graphene rolled into a tube such that no edges overlap. This concept is used to define the chirality of a SWNT.[16] The chiral vector, C_h, of a SWNT is usually written in the form (n,m) where n and m are integers and $n \geq m$ – e.g. a (6,3)-SWNT. It determines the diameter of a SWNT and allows a SWNT to be classed as one of three structural types, named after the pattern along the edge of the graphene sheet which can be rolled up to give the SWNT. When $n = m$, a SWNT has an armchair structure and when $m = 0$, a SWNT has a zigzag structure. For other values of n and m, a SWNT has a chiral structure, and can be further described by a chiral angle.[16,17] The chiral vector can also be used to predict the electronic properties of SWNTs; in cases where the equation $2n + m = 3q$ gives an integer value of q, the SWNT should be metallic, otherwise it is a semiconductor.[16] Notably that this means that all armchair SWNTs are expected to be metallic. For small-diameter SWNTs this equation does not always correctly predict properties and more complex calculations are required.[17] SWNTs typically have diameters of around 1 nm,[3,4] and lengths on at least the μm scale.[3] Lengths in excess of 18.5 cm have been reported.[18] This disparity between length and diameter has led SWNTs to be considered as "one-dimensional" materials, and has an influence on both their physical properties and toxicity (see below). If SWNTs of different chiralities are separated it becomes possible to take advantage of either their metallic or semiconducting properties.[19]

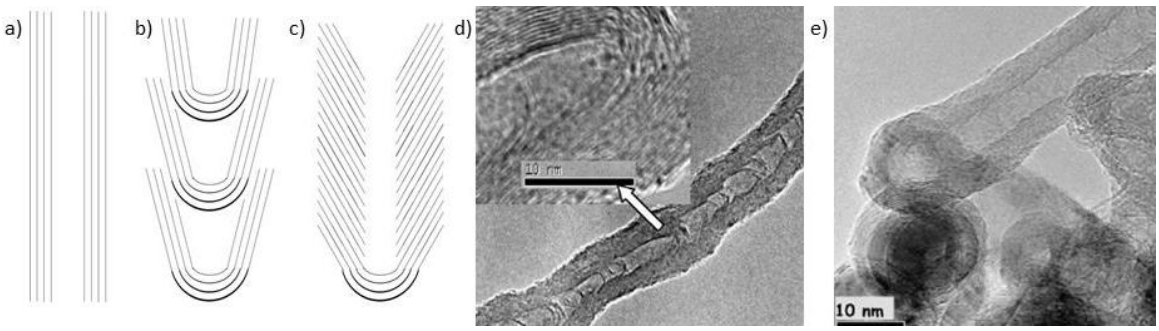

Figure 1.03: MWNT morphologies illustrated using schematic, cross-sectional views and TEM images: a) concentric cylinder; b) bamboo; c) herringbone; d) bamboo MWNT from reference 21; e) herringbone MWNTs from reference 22.

MWNTs typically consist of a number of concentric SWNTs of increasing diameter, although other morphologies have been reported.[20-22] Figure 1.03 shows cross-sectional representations of three morphologies: "concentric cylinder", "bamboo" and "herringbone" MWNTs, and TEM images of bamboo and herringbone MWNTs. Bamboo and herringbone MWNTs resemble stacked cups or cones. The layered structure of MWNTs means they are

less well-defined than SWNTs and cannot be assigned a chiral vector. It also causes all MWNTs to be metallic as current can travel between, as well as along, layers.[23] Another consequence is that MWNTs have a larger diameter than SWNTs, typically 10 nm to 100 nm for commercial materials. Like SWNTs they have a high aspect ratio, with lengths around three orders of magnitude greater than their diameter.

1.2.2: Properties and Applications of CNTs

The stand out properties of CNTs include high thermal and electrical (in the case of metallic CNTs) conductivity, exceptional mechanical properties such as a Young's modulus of almost 1 TPa,[24] low weight, high aspect ratio, high surface area and near-transparency in thin films. This has led to a host of proposed applications for both SWNTs and MWNTs. These include applications as electronic components, in catalysis, in composite materials, as sensors, and for biomedical applications.[13] More specific examples are CNT electrodes for flexible displays[25,26] and lithium ion batteries.[27] Recent developments include the 'carbon nanotube computer,' which uses only transistors made entirely from CNTs,[28] and super lightweight 'carbon aerogels' made from CNTs and graphene oxide (GO) (Figure 1.04).[29] The latter have densities as low as 0.16 mg cm^{-3} and are capable of absorbing many times their own mass in organic liquids.

Figure 1.04: A cylinder of carbon aerogel (volume *ca.* 100 cm^3) is sufficiently lightweight that it does not deform fine plant fibres. Image reproduced from reference 29.

Most proposed applications remain confined to laboratory prototypes; however there are some examples of commercial products using lightweight, high-strength nanotube composites, including tennis racquets and bicycle components. It has also been suggested that CNTs could be used to dampen vibrations in skis.[30] CNTs have famously been proposed as a means of creating a space elevator due to their exceptional tensile strength and low weight.

CNT-based technologies may be affected by concerns about their toxicity and biological and environmental effects.[31-35] CNTs could have an asbestos-like effect on the lungs due to their high aspect ratio.[31,32] Other concerns are risks associated with any catalyst contaminant on CNT surfaces and the binding of proteins and other biomolecules to CNT surfaces.[33] Studies indicate that biological effects differ depending on CNT length, diameter and functionality.[32-34]

1.2.3: Synthesis of CNTs

Several methods have been developed for the production of CNTs. The most commonly used are arc discharge, laser ablation and chemical vapour deposition (CVD), including the high pressure carbon monoxide (HiPco) process.[36-38] CVD is the easiest of the processes to scale up for industrial production.[39,40] Many variants exist using slightly different conditions, but the basis of the process is the growth of CNTs on a catalyst surface using carbon derived from a volatile feedstock.[36] The HiPco process combines the catalyst with the feedstock by using $Fe(CO)_5$ together with additional carbon monoxide to grow CNTs on a gas-phase catalyst: iron catalyses the disproportionation of carbon monoxide to carbon and CO_2.[37] CVD can be used to produce both SWNTs and MWNTs, including MWNTs with bamboo and herringbone morphologies.[21,22]

The arc discharge technique was already known as a method of fullerene synthesis when it was used by Ijima in his first report of MWNTs.[2] It can also be applied to the synthesis of SWNTs.[41] In this technique a high electrical current is allowed to arc between two graphite electrodes, which causes some of the carbon present in the graphite to be evaporated. The material formed on cooling contains bundles of CNTs.

Laser ablation is often used in the synthesis of SWNTs and is also based on a method of fullerene synthesis.[1,42] In this technique a target consisting of graphite and metal catalyst is heated to high temperature and exposed to a laser pulse which vaporises the target. Upon cooling under a flow of inert gas CNTs are obtained. A useful feature of this process is that the SWNTs produced have a near-uniform diameter and are obtained in high yield.[36,42] It cannot, however, be scaled up for large scale CNT production.[36]

Compared to SWNTs, MWNTs are currently considerably easier and cheaper to produce on large scale which makes them a more viable material for any future commercial applications.

However, the prices of both materials are continuing to fall as industrial processes become more efficient.

1.3: Properties of Graphene

1.3.1: Discovery and Structure

First reported in 2004,[5] although studied theoretically almost 50 years earlier,[43] graphene is best described as a single layer of graphite, i.e. an atomically thin, planar, hexagonal lattice of sp^2-bonded carbon atoms. Although closely related materials now known as graphene oxide (GO) and reduced graphene oxide (RGO) were described previously they did not possess the unique properties displayed by graphene.[44] Since 2004, when the first method of isolating graphene was published, this fascinating material has attracted a great deal of attention. A further surge in interest followed the award of the 2010 Nobel Prize in physics to Geim and Novoselov for their discoveries in this area. The properties of materials consisting of more than one graphene layer can be similar to those of true graphene. This means the terms "few layer graphene" (FLG) and "multi-layer graphene" (MLG) are often used, particularly in reference to material produced by liquid-phase exfoliation of graphite. These terms are not clearly defined, and are often used interchangeably to refer to graphitic flakes with 10 or fewer layers.[45-47] A proposed nomenclature defines MLG as flakes of 'between 2 and about 10' graphene layers and FLG as a subset 'with layer numbers from 2 to about 5.'[48] A recommended term for exfoliated graphite flakes of more than about 10 layers but thicknesses below 100 nm is graphite nanoflakes.[48] The electrical properties of graphite nanoflakes are closer to those of bulk graphite than graphene. We will adopt these conventions when referring to exfoliated graphite. Figure 1.05 shows TEM images of a graphene sheet and some MLG flakes.

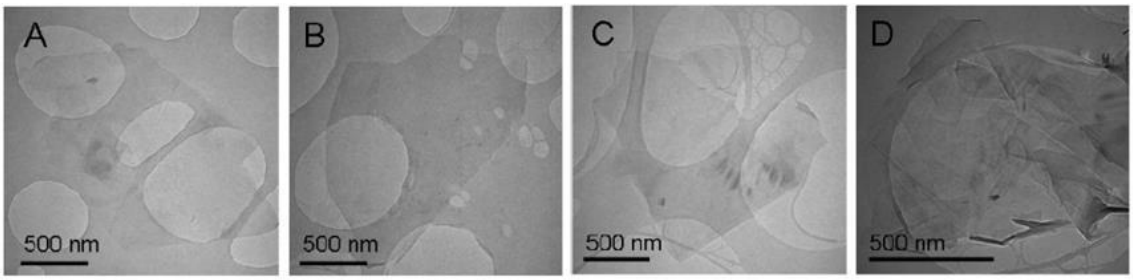

Figure 1.05: TEM images of graphitic flakes adapted from reference 46. A: graphene monolayer with some small overlying flakes; B: bilayer FLG; C: trilayer FLG; D: disordered MLG.

1.3.2: Properties and Applications of Graphene

Graphene has remarkable physical properties, many of which are comparable to those of CNTs. For example it is extremely lightweight and has a large surface area.[47] It was described by Lee *et al.* as "the strongest material ever measured," when they reported properties such as its Young's modulus of 1.0 TPa.[49] Graphene is also almost transparent[50] and has unprecedented electron and hole mobility, which suggests applications as an electrode in solar cells or organic LEDs.[51] Another possible application is use in materials for storage of hydrogen and other gases, as it is impermeable.[47] Other applications similar to those proposed for CNTs are also possible, such as use in composites or molecular electronics. The exploitation of graphene is a field which is still in its infancy, and there are many challenges to overcome before the properties of this material can be fully exploited. This means it is difficult to predict which applications will find widespread use.[52] The viability of large scale graphene production is likely to have a significant impact.

Investigation of the toxicity of graphene and its derivatives is an area of growing interest.[53,54] Current results are limited and inconclusive, but suggest that graphene, FLG, GO and RGO may all have different biological effects. Some of the concerns associated with CNTs are not relevant to graphene as it does not have the same high aspect ratio and is typically produced without metallic impurities.[54]

1.3.3: Production of Graphene

Similarly to the debundling of CNTs, isolation of individual graphene sheets from graphene requires that the strong van der Waals interactions between the closely stacked (3.41 Å) graphene layers be overcome.[55] Graphene was first isolated using a method based on repeated mechanical cleavage of graphite using Scotch tape.[5] While this allowed for the isolation of small amounts of stable single-layer graphene and FLG, this technique is somewhat impractical beyond laboratory scale.[44] This ground-breaking work inspired the development of further methods for graphene production. These can be described as either "top down" or "bottom up" approaches depending on the choice of starting material.[45,47] The former includes various techniques based on exfoliation of graphite to give graphene layers, ranging from the original mechanical cleavage approach[5] to the methods based on intercalation of solvents, surfactants or alkali metal ions.[45,55] Surfactant-aided exfoliation is discussed in further detail in Section 1.5. Recent publications show a growing interest in "top

down" approaches based on ball-milling.[56,57] Examples of "bottom up" approaches include CVD methods[45] similar to those used to produce CNTs, and growth from smaller polycyclic aromatic hydrocarbons.[44,58] A method which includes aspects of both approaches is the 'unzipping' of CNTs to give graphene nanoribbons,[14] i.e. graphene sheets which are much longer than they are wide. "Bottom up" methods produce high quality graphene, but are unlikely to be practical for bulk scale production, for which "top down" approaches are favoured.[55] Challenges remain in achieving high conversion of graphite to graphene using "top down" approaches. A priority of current work on graphene is the development of scalable, reproducible methods which produce high quality material.

Alternative approaches produce the graphene-like material RGO. These are practical on a much larger scale than most other methods.[59] To obtain RGO, graphite is first subjected to highly oxidising conditions which convert it to graphite oxide. Hummers' method, published in 1958, uses potassium permanganate, sulphuric acid and sodium nitrate to oxidise graphite and (with some modifications) remains a popular procedure.[60,61] The structure of graphite oxide is poorly defined.[59] It contains a variety of oxygen functionalities such as carbonyls and epoxides, which increase the layer separation relative to pristine (i.e. untreated) graphite.[61,62] GO is the oxidised analogue of graphene, i.e. a single layer of graphite oxide. Due to its increased layer spacing in comparison to graphite and the presence of hydrophilic moieties it is considerably easier to exfoliate graphite oxide to give GO in aqueous media (or other solvents); this is possible without the addition of surfactants or other stabilisers.[62,63] Reduction of GO by chemical, thermal or other means affords RGO; a common reducing agent is hydrazine.[61-63] The oxidative and reductive conditions used in the synthesis of RGO result in structural differences compared to graphene which include defects in the hexagonal lattice and the presence of heteroatoms, particularly oxygen.[62,64] These have a substantial effect on some properties of RGO; for example its thermal and electrical conductivity is considerably lower than that of graphene.[55,64,65] Nonetheless, RGO does predominantly consist of large 2-dimensional sheets comprised chiefly of sp^2 carbon. This means that it may be suitable in applications where only selected properties of graphene are desirable. It is hoped that by further improving reductive methods it will become possible to produce RGO with properties comparable to graphene.[59,62]

1.4: Aqueous Dispersion of CNTs

1.4.1: Overview

Various methods have been employed to improve the processability of CNTs by dispersing them in water and other solvents. Although the terms "solution" and "solubilisation" are commonly found in the literature, we will refer to CNTs (and similar carbonaceous materials such as graphene) individualised and stabilised in a solvent as "dispersions" in agreement with the recommendation of Premkunar *et al.*,[66] who reasoned that CNT dispersions, are colloidal and therefore not true solutions. A 'true solution' of SWNTs has been reported but this required the use of chlorosulphonic acid as a solvent and was limited to a concentration of 0.5 wt%.[67]

Both SWNTs and MWNTs are usually produced as "bundles" of tubes held together through strong inter-tube π-π and van der Waals interactions, on the order of 500 eV μm^{-1}.[68,69] In order to exploit many of the desirable properties of CNTs it is necessary to break up these bundles into individual CNTs. This requires energetic processing and, unless the dispersion is prepared in aromatic solvents such as xylene, functionalisation of the CNT. This is usually achieved in one of three ways: i) direct, covalent functionalisation of the CNT surface; ii) non-covalent functionalisation by wrapping the surface in a polymer or biopolymer; or iii) non-covalent functionalisation of the surface with small molecules, typically surfactants. Covalent functionalisation disrupts the structure of the CNT surface and can have a negative impact on many of the material's useful properties.[70,71] Non-covalent approaches do not alter the CNT structure, ensuring their properties can be exploited.[72] Polymer-wrapping can be a very effective method for CNT dispersion but it can be difficult to remove the polymer and obtain pristine individualised CNTs.[73] Surfactants are equally effective dispersants and can be more easily removed from CNT surfaces after processing.

The use of polymers or surfactants allows CNTs to be dispersed in water. This offers a distinct advantage as most organic solvents used to disperse CNTs are toxic or have high boiling points. The ability to efficiently disperse large quantities of CNTs in water would facilitate industrial processing of this material in a useful, unbundled state. Handling CNTs in dispersions may help to overcome some of the hazards associated with these materials in the solid state, such as possible toxicity associated with inhalation, as they are no longer fine, lightweight particles.

1.4.2: Factors Affecting Aqueous Dispersion of CNTs using Surfactants

To prepare an aqueous CNT dispersion, the typical method is to ultrasonicate a mixture of SWNTs or MWNTs with a solution of either surfactant or polymer. This provides the energy needed to overcome the strongly attractive inter-tube forces. Centrifugation is applied to the obtained suspension to separate any remaining large aggregates from the individualised, dispersed CNTs. The supernatant CNT dispersion can then be decanted and analysed – common studies include measuring the UV-visible absorbance of a dispersion to determine the concentration of CNTs using the Beer-Lambert law, and microscopy. Dispersions are typically stable for several months or longer. Figure 1.06 summarises surfactant-aided dispersion.

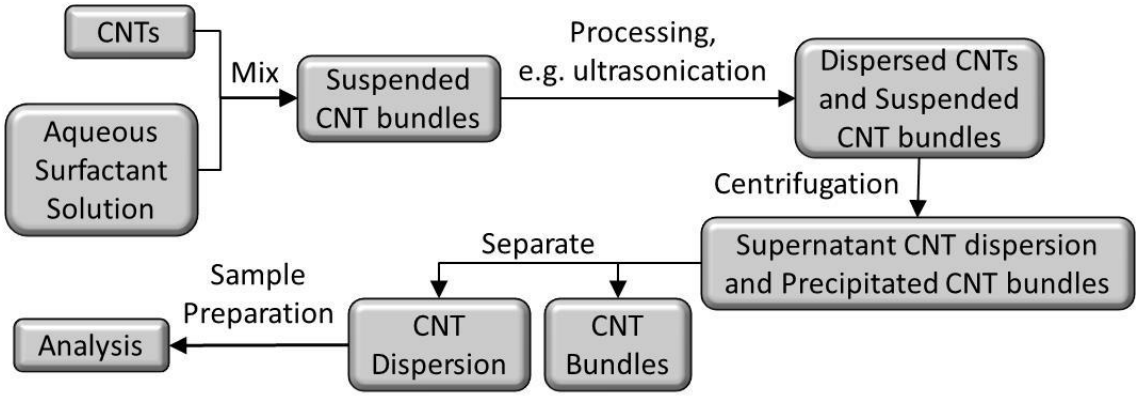

Figure 1.06: Summary of a typical method for preparing aqueous CNT dispersions using surfactants.

Although the dispersion process appears straightforward, comparisons of different studies are difficult. Variables which differ between studies include: CNT type (SWNT or MWNT), supplier, production method and (average) dimensions, any pre-treatment of CNTs, the ratio of CNT mass to volume of surfactant solution, surfactant concentration, experimental scale, sonication type, power, time and temperature, centrifugation time and force, and analysis technique used. Prior to a discussion of published dispersion studies we will elaborate briefly on these variables.

Predictably, SWNTs and MWNTs often give conflicting results due to differences between their diameters and surface curvatures. Other factors such as manufacturing method, supplier, typical dimensions (which can also vary significantly within a heterogeneous CNT sample) and any pre-treatment of the material can all affect the ease with which studies can be compared as the properties of the CNTs will differ.[74,75] Changing the ratio of surfactant to CNT would be expected to affect the efficiency of CNT dispersion. If insufficient surfactant is

present then the CNT surface coverage will be incomplete and the hydrophilicity of the functionalised CNT will be less than optimum, possibly producing misleading results. An initial increase in CNT concentration with surfactant concentration, followed by a plateau, has been observed for both SWNTs and MWNTs.[71,75] The onset of this plateau is close to the critical micelle concentration (CMC) of the surfactant used. Too much surfactant is not only wasteful but may lower the level of dispersion through the effect of depletion forces.[76,77]

Ultrasonication is usually conducted either in an ultrasonic bath or using a 'tip' (or 'probe') sonicator. In the case of the former samples are immersed in a water bath through which ultrasonic vibrations are passed, whereas for the latter the vibrating tip can be immersed directly into the sample. Bath sonication is a gentler technique and as such typically uses longer sonication times than the more energetic tip sonication. It has been reported that (at least in organic media) both sonication methods can break up long CNTs into shorter fragments,[78] which may have implications depending on the intended application of the CNT dispersion. Like surfactant concentration, increasing sonication time can increase the concentration of dispersions up to a point.[71,74] Sonicator power can also influence dispersion quality.[79]

Sufficient centrifugation at an appropriate force is important to remove any larger CNT aggregates from the dispersion. Although these precipitate over time upon standing, this can take several days.[80] The presence of such aggregates in a dispersion could result in errors in any analysis performed, for example aggregates would increase the UV-visible absorbance of dispersions. Very high centrifugal forces could be sufficient to remove some of the dispersed CNTs from the bulk liquid – techniques such as density gradient ultracentrifugation can be used to purify SWNTs of different chiralities.[81,82] It is therefore important to find intermediate centrifugation conditions which ensure any aggregates are removed from the dispersion without causing precipitation of individualised CNTs.

1.4.3: Aqueous Dispersion of CNTs using Surfactants

O'Connell *et al.* published one of the first examples of ultrasonic dispersion of individualised CNTs in 2002.[83] SWNTs were dispersed using 1 wt% sodium dodecyl sulphate (**SDS**) by subjecting the mixture to high shear mixing followed by cup horn sonication (an intermediate technique between bath and tip sonication). SWNT concentrations of 20-25 mg L^{-1} were achieved. More recent research into the dispersion of CNTs in aqueous media includes the

use of common, commercially available surfactants and bespoke surfactants designed specifically for the dispersion of CNTs. Widely studied commercial surfactants include **SDS**, sodium dodecylbenzenesulphonate (**SDBS**), cetyltrimethylammonium bromide (**CTAB**), octadecyltrimethylammonium bromide (**OTAB**) and **Triton X-100** (Figure 1.07).

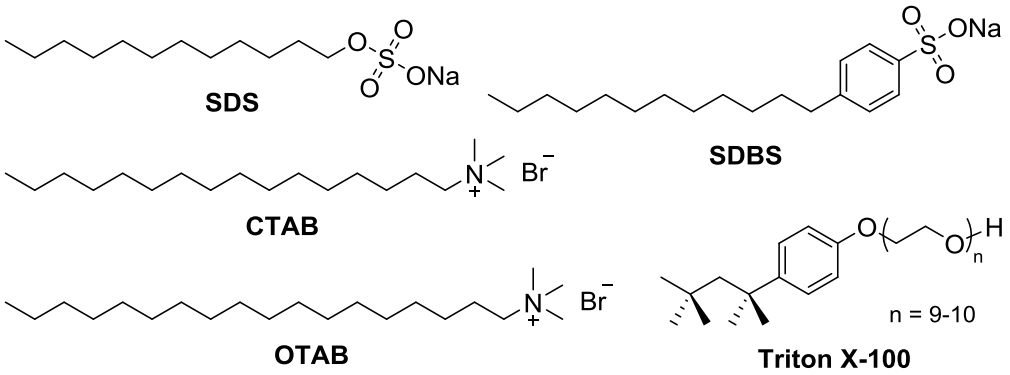

Figure 1.07: Structures of commercial surfactants used to form aqueous CNT dispersions.

Investigations into the precise nature of the binding of surfactants to a CNT surface have given disparate results.[74] Figure 1.08 shows schematic illustrations of possible surfactant structures as summarised by Hirsch and co-workers.[73] Work by Yurekli *et al.* in which SWNTs dispersed in **SDS** were investigated using small angle neutron scattering indicates that the orientation of surfactant molecules on the SWNT surface is random.[70] This contrasts with observations by Matarredona *et al.* who describe a change between behaviour at low and high surface coverage in a study where **SDBS** was used to disperse SWNTs.[71] They proposed an initial regime in which surfactant molecules lie parallel to the SWNT surface. Upon an increase in surfactant concentration rearrangement into a cylindrical micelle surrounding the SWNT occurs, resulting in a higher (monolayer) surface coverage.[71] These cylindrical micelles are templated by the SWNT and cannot exist freely. Matarredona *et al.* also comment that the formation of hemicylindrical micelles is unlikely on a SWNT surface as its high curvature would render them unstable. Conversely, Richard *et al.* reported that hemicylindrical micelles form on SWNTs and MWNTs dispersed using anionic **SDS**, cationic **OTAB** and several novel amphiphiles containing carboxylic acid moieties.[72] These micelles lie perpendicular, or close to perpendicular, to the CNT axis such that they form toroidal or helical structures. Interestingly, no ordered surface structures were observed when **Triton X-100** was used to prepare dispersions. The authors attribute this to the π-stacking interaction which can occur between the aromatic ring of **Triton X-100** and the CNT surface.[72] The non-ionic polyethylene glycol (PEG) hydrophile of this surfactant may be equally relevant. Hemicylindrical and hemispherical micelles are also known to form on graphitic surfaces.[84-86]

A more recent computational study simulated the formation of all of the above surface assemblies by varying surfactant concentration and alkyl chain length.[87] Surface functionalisation using amphiphiles with short alkyl hydrophobic units is reversible as binding of these materials is an equilibrium process.[74] Richard *et al.* showed that more stable supramolecular structures are formed when longer alkyl chains are used.[72] Another way to accomplish strong, stable surfactant binding to a CNT surface is to use an aromatic, rather than an aliphatic, hydrophile to take advantage of π-stacking interactions. This is commonly exploited when designing surfactants specifically for the dispersion of CNTs and graphene, as discussed below.

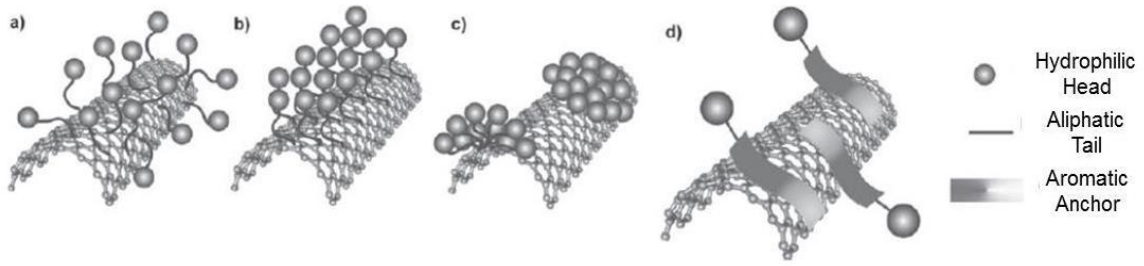

Figure 1.08: Illustration of possible non-covalent surfactant-CNT interactions (using SWNTs) adapted from Reference 73. These consist of a) random surfactant absorption; b) formation of cylindrical micelles; c) formation of hemispherical micelles; d) absorption of surfactants incorporating an aromatic anchor through π-π interactions.

Wenseleers *et al.* compared the ability of 18 commercially available surfactants (and one polymer) to disperse SWNTs.[80] Interestingly, in this work sonication was not used, rather SWNTs were stirred gently in surfactant solution over a period of 3 days. The authors also note that allowing the dispersions to settle over an additional 3 days achieved similar results to centrifugation for 10 min at 3000 g. It was found that the bile salt surfactants sodium deoxycholate (**SDOC**) and sodium taurodeoxycholate (**STDOC**) (Figure 1.09) were very effective dispersants under these conditions. **CTAB**, **SDBS**, sodium cholate (**SC**) and sodium pyrenebutyrate (**SPB**) also performed well, but **SDS** gave lower SWNT concentrations than most of the other surfactants studied. Non-ionic surfactants were generally less effective than ionic surfactants.

Other studies of commercial surfactants gave contrasting results. For example, Sun *et al.* found **SDS** to be a better dispersant for SWNTs than **SDBS** or **SC**.[77] Rastogi *et al.* achieved higher MWNT dispersion levels using **Triton X-100** and other non-ionic surfactants rather than **SDS**,[88] whereas Clark *et al.* found **CTAB** to be a better dispersant of MWNTs than **SDBS** and **SDS**, and all three ionic species to be better than **Triton X-100**.[75]

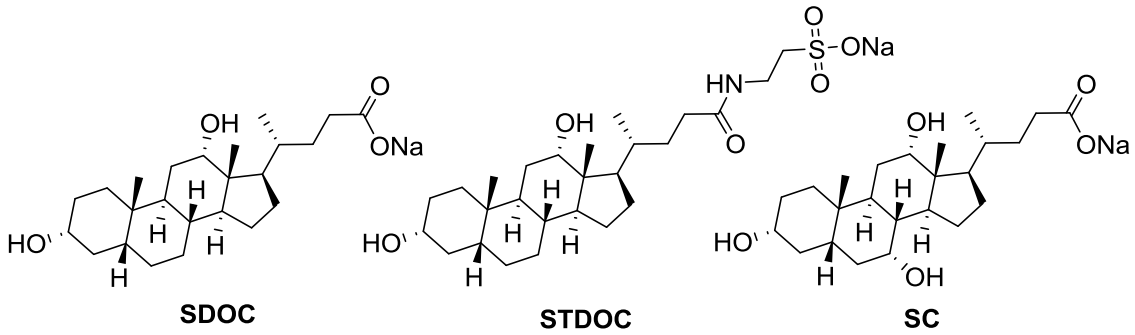

Figure 1.09: Structures of bile salts used by Wenseleers *et al.* to disperse SWNTs.[80]

The hydrophobic moiety of commercial surfactants is usually based on an alkyl chain. In surfactants designed specifically for dispersion of CNTs a polycyclic aromatic moiety is preferentially used to take advantage of strong π-π interactions between the surfactant and CNT surface. These include pyrene,[69] perylene,[73,89] anthracene[90] and porphyrins.[91] The effectiveness of surfactants with polycyclic aromatic anchors was demonstrated by Tomonari *et al.* who showed that pyrene-based surfactant **1** was more effective than its phenanthrene analogue at dispersing SWNTs, and that naphthyl and phenyl analogues failed to disperse SWNTs.[92] A larger aromatic anchor clearly allows for more effective dispersion. Pyrene derivatives functionalised with simple hydrophilic moieties, such as **SPB**, **1**, **2**[93] and **3**[94] (Figure 1.10), have been shown to disperse CNTs in water.

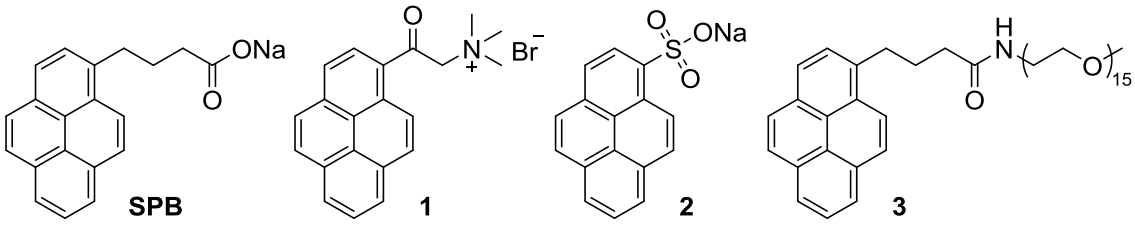

Figure 1.10: Simple pyrene surfactants used to disperse CNTs in water.

More complex surfactant architectures can give improved CNT dispersion ability. Hydrophilic dendrons are commonly used in conjunction with polycyclic aromatics in surfactants for CNT dispersion. The Hirsch group have conducted many studies using molecules based on this concept, such as pyrene derivative **4**[69] and perylene bisimide derivatives **5** and **6** (Figure 1.11).[73,95] Analogues with different generation dendrons as head groups and, in the case of **6**, with branched alkyl chains have been investigated under neutral and basic conditions. The importance of the aromatic perylene moiety was shown using a second generation dendron functionalised instead with a long alkyl chain, which did not form stable SWNT dispersions.[73]

4 and **5** gave higher SWNT concentrations than their second generation (G2) analogues; however **6** performed similarly to **5**. Trends in SWNT dispersing ability were related to packing density on the SWNT surface. **5** and **6** were found to be almost 5 times better than **SDS** at individualising SWNTs.[73]

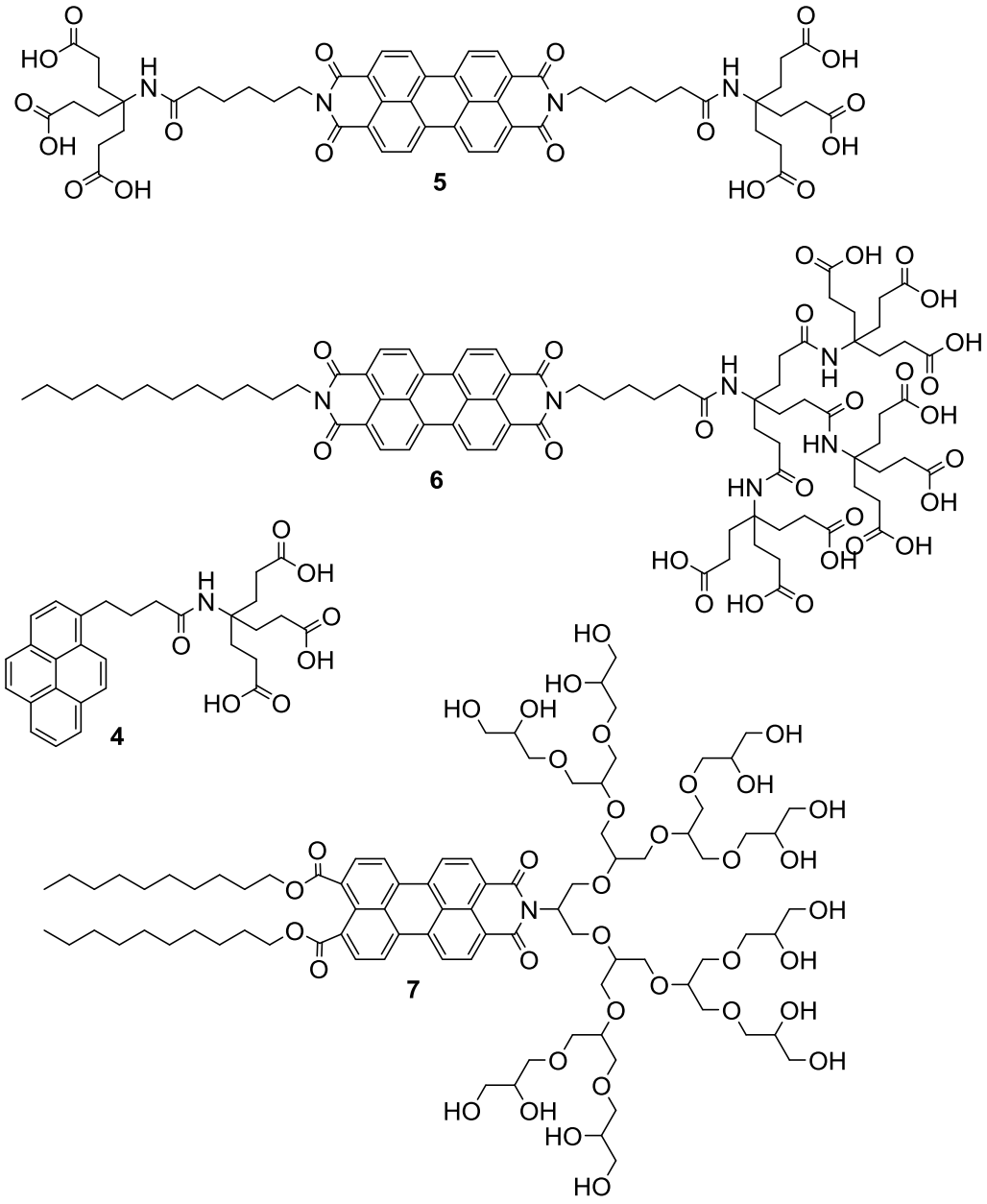

Figure 1.11: Dendron-functionalised polycyclic aromatic surfactants used to disperse CNTs.

Perylene-based surfactants have also been studied by the groups of Haag and Reich.[89,96] They use polyglycerol dendrons as hydrophilic moieties in non-ionic surfactants such as **7** (Figure 1.11). They show that changes to the alkyl unit can have a significant impact on surfactant properties. Analogues of **7** with longer, shorter or no alkyl chains are less efficient at dispersing SWNTs. This relates to the hydrophobic contribution of the alkyl chains, as

efficient SWNT dispersion can be achieved using shorter chain analogues if an additional alkyl linker is added between the perylene moiety and the dendron.[89] The use of a long, hydrophilic PEG chain in place of the glycerol dendron reduced SWNT individualisation, suggesting that dendritic head groups are more favourable.

Takaguchi *et al.* used an amidoamine dendron-functionalised fullerene derivative to disperse SWNTs in water,[97] and they subsequently showed that an anthracene analogue was also effective.[90] The concentration of the SWNT dispersions is not reported in either case.

A different approach is to design surfactants with aromatic anchors which fit the curvature of a CNT surface (Figure 1.12). A simple example of this is the use of triptycene derivatives such as **8**.[98] More elaborate examples are "nanotweezers" in which two aromatic moieties are held at an angle by a linking unit, such as tetrathiafulvalene derivative **9**, which can be used to disperse both SWNTs and MWNTs in water.[99] It is hoped that nanotweezer designs which are selective to SWNT chiralities can be developed.

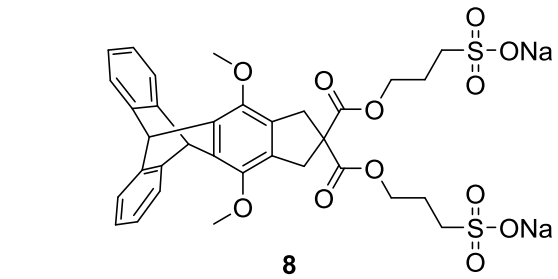

8

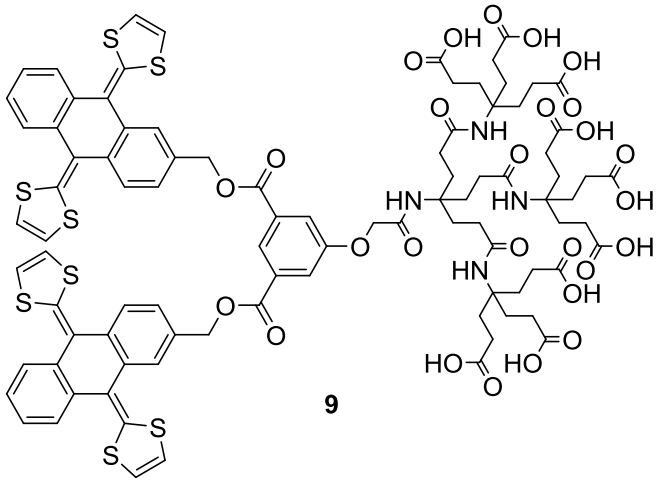

9

Figure 1.12: Aromatic surfactants which can fit to the curved surface of CNTs.

1.5: Surfactant-Aided Exfoliation of Graphite to Graphene

The exfoliation of graphite using surfactants can be accomplished using methods similar to those used to disperse CNTs (Section 1.4.2).[46,100,101] This is a developing area of research; the first surfactant-stabilised dispersion of graphene (using **SDBS**) was reported in 2009.[46] It should be noted that the dispersions produced consist not only of single-layer graphene but also FLG and MLG. As for CNTs the methods used vary between laboratories, complicating direct comparison of results. The variables are similar, relating to the graphite feedstock, sonication and centrifugation conditions, and analysis techniques. Aqueous dispersions of RGO can be produced by adding suitable surfactants prior to the reduction of GO,[63] but this approach will not be considered in detail here.

Commercial surfactants have been widely applied to graphite exfoliation. Guardia *et al.* report that non-ionic surfactants are particularly effective,[102] whereas Sun *et al.* found **STDOC** to be the best of 8 surfactants, including 4 non-ionics.[103] Other bile salts such as **SC** and **SDOC** have also been used for graphite exfoliation.[65,100] A detailed comparison including analysis of different concentrations found **SDOC** to be superior to **SC**.[104] Using a range of commercial surfactants Notley found that the concentration of dispersed graphene and FLG could be greatly increased by adding surfactant continuously during the sonication process.[105] This method consequently uses much larger quantities of surfactant.

Exfoliation of graphite using pyrene derivatives including **SPB** and **2** has been discussed in a recent review.[47] Other small aromatics can also be effective dispersants; Sampath *et al.* exfoliated graphite in water using diazaperopyrenium salt **10**, but found its smaller diazapyrene analogue **11** to be ineffective (Figure 1.13).[106] This is attributed to the larger aromatic footprint of **10**. **10** is of interest as it can be prepared easily from perylene derivatives.

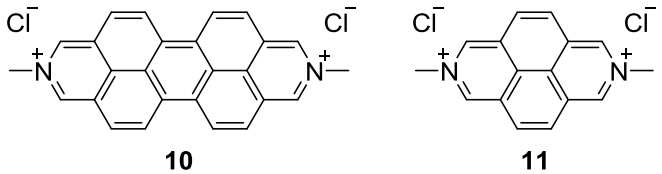

10 **11**

Figure 1.13: Cationic aromatics used by Sampath *et al.* in graphene exfoliation studies.

The use of more elaborate surfactants for graphite exfoliation is a developing field. The Hirsch group have recently investigated perylene bisimide surfactants related to **5** and **6** as

graphene dispersants.[101] The tetrapyrene species **12** (Figure 1.14) can exfoliate graphite in a mixture of water and methanol.[107] Its planar footprint means it is ineffective as a dispersant for SWNTs, which have too large a curvature for the surfactant to bind effectively to their surface.

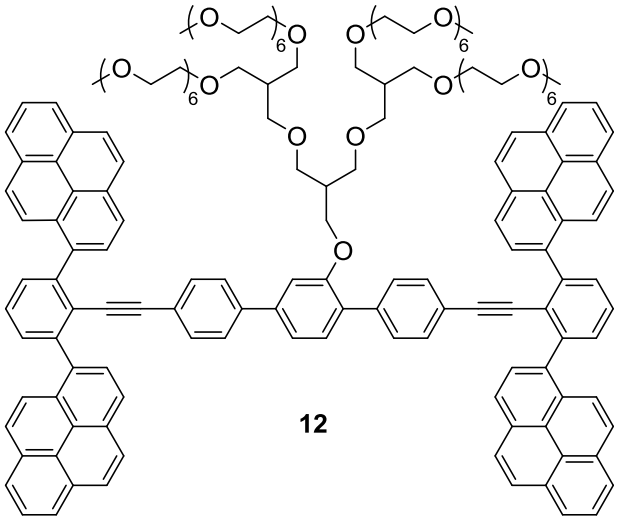

Figure 1.14: Structure of a large tetrapyrene surfactant used to exfoliate graphite.

1.6: Responsive Aqueous CNT and Graphene Dispersions

Work on not only dispersing CNTs or graphene, but also incorporating responsive properties to the dispersion is another emerging area of study. Here we will discuss examples of responsive dispersions which rely on polymeric dispersants and covalent functionalisation in addition to surfactant-stabilised CNTs and graphene.

The most common method of producing a responsive CNT or graphene (usually GO) dispersion is the use of thermally responsive polymers, with which graphitic surfaces can be functionalised both covalently and non-covalently. Polymers used for this purpose have a lower critical solution temperature (LCST) above which they become water immiscible. Covalent functionalisation of CNTs with responsive polymers can be accomplished by growing polymer chains from reactive sites on functionalised CNT surfaces.[108-110] The polymer-functionalised CNTs can then be dispersed in water but will precipitate if heated above the LCST of the polymer. This can be reversed upon cooling.[109] A similar response can be achieved if GO is functionalised in the same way.[111,112] Responsive GO can be used to prepare films which have differing wettability at different temperatures.[112] Non-covalent functionalisation with thermoresponsive polymers can give comparable results.[113,114] Block

copolymers can be used to strengthen interactions with the graphitic surface or to tune the temperature of the response.[115,116] They can also be used to give more complex responsive behaviour; MWNTs dispersed in a block copolymer including poly-*N*-isopropylacrylamide and poly-1-ethyl-3-vinylimidazolium bromide were stable when heated or upon addition of KBr, but precipitated when both stimuli were applied together.[117] A thermal response using a small molecule dispersant was reported by Ikeda *et al.* who dispersed SWNTs in folic acid solution under basic conditions.[118] Heating induced precipitation of SWNTs as folic acid was stripped from their surface. This meant that the process was irreversible without sonication comparable to that used to prepare the original dispersion.

Another common stimulus for responsive dispersions is pH change. This is also usually achieved using polymeric dispersants. A CNT dispersion in polymethacrylic acid was stable under basic conditions but precipitated reversibly if acidified due to protonation of anionic carboxylate moieties.[114] Conversely, SWNTs dispersed in poly-*L*-lysine were stable under acidic, neutral and weakly basic conditions but not at high pH.[113] This is caused by deprotonation of cationic ammonium moieties. These effects have been combined into a terpolymer with polystyrene, polyvinylpyridine and poly(acrylic acid) blocks. The combination of acidic and basic moieties resulted in MWNT dispersions which were stable below pH 4 and above pH 7, but unstable inbetween.[119] The thermally responsive SWNT dispersion in folic acid discussed above was also found to be pH sensitive.[118] Precipitation of SWNTs occurred upon acid treatment, however in this case re-dispersion could be achieved without sonication upon addition of base, indicating that the folic acid remained bound to the SWNT surface.

1.7: Project Aims

Although it has been reported that a range of molecules can disperse CNTs and exfoliate graphite in organic solvents and water based on adsorption to graphitic surfaces, there remains a need for surfactants which allow for further exploitation of dispersed carbon nanomaterials. Stimulus-responsive dispersions are an area of growing interest. The aim of the current work is to design, synthesise and test novel surfactants which can not only efficiently disperse CNTs and exfoliate graphene in aqueous media, but also result in responsive dispersions. The ability to tune this responsive behaviour through structural variation is also highly desirable. We have devised a surfactant template comprised of three parts, shown schematically in Figure 1.15. These will be referred to as 'anchor,' 'linker' and

'head' groups; variation of these groups allows the development of a library of 'anchor-linker-head' (ALH) surfactants.

Figure 1.15: A schematic representation of our ALH surfactant template.

The anchor group is designed to bind strongly to graphitic surfaces through π-π interactions to ensure that CNTs and graphene are efficiently functionalised. To achieve this it should be hydrophobic and include multiple aromatic rings. We have selected pyrene for this unit as it is known to bind strongly to CNTs and can be easily functionalised with a hydrophilic substituent. Functionalisation with a side chain can further increase the strength of binding to graphitic surfaces.[120] In the event that stronger binding is required we would consider larger macrocyclic species such as porphyrins and phthalocyanines.

A defined linker unit with a functional role is largely unexplored in existing work. Typically the link between the anchor and head groups is either direct or a simple, short aliphatic chain. We plan to examine the role of the linker unit more systematically by incorporating oligomeric linkers of varying lengths and functionality. We propose that longer linkers may allow for more efficient surface coverage when using aromatic anchors as the head group will have greater freedom of movement relative to the anchor group. This could allow for micelle formation on the graphitic surface. We anticipate that the presence of hydrophilic moieties in these oligomeric linkers will have a positive impact on the ability of our surfactants to disperse CNTs and graphene in water. Amide and ether based linkers were targeted on this basis.

The head group is designed to impart hydrophilicity to functionalised CNTs and graphene. As discussed in Sections 1.4 and 1.5, many hydrophilic moieties have been successfully used in this role, including sulphonates, sulphates, ammonium ions, carboxylic acids, carboxylates, polyols and polyethers. We selected carboxylate head groups for our initial investigations as they were anticipated to be synthetically convenient and likely to result in at least a pH response. We also chose to investigate carboxylate dendrimers as these have previously been shown to be effective in surfactants for CNTs and graphene.[73] Alternative head groups could be considered based on the performance of carboxylate materials.

Stimuli of interest include temperature, pH change and the presence of salts. By incorporating functionalities which are sensitive to one or more stimuli we hope to produce dispersions with a similar response. For example, the hydrophilicity of carboxylate head groups will be reduced at low pH as they are converted to carboxylic acids. This could induce precipitation of functionalised CNTs or graphene as observed for polymeric dispersants in Section 1.6. Ion sensitivity could be achieved by using moieties such as crown ethers which have an affinity for specific ions. A temperature response could be achieved through thermally induced changes to the favoured linker conformation, which may alter head group availability. By choosing appropriate amide or ether linkers with thermoresponsive properties (e.g. an LCST) it may be possible to cause functionalised carbonaceous materials to aggregate above a certain temperature. A reversible stimulus response of this type is particularly desirable. Figure 1.16 schematically illustrates the dispersion process and possible stimulus responses of functionalised CNTs.

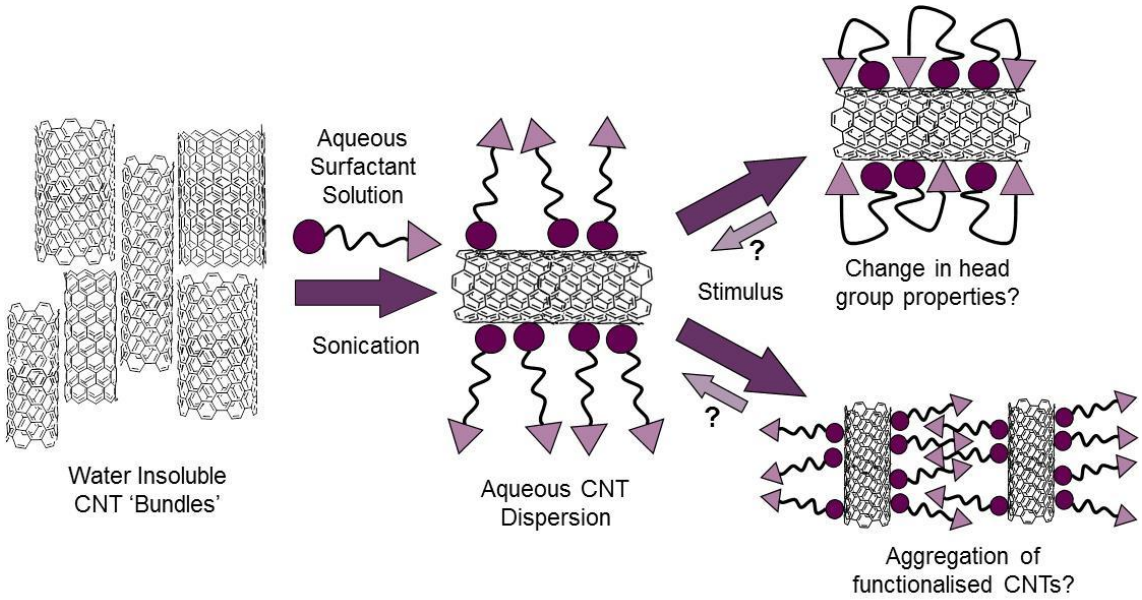

Figure 1.16: A schematic representation of how an ALH surfactant could functionalise and disperse CNTs and how the functionalised materials may respond to stimuli.

Surfactant synthesis within this project was divided into development of 'ether linker' and 'amide linker' surfactants. This thesis will detail the synthesis of the 'ether linker' surfactants and compare their properties as dispersants with 'amide linker' surfactants whose synthesis was developed in our laboratory by Dr Kara Howes and Dr Daniel Welsh.

We aim to investigate the ability of both series of surfactants to disperse MWNTs and graphene. The higher curvature of SWNTs is expected to make π-π interactions less efficient

than with MWNTs, so they will not be studied. The structural similarities between the surfaces of large-diameter, low curvature MWNTs and graphite or MLG should mean that both materials will interact strongly with aromatic anchoring units. As functionalisation of the materials should be similar, we expect any surfactant-induced responsive behaviour will be transferable between the two materials.

Chapter 2: Synthesis of Anionic Surfactants

This chapter describes the synthesis of two series of anionic surfactants designed to disperse CNTs and graphene in aqueous media. It will begin with an overview of the materials which were targeted. This is followed by discussion of the various synthetic strategies which were utilised, including those which were found to be unsuitable due to poor yields, by-product formation or failed reactions, concluding with the route which was employed successfully in the synthesis of the novel surfactants.

2.1: Synthetic Targets

Two related general structures were proposed for ether linker anionic surfactants (Figure 2.01). These both followed the ALH architecture discussed in Section 1.7, and included the targeted pyrene anchor unit, polyether linker and carboxylate head group. We planned to synthesise and compare two related series of surfactants in which the linker length was systematically varied; one series with simple monocarboxylate head groups and the other with more complex, dendritic head groups comprising three carboxylate moieties. The latter series can be derived from the former *via* formation of an amide bond. Additional comparisons were planned between these species and 'amide linker' surfactants which were also prepared in our laboratory.

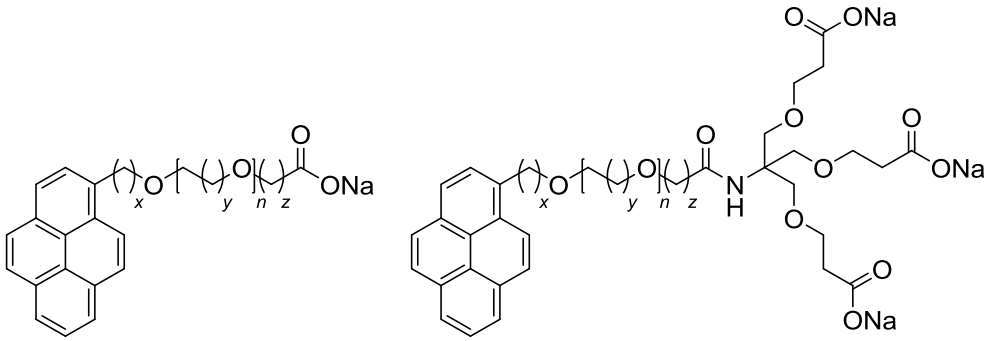

Figure 2.01: The general structures of targeted monocarboxylate surfactants (left) and tricarboxylate surfactants (right).

The most convenient commercial pyrene derivatives on which to base a synthetic route are 1-pyrenemethanol, **PyrMOH**, and 1-pyrenebutanol, **PyrBOH**; the latter can also be derived from another commercial material, 1-pyrenebutyric acid, **PBA**, by simple reduction (Figure 2.02).

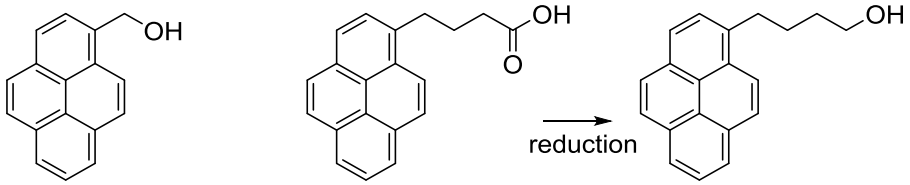

Figure 2.02: Structures of commercially available pyrene derivatives from which the anchor group can be derived.

At the outset, precise alkyl chain lengths within the target structures were not specified, rather the variables *x*, *y*, and *z* (Figure 2.01) would be determined by synthetic convenience. Several synthetic routes were attempted and these are discussed in Sections 2.2, 2.3 and 2.4. It was planned to systematically vary *n* to assess the effect of linker chain length on the ability of the surfactant to disperse CNTs and graphene. The values of *n* used would be somewhat dependent on the choice of *y*, to achieve a balance between synthetic accessibility and chain length variability.

The target tricarboxylate head group is a first generation Newkome-type dendron[121-123] which will be referred to as the "G1" head group. The monocarboxylate head group will be referred to as "G0". Newkome-type dendrons have been used as hydrophilic moieties in areas including supramolecular chemistry,[124,125] biochemical and medicinal applications (including fluorescent probes)[126-129] and functionalisation of nanoparticles.[130] Of particular relevance is work of the Hirsch group discussed in Chapter 1, where Newkome-type dendrons were used as hydrophilic groups in surfactants used to form dispersions of SWNTs and graphene.[69,73] Better CNT solubilising ability was observed for pyrene-anchored surfactants with a first rather than a second generation dendron as the hydrophile.[69] It was hypothesised that the higher coulombic repulsion between nonacarboxylate (G2) head groups results in poorer CNT surface coverage for G2 compared with G1 surfactants. Similar trends were observed in some cases when perylene anchors were used.[73] On this basis we decided not to initially target a G2 dendron as a head group for ether linker surfactants. The concurrent work on amide linker surfactants would assess the impact of linker units on surfactants with both G1 and G2 head groups, with a view to extending the ether series to include G2 head groups if they appeared favourable.

It is convenient to synthesise Newkome-type dendrons as *tert*-butyl esters in order to protect the acid moieties and allow the amine at the dendron core to be used to form amides without side reactions. *tert*-Butyl esters are more robust under the basic conditions used in amide

couplings than methyl or ethyl esters. The dendrons used by the Hirsch group are derived from nitromethane, exemplified in the two-step synthesis of *tert*-butyl protected first generation dendron, **13**, in Scheme 2.01.[69,131] Our work uses a slightly larger dendron derived from tris(hydroxymethyl)aminomethane, **TRIS**. A reported synthesis of this *tert*-butyl protected first generation dendron, **14**, directly from **TRIS** and *tert*-butyl acrylate **15** is also shown in Scheme 2.01.[123] The use of **TRIS** means dendron **14** contains ether moieties which differentiate it from dendron **13**. It was anticipated that these ether moieties would enhance the hydrophilicity of surfactants incorporating **14** rather than **13** as additional hydrogen bonding interactions are made possible. This should in turn improve the ability of surfactants to disperse CNTs. It was hoped that the increased hydrophilicity will be more significant than any unfavourable effects associated with the slightly increased steric bulk of dendron **14** *vs.* **13**. The reported synthesis of **13** is slightly higher-yielding than that of **14** (63% overall for 2 steps, *vs.* 54% in a single step); however, a synthesis of **13** in our laboratory afforded a significant quantity of inseparable cyclised by-product **16** (Scheme 2.01), despite claims to the contrary in the literature.[131] This complication is avoided entirely by using dendron **14** as the analogous lactam would be a less favourable 7-membered ring. The synthesis of **14** also benefits from milder reaction conditions.

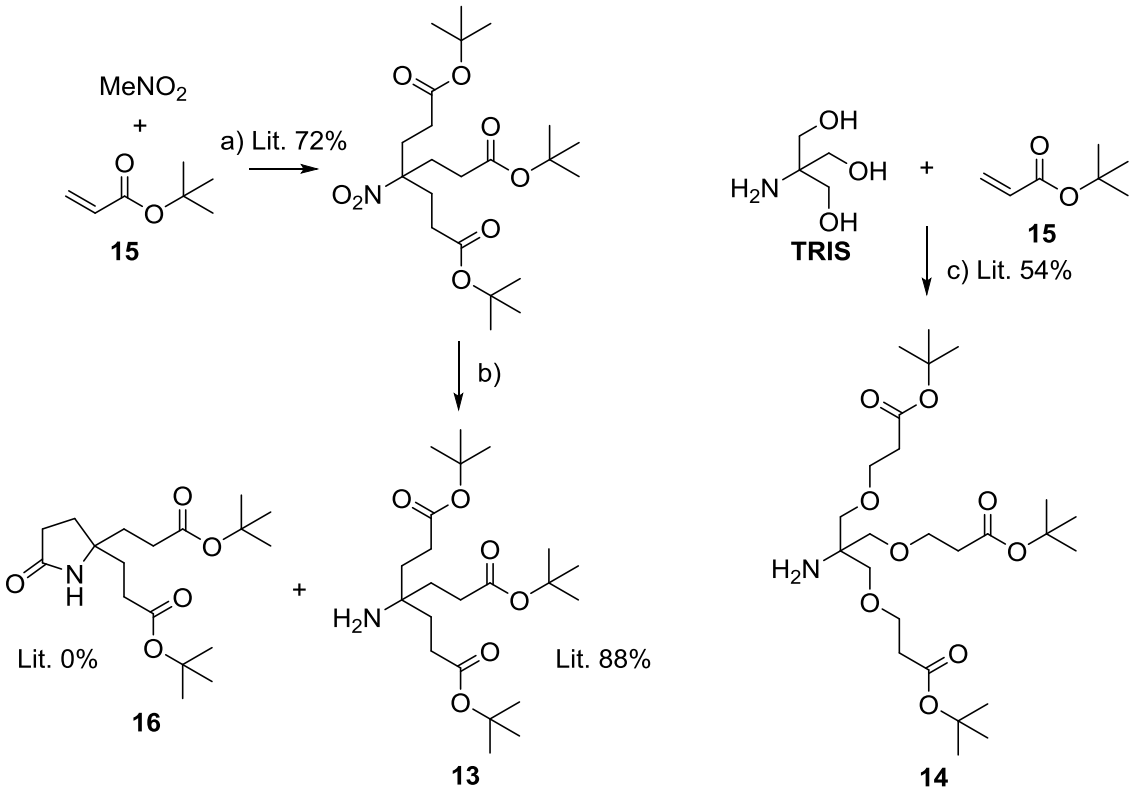

Scheme 2.01: Literature reagents and conditions: a) benzyltrimethylammonium hydroxide, MeOH, dimethoxyethane, 70 °C, 1 h; b) Raney Ni, EtOH, 50 psi H_2, 60 °C, 24 h; c) $NaOH_{(aq)}$, DMSO, 15 °C – RT, 24 h.

Our strategy was to isolate the targeted surfactants as their sodium salts in order to enhance their hydrophilicity and dispersion ability without the addition of further base. This was expected to be a more convenient method than the preparation of dispersions in basic or buffered solutions,[73,132] as the use of deionised water as a solvent would mean the only species present in solution would be the carboxylate surfactant and its counter-ions. The effects of other species used to form a buffer solution or the use of excess base to control pH will not need to be considered. This approach will also facilitate comparisons with commercial anionic surfactants such as **SDS** and **SC** which are also sodium salts. Investigation of the effect of electrolytes should also be possible by using salt solutions in place of deionised water, with a view to determining whether the surfactants and dispersions are sensitive to ions.

2.2: Iterative Addition of Ethers

The synthesis of the amide linker surfactant series against which the targeted ether linker series would be compared was initially based on the iterative addition of 6-aminohexanoic acid, **17**, to **PBA** (using acids activated as *N*-hydroxysuccinimide esters), followed by attachment of a head group precursor such as dendron **14** (Scheme 2.02). This was subsequently reversed, instead building iteratively from the head group using benzyl carbamate protected **17**. Inspired by these approaches, our initial strategy for the synthesis of ether linker surfactants was to develop a similar, iterative route.

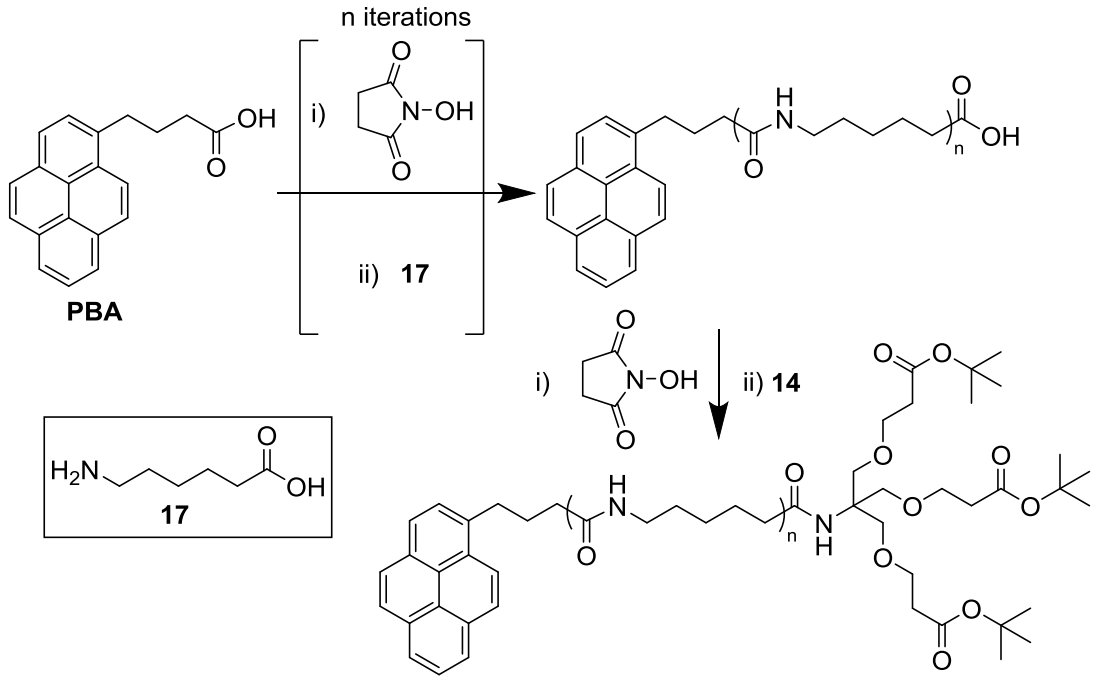

Scheme 2.02: The first route developed for the synthesis of amide linker surfactants.

As the target surfactants were based on polyether linkers with a terminal carboxylic acid it was desirable to incorporate the acid moiety during the synthesis of the linker. Reduction of this terminal acid to an alcohol could then allow another linker repeat unit to be added *via* a further ether synthesis, or at any point the acid could be converted to its salt or reacted with dendron **14** to give a G1 surfactant precursor. Two routes which exploit the Williamson ether synthesis were proposed to achieve the first iteration; these are shown as retrosyntheses in Figure 2.03. Where a hydroxy-acid is required, the derived lactone is an equivalent reagent (and in some cases exists preferentially).

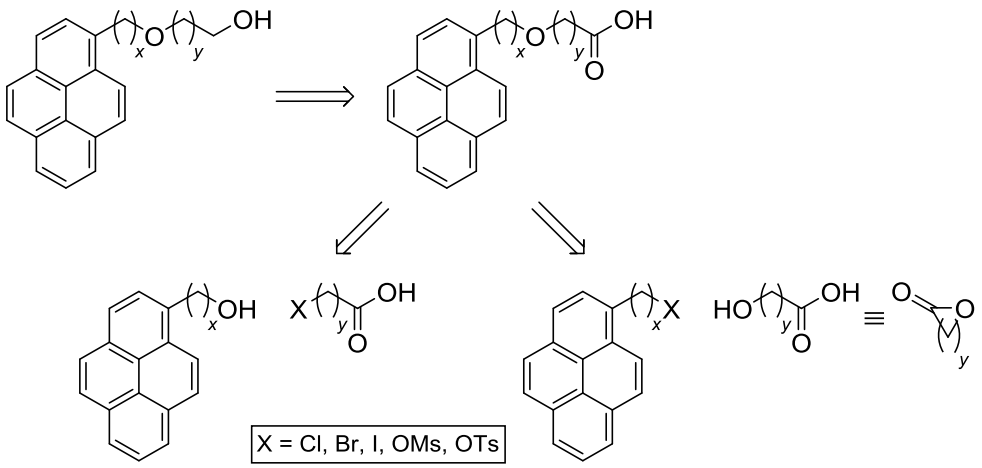

Figure 2.03: Retrosynthetic approaches to possible first iterations of ether linker addition.

Our first route used a halogenated pyrene derivative and a lactone, based on an analogous reaction between benzyl bromide, **BnBr**, and γ-butyrolactone, **18**, which affords 4-benzyloxybutyric acid, **19**.[133] We planned to replace **BnBr** with 1-bromomethyl pyrene, **PyrMBr**. **PyrMBr** was first prepared from **PyrMOH** using the method reported by Zhang *et al.* which gave a yield of 71% (literature yield 73%) (Scheme 2.03).[134] Subsequently, an improved procedure based on that reported by Ocak *et al.* afforded **PyrMBr** in 94% yield (Scheme 2.03).[135] We observed that **PyrMBr** partially decomposed when stored for longer than 1-2 weeks, even if kept in darkness and refrigerated; this is not reported in the literature. We could not identify the decomposition product(s) as they were insoluble.

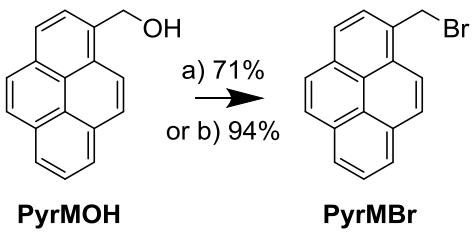

Scheme 2.03: Reagents and conditions: a) PBr_3, DCM, RT, 3 h; b) PBr_3, toluene, 110 °C, 19 h.

The reported reaction between **BnBr** and **18** uses an excess of the bromide. This was undesirable if **PyrBBr** was to be used due to its observed decomposition, which was expected to hinder recovery of unreacted material. **PyrBBr** is much more costly than **BnBr** and its use in excess was not viable. Therefore tests were conducted using **BnBr** and **18** to see if the stoichiometry of the reaction could be altered whilst still attaining an acceptable yield of **19**. Disappointingly scaling down the reported reaction resulted in a crude yield of only 16% (c.f. reported 92%[133]), and when **18** was used in excess no product was isolated (Scheme 2.04 and Table 2.01). Based on these results it was decided to investigate an alternative route rather than attempt to optimise this low-yielding reaction for use with **PyrBBr**.

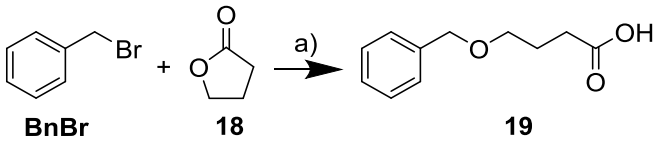

Scheme 2.04: Reagents and conditions: a) KOH, toluene, 110 °C, 72 h. See Table 2.01 for yields.

Table 2.01: Conditions used for the synthesis of acid **19**

Conditions	Scale (moles of BnBr / mmol)	Equivalents of BnBr	Equivalents of 18	Equivalents of KOH	% Yield of 19
Literature[133]	700	1	0.25	1.06	92
Excess BnBr	2.9	1	0.25	1.07	16 (crude)
Excess 18	2.9	1	2	1.07	0

6-Bromohexanoic acid, **20** was selected to trial the halo-acid based ether synthesis route in Figure 2.03 as, if successful, it would afford a series of surfactants with ether linkers of directly comparable lengths to the amide linker species (based on **17**), facilitating comparison of the effects of the two functional groups. Three sets of reaction conditions were applied to the attempted ether synthesis between **PyrMOH** and **20**, but none afforded the desired product, pyrene-acid **21** (Scheme 2.05). Using sodium hydroxide in DMF resulted in isolation of only the starting materials, suggesting a stronger base was required to bring about the reaction. The use of LDA in THF also returned only the starting materials whereas using NaH in THF resulted in the unexpected isolation of 1-pyrenecarboxylic acid, **22**, in 39% yield. The occurrence of this oxidation reaction in the presence of hydride is counterintuitive, but not without precedent. Indeed such reactions have become of interest in recent years as green, transition metal-free alternatives to conventional oxidations. A communication published in 2009 regarding oxidation of benzylic secondary alcohols to ketones by NaH[136] was subsequently withdrawn after attracting considerable attention (summarised in a *Nature Chemistry* editorial[137]) which made it clear that the observed reactions were most likely caused by the presence of an oxidising contaminant (such as dissolved O_2) in addition to NaH.

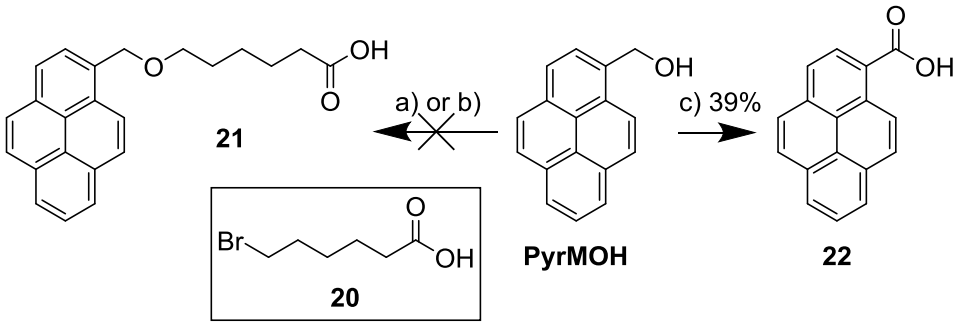

Scheme 2.05: Reagents and conditions: a) i. NaOH, DMF, RT, 2h, ii. **20,** 110 °C, 18 h; b) i. LDA, THF, -78 °C, 2 h, **20**, -78 °C – RT, 90 min; c) i. NaH, THF, RT, 2h, ii. **20**, 40 °C, 24 h.

Work published subsequently by Zhou *et al.* showed that sodium metal could also bring about oxidation of benzylic secondary alcohols to ketones, but only in the presence of air (or transition metal catalysts).[138] They report that the conditions afford only trace quantities of aldehyde in the case of primary alcohols and do not discuss any carboxylic acid formation as observed in our work. No mechanism is proposed for the oxidation, although the requirement for air to be present suggests oxygen is involved in some way.

Joo *et al.* reported a similar oxidation of benzoins to benzils in 2010, acknowledging the importance of oxygen to the process.[139] Subsequent publications by the same group discuss the further oxidation of these benzils to benzoic acids if the reaction time is increased,[140] and the application of similar conditions to the oxidation of cyclic 1,2-diketones to dicarboxylic acids.[141] Hydroperoxide formed from O_2 appears to be the oxidising agent. Both works illustrate its key role; in the former the equivalent oxidation of benzils is shown to occur upon direct treatment with hydroperoxide, and both show that ketone oxidation with NaH/O_2 will proceed only in the presence of an alcohol from which hydroperoxide can be generated. The proposed mechanism (Scheme 2.06) for oxidation of benzoins (general structure **23**) to benzils (general structure **24**) involves formation of the sodium alkoxide of **23** (with loss of H_2) followed by abstraction of its α-hydrogen as hydride to form a hydroperoxide anion and benzil **24** (which can be isolated[139]). The further oxidation of **24** to benzoic acids **25** and **26** is hypothesised to occur *via* attack of a benzil carbonyl by hydroperoxide to give intermediate **27** which can form an anhydride through loss of hydroxide. Nucleophilic attack on the anhydride by a hydroxide ion leads to the formation of a carboxylate anion and a carboxylic acid, the latter of which is readily deprotonated due to the basic conditions of the reaction. Acidic work up then affords **25** and **26**.

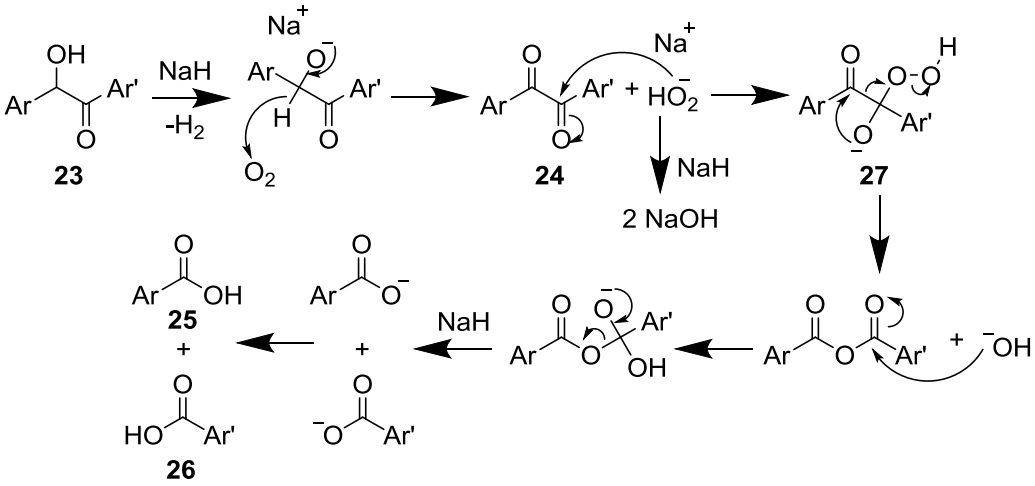

Scheme 2.06: Mechanism proposed by Kang *et al.* for the oxidation of benzoins in the presence of sodium hydride and oxygen.[140]

Wang and Wang, two co-authors of the withdrawn 2009 paper discussed above, have subsequently published a more detailed study of these "aerobic oxidations," where they also refer to previous reports of similar chemistry.[142] One of these is the 1965 work of Lewis, which shows that *para*-nitrobenzaldehyde and *para*-nitrobenzyl alcohol are oxidised to *para*-nitrobenzoic acid by NaH in the presence of air, and claims that one role of NaH in the reaction is the "conversion of oxygen to oxygenated nucleophiles," an idea not dissimilar to the mechanisms put forward some forty years later.[143] Wang and Wang discuss two possible mechanisms for the oxidation of benzylic secondary alcohols (general structure **28**) to ketones (general structure **29**) by NaH/O_2. The first of these involves formation of the alkoxide of **28** and subsequent abstraction of the α-hydrogen as hydride by O_2, forming a hydroperoxide ion as proposed by Kang *et al.*[140] and shown in Scheme 2.06 above. In the second possible mechanism (Scheme 2.07) the α-hydrogen is removed *via* a radical pathway followed by recombination of the resulting hydroperoxyl and benzylic radicals. Elimination of NaOOH then affords **29**. By using secondary alcohols with cyclopropyl substituents Wang and Wang were able to provide evidence favouring the radical pathway: a variety of additional products were isolated which can be accounted for by this mechanism but not the hydride abstraction mechanism.[142] They also extended the methodology to an interesting oxidative amidation reaction between aryl aldehydes and secondary amines.[142]

The radical mechanism is further supported by the work of Lei and co-workers who investigated the oxidation of primary alcohols to carboxylic acids using NaOH and either O_2 or air.[144] In this case hydrogen abstraction must occur twice, once from the alcohol and again from an aldehyde intermediate. If the radical scavenger BHT

(2,6-di-*tert*-butyl-4-methylphenol) is added to the reaction the expected oxidation product is not isolated, strongly indicating a radical mechanism.

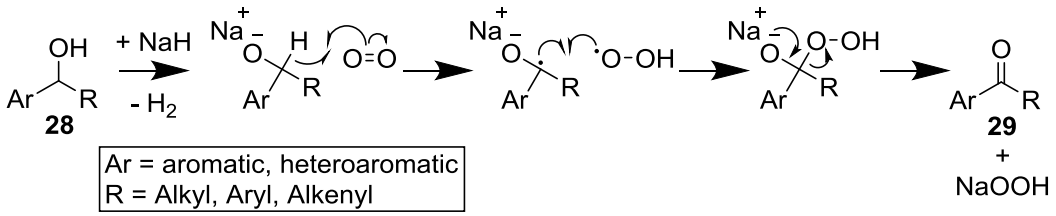

Scheme 2.07: Mechanism proposed by Wang and Wang for the oxidation of benzylic secondary alcohols in the presence of sodium hydride and oxygen.[142]

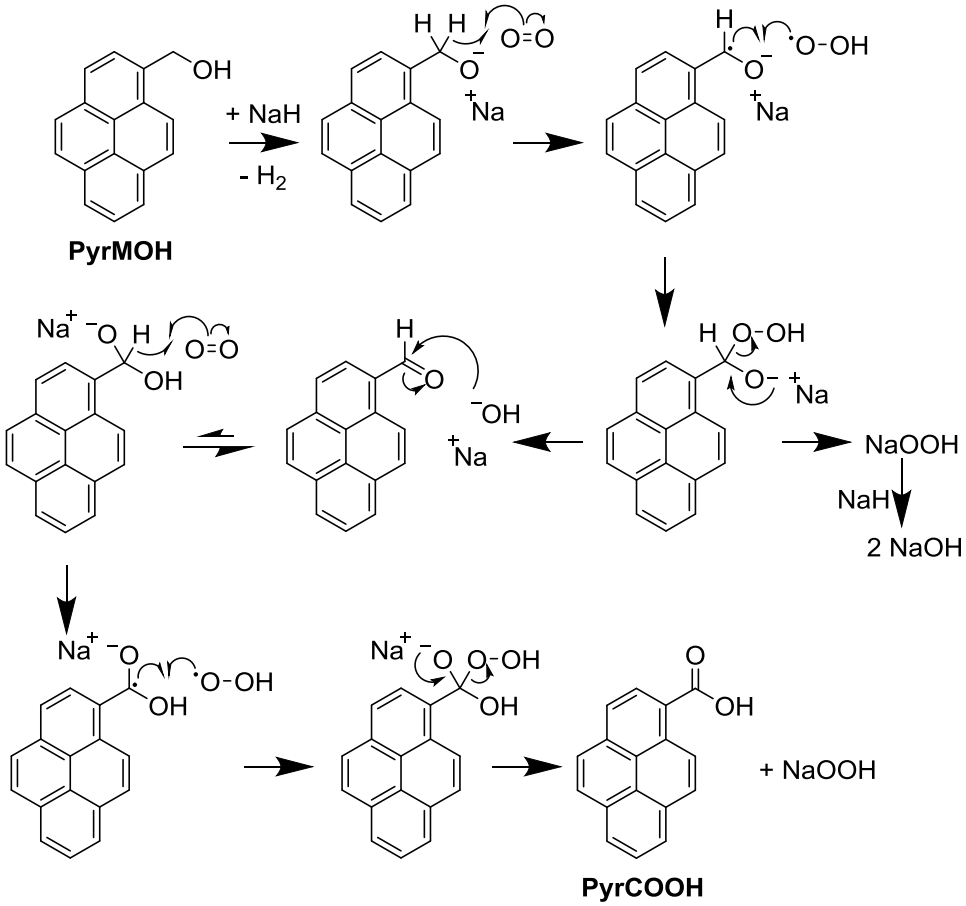

Scheme 2.08: A possible mechanistic explanation of the observed oxidation of **PyrMOH** (Scheme 2.05) based on proposed mechanisms in the literature.[140,142,144]

These reports allow the observed oxidation of **PyrMOH** to **22** in the presence of NaH to be rationalised. Despite the use of anhydrous solvents and an argon atmosphere, it is evident that some oxygen was present in the reaction, most likely dissolved in the solvent. The isolated yield of 39% is consistent with the works discussed above, where lower yields are observed when efforts are made to exclude oxygen.[139,142] A possible mechanism for the oxidation is shown in Scheme 2.08. This is based on a combination of the mechanisms of

Wang and Wang[142] (radical pathway, oxidation of alcohol to aldehyde), Kang *et al.*[140] (formation of NaOH) and Lei and co-workers[144] (radical pathway, oxidation of aldehyde to acid). The presence of NaOH could also be due to partial decomposition of stored NaH. **PyrMOH** was stirred with NaH for 2 h prior to the addition of **20**; the oxidation likely occurred during this period. This would imply that the **PyrMOH** had been at least partially consumed before adding **20** and that the various side products of the oxidation would have been present at this point, presumably preventing the desired ether formation from occurring.

The formation of benzylic ethers by Williamson ether synthesis is much more commonly accomplished using a benzylic halide rather than a benzylic alcohol, suggesting that **PyrMBr** would be a more suitable reagent. Alternatively, a different approach to ether synthesis using **PyrMOH** could be adopted. α,β-Unsaturated carbonyls can form ethers in 1,4-nucleophilic addition reactions, exemplified in the synthesis of dendron **14** (Scheme 2.01 above). The reaction of **PyrMOH** with NaOH and **15** produced ester **30** in high yield (Scheme 2.09). It was hoped that an iterative linker extension based on the reduction of **30** to alcohol **31** followed by further 1,4-nucleophilic addition reactions and reductions would afford esters of general structure **32**. Deprotection of **30** and esters of structure **32** would afford a series of acids of general structure **33** which could be used to form G0 salts or coupled to dendron **14**. Reduction of **30** to **31** was facile and high yielding, but deprotection of the *tert*-butyl ester to afford acid **34** could not be achieved (Scheme 2.09).

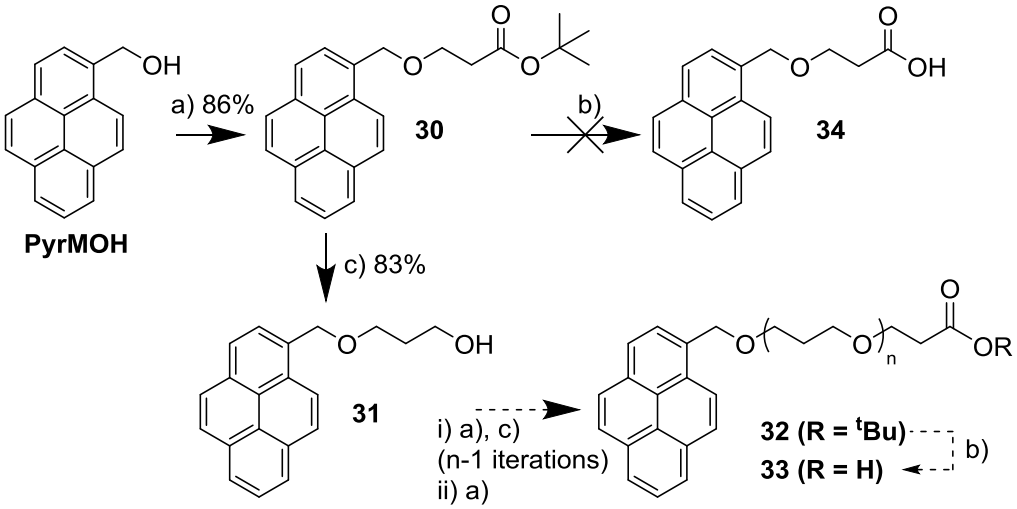

Scheme 2.09: Reagents and conditions: a) $NaOH_{(aq)}$, **15**, DMSO, 15 °C – RT, 20 h; b) See Table 2.02; c) $LiAlH_4$, THF, 0 °C – RT, 22 h.

It was expected that treatment of ester **30** with formic acid would accomplish deprotection quantitatively as in the synthesis of higher generation dendrons.[123] This method had also been successfully applied in the synthesis of the amide linker surfactants. However, analysis of the crude product by ^{1}H NMR spectroscopy showed a complex mixture which could not be purified. Addition of DCM to the reaction in an attempt to ensure **30** was fully dissolved did not afford any characterisable product, nor did using an acid-base workup to separate any carboxylic acid products. Similar results were obtained using alternative, mild conditions from the literature.[145] The final set of conditions we investigated[146] afforded a solid following neutralisation with NaOH. This material was insoluble in a wide range of solvents, including hexane, toluene, DCM, ethyl acetate, acetone, DMSO, acetic acid and water, and so could not be characterised. To check whether this insoluble material was a carboxylate salt, the reaction was repeated but not treated with NaOH. What appeared to be the same insoluble solid was isolated. Table 2.02 summarises the attempted deprotections of **30**. We concluded at this point that the insoluble material obtained was **34**, and that a combination of π-stacking and intramolecular hydrogen bonding interactions led to its insolubility. Subsequent results (discussed in Section 2.3) indicated that in fact the benzylic ether of **30** was likely cleaved under the deprotection conditions.

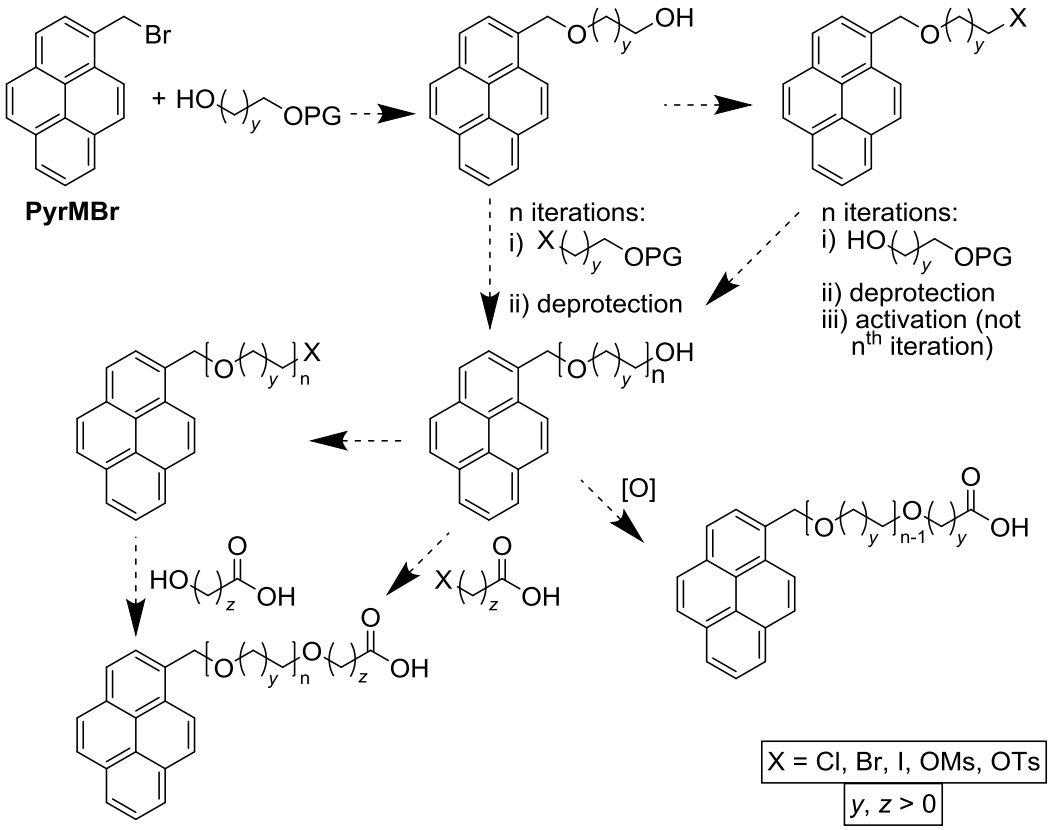

Scheme 2.10: Variations on a proposed iterative route to polyether surfactant precursors using monoprotected diols and **PyrMBr**.

Table 2.02: Attempted deprotections of ester **30**.

Conditions	Notes	Product
Formic acid, 20 °C, 24 h[123]	Followed literature procedure	Inseparable mixture of materials
Formic acid, DCM, 20 °C, 24 h[123]	DCM added to improve solubility	Inseparable mixture of materials
Formic acid, DCM, 20 °C, 24 h[123]	Acid-base workup attempted	Inseparable mixture of materials
SiO_2, toluene, 110 °C, 16 h[145]	Followed literature procedure	Inseparable mixture of materials
H_2SO_4, DCM, 0 °C, 5 h[146]	Followed literature procedure	Insoluble yellow solid
H_2SO_4, DCM, 0 °C, 5 h[146]	Did not treat with NaOH	Insoluble yellow solid

Our final iterative approach was a Williamson ether synthesis using **PyrMBr** as the halogenated reagent. This strategy was based on protected diols rather than alcohols functionalised with acids or esters. In this route a polyether linker could be constructed by iterative ether syntheses, deprotections and alcohol activations (e.g. as a sulphonate ester or by conversion to a halide), and the desired terminal acid moiety introduced by oxidation or ether synthesis. Possible approaches to this strategy are outlined in Scheme 2.10.

Our initial investigation of this route used a *tert*-butyldimethylsilyl (TBDMS) protecting group. A high-yielding monoprotection of 1,6-hexanediol, **35**, with this group had been previously reported,[147] and use of this diol would facilitate comparison with the amide linker surfactants based on **17** as in both cases each iteration would increase the linker chain length by 6 carbon atoms and a heteroatom. The reported monoprotection of **35** to give alcohol **36** uses stoichiometric amounts of **35**, NaH and TBDMS chloride **37**, which would usually be expected to afford a statistical mixture of **35**, **36** and *bis*-protected species **38** in a 1:2:1 ratio. Contrastingly, McDougal *et al.* report yields in excess of 90% for this and several other monosilylations.[147] They attribute this fortuitous result to the poor solubility of the alkoxide salt formed during the reaction. In THF, the rapid reaction between NaH and a diol such as **35** affords a precipitate believed to be the sodium salt of the monoalkoxide. A small amount of alkoxide is believed to remain in solution, and is free to react with **37** upon its addition to the solution. As the dissolved alkoxide is silylated, the precipitate is slowly dissolved to replace it. McDougal *et al.* propose that the rate of silylation of dissolved alkoxide is faster than that of proton transfer between alcohol and alkoxide groups, favouring the formation of monoprotected diols.[147] In our hands the high yield reported by McDougal *et al.* was not reproduced; two attempts following their published procedure afforded **36** in only 41-42% yield (Scheme 2.11), alongside a small quantity of **38** (19%) – close to the expected yields for a statistical reaction. **36** was then used in a Williamson ether synthesis reaction with **PyrMBr** to afford protected ether **39** in 55% yield. If this was representative of the yields for subsequent iterations it is unlikely that this route would prove viable; much higher yields would be necessary for each ether synthesis. Although it was expected that deprotection of

the TBDMS-protected alcohol would be facile using tetra-*n*-butylammonium fluoride (TBAF), further investigation of this route was deferred in favour of the methodology discussed in Sections 2.3 and 2.4, which no longer relies upon iterative synthesis.

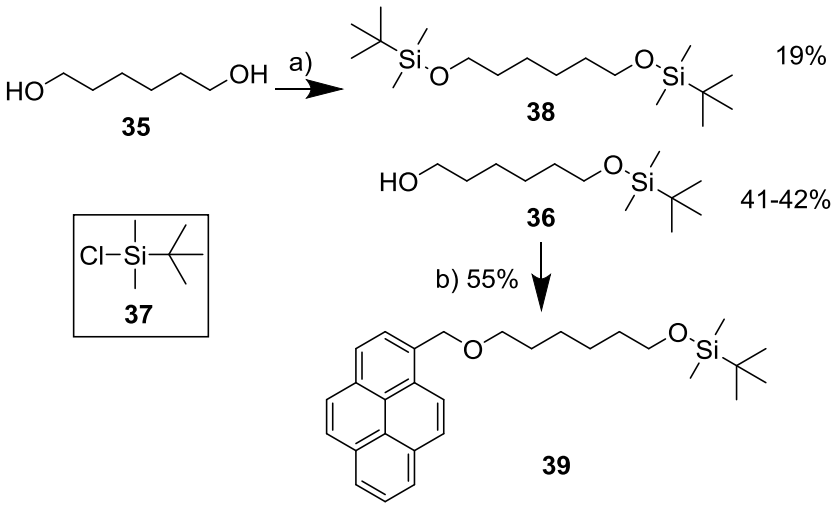

Scheme 2.11: Reagents and conditions: a) i. NaH, THF, RT, 1 h, ii. **37**, RT, 90 min; b) i. NaH, THF, 40 °C, 2 h, ii. PyrMBr, 40 °C, 16 h.

2.3: Use of OEG Linkers with Pyrenemethanol-Derived Anchors

This section will discuss the use of commercial polyether species as the linker group. This approach is advantageous as it should allow the synthesis of surfactants incorporating many ether moieties to be achieved in far fewer steps than with an iterative method. It does, however, introduce limitations on the polyether linker chosen, based on available materials.

Polyethylene glycol (PEG) is the hydrophilic component of commercial surfactants such as **Triton X-100** and **TWEEN 20** and is widely used to functionalise materials to improve biocompatibility and water solubility. The non-toxic nature of PEG means biochemical and pharmaceutical applications are particularly common; the term 'PEGylation' is widely used in these fields.[148] Other materials which have been functionalised with PEG include quantum dots,[149] other nanoparticles (e.g. iron oxide[150] and gold[151]) and CNTs.[152] Due to their hydrophilicity polyether linkers derived from PEG are excellent candidates for this work. The CNT and graphene dispersing ability of surfactants containing such linkers could be improved in comparison to species with less hydrophilic linkers as both the surfactants and materials functionalised with them should interact more favourably with water.

Short (2-8 repeat units) oligoethylene glycol (OEG) species are commercially available as well as some longer oligomers (e.g. 12 repeat units). We will refer to specific oligomers as OEGs or

PEGn (where n is the number of repeat units) and polydisperse material as PEG (further defined in terms of average molecular weight if necessary). Oligomer-pure material increases rapidly in price beyond PEG4, so the use of short OEGs or polydisperse PEG is more viable for any large scale applications. OEGs were selected for use as "pre-made" polyether linkers, removing the need to synthesise this unit iteratively. Specific oligomers were chosen in order to avoid polydispersity in intermediates and surfactants with the expectation that this would facilitate purification, characterisation, and evaluation of surfactant performance. Using a series of commercial OEGs should allow surfactants with a range of ether linker lengths to be investigated without using an iterative synthetic route.

Bouzide and Sauvé report the use of Ag_2O in monobenzylations[153] and monotosylations[154] of diols, and observe particular effectiveness for OEGs. KI can be used to catalyse these reactions. They rationalise the selectivity of such reactions in terms of intramolecular hydrogen bonding and coordination to Ag^+ or K^+ ions (Figure 2.04). They propose that the alcohol groups of a diol molecule can form a hydrogen bond such that the hydrogen not involved in this bond (H_A) becomes more acidic than that in the hydrogen bond (H_B) and therefore more labile. As H_A is more labile than H_B it reacts preferentially, favouring monosubstitution. The formation of the intramolecular hydrogen bond may be favoured if the two alcohol groups are also coordinated to a metal ion. In the case of OEGs, selectivity is further enhanced due to the chelation of additional ether oxygen atoms to the metal ion to form a crown ether-like motif which increases the likelihood of intramolecular hydrogen bonding. Bouzide and Sauvé comment that they have no material evidence for this mechanism[154] and although it fits their observations the explanation seems somewhat incomplete. For example, the presence of Ag^+ ions is not explained (Ag_2O should be insoluble in the solvent used) and K^+ ions are not present in all cases. For monotosylations the presence of excess Ag_2O allows otherwise unobserved cyclisations to occur,[154] suggesting that Ag_2O is consumed in some way during the reaction, possibly by reaction with HCl to form AgCl and water.

Based on the above method, Loiseau *et al.* used Ag_2O to selectively monosubstitute OEGs with benzyl (Bn) and tosyl (Ts) groups and also extended the protocol to *para*-methoxybenzyl (PMB) and trityl (Tr) protecting groups.[155] These syntheses are summarised in Scheme 2.12. More forcing conditions are required for the PMB and Tr protecting groups, particularly for the longer OEG, **PEG6**. Springer and co-workers report a lower yield for monobenzylation of **PEG6** than Loiseau *et al.* (53%[156] *vs.* 83%[155]), however, they do not specify the use of freshly

prepared Ag_2O as reported previously.[153,155] Svedhem *et al.* report similar conditions for monomesylation of OEGs,[157] although their study is less detailed and achieves lower selectivity (60:25% mono/*bis*-substitution[157]) than comparable monotosylations (e.g. 85:7% mono/*bis*-substitution[154]). Some reports of monomethylation using Ag_2O and methyl iodide have also been published[158,159] but the protocol does not seem to have been extended to longer alkyl chains. The reported 50% yield is not indicative of significant selectivity. Alternative monosubstitution methods rely on using an excess of OEG to favour monosubstitution over *bis*-substitution in a statistical reaction which can be wasteful and is less practical for longer, more expensive OEGs.[155] Such conditions have been reported for several substituents, including mesyl and silyl groups,[160] and benzyl groups.[156,161]

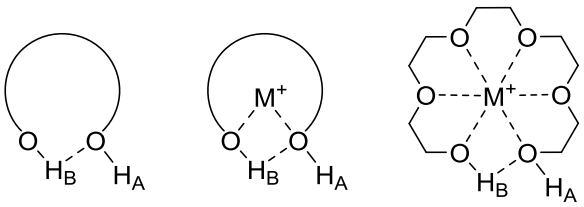

Figure 2.04: Bouzide and Sauvé explain Ag_2O mediated monosubstitutions of diols using the concept of intramolecular hydrogen bonding (left) which can be enhanced in the presence of ions (middle) and chelating moieties (right). M = Ag or K.

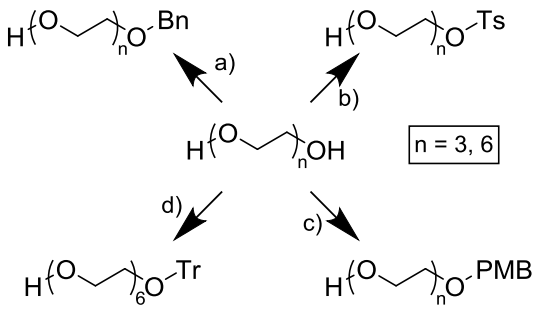

Scheme 2.12: Monosubstitutions of OEGs reported by Loiseau *et al.*[155] Reagents and conditions: a) **BnBr**, Ag_2O, KI, DCM, 2 h, RT; b) TsCl, Ag_2O, KI (n = 6), DCM, 0 °C, 15-20 min; c) PMBCl, Ag_2O, KI, toluene, RT (n = 3) or 110 °C (n = 6), 2 h (n=3) or 17 h (n=6); d) TrCl, Ag_2O, KI, DCM, 40 °C, 14 h.

The final approach investigated in Section 2.2 was the reaction of **PyrMBr** with monoprotected diols. As OEGs are diols, a similar approach could have been applied. However, as OEGs can be monosubstituted using **BnBr** we reasoned that its pyrene analogue, **PyrMBr**, could be used in its place. This would circumvent the use of protecting groups and allow the polyether linker to be attached directly to a pyrene anchor in a single synthetic step whilst leaving the second terminal alcohol free for further functionalisation. Pleasingly this convenient method was found to be extremely effective. Using **PyrMBr**, Ag_2O and catalytic KI, **PEG6** was converted to **PyrM-PEG6** in 80% yield (Scheme 2.13). **PEG6** was chosen as the

work of Loiseau *et al.* shows that more forcing conditions are sometimes needed for this oligomer in comparison to **PEG3**; therefore conditions which are effective for **PEG6** should also be applicable to shorter oligomers. The high yielding monosubstitution was accomplished using commercial Ag_2O which was stored in darkness and was comparable to the 83% yield reported by Loiseau *et al.* for the analogous reaction using **BnBr** and freshly-prepared Ag_2O.[155] It therefore appears that the preparation of fresh Ag_2O is unnecessary. The high yield of **PyrM-PEG6** suggests that the increased size of the pyrene ring system (relative to benzene) has little effect on the selectivity or efficacy of the reaction. This can be attributed to the planarity of the pyrene moiety and contrasts with the work of Loiseau *et al.* in which the analogous reaction using bulky trityl chloride, TrCl, had to be heated in order to afford reasonable quantities of product.[155] The reaction gave the same yield with either 1.0 or 1.05 equivalents of **PyrMBr**, which compares favourably with the 1.1 eq. of **BnBr** used by both Loiseau *et al.*[155] and Springer and co-workers[156] in monobenzylations.

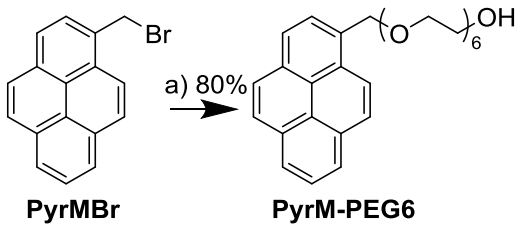

Scheme 2.13: Reagents and conditions: a) PEG6, Ag_2O, KI, DCM, RT, 3 h.

Zhang *et al.* reported the monosubstitution of 6660 g mol^{-1} PEG with a PyrM group in 62% yield without using Ag_2O.[134] When monosubsitution of PEG6 (only 282 g mol^{-1}) was attempted using these conditions the only isolated product was the *bis*-substituted species **PyrM-PEG6-PyrM** (Scheme 2.14). This confirmed the key role of Ag_2O in monosubstitution of the short OEGs which are of interest in our work. The conditions used by Zhang *et al.* are presumably only applicable to PEGs of much higher molecular weight.

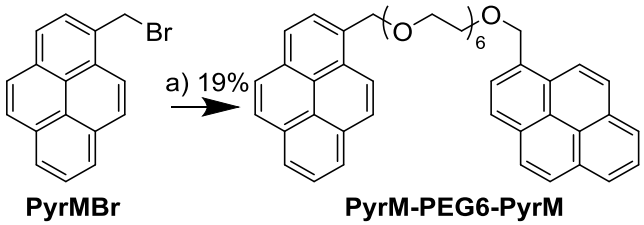

Scheme 2.14: Reagents and conditions: a) PEG6, NaH, THF, 40 °C, 2 h.

To approach our targeted structures a carboxylic acid moiety was required at the end of the OEG linker. Oxidation of **PyrM-PEG6** to **PyrM-PEG5-CH_2COOH** was attempted using Jones reagent (Scheme 2.15) based on conditions reported for the oxidation of a PEG4 derivative which was monosubstituted with an aliphatic group.[162] Disappointingly the crude product could not be purified and **PyrM-PEG5-CH_2COOH** was not isolated. The literature offers examples of oxidation of monobenzylated diols,[163] including OEGs,[164] but also suggests possible incompatibility of benzylic ethers with Jones reagent.[165]

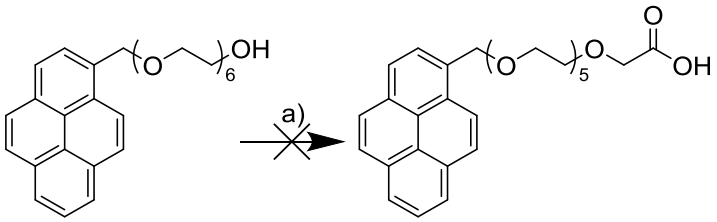

PyrM-PEG6 **PyrM-PEG5-CH_2COOH**

Scheme 2.15: Reagents and conditions: a) $CrO_3/H_2SO_{4(aq)}$, acetone, RT, 30 min.

As an alternative route we used **PyrM-PEG6** in Williamson ether synthesis reactions with both bromoacetic acid, **40**, and methyl bromoacetate, **41**. Initial reactions using acid **40**, based on literature conditions using other PEG derivatives,[166,167] were unsuccessful (Table 2.03); **PyrM-PEG6** was recovered in high yield. Using more forcing conditions (adapted from those used by Zhang *et al*.[134]) **PyrM-PEG6-CH_2COOH** was isolated in 79% yield (Scheme 2.16 and Table 2.03). Purification was achieved *via* acid-base workup which removed all impurities except unreacted **40**, which could then be removed by distillation. This method helpfully avoids time-consuming chromatographic separation of polar materials. A route using ester **41** was tested to check whether protecting the acid moiety would improve results. Adapted literature conditions,[168] which were less forcing than those used with **40**, afforded **PyrM-PEG6-CH_2COOMe** in only 54% yield following column chromatography. Subsequent saponification gave **PyrM-PEG6-CH_2COOH** in 48% overall yield from **PyrM-PEG6** (Scheme 2.16 and Table 2.03). An attempt to improve the yield by saponification of crude **PyrM-PEG6-CH_2COOMe** afforded less product which was also of lower purity. We therefore favoured the use of **40** to incorporate a terminal acid moiety in analogous compounds (Sections 2.4 and 4.2).

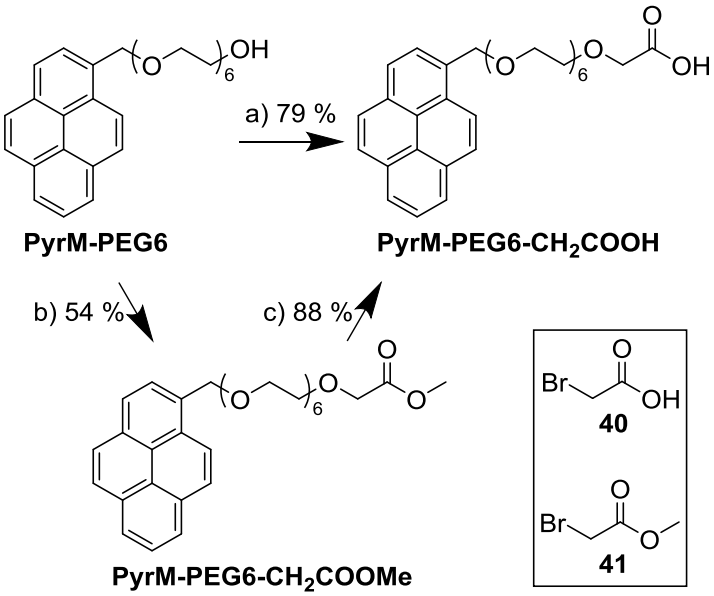

Scheme 2.16: Reagents and conditions: a) i. NaH, THF, 40 °C, 1 h, ii. **40**, 40 °C, 18 h; b) i. KO^{t}Bu, THF, 0 °C, 30 min, ii. **41**, 0 °C – RT, 19 h; c) i. LiOH, MeCN, RT, 10 min, ii. HCl, RT, 2 min.

Table 2.03: Summary of attempted syntheses of **PyrM-PEG6-CH$_2$COOH** from **PyrM-PEG6**.

Bromide	Base	Temperature	Reaction Time / h	Comments	Yield of PyrM-PEG6-CH$_2$COOH
40 (1.2 eq.)	NaH (6 eq.)[a]	20 °C	3	Based on literature conditions.[166] No reaction, recovered **PyrM-PEG6**	-
40 (1 eq.)[b]	NaH (2 eq.)	0 °C	24	Based on literature conditions.[167] No reaction, recovered **PyrM-PEG6**	-
40 (1.2 eq.)[b]	NaH (13 eq.)	40 °C	18	Adapted from literature conditions.[134] Initially contaminated with excess **40**, removed *in vacuo*	79%
41 (1.2 eq.)[b]	KO^{t}Bu (2 eq.)	0 °C	19[c]	Based on literature conditions.[168] Purified by column chromatography before ester saponification	48% (2 steps)
41 (1.2 eq.)[b]	KO^{t}Bu (2 eq.)	0 °C	19[c]	Based on literature conditions.[168] Ester saponification performed on crude material gave impure acid which could not be purified by acid/base treatment	**Impure**. <46% (2 steps)

In all cases THF was used as the solvent. [a] Base was added to a stirred mixture of alcohol and bromide; [b] Bromide was added to a stirred mixture of alcohol and base; [c] for the ether synthesis step.

PyrM-PEG6-CH$_2$COOH is a precursor of surfactants from both target series. We first set about the synthesis of the G1 surfactant, which required the formation of an amide bond between **PyrM-PEG6-CH$_2$COOH** and dendron **14**. Using the method described in Section 2.1 it was possible to isolate **14** in 48% yield (Scheme 2.17), which compares reasonably with the 54% yield reported by Cardona and Gawley.[123]

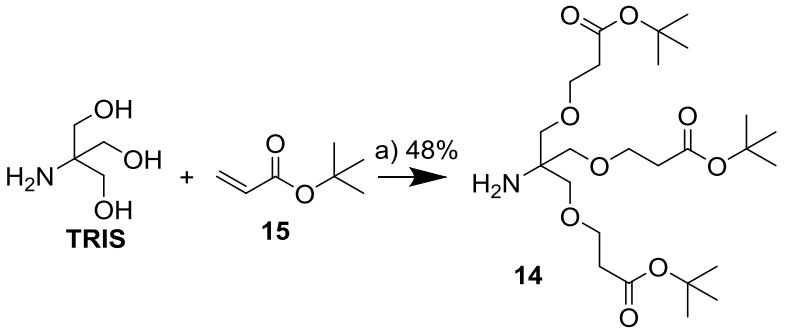

Scheme 2.17: Reagents and conditions: a) DMSO, $NaOH_{(aq)}$, 15 °C – RT, 48 h.

The coupling agent *N,N,N',N'*-tetramethyl-*O*-(benzotriazol-1-yl)uronium tetrafluoroborate (**TBTU**) was used to form an amide bond between **PyrM-PEG6-CH$_2$COOH** and **14** (Scheme 2.18). Difficulty separating unreacted **14** from amide product **PyrM-PEG6-CH$_2$COOG1(O^{t}Bu)$_3$** (both chromatographically and by acid extraction) meant the isolated yield was only 38% at ~90% purity based on integrals in the ^{1}H NMR spectrum. The nature of the impurity was supported by the ^{13}C NMR spectrum.

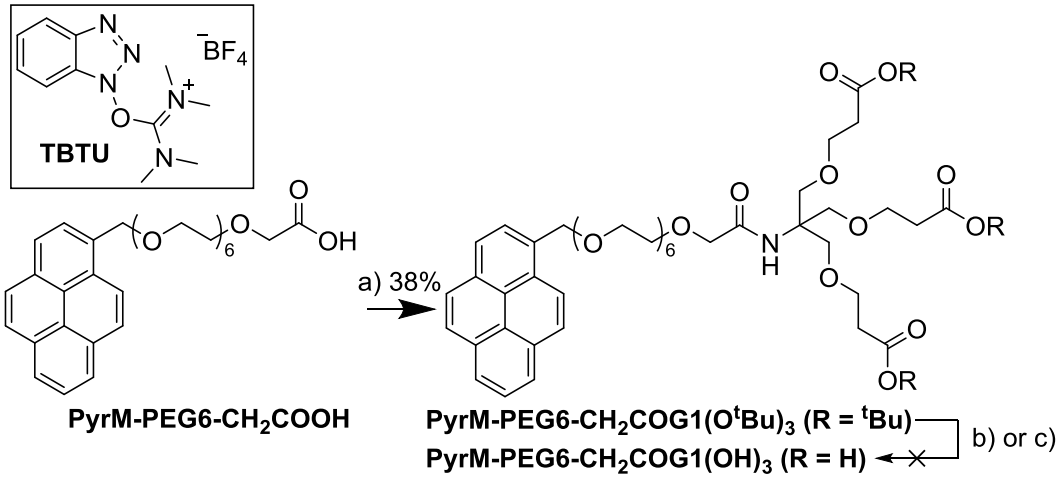

Scheme 2.18: Reagents and conditions: a) i. DIPEA, TBTU, DCM, 0 °C, 10 min, ii. **14**, 0 °C – RT, 70 h; b) formic acid, RT, 18 h; c) 4M HCl, 1,4-dioxane, RT, 18h.

Before attempting to optimise the synthesis and purification of **PyrM-PEG6-CH$_2$COOG1(O^{t}Bu)$_3$** the remaining steps needed to obtain a G1 surfactant were tested. As discussed in Section 2.2, formic acid was used to quantitatively deprotect *tert*-butyl esters in the synthesis of amide linker surfactants. When the same conditions were applied to **PyrM-PEG6-CH$_2$COOG1(O^{t}Bu)$_3$** the expected triacid product **PyrM-PEG6-CH$_2$COOG1(OH)$_3$** was not found (Scheme 2.18). Unlike the failed deprotections of **30**, in this case it was possible to investigate the isolated material using ^{1}H NMR spectroscopy. This indicated that in addition to the desired ester deprotection the PyrM ether bond had also been cleaved –

crude material isolated from the small scale reaction appeared to be triacid **42** contaminated with minor aromatic impurities, formic acid and ethyl acetate (Figure 2.05). The ^{1}H NMR chemical shifts and integrals observed correspond well with the proposed product. Treatment of **PyrM-PEG6-CH$_2$COOG1(O^{t}Bu)$_3$** with 4 M HCl in 1,4-dioxane gave further support for PyrM ether cleavage; in this case crude isolated product appeared by ^{1}H NMR spectroscopy to be a PyrM species with no OEG linker or head group attached (Figure 2.06). Although a peak can be seen at a similar shift to the benzylic environment of **PyrMOH** (~5.4 ppm), the aromatic region exhibits a considerably different splitting pattern. Investigation of both crude materials by mass spectrometry was inconclusive, making it difficult to confirm the exact nature of the apparent ether cleavage. These data suggest that a similar PyrM ether cleavage was also occurring during the attempted deprotections of **30**, although in this case the non-aromatic product was presumably either volatile and lost during solvent removal, or hydrophilic and removed during work-up.

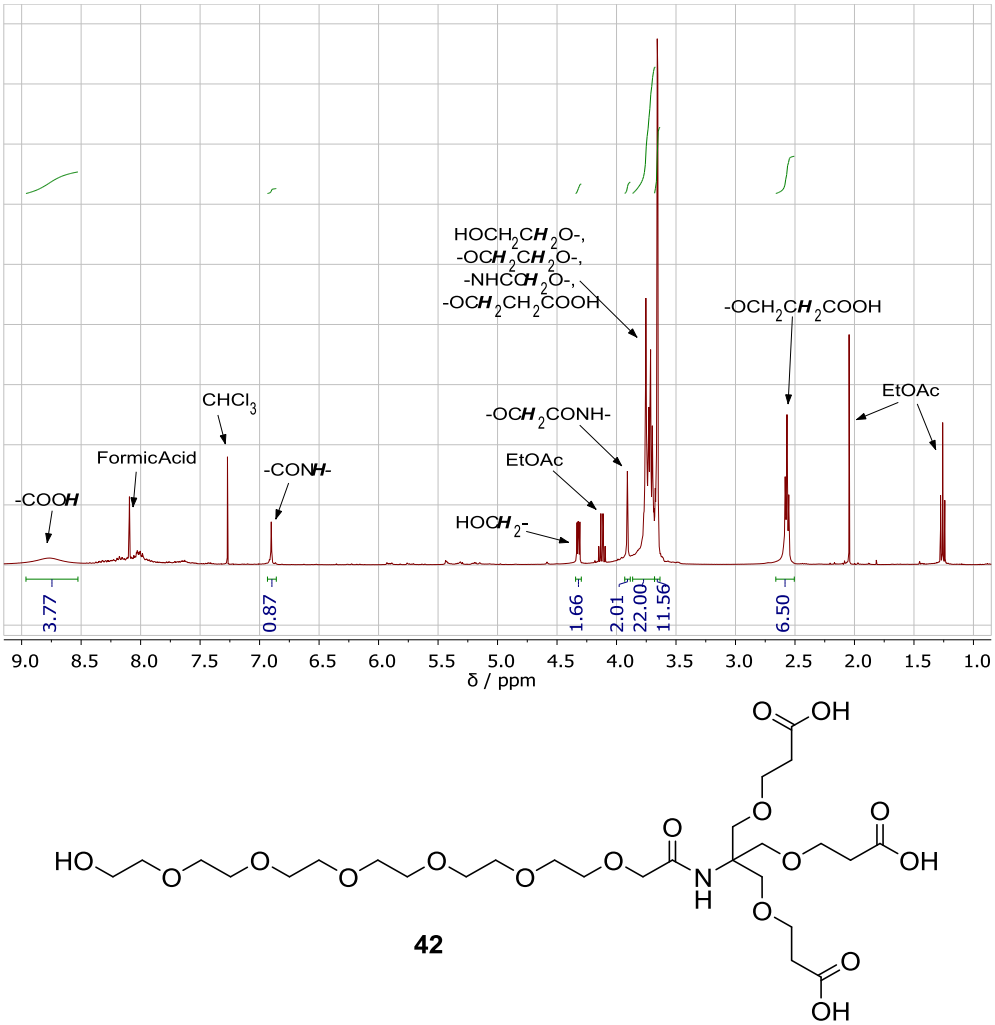

Figure 2.05: ^{1}H NMR spectrum (in $CDCl_3$) of crude material obtained from an attempted deprotection of **PyrM-PEG6-CH$_2$COG1(O^{t}Bu)$_3$** using formic acid, the major component of which appears to be triacid **42**.

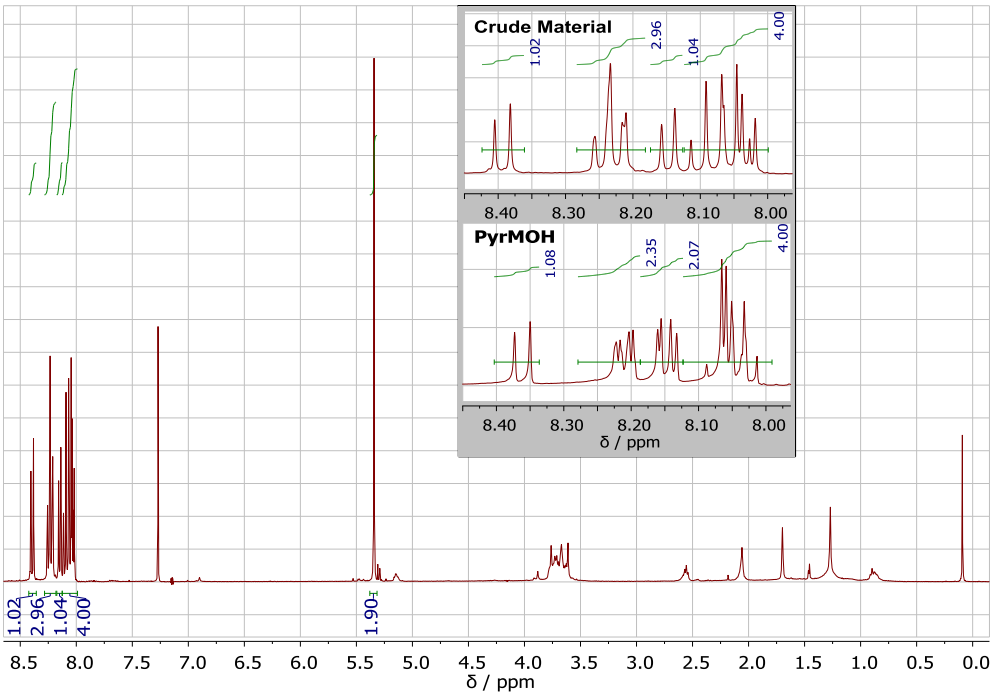

Figure 2.06: ^{1}H NMR spectrum (in $CDCl_3$) of crude material obtained from an attempted deprotection of **PyrM-PEG6-CH_2COOG1(O^{t}Bu)$_3$** using 1 M HCl in 1,4-dioxane. Inset: Aromatic region of this spectrum and that of commercial **PyrMOH**.

There is literature precedent that 2-naphthylmethyl (NAP) ethers can be preferentially cleaved in the presence of Bn ethers using catalytic hydrogenation.[169] This is in part attributed to the increased electron density associated with the larger naphthalene π-system. Although more electron rich than Bn ethers, NAP ethers are more stable under acidic conditions than PMB ethers.[170] The latter are also electron rich – the impact of this upon the ease with which they can be cleaved makes them popular for orthogonal protections.[171] The larger aromatic system of pyrene appears to contain sufficient electron density to render PyrM ethers susceptible to acidic cleavage under relatively mild conditions.

It was clear that the use of PyrM ethers was incompatible with the use of *tert*-butyl esters. Some different methods of incorporating the G1 head group were therefore briefly examined. An attempted amide coupling between dendron **14** and acid **40** returned only starting materials. Had this reaction been successful it was hoped that deprotection of the triester product **43** would have been possible, followed by a Williamson ether synthesis to attach **PyrM-PEG6** and give **PyrM-PEG6-CH_2COOG1(OH)$_3$** (Scheme 2.19). Purification of materials produced using this route was a concern as it would involve highly polar triacids, and so further efforts were focussed elsewhere.

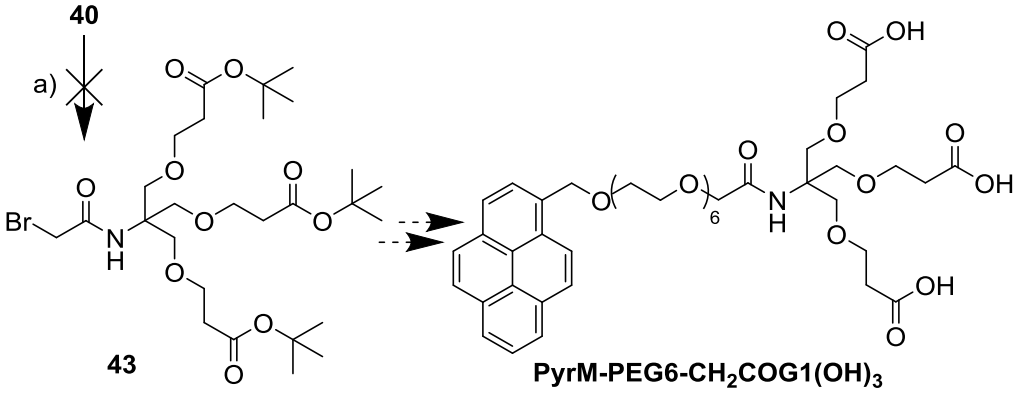

Scheme 2.19: Reagents and conditions: a) i. DIPEA, TBTU, DCM, 0 °C, 10 min, ii. **14**, 0 °C – RT, 70 h.

An alternative protecting group for the acids of the dendron was explored using a 2-(trimethylsilyl)ethyl ester protecting group, which can be readily deprotected using a fluoride source such as tetrabutylammonium fluoride (TBAF). It was hoped that these deprotection conditions would be compatible with PyrM ethers as they do not involve acid. A key intermediate in this route was 2-(trimethylsilyl)ethyl acrylate **44**. It was planned to use **44** in place of **15** in a reaction with **TRIS** to afford an alternative Newkome-type dendron, **45** (Scheme 2.20). Although the synthesis of **44** has been reported in the literature,[172] detailed reaction conditions are not provided and we were unable to isolate **44** from an attempted synthesis from acryloyl chloride, **46**, and 2-(trimethylsilyl)ethanol, **47**. We then decided to switch our attention to use of a different pyrene derivative, which would be compatible with *tert*-butyl esters, as the anchor unit.

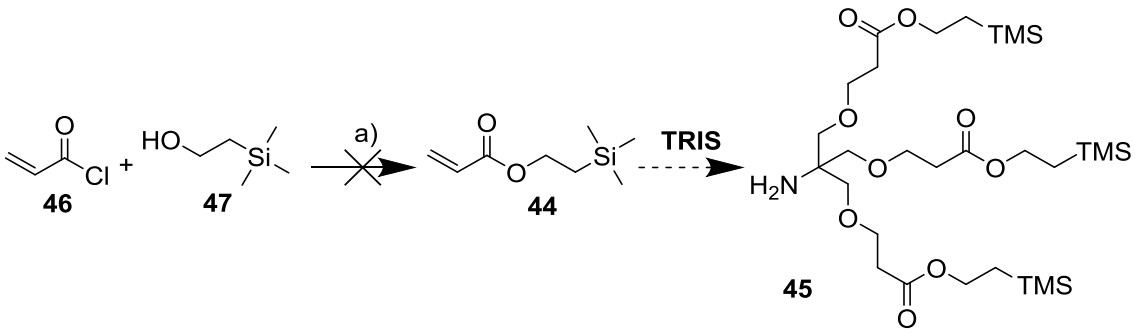

Scheme 2.20: Reagents and conditions: a) NEt_3, DCM, 0 °C, 2.5 h.

2.4: Use of OEG Linkers with Pyrenebutanol-Derived Anchors

In Sections 2.2 and 2.3 **PyrMOH** was the starting point of all the synthetic routes. However, **PyrBOH** now appeared more suitable as compounds derived from it do not contain a benzylic ether and should therefore be compatible with the conditions required for *tert*-butyl ester deprotection. **PyrBOH** was prepared by near-quantitative reduction of **PBA** using borane

THF complex (Scheme 2.21). To test the suitability of this change **15** was reacted with **PyrBOH** to afford **48** (Scheme 2.21). Unlike the PyrM analogue **30** (Scheme 2.09 above), treatment of **48** with formic acid achieved clean deprotection of the *tert*-butyl ester to afford acid **49** in high yield (Scheme 2.21). This confirmed that the benzylic nature of PyrM ethers was the problem in previous deprotection attempts (e.g. Schemes 2.09 and 2.18). We therefore developed a route based on a PyrB anchor which would allow dendron **14** to be used in the synthesis of G1 surfactants.

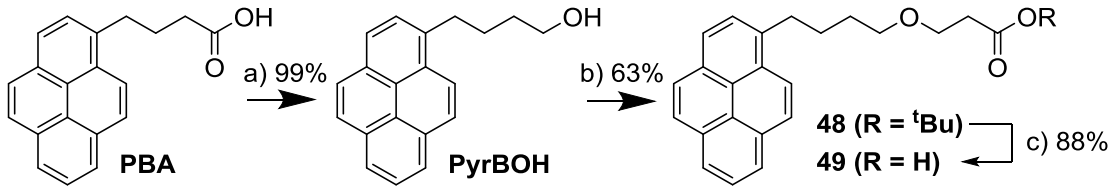

Scheme 2.21: Reagents and Conditions: a) BH_3·THF, THF, RT, 72 h; b) **15**, $NaOH_{(aq)}$, DMSO, 15 °C – RT, 20 h; c) formic acid, RT, 18 h.

A consequence of this change was that selective monosubstitution of OEGs with the new PyrB anchor group could not be achieved in a single step. Using the Appel reaction, **PyrBBr** was easily synthesised from **PyrBOH** in high yield (Scheme 2.22), comparable to that reported by Lampkins *et al*.[173] However, using **PyrBBr** in place of **PyrMBr** under the conditions used to monosubstitute **PEG6** in Section 2.3 returned only starting materials (Scheme 2.22). This was unsurprising as such monosubstitutions have only previously been reported using benzylic halides, sulphonyl chlorides and methyl iodide.[155,157-159]

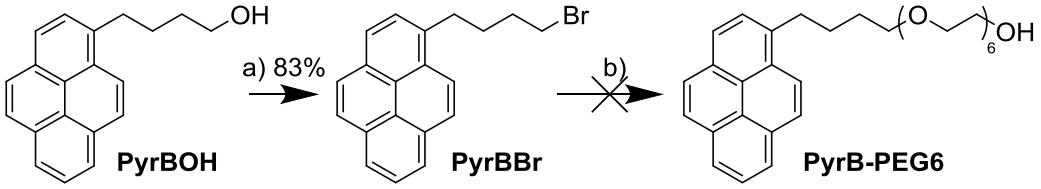

Scheme 2.22: Reagents and conditions: a) CBr_4, PPh_3, K_2CO_3, DCM, 0 °C – RT, 18 h; b) PEG6, Ag_2O, KI, DCM, RT, 3 h.

A longer synthetic route was therefore devised in which **PEG6** was selectively monoprotected prior to reaction with **PyrBBr**. The benzyl protecting group was chosen because Loiseau *et al.* reported that monobenzylation of OEGs was the highest-yielding of their monoprotections under Ag_2O-mediated conditions.[155] Accordingly, monobenzylation of **PEG6** was achieved in 83% yield (Scheme 2.23), matching that reported previously.[155]

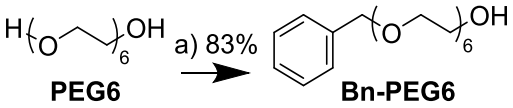

Scheme 2.23: Reagents and Conditions: **BnBr**, Ag_2O, KI, DCM, RT, 2 h.

Subsequent attempts at ether synthesis between **PyrBBr** and **Bn-PEG6** to give **PyrB-PEG6-Bn** were low yielding under various conditions (Table 2.04) due to a competing E2 elimination reaction which gave alkene **50** (Scheme 2.24). Separation of the mixtures obtained was challenging and not all starting material could be accounted for in some cases. The highest isolated yield of **PyrB-PEG6-Bn** was 27%, alongside a 56% yield of **50**. Changing the base from KO^{t}Bu to NaH reduced the amount of **50** obtained, but also lowered the yield of **PyrB-PEG6-Bn**. The strong bases needed to deprotonate the aliphatic alcohol of **Bn-PEG6** appear to favour the E2 elimination reaction over the S_N2 Williamson ether synthesis, which is by no means unreasonable and could perhaps have been anticipated.

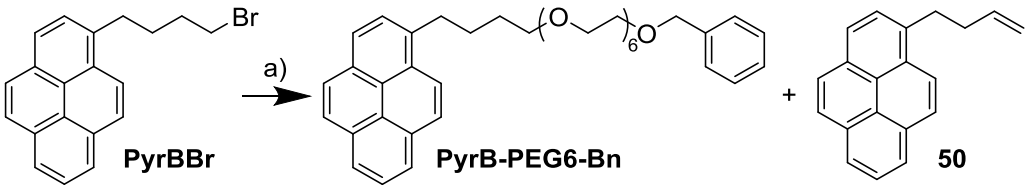

Scheme 2.24: Reagents and Conditions: a) **Bn-PEG6**, base – See Table 2.04 for full details.

Table 2.04: Synthesis of **PyrB-PEG6-Bn** from **PyrBBr** and **Bn-PEG6** under various conditions.

Conditions	Scale (mass of PyrBBr) / mg	Isolated % yield of PyrB-PEG6-Bn	Isolated % yield of 50	% PyrBBr Recovered
1 eq. **Bn-PEG6**, 2 eq. KO^{t}Bu in THF at 0 °C – RT, 21 h	200	27	56	n/a
1.1 eq. **Bn-PEG6**, 1.2 eq. NaH in THF at 40 °C, 19 h	300	15	42	39
1.1 eq. **Bn-PEG6**, 4.4 eq. NaH in DMF at 0 °C - RT, 22 h	282	18	27	n/a

In order to avoid any significant E2 elimination reaction, rather than reacting **PyrBBr** with a monoprotected OEG, the functionalities were reversed and **PyrBOH** was reacted with a monotosylated, monoprotected OEG. Such species have been previously used to synthesise long, monodisperse OEGs from shorter, readily available OEGs.[155,156,161] In some cases small quantities of an E2 elimination by-product can be isolated when such species are used in ether syntheses,[155] but formation of the ether product dominates. The tetrahydropyran (THP) protecting group was selected based on the following factors. i) Reaction of a tosylated, THP-protected OEG, **Ts-PEG3-THP**, with 1-pyrenepropanol has been reported in the

literature.[174] ii) Loiseau *et al.* report their highest yields (over two steps) of monotosylated, monoprotected derivatives of PEG3 and PEG6 by protecting tosylated OEGs with a THP group.[155] iii) Compared to e.g. the catalytic hydrogenation typically used to remove benzyl ethers, the conditions required for deprotection (10% HCl in THF) are simpler, require a shorter reaction time (c.f. reported 12 h[174] for THP *vs.* reported 17 h[155] or 4 days[156] for Bn) and conveniently can be used on crude material prior to purification of the deprotected alcohol.[174] A reaction between **PyrBOH** and a monotosylated OEG with no protecting group was not attempted in order to avoid possible side reactions such as polymerisation of the OEG through the free alcohol in the presence of excess base.

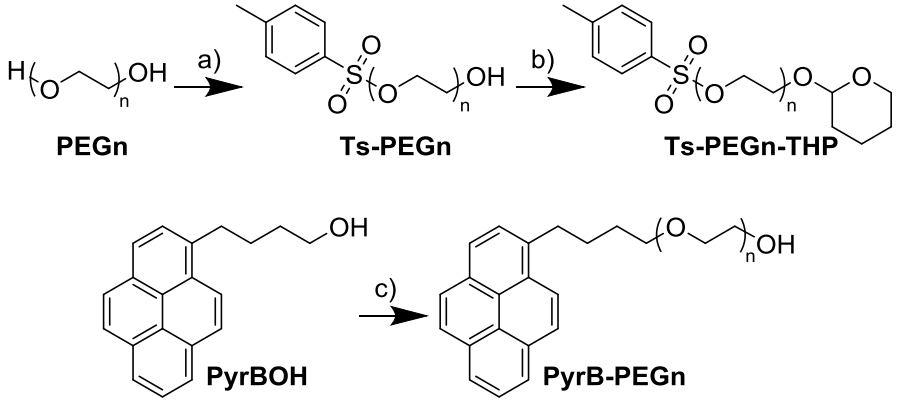

Scheme 2.25: Reagents and conditions: a) TsCl, Ag_2O, KI, DCM, 0 °C, 15-60 min; b) pyridinium *p*-toluenesulphonate, dihydropyran, DCM, 40 °C, 20 h; c) i. NaH, THF, 67 °C, 1-2 h, ii. **Ts-PEGn-THP**, 67 °C, 18 h, iii. HCl/THF, RT, 18 h. Yields are given in Table 2.05.

Table 2.05: Synthesis of OEGs monosubstituted with a PyrB moiety. Comparable literature values are shown in parentheses where appropriate.

OEG	% Yield of Monotosylation (a)	% Yield of THP Protection (b)	Overall % Yield for Ts-PEGn-THP from PEGn	% Yield of Ether Synthesis + Deprotection (c)
PEG2	53 (92[154])	89	47	54
PEG4	62 (85[154])	96	60	58
PEG6	87 (85[154,155])	91 (96[155])	79 (82[155])	66
PEG12	50	82	41	50

Using the new route a series of monosubstituted OEGs, **PyrB-PEGn** (n = 2, 4, 6, 12), was isolated as summarised in Scheme 2.25 and Table 2.05. Monotosylation of OEGs was accomplished using previously reported conditions.[154,155] Difficulties were encountered when synthesising **Ts-PEG2**; attempts are summarised in Table 2.06. With **PEG2**, using commercial Ag_2O and a 5 min reaction time as reported by Bouzide and Sauvé[154] only starting materials could be recovered. However, increasing the reaction time to 15 min resulted in a 37% yield, whereas switching to the use of freshly-prepared Ag_2O gave a disappointing yield of only 19% for both 5 and 15 min reaction times. An acceptable yield of 53% was achieved using a

reaction time of 30 min, but this is significantly lower than Bouzide and Sauvé's report of 92%.[154] This higher yielding reaction was also conducted on a larger scale than the previous attempts. We subsequently became aware that the analogous chloride was available commercially; using this reagent in place of **Ts-PEG2** would have been more convenient. The synthesis of **Ts-PEG4** was higher yielding, although again lower than that reported in the literature, whereas the isolated yield of **Ts-PEG6** was marginally higher than reported.[154,155] Although they do not provide any further details Loiseau *et al.* state that "Attempted monotosylation of PEG12 (…) led to a mixture of the starting material, as well as mono- and ditosylated products in roughly statistical ratios," which agrees with our 50% yield of **Ts-PEG12**. In contrast to the work on which this step was based, in our hands the highest-yielding monotosylation was that of PEG6, rather than the shorter oligomers.

Table 2.06: Synthesis of Ts-PEG2 under various conditions

Ag_2O Source	Scale: Volume of PEG2 / ml	Reaction Time / min	% Yield
Commercial[a]	1	5	0
Freshly-prepared	1	5	19
Commercial[a]	1	15	37
Freshly-prepared	1	15	19
Commercial[a]	3	30	53

[a] Stored in darkness to minimise any decomposition.

THP protection of the monotosylated OEGs was high yielding in all cases, although it was found that a longer reaction time than the reported 3 h[155] was required to achieve these yields (only 62% yield of **Ts-PEG4-THP** was obtained after a 3 h reaction). Ahmed and Tanaka claim that a side reaction can occur in this step due to the presence of *bis*-tosylate impurities,[161] and instead opted to use monotosylated, monobenzylated OEGs. Loiseau *et al.* do not discuss any by-product formation,[155] nor was any observed in our work, in which it was found that *bis*- and monotosylates were usually easily separated chromatographically prior to the THP protection step. The **PEG12** species was considerably more difficult to purify due to the high polarity of both the monotosylated product and *bis*-substituted by-product. The purification of **Ts-PEG12-THP** was somewhat easier than that of **Ts-PEG12** but still more challenging than that of the shorter OEG analogues.

Williamson ether synthesis between **Ts-PEGn-THP** species (n = 2, 4, 6, 12) and **PyrBOH** was conducted using the method of Fujimoto *et al.*[174] Accordingly, the crude product was subjected to THP deprotection conditions and the resulting material then purified to obtain the monosubstituted OEG, **PyrB-PEGn** (Scheme 2.25 and Table 2.05). Yields over the two step process ranged from 50-66% across the series (c.f. 70% for the analogous reaction[174]).

The route developed in Section 2.3 was then followed for the remainder of the synthesis. The isolated **PyrB-PEGn** species (n = 2, 4, 6, 12) were reacted with **40** to obtain the series of general structure **PyrB-PEGn-CH_2COOH** (Scheme 2.26 and Table 2.07). Similarly to the isolation of **PyrM-PEG6-CH_2COOH**, purification by acid-base workup and distillation was facile and avoided the need to purify these very polar materials using column chromatography. Yields for the shorter **PEG2** and **PEG4** species are >90%, whereas those for the **PEG6** and particularly **PEG12** species are somewhat lower. It may be that the oxygen atoms of OEG linkers interact with the sodium counter-ion of the alkoxide formed during the reaction, sterically shielding the alkoxide to an increasing extent as the OEG length increases (Figure 2.07).

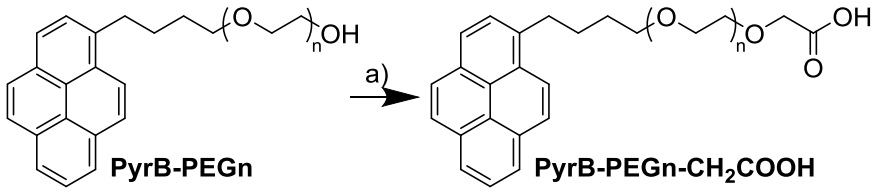

Scheme 2.26: Reagents and conditions: a) i. NaH, THF, 40 °C, 1 h, ii. **40**, 40 °C, 16 h. Yields are given in Table 2.07.

Table 2.07: Yields of Williamson ether syntheses from Scheme 2.26.

Product	% Yield
PyrB-PEG2-CH_2COOH	92
PyrB-PEG4-CH_2COOH	91
PyrB-PEG6-CH_2COOH	70
PyrB-PEG12-CH_2COOH	55

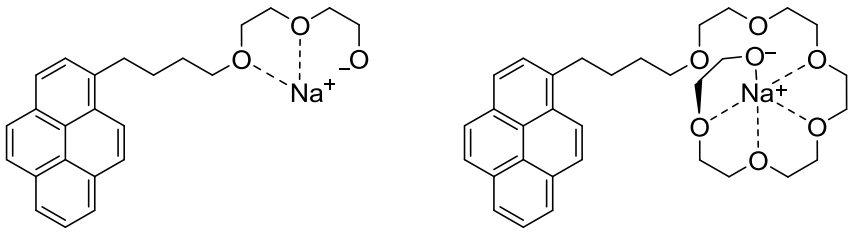

Figure 2.07: OEG oxygen atoms may interact with the sodium counter-ions of the alkoxides formed in the synthesis of acids from the series **PyrB-PEGn-CH_2COOH**. For short OEGs (e.g. PEG2, left) this is unlikely to have any significant effect, but for longer OEGS (e.g. PEG6, right) the chain may, partially shield the alkoxide (for clarity not all O-Na interactions are indicated).

Amide coupling with dendron **14** was successful for the **PEG2**, **PEG4** and **PEG6** species, affording the triester series **PyrB-PEGn-CH_2COG1(O^tBu)$_3$**. Isolated yields were from 54-78% (Scheme 2.27 and Table 2.08). The reaction was not attempted with **PyrB-PEG12-CH_2COOH**. Purification of these products was somewhat easier than for **PyrM-PEG6-CH_2COG1(O^tBu)$_3$**. It was important to ensure that the triesters were as pure as possible at this point to avoid

carrying impurities through the two subsequent steps which were expected to be quantitative. Deprotection of the *tert*-butyl ester products using formic acid was facile and quantitative, thereby justifying the change from a PyrM to PyrB anchor group (Scheme 2.27).

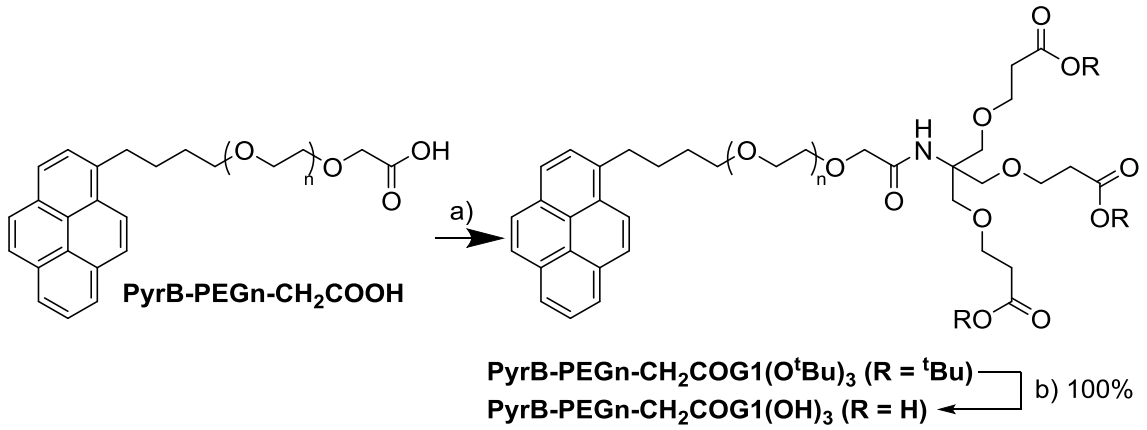

Scheme 2.27: Reagents and conditions: a) i. DIPEA, TBTU, DCM, 0 °C, 15 min, ii. **14**, 0 °C – RT, 22-72 h; b) formic acid, RT, 18 h.

Table 2.08: Yields of amide couplings from Scheme 2.27.

Product	% Yield
PyrB-PEG2-CH_2COG1(O^tBu)$_3$	54
PyrB-PEG4-CH_2CO(O^tBu)$_3$	54
PyrB-PEG6-CH_2CO(O^tBu)$_3$	78

Both the simple monocarboxylic acids and the G1 triacids were then converted quantitatively to their sodium salts to afford the first two series of target surfactants: **PyrB-PEGn-CH_2COONa** (n = 2, 4, 6, 12) and **PyrB-PEGn-CH_2COG1(ONa)$_3$** (n = 2, 4, 6) (Scheme 2.28). Lyophilisation of aqueous solutions gave material which was easier to handle in subsequent studies. These dry materials were hygroscopic and were therefore stored under vacuum.

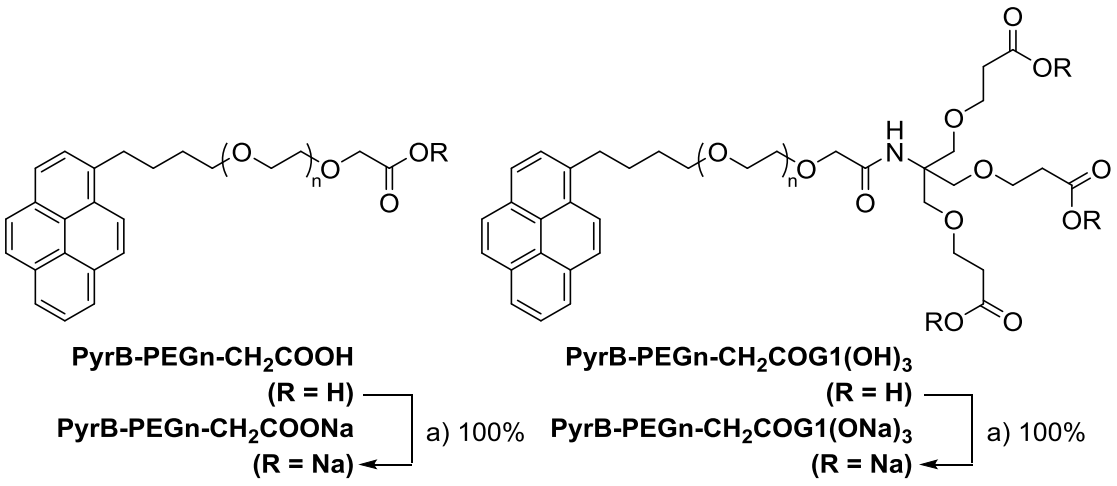

Scheme 2.28: Reagents and conditions: a) $NaOH_{(aq)}$, MeOH, RT, 30 min.

Interestingly, when the ^{1}H NMR spectra of the G0 and G1 surfactants were compared to those of the precursor acids (and esters for the G1 series) the peaks associated with protons in the OEG moiety usually showed a much greater range of shifts. In the case of the G1 materials, for the esters (in $CDCl_3$) and acids (in CD_3OD) the majority of these peaks overlap, exemplified in the proton spectra of **PyrB-PEG6-CH$_2$COG1(O^{t}Bu)$_3$** (Figure 2.08a) in which OEG protons lie within the multiplet of integral 30 between 3.56 and 3.68 ppm, and **PyrB-PEG6-CH$_2$COG1(OH)$_3$** (Figure 2.08b) in which the OEG protons lie within a broader multiplet which can be divided into 3 segments, one of integral 6 between 3.58 and 3.63 ppm, the second of integral 12 between 3.51 and 3.58 ppm, and the third of integral 8 between 3.44 and 3.51 ppm – the last of these appears to overlap an environment associated with the butyl moiety. In the case of the carboxylate surfactants (in D_2O) a greater range of distinct environments are resolved, as exemplified in the proton spectrum of **PyrB-PEG6-CH$_2$COG1(OH)$_3$** (Figure 2.08c). Here the OEG protons give a range of broad peaks of integral 2 between 3.0 and 3.5 ppm, and a larger peak of integral 12 between 3.05 and 3.24 ppm (with shoulders which could be further distinct environments overlaid by a larger peak). Additionally the peaks associated with the butyl moiety present in the ester and acid spectra at ~1.8 and ~1.9 ppm have been shifted upfield and now overlap in a broad singlet at 1.12 ppm. It may be that for the esters and acids the OEG chains coil and experience intramolecular interactions such that proton environments become similar, whereas for the salts interactions between the OEG chain and D_2O are more favourable, causing the chain to become extended and thereby differentiating the proton environments. Micelle formation could also play a role in the case of the salts, with different sections of the OEG chain lying closer to either the hydrophilic or hydrophobic environments of the micelle.

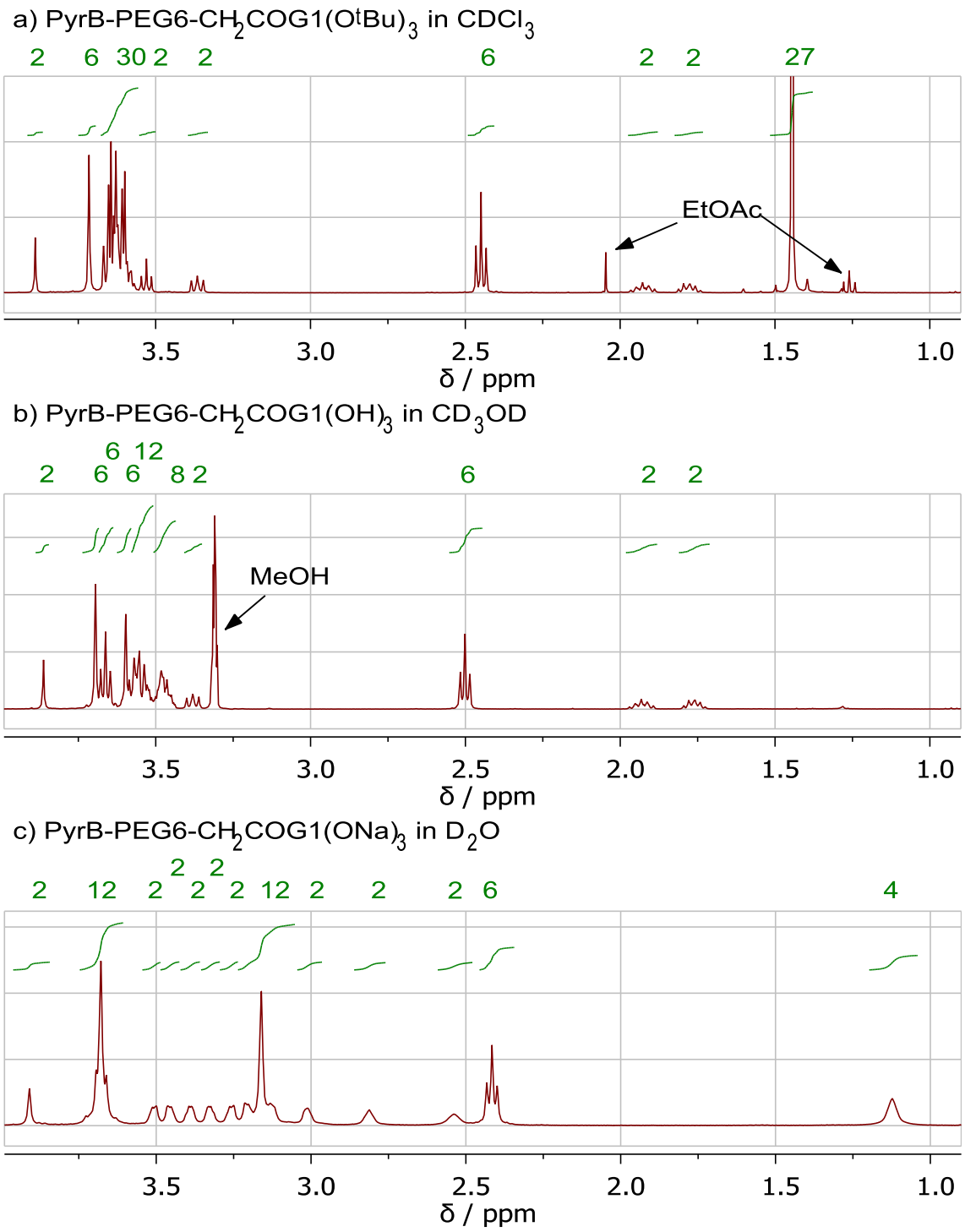

Figure 2.08: Aliphatic region (1.0 – 4.0 ppm) of the ^{1}H NMR spectra of a) **PyrB-PEG6-CH_2COOG1(O^{t}Bu)$_3$** in $CDCl_3$; b) **PyrB-PEG6-CH_2COOG1(OH)$_3$** in CD_3OD and c) **PyrB-PEG6-CH_2COOG1(ONa)$_3$** in D_2O. Any solvents are labelled where present.

2.5: Conclusions

This chapter has discussed the synthesis of two series of anionic surfactants with our ALH target architecture. Various strategies which were applied to the incorporation of a polyether linker have been discussed. Early work using iterative ether syntheses proved more challenging than anticipated and was discontinued in favour of the use of commercial OEGs. This allowed linkers of varying lengths to be attached directly to an anchor unit. Anchors derived from **PyrMOH** initially appeared attractive as it was possible to selectively monosubstitute OEGs with a PyrM anchor using Ag_2O and **PyrMBr**. However, PyrM ether derivatives proved to be unstable under the conditions required for *tert*-butyl ester deprotection, meaning that the desired G1 head group could not be used easily. To circumvent this problem a slightly longer route using **PyrBOH** as a starting material was required. This allowed the successful isolation of two series of surfactants: "G0" surfactants **PyrB-PEGn-CH_2COONa** (n = 2, 4, 6, 12) and "G1" surfactants **PyrB-PEGn-CH_2COG1(ONa)$_3$** (n = 2, 4, 6), shown in Scheme 2.28.

Chapter 3: Dispersion of MWNTs using Anionic Surfactants

This chapter discusses the use of the ether linker surfactants synthesised in Chapter 2 to prepare dispersions of MWNTs in deionised water and salt solutions. The ability of these surfactants to disperse MWNTs will be compared to commonly used commercial surfactants, analogous surfactants with no linker group, and related surfactants with linkers based on amides. Trends in MWNT dispersing ability, including the effect of salts, will be analysed in terms of surfactant structure. The effect of pH change and temperature on dispersion stability is also investigated.

3.1: Methodology

The ability of the novel ionic surfactants from Chapter 2 to disperse CNTs was tested using MWNTs*. To ensure data were representative the same batch of MWNTs was used throughout our study. Dispersion experiments were based on the method of Ulijn and co-workers[132] for the dispersion of both SWNTs and MWNTs. We cooled the sample in an ice bath and used a lower amplitude of 20% during tip sonication as we found that ensuring the sample remained at a low temperature resulted in higher MWNT concentrations. The Ulijn group used 0.6 mM aqueous surfactant solutions in phosphate buffered saline (PBS)[132] whereas our work uses 1.0 mM solutions in Millipore deionised water. We expected that this increased concentration would give equivalent or improved dispersion ability due to higher surfactant availability. These surfactant concentrations lie within the range for which Clark *et al.* showed that MWNT dispersion efficiency increased or remained constant with increasing concentration,[75] and are much lower than the concentrations at which depletion forces have been observed to reduce CNT concentration.[76,77] Many of the published CNT dispersion studies discussed in Chapter 1 compare surfactant solutions at a fixed weight percentage, but this means that surfactant molarity varies with molecular weight. We reasoned that a fixed molarity would better represent surfactant performance as dispersion ability would be compared on a 'per molecule' basis. For the pyrene-anchored surfactants this would mean the same number of pyrene moieties would be present in all cases, simplifying comparisons of differing linker and head groups.

*MWNTs were purchased from NanoAmor. The following values were quoted: purity: 95+%, outer diameter: 20-30 nm, internal diameter: 5-10 nm, length: 10-30 μm.

MWNT dispersions were prepared by treating MWNTs (1.0 mg) with 1 mM surfactant solution (3 ml) and ultrasonicating the mixture. Full details of this process can be found in the experimental section. These conditions were not optimised; rather they were selected as a means of comparing surfactant performance using small amounts of both surfactant and MWNTs. Any large, suspended aggregates were removed by centrifugation and the supernatant investigated by UV-visible spectroscopy. The spectrometer was fitted with an integrating sphere to account for any light scattering by dispersed nanoparticles. This analysis required dilution of the sample to ensure the absorption was within the range of the spectrometer; ten-fold dilutions (using the parent surfactant solution) were used throughout. The parent surfactant solution was used as a reference for these measurements. To further ensure there was no interference from the absorption of the surfactants any quantitative analysis was conducted at wavelengths at which they did not absorb. Based on the absorbance data the concentration of MWNTs in the dispersion, C_{MWNT}, could be calculated using the Beer-Lambert law (see below). The maximum possible C_{MWNT} under the conditions used is 333.333 mg L^{-1}. Further optimisation of the obtained C_{MWNT} values should be possible, but is yet to be investigated in detail.

It has been widely reported that CNT dispersions obey the Beer-Lambert law, $A = \varepsilon c l$, where A is the absorbance of a dispersion at a given wavelength, ε is the extinction coefficient of the dispersed CNTs at that wavelength, c is the concentration of the dispersion and l is the path length of the sample.[175-177] To calculate the concentration of dispersions using the Beer-Lambert law a value for ε is required. Relatively few literature values of ε are available for MWNTs. These include values of 46.0 ± 1.4 ml mg^{-1} cm^{-1} at 500 nm reported for covalently functionalised MWNTs,[177] 42.2 ± 0.3 ml mg^{-1} cm^{-1} at 500 nm for polymer-functionalised MWNTs dispersed in chloroform,[178] 39.92 ml mg^{-1} cm^{-1} for acid treated MWNTs dispersed in water,[175] and 41.14 ml mg^{-1} cm^{-1} at 500 nm for MWNTs dispersed in xylene.[175] Other works do not report a value for ε, although they state that the Beer-Lambert law was used.[132,176] Calibration plots are included, but ε cannot be deduced from these without knowledge of the path length, l. Although it has been claimed that ε is independent of MWNT diameter and length for sufficiently dispersed material,[175] it has also been reported that functionalisation of SWNTs has a large effect on ε.[179] Therefore it was important to establish a value of ε that was based on dispersions of non-covalently functionalised MWNTs and was specific to the batch of MWNTs used throughout our study. This required UV-visible analysis of a dispersion of known concentration at several dilutions.

Accurately determining the concentration of a surfactant-stabilised CNT dispersion is complicated by the need to account for material which is not dispersed.[180] Some works on SWNTs simply use freshly prepared dispersions which have not been centrifuged, and assume bundled SWNTs remain suspended on the timescale of the experiment.[179,180] We were not confident that the effect of suspended MWNT bundles would be negligible, and so investigated other methods. An approach which has been used for graphene dispersions is to pass a known volume through a filter of known mass to determine the mass of dispersed material,[46,181] which can be followed by gravimetric analysis to account for any remaining adsorbed surfactant or solvent. We were unable to achieve consistent results using this method. We were also unable to obtain satisfactory results by adapting the method of Brahmachari *et al.* where the concentration of an SWNT dispersion was calculated based on the mass of the residue recovered after centrifugation.[182] We successfully determined ε by adapting the method of Liu *et al.*,[94] who showed that MWNTs dispersed in aqueous SDS solution can be precipitated by adding excess acetone. Repeated centrifugation, decanting of the supernatant, and acetone treatment removes SDS and water from the MWNTs which can then be dried and weighed.[94] Compared to our standard dispersion conditions this method required an increased volume of dispersion so that sufficient was available for both UV-visible absorption and precipitation procedures. We also used an increased MWNT loading to afford more concentrated dispersions, which would increase the mass of precipitated MWNTs and reduce the impact of any weighing errors.

The data used to calculate ε are shown in Figure 3.01. Each data set shows a linear relationship between absorbance and C_{MWNT}. As 1 cm path length cuvettes were used, for each sample ε (in ml mg^{-1} cm^{-1}) is equal to the gradient of the trend line. The results of three experiments show excellent agreement; averaging the three runs gives ε = 49.9 ± 1.2 ml mg^{-1} cm^{-1} at 500 nm (where the error is the standard deviation of the three results). Although MWNTs absorb across the entire UV-visible range, ε at 500 nm is commonly used as surfactants and other materials used for their dispersion do not absorb at this wavelength. This value was used to calculate C_{MWNT} for all other dispersions and agrees reasonably with the values obtained using different dispersion methods discussed above (39.9 - 46.0 ml mg^{-1} cm^{-1}).[175,177,178]

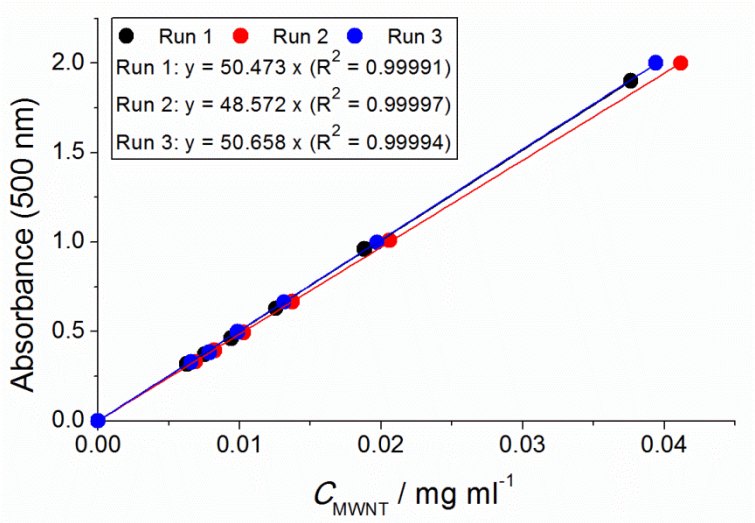

Figure 3.01: The extinction coefficient, ε, (at 500 nm) of the MWNTs used in our work was obtained by plotting the absorbance of dilutions prepared from a sample of known concentration against their concentration.

The structures of the surfactants used to prepare MWNT dispersions are summarised in Appendix 1. In addition to the ether linker surfactants, five commercially available surfactants were used to prepare MWNT dispersions for comparison. These were **SDS**, **SDBS**, **SC**, **SDOC** and **Triton X-100**. The sodium salt of **PBA**, **SPB**, was also tested as a reference. Comparisons were also made with surfactants concurrently synthesised by colleagues. These include 'linker-free' surfactants **PBA-G1(ONa)$_3$**, **PBA-H1(ONa)$_3$** (the sodium salt of surfactant **4** reported by the Hirsch group[69] – see Chapter 1) and **PBA-G2(ONa)$_9$**, in which a dendron was linked directly to **PBA** *via* amide coupling. The three 'linker-free' surfactants have head groups derived from dendron **14** (i.e. that which was used in the ether linker species), dendron **13**, and the second generation dendron derived from **14**, respectively. These head groups will be referred to as G1, H1 and G2. Further surfactants incorporated amide linkers derived from **17** (these will be referred to as "C6 linkers") with both G1 and G2 head groups; this series consists of **PBA-C6-G1(ONa)$_3$**, **PBA-C6-G2(ONa)$_9$**, **PBA-(C6)$_2$-G1(ONa)$_3$** and **PBA-(C6)$_2$-G2(ONa)$_9$**. Work on the synthesis of these two series was initiated by Dr Kara Howes and completed by Dr Daniel Welsh in our laboratory. Dr Welsh conducted all MWNT dispersion studies using these surfactants as well as **SDBS**, **SC**, **SDOC**, **Triton X-100** and **SPB**. Dispersion studies were conducted in triplicate for all surfactants except **SDS**, **SDBS**, **SC**, **SDOC** and **SPB** from which six dispersions were prepared, and **PBA-(C6)$_2$-G2(ONa)$_9$** from which only one dispersion was prepared as only a small quantity of material was available.

3.2: Dispersions in Deionised Water - Results and Discussion

3.2.1: Results

The results of MWNT dispersion studies in Millipore deionised water are shown in Figure 3.02 and Table 3.01. The percentage of MWNTs dispersed is relative to the maximum possible value under the conditions used, i.e. 333.333 mg L^{-1}. Control experiments using deionised water with no surfactant showed no MWNT dispersion. Good reproducibility was observed; for most surfactants the standard deviation of C_{MWNT} was less than 10% of the mean. As this error was always larger or comparable to that associated with ε, the latter was discounted throughout. The most significant error was observed for **SDBS**, despite this being one of the materials for which 6 results were averaged. The dispersions appeared to be stable over periods of at least several months under ambient conditions; they remained visibly homogeneous with no precipitation of MWNTs.

Table 3.01: C_{MWNT} in a range of 1 mM aqueous surfactant solutions. Errors are the standard deviation of 3 results except for **SDS**, **SDBS**, **SC**, **SDOC** and **SPB**, which are from 6 results, and **PBA-(C6)$_2$-G2(ONa)$_9$** which represents a single experiment only.

Surfactant	C_{MWNT} / mg L^{-1}	Error (σ) / mg L^{-1}	% MWNTs Dispersed
SDS	108	7	32
SDBS	94	18	28
SC	95	6	29
SDOC	91	9	27
SPB	57	7	17
Triton X-100	134	5	40
PBA-H1(ONa)$_3$	85	12	26
PBA-G1(ONa)$_3$	86	2	26
PBA-C6-G1(ONa)$_3$	73	10	22
PBA-(C6)$_2$-G1(ONa)$_3$	74	3	22
PBA-G2(ONa)$_9$	76	1	23
PBA-C6-G2(ONa)$_9$	69	11	21
PBA-(C6)$_2$-G2(ONa)$_9$	88	-	26
PyrB-PEG2-CH$_2$COONa	107	5	32
PyrB-PEG4-CH$_2$COONa	137	9	41
PyrB-PEG6-CH$_2$COONa	148	1	44
PyrB-PEG12-CH$_2$COONa	129	9	39
PyrB-PEG2-CH$_2$COG1(ONa)$_3$	110	3	33
PyrB-PEG4-CH$_2$COG1(ONa)$_3$	104	4	31
PyrB-PEG6-CH$_2$COG1(ONa)$_3$	105	8	32

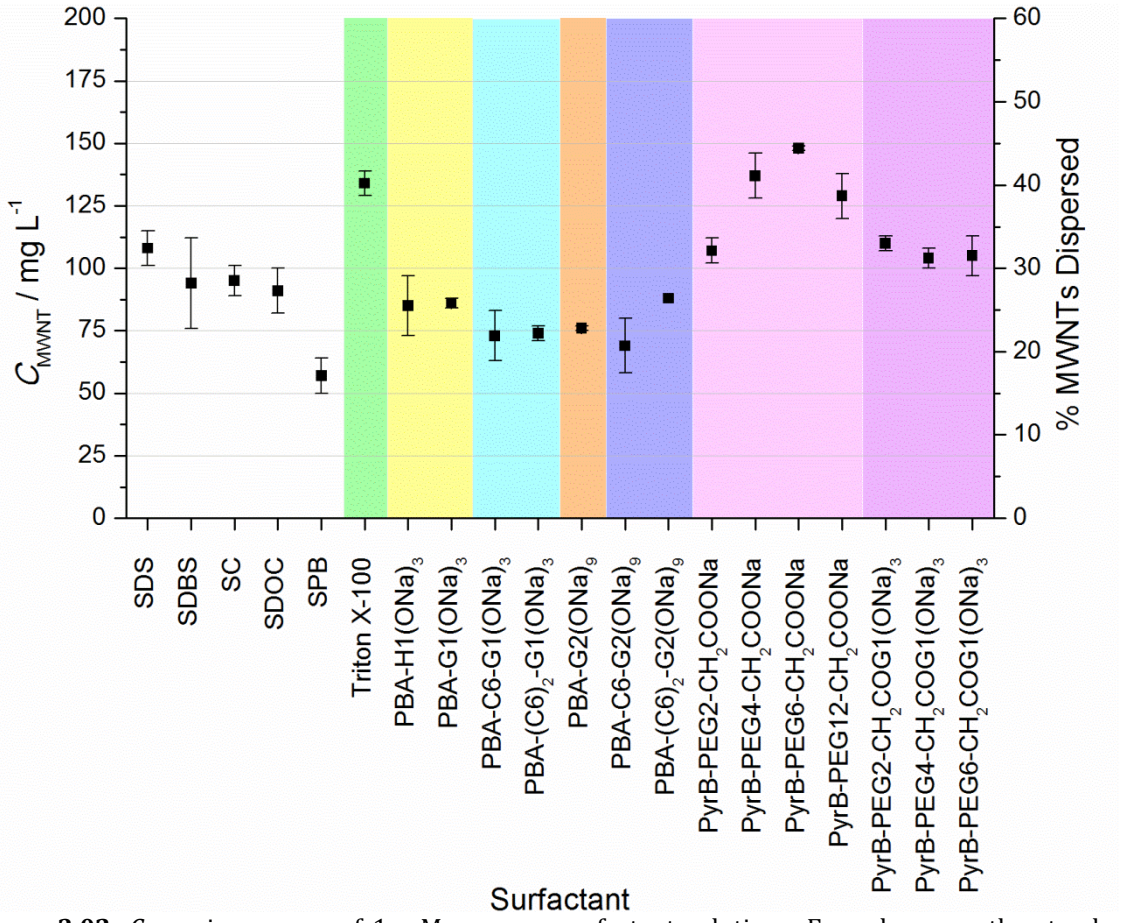

Figure 3.02: C_{MWNT} in a range of 1 mM aqueous surfactant solutions. Error bars are the standard deviation of 3 results except for **SDS**, **SDBS**, **SC**, **SDOC** and **SPB**, which are from 6 results, and **PBA-(C6)$_2$-G2(ONa)$_9$** which represents a single experiment only. Colours indicate surfactant groups: white - reference anionic; green – reference non-ionic; yellow – linker-free G1; light blue – amide linker G1; orange – linker-free G2; dark blue – amide linker G2; pink – ether linker G0; purple – ether linker G1.

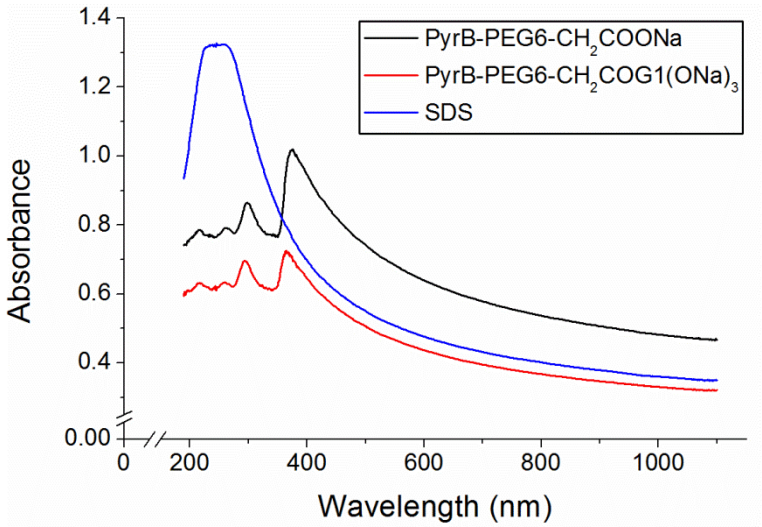

Figure 3.03: Representative UV-visible absorbance spectra of MWNT dispersions in 1 mM solutions of the indicated surfactants. A 1 mM surfactant solution was used as a reference.

Figure 3.03 shows representative spectra for MWNT dispersions in **PyrB-PEG6-CH_2COONa**, **PyrB-PEG6-CH_2COG1(ONa)$_3$** and **SDS**. It can be seen that above *ca.* 380 nm absorbance is broad and featureless, which is characteristic of dispersed MWNTs.[94] Where pyrene-containing surfactants are used, we attribute the features at lower wavelengths to adsorption of surfactant to the MWNT surface, which creates a discrepancy in surfactant concentration between the dispersion and the surfactant solution used as a reference. This is supported by the absence of such features in the case of **SDS**, which has no significant absorbance.

3.2.2: Commercial and Reference Surfactants

The commercial anionic surfactants (**SDS**, **SDBS**, **SC** and **SDOC**) dispersed similar levels of MWNTs (27-32%) under our conditions. **SDS** was the best-performing of these materials, affording 108 ± 7 mg L^{-1} of MWNTs. Ulijn and co-workers report a somewhat higher C_{MWNT} of 200 ± 30 mg L^{-1} for **SDS** under near-identical conditions.[132] In contrast to our results, they observe slightly higher dispersion levels using **SDBS** (210 ± 10 mg L^{-1}) rather than **SDS**. Again, this value is much higher than the 94 ± 18 mg L^{-1} (28%) we achieved. We suspect that the discrepancy between our results and those of the Ulijn group could be due to differing surfactant behaviour in Millipore deionised water and PBS. A C_{MWNT} of 10 mg L^{-1} is reported for a control experiment in PBS,[132] whereas we observed no MWNT dispersion in our control experiment. The ionic strength of the dispersion medium is known to affect C_{MWNT};[183] this is discussed in more detail in Section 3.3. Other factors could also contribute, e.g. the Ulijn group used MWNTs which were produced in-house, whereas we used commercial material. We also note that they calculated ε using acid treated MWNTs, and applied this value to untreated MWNTs dispersed by a surfactant. Our slightly higher surfactant concentration should at worst result in similar C_{MWNT} to that of the Ulijn group. We also do not believe that our alterations to the processing conditions (lower sonicator amplitude and ice cooling) are responsible, as this was found to increase C_{MWNT}. **SC** and **SDOC** performed similarly to **SDBS**, in contrast to the work of Wenseleers *et al.* who found that **SDOC** was much more efficient at dispersing SWNTs than the other commercial materials we have investigated.[80]

SPB gave a significantly lower C_{MWNT} compared to the commercial anionic surfactants, only 57 ± 7 mg L^{-1} (17%). This was unexpected as we had anticipated that the strong interactions between the pyrene moiety and CNT surfaces would enhance dispersion ability by ensuring the surfactant is firmly bound to the CNT surface (See Chapter 1). To bind strongly to the MWNT through π-π interactions the planar pyrene anchor must lie parallel to the surface,

whereas **SDS** and **SDBS** can form micellar structures which could allow for increased surface coverage and therefore a higher overall charge density. This could explain the improved C_{MWNT} observed using the surfactants with aliphatic chains.

The commercial non-ionic surfactant **Triton X-100** afforded a high C_{MWNT} of 134 ± 5 mg L^{-1} (40%), considerably higher than any of the anionic species used as references. Non-ionic surfactants achieve CNT dispersion through a combination of hydrophilicity and steric effects, rather than through charge interactions as in the case of ionic surfactants.[184] This result indicated that this could be a superior approach and prompted the development of the non-ionic surfactants discussed in Chapters 4 and 5.

3.2.3: Linker-free and Amide Linker Surfactants

The surfactants **PBA-G1(ONa)$_3$** and **PBA-H1(ONa)$_3$** allow for direct comparison between the first generation Newkome-type dendrons used in our work (**14**) and those favoured by the Hirsch group (**13**). Surprisingly, neither shows any clear advantage over the other in terms of C_{MWNT}, although **PBA-G1(ONa)$_3$** gave more consistent results. We had hoped that **PBA-G1(ONa)$_3$** might give a higher C_{MWNT} than **PBA-H1(ONa)$_3$** due to the presence of hydrophilic ether moieties in the head group. However, the use of head groups derived from **14** is still justifiable in terms of their more convenient synthesis and the better reproducibility observed in the MWNT dispersion study. **PBA-G2(ONa)$_9$** performs slightly worse than the two 'linker-free' surfactants with first generation dendrons. This agrees with Hirsch's report that **PBA-H1(ONa)$_3$** dispersed SWNTs more efficiently than its second-generation analogue.[69] This was rationalised in terms of surface coverage by the surfactants: larger, more charged G2 head groups cannot pack as closely together as G1 head groups due to increased coulombic repulsion which results in lower C_{MWNT}.[69] The lower CNT dispersing ability of the 'linker-free' surfactants relative to **SDBS** also agrees with the observations of the Hirsch group.

Relating surfactant performance to surface coverage is a useful concept when analysing the results for our novel surfactants. For a given head group charge, the MWNT surface area coverage per surfactant molecule, A_{surf}, can be related to the charge density of a functionalised MWNT, which in turn should impact on the extent of MWNT dispersion. As A_{surf} increases, charge density is reduced and C_{MWNT} is expected to decrease. This is illustrated schematically in Figure 3.04. The point at which maximum surfactant coverage is reached (and A_{surf} is

minimised) will be whichever of the following occurs first: i) the entire MWNT surface is coated with pyrene and any hydrophobic moieties; or ii) the volume around the MWNT surface is filled by head (and linker) groups.

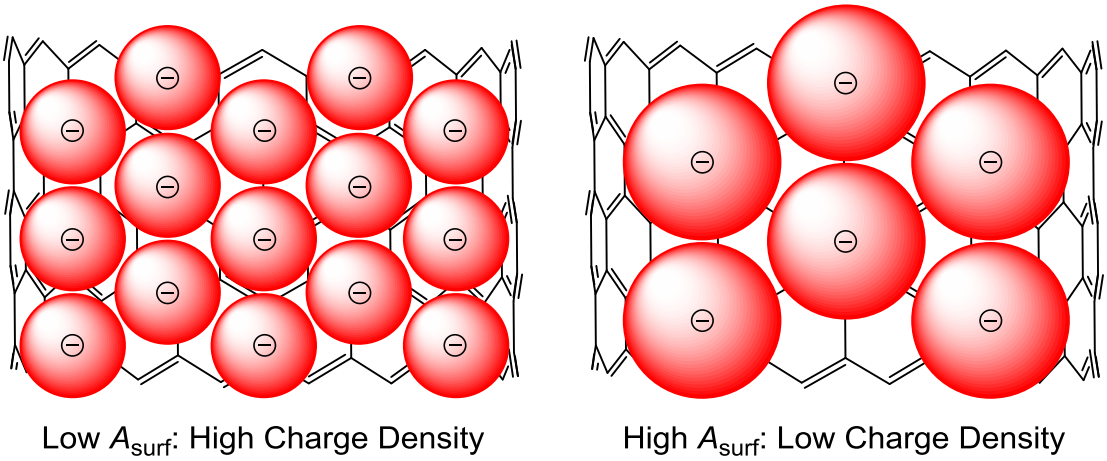

Figure 3.04: For a given head group charge (illustrated as monoanionic), as the MWNT surface area covered by a surfactant molecule, A_{surf}, increases, the overall charge density of the functionalised MWNT decreases. These illustrations assume A_{surf} is limited by the volume of the head (and linker) groups.

The amide linker surfactants show little variation in MWNT dispersion ability. Addition of C6 linker units causes a slight decrease in C_{MWNT}. This is most noticeable in the G1 series; **PBA-C6-G1(ONa)$_3$** and **PBA-(C6)$_2$-G1(ONa)$_3$** gave similar C_{MWNT} values of 73 ± 10 and 74 ± 3 mg L^{-1} respectively (both 22%), slightly lower than 86 ± 2 mg L^{-1} (26%) for the linker-free analogue **PBA-G1(ONa)$_3$**. Interestingly, the addition of the second C6 unit appears to have no effect on MNWT dispersing ability within experimental error. It is more difficult to draw conclusions for the G2 series. Addition of a single C6 linker again gives a lower C_{MWNT} than the linker-free species, although in this case the decrease is smaller and has a degree of uncertainty due to the relatively large error associated with the result for **PBA-C6-G2(ONa)$_9$**. In contrast to the G1 series, the highest C_{MWNT} obtained for the G2 materials was that for **PBA-(C6)$_2$-G2(ONa)$_9$**, 88 mg L^{-1} (26%), although this represents a single experiment rather than the average of a triplicate set as for the other novel surfactants. If the margin of error is similar to that for the other surfactants it means that for the G2 series the addition of a second C6 linker improves MWNT dispersing ability compared to both the linker-free analogue and that with only a single C6 linker. It is not clear why this should be beneficial in the case of the G2 but not the G1 series.

Although the addition of C6 linkers incorporates further hydrophilic amide moieties into the molecule, this is counteracted by the addition of hydrophobic pentyl chains. These may cause

the linkers to preferentially lie flat on the MWNT surface, increasing A_{surf} and lowering C_{MWNT}. Depending on the preferred orientation of linkers on the MWNT surface, addition of a second C6 unit may not cause as significant an increase in A_{surf}, as the linker could, for example, fold back on itself. This interpretation accounts for the trends in the G1 series, and the reduced C_{MWNT} achieved by **PBA-C6-G2(ONa)$_9$** compared with **PBA-G2(ONa)$_9$**. For the G2 materials the relative increase in A_{surf} when a C6 linker is added is less than for the G1 materials due to the presence of the larger G2 head group. This may explain the smaller difference in C_{MWNT} in this case.

Comparing the G1 and G2 series, neither head group provides a distinct advantage in terms of MWNT dispersing ability. While for the linker-free species the G1 head group performed slightly better, for surfactants with a single C6 linker there was no appreciable difference between the G1 and G2 head groups. The C_{MWNT} obtained using **PBA-(C6)$_2$-G2(ONa)$_9$** is a little higher than that using **PBA-(C6)$_2$-G1(ONa)$_3$**, but we do not believe this increase is sufficient to justify the more complex synthesis of the G2 materials. This supports the decision not to investigate the use of G2 head groups in ether linker surfactants.

3.2.4: Ether Linker Surfactants

All of the ether linker surfactants show a level of MWNT dispersion that is at least comparable to the best of the commercial anionic surfactants, **SDS**. They outperform all of the linker-free and amide linker species, indicating that the inclusion of the hydrophilic OEG linker is beneficial in terms of surfactant performance, as proposed in Section 2.3. Comparing the G0 series to **SPB** (which can be considered as a linker-free analogue) makes this very clear. **SPB** gave a C_{MWNT} of 57 ± 7 mg L^{-1} (17%) whereas the G0 species with the shortest ether linker, **PyrB-PEG2-CH$_2$COONa**, gave 107 ± 5 mg L^{-1} (32%). The overall structural difference between these species is equivalent to the addition of three PEG repeat units, as illustrated in Figure 3.05. A marked increase in C_{MWNT} has therefore been achieved by only the addition of a short OEG moiety. The use of longer OEG linkers further increases C_{MWNT}, giving 137 ± 9 mg L^{-1} (41%) for **PyrB-PEG4-CH$_2$COONa**, and 148 ± 1 mg L^{-1} (44%) for **PyrB-PEG6-CH$_2$COONa**. The latter gives a C_{MWNT} almost triple that of **SPB**. Investigation of the much longer PEG12 linker showed that it was less effective than either a PEG6 or PEG4 linker; **PyrB-PEG12-CH$_2$COONa** afforded only 129 ± 9 mg L^{-1} (39%) of MWNTs. This suggests that there is an optimal linker length at which MWNT dispersing ability is maximised.

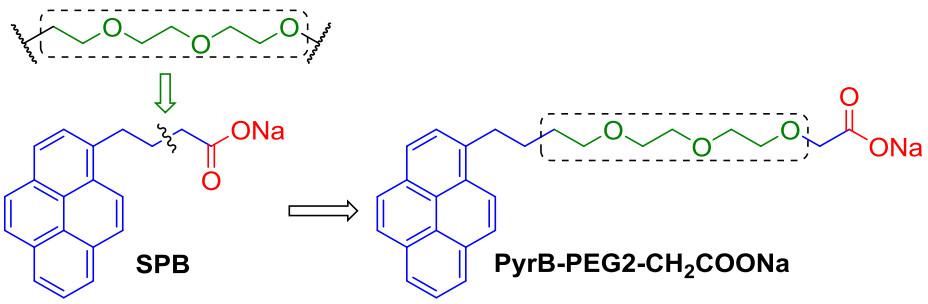

Figure 3.05: The structural difference between SPB and PyrB-PEG2-CH_2COONa is equivalent to the addition of 3 PEG repeat units.

Analysing these data in terms of PEG units added to **SPB** (defined as the n+1 for the **PyrB-PEGn-CH_2COONa** series, and 0 for **SPB**) shows that C_{MWNT} appears to increase linearly from **SPB** to **PyrB-PEG4-CH_2COONa**, as shown in Figure 3.06. The increase in C_{MWNT} between **PyrB-PEG4-CH_2COONa** and **PyrB-PEG6-CH_2COONa** is much smaller, suggesting that the beneficial effect of further PEG units becomes less significant beyond this point. The decrease in C_{MWNT} between **PyrB-PEG6-CH_2COONa** and **PyrB-PEG12-CH_2COONa** indicates that there is a point at which the addition of further PEG repeat units becomes disadvantageous. However, without further data we cannot define the optimal linker length more accurately than between PEG5 and PEG11. This is convenient as the use of oligomer-pure linkers beyond PEG12 would be synthetically challenging and require very costly starting materials.

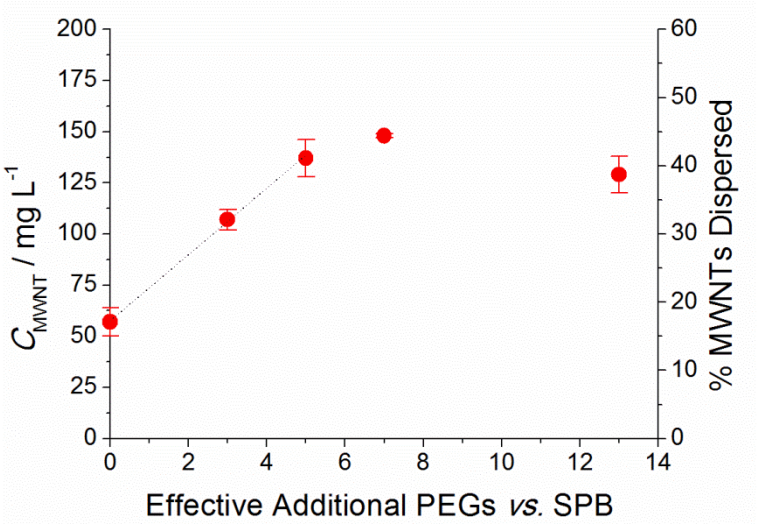

Figure 3.06: C_{MWNT} using 1 mM aqueous solutions of SPB and the series **PyrB-PEGn-CH_2COONa**. Error bars are the standard deviation of 3 results except for SPB, where it is the standard deviation of 6 results.

These data can also be rationalised in terms of A_{surf}. For shorter linkers, the increased hydrophilicity associated with the OEG has a beneficial effect that outweighs any negative contribution from the increase in A_{surf}. The increased distance between the pyrene anchor

and the charged head group compared to **SPB** may also allow micellar structures to form; if the linker and head group form structures that tend to extend away from the MWNT surface into the water any change in A_{surf} would be minimal. Although hydrophilicity continues to increase for longer PEG chains, it becomes increasingly entropically unfavourable for the linker and head to extend out into the water – entangled, bulky, random coil structures close to the MWNT surface would be expected to be preferable. This would increase A_{surf} by occupying a large volume above the MWNT surface. We suggest that for shorter linkers the surface coverage is the limiting case as the footprint of pyrene is large relative to the head group. For longer linkers the increased volume occupied by the linker becomes the limiting factor. A model of this idea is shown in Figure 3.07. C_{MWNT} remains high even for **PyrB-PEG12-CH$_2$COONa** which may indicate a transition in the mechanism by which dispersed MWNTs are stabilised. This may rely less on the coulombic repulsion effect associated with ionic surfactants and more on steric bulk and hydrophilicity, i.e. the mechanism commonly attributed to non-ionic surfactants. The similarity in C_{MWNT} between **PyrB-PEG12-CH$_2$COONa** and **Triton X-100** (which has an average PEG chain length of 9.5 repeat units) may not be entirely coincidental.

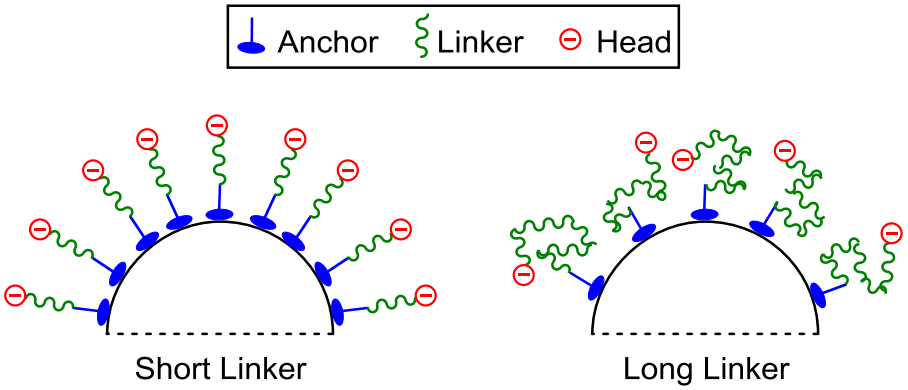

Figure 3.07: Cross-sectional representations of surfactants of different linker lengths maximising surface coverage on a MWNT.

The G1 ether linker series shows much less variation than the G0 series; all three surfactants give C_{MWNT} in the range 104-110 mg L^{-1} (31-33%) and within experimental error of one another. As the analogous G0 surfactants show a distinct positive correlation between C_{MWNT} and linker length for the comparable n = 2, 4, 6 species, it follows that this difference is attributable to the G1 head group. It is again clear that the inclusion of an OEG linker is advantageous when the results are compared to the linker-free analogue **PBA-G1(ONa)$_3$** (C_{MWNT} = 86 ± 2 mg L^{-1}). This contrasts with the effect observed for the G1 amide linker species where inclusion of C6 linkers gave lower C_{MWNT} values than **PBA-G1(ONa)$_3$**, although

again the number of linker units had little effect. This shows that the nature of the linker unit is important.

These observations can also be rationalised based on A_{surf}. **PBA-G1(ONa)$_3$** has a large head group which will be held close to the MWNT surface by the pyrene anchor group. This will increase A_{surf} by occupying a large volume close to the surface, limiting coverage through coulomb interactions. The mutual repulsion between anionic head groups is strong in Millipore water as their charge is screened only by small quantities of ionised water. The effect of this is that coulomb interactions have a much larger effect on the volume occupied by a head group than its steric bulk. The addition of a hydrophilic linker unit can increase the available volume and decrease A_{surf} by allowing the head group to extend further from the MWNT surface, although this volume will be in part occupied by the linker itself. This is in contrast to the more hydrophobic linkers used in the amide linker surfactants, which increase A_{surf} due to their affinity for the MWNT surface. Figure 3.08a shows a representation of maximised surface coverage by linker-free surfactants with large head groups. Figure 3.08b includes a hydrophobic linker intended to represent the C6 linkers of the amide linker surfactants. The use of hydrophilic linkers such as OEGs is illustrated in Figure 3.08c. These diagrams are a simplified view and fail to account for effects such as 3-dimensional packing and any inter- and intra-linker interactions. The latter could play a role in limiting the extent to which the head groups can extend from the surface, which may account for the lack of variation along the G1 series.

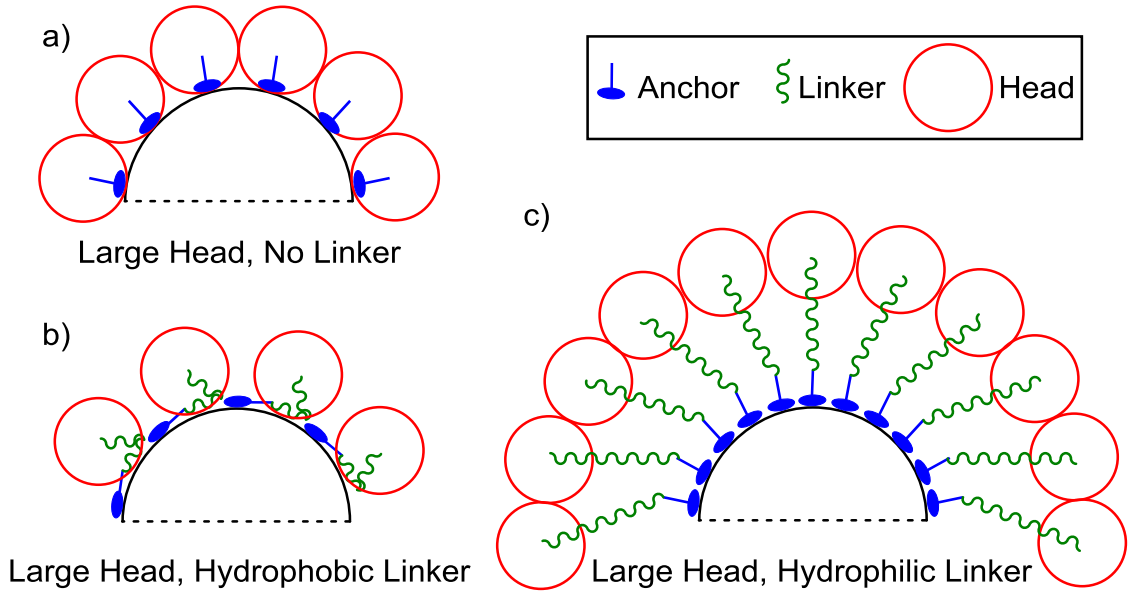

Figure 3.08: Cross-sectional representations of different types of surfactants maximising surface coverage on a MWNT. Not to scale.

3.2.5: TEM Studies

To support the UV-visible spectroscopic data, which confirmed that MWNTs are dispersed in aqueous solution, TEM imaging was used to qualitatively assess the degree to which MWNTs were individualised in the dispersions. Images were obtained by Dr Budhika Mendis of the Department of Physics, Durham University. Samples were prepared by dropping *ca.* 20 μL of MWNT dispersion onto a holey-carbon TEM grid which was dried in air overnight. Representative TEM images for samples prepared from MWNT dispersions in **PBA-G1(ONa)$_3$**, **PBA-C6-G1(ONa)$_3$**, **PBA-(C6)$_2$-G1(ONa)$_3$**, **PBA-G2(ONa)$_9$**, **PBA-C6-G2(ONa)$_9$**, **PyrB-PEG4-CH$_2$COONa**, **PyrB-PEG2-CH$_2$COG1(ONa)$_3$** and **PyrB-PEG6-CH$_2$COG1(ONa)$_3$** are shown in Figures 3.09a-h respectively. In all cases individualised MWNTs can be seen lying on the holey-carbon grid, confirming that the dispersion procedure is effective. Although some larger bundles can be seen, it is impossible to say based solely on these images whether these are representative of the dispersed material or are artefacts formed upon drying (i.e. during sample preparation). Various lengths of MWNT can be seen in the images; the presence of objects shorter than 10 μm indicates that some MWNTs have been broken into shorter pieces during the sonication procedure, as the as-supplied material has a specified length of 10-30 μm. Many examples of MWNTs within this length range can also be seen. Shortening of CNTs during sonication is a known phenomenon,[78] and could be reduced by utilising gentler but more time-consuming processing conditions.

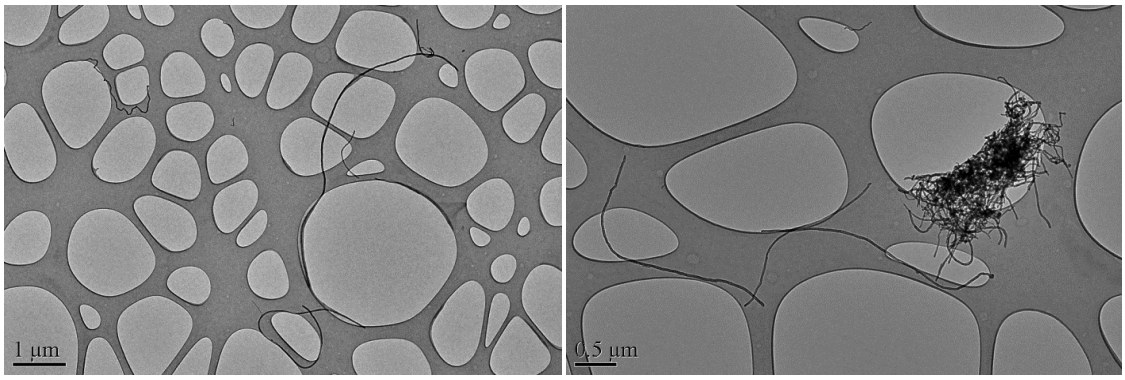

Figure 3.09a: Representative TEM images of MWNTs from a sample dispersed using 1 mM **PBA-G1(ONa)$_3$** in Millipore water.

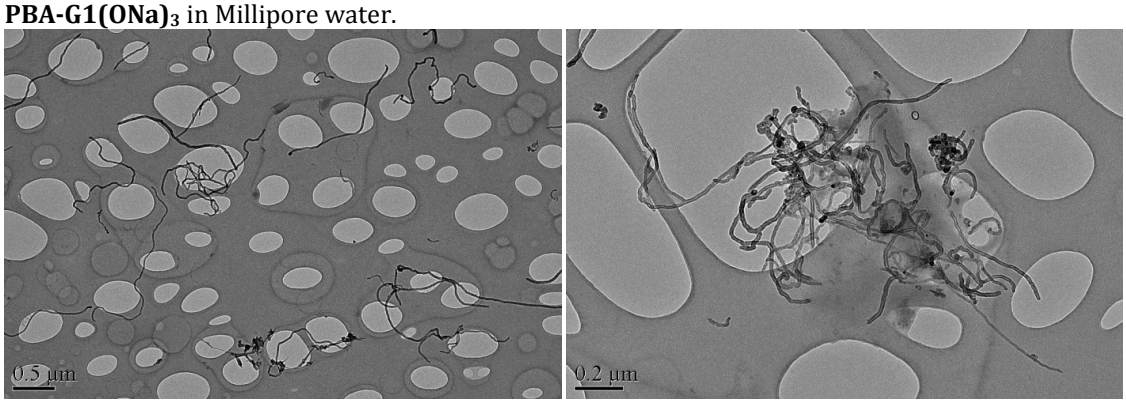

Figure 3.09b: Representative TEM images of MWNTs from a sample dispersed using 1 mM **PBA-C6-G1(ONa)$_3$** in Millipore water.

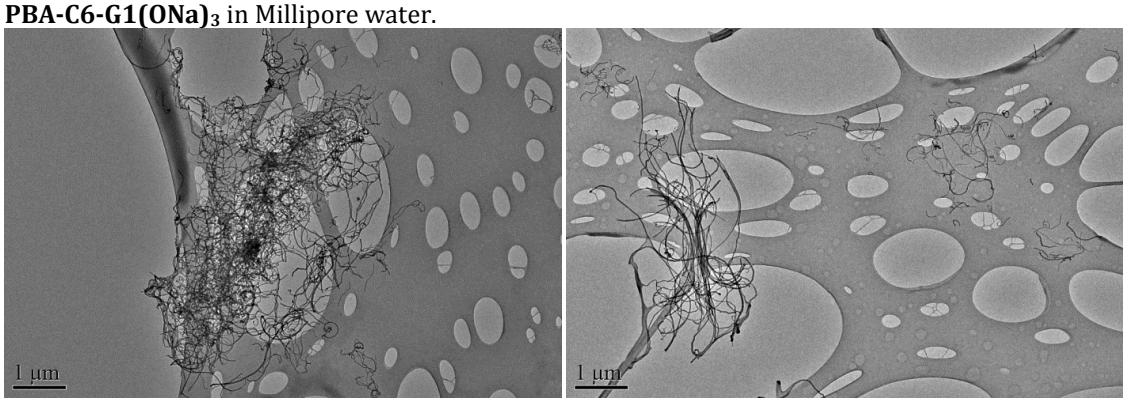

Figure 3.09c: Representative TEM images of MWNTs from a sample dispersed using 1 mM **PBA-(C6)$_2$-G1(ONa)$_3$** in Millipore water.

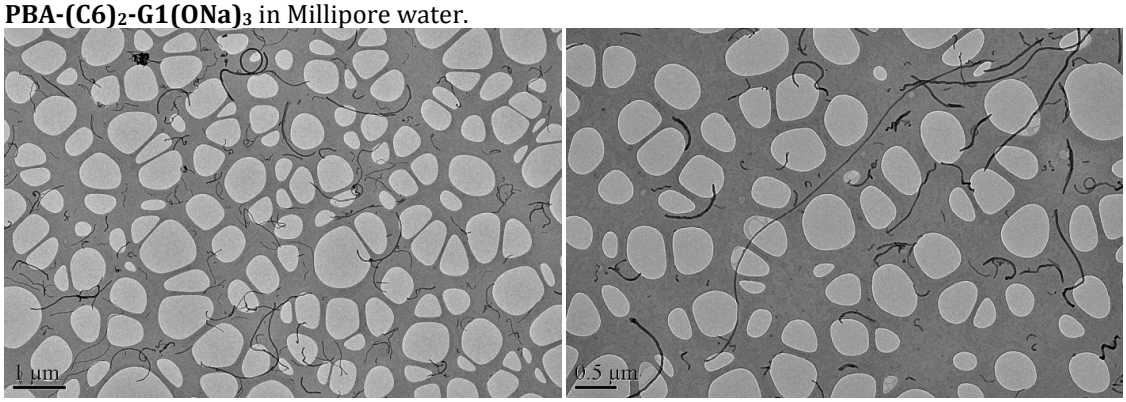

Figure 3.09d: Representative TEM images of MWNTs from a sample dispersed using 1 mM **PBA-G2(ONa)$_9$** in Millipore water.

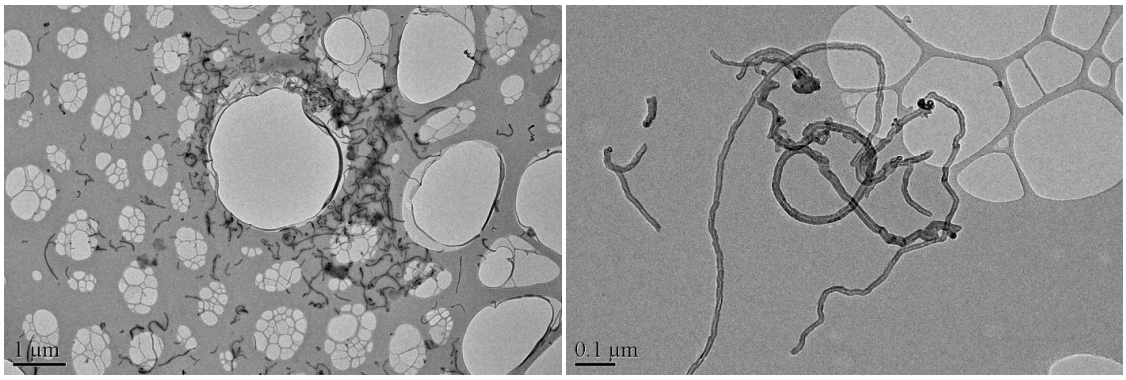

Figure 3.09e: Representative TEM images of MWNTs from a sample dispersed using 1 mM **PBA-C6-G2(ONa)$_9$** in Millipore water.

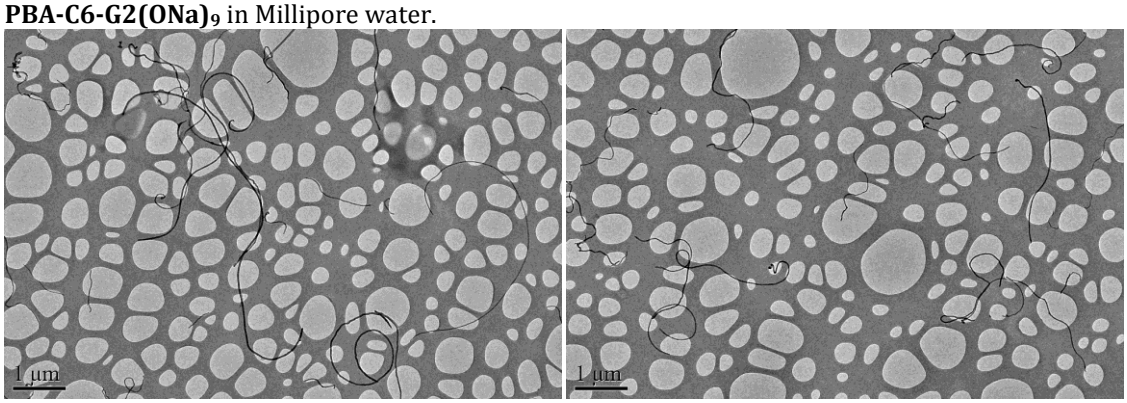

Figure 3.09f: Representative TEM images of MWNTs from a sample dispersed using 1 mM **PyrB-PEG4-CH$_2$COONa** in Millipore water.

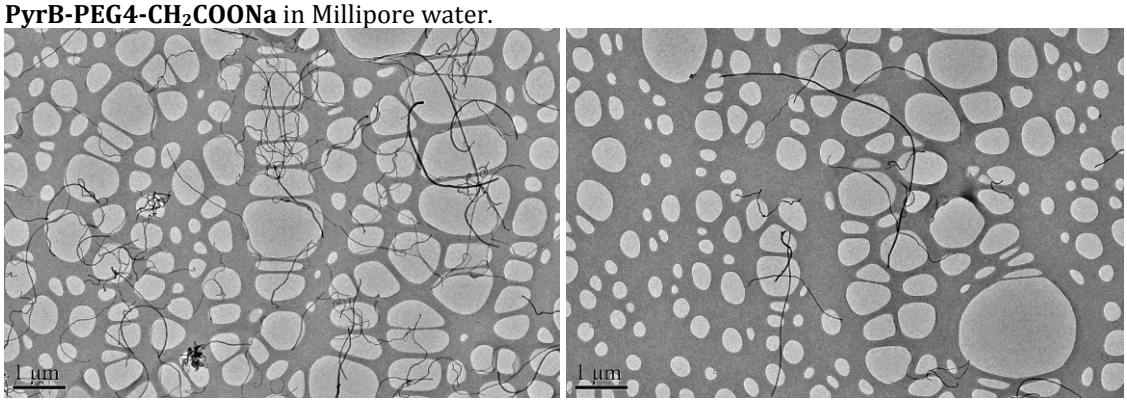

Figure 3.09g: Representative TEM images of MWNTs from a sample dispersed using 1 mM **PyrB-PEG2-CH$_2$COG1(ONa)$_3$** in Millipore water.

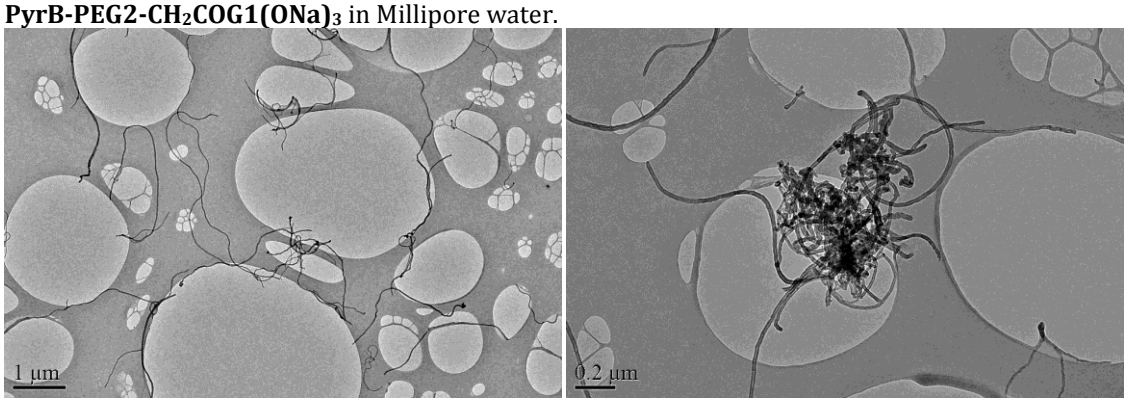

Figure 3.09h: Representative TEM images of MWNTs from a sample dispersed using 1 mM **PyrB-PEG6-CH$_2$COG1(ONa)$_3$** in Millipore water.

3.3: Dispersions in Salt Solutions – Results and Discussion

3.3.1: Overview

One area of interest when examining possible responsive behaviour in MWNT dispersions was the influence of ions. This section examines the effect of ions on the ability of surfactants to disperse MWNTs. As well as indicating any ion sensitivity this study aimed to further our understanding of the mechanisms by which our surfactants disperse MWNTs. A recent publication by Hirsch and co-workers examines the effect of ionic strength and pH on the ability of a perylene bisimide surfactant **5** (Figure 1.11) to disperse SWNTs.[183] Their aim was to develop a means of sorting SWNTs of different chiralities based on sensitivity to ionic strength, and preliminary evidence of such an effect was shown. They show that dispersions prepared in phosphate buffered solutions of **5** at different ionic strength and pH vary significantly in SWNT concentration. They find that dispersion efficiency is improved at higher pH and higher ionic strength, and relate this to SWNT charge density and A_{surf}.[183] Working at high pH causes ionisation of the carboxylic acid moieties of **5**, increasing the charge density of functionalised SWNTs. However, compared to neutral pH A_{surf} is increased due to coulombic repulsions between the now charged head groups. Dispersion efficiency at an ionic strength of 0.09 M is found to be higher than at 0.005 M at both pH 7 and pH 10. This is attributed to increased charge screening at higher ionic strength which reduces the extent of coulombic repulsions. This allows a higher A_{surf} which in turn increases SWNT charge density.[183] Although this increases dispersion efficiency, increased ionic strength is observed to have a negative impact on SWNT individualisation.

We conducted our investigation on a similar basis, but used salt solutions rather than buffers and did not vary pH as our surfactants were prepared as carboxylates. The MWNTs were dispersed in salt solutions in order to analyse the effect of ions on the dispersion process as a whole. Our protocol makes it possible to examine whether the presence of salts is favourable or unfavourable, whereas treating an aqueous dispersion with a salt would show a response only if the salt had an adverse effect on the dispersion's stability. As in Section 3.2, 1 mM surfactant solutions were used, however, these were now prepared in standard salt solutions. A concentration of 0.6 M was selected for monovalent salts – this approximates the ion concentration in standard sea water (which has a salinity, or salts content, of *ca.* 35 g kg^{-1},[185] approximately 35 g L^{-1}. This is equivalent to 0.6 M NaCl). For multivalent ions the concentration was adjusted to maintain the same overall charge density (e.g. $CaCl_2$ was used

at 0.3 M to maintain a 0.6 M concentration of chloride ions and an overall 0.6 M 'concentration' of positive charge), although this does not represent the same ionic strength due to the higher contribution of multivalent ions to this parameter. These salt concentrations meant we were examining the behaviour of our surfactants at much higher ionic strengths than those studied by the Hirsch group,[183] and charge screening effects would be enhanced. TEM imaging was not undertaken for dispersions prepared in salt solutions as salt crystals formed upon sample drying were expected to obscure the images.

3.3.2: NaCl Solutions: Results

The results of MWNT dispersion studies in 0.6 M NaCl are shown in Figure 3.10 and Table 3.02. For comparison the results of the dispersion experiments in Millipore water are also shown in Figure 3.10. It was not possible to compare as with many reference surfactants under these conditions as most had insufficient solubility in 0.6 M NaCl. Similarly to the aqueous dispersions, reproducibility was generally good, although a larger variance was observed for some of the best performing surfactants. As before, the small error associated with ε is not included in the stated values. Figure 3.11 shows triplicate sets of centrifuged dispersions of MWNTs in 0.6 M NaCl solutions of **PyrB-PEG2-CH_2COG1(ONa)$_3$**, **PyrB-PEG4-CH_2COG1(ONa)$_3$** and **PyrB-PEG6-CH_2COG1(ONa)$_3$**. As for the aqueous dispersions, no precipitation of MWNTs was observed in dispersions stored for several months.

Table 3.02: C_{MWNT} in a range of 1 mM surfactant solutions in 0.6 M NaCl. Errors are the standard deviation of 3 results except for **PBA-(C6)$_2$-G2(ONa)$_9$** for which the data represents a single experiment only.

Surfactant	C_{MWNT} / mg L^{-1}	Error (σ) / mg L^{-1}	% MWNTs Dispersed
Triton X-100	73	4	22
PBA-G1(ONa)$_3$	4	0	1
PBA-C6-G1(ONa)$_3$	54	4	16
PBA-(C6)$_2$-G1(ONa)$_3$	76	6	23
PBA-G2(ONa)$_9$	18	0	5
PBA-C6-G2(ONa)$_9$	66	6	20
PBA-(C6)$_2$-G2(ONa)$_9$	78	-	23
PyrB-PEG2-CH_2COONa	48	3	15
PyrB-PEG4-CH_2COONa	88	7	27
PyrB-PEG6-CH_2COONa	131	18	39
PyrB-PEG12-CH_2COONa	165	22	49
PyrB-PEG2-CH_2COG1(ONa)$_3$	74	6	22
PyrB-PEG4-CH_2COG1(ONa)$_3$	114	11	34
PyrB-PEG6-CH_2COG1(ONa)$_3$	154	7	46

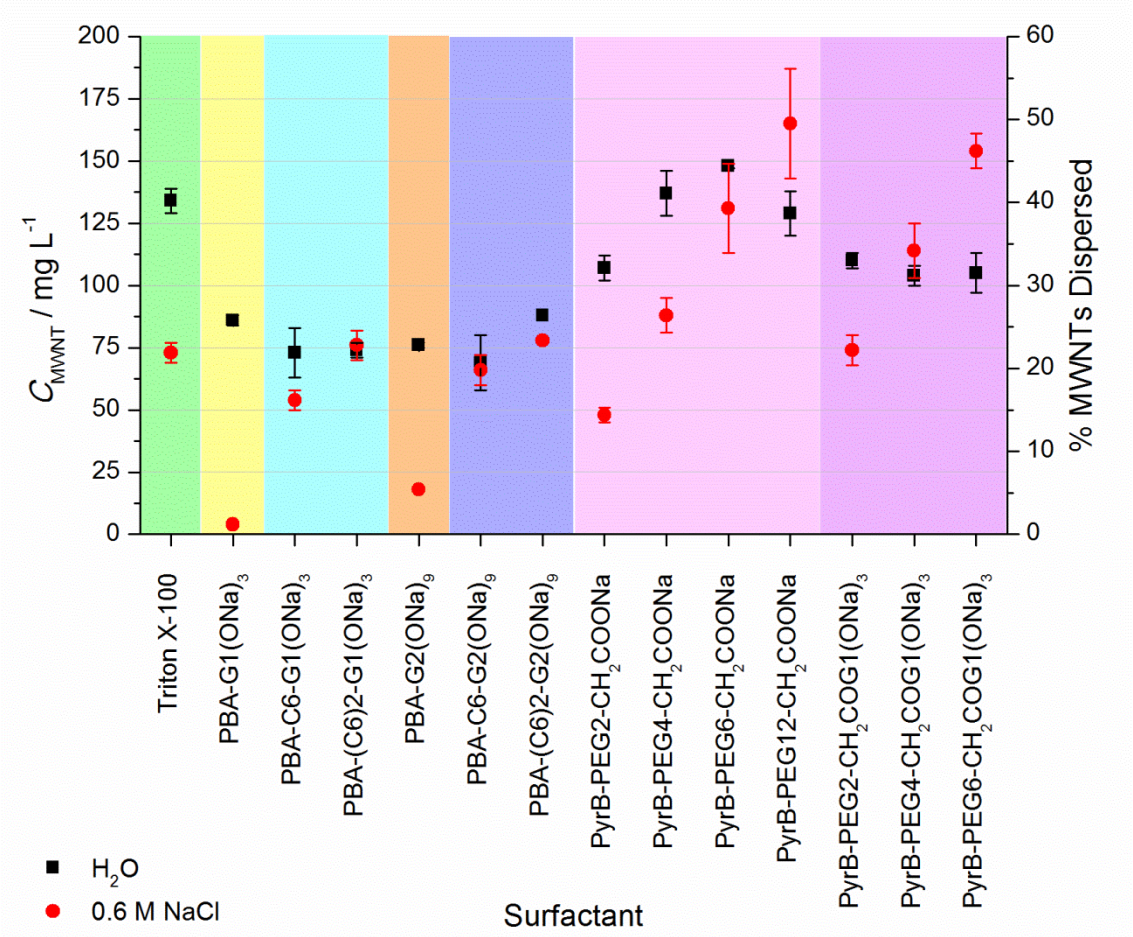

Figure 3.10: C_{MWNT} in a range of 1 mM surfactant solutions in Millipore water and 0.6 M NaCl. Error bars are the standard deviation of 3 results except for **PBA-(C6)$_2$-G2(ONa)$_9$** which represents a single experiment only. Colours indicate surfactant groups: green – commercial non-ionic; yellow – linker-free G1; light blue – amide linker G1; orange – linker-free G2; dark blue – amide linker G2; pink – ether linker G0; purple – ether linker G1.

Figure 3.11: Photographs of MWNTs dispersions in 0.6 M NaCl solutions of **PyrB-PEG6-CH$_2$COG1(ONa)$_3$** (first to third from left), **PyrB-PEG4-CH$_2$COG1(ONa)$_3$** (fourth to sixth from left) and **PyrB-PEG2-CH$_2$COG1(ONa)$_3$** (seventh to ninth from left).

3.3.3: NaCl Solutions: Commercial and Reference Surfactants

The only commercial surfactant tested in 0.6 M NaCl was **Triton X-100**. **SDS**, **SDBS**, **SC**, **SDOC** and **SPB** are insufficiently soluble to use under these conditions at the desired 1mM concentration. The C_{MWNT} for **Triton X-100** in 0.6 M NaCl was 73 ± 4 mg L^{-1}, almost half that obtained in Millipore water. This indicates that NaCl has a significant negative effect on this surfactant's performance as a MWNT dispersant. Phillies and Yambert have shown that both the size and micelle aggregation number (i.e. the average number of surfactant molecules making up a micelle) of **Triton X-100** micelles increase with NaCl concentration, and also suggest that a change of micelle shape may occur.[186] Conveniently they include data collected in both Millipore water and 0.6 M NaCl, which shows an increase in micelle radius from 43 to 56 Å (equivalent to a more than two-fold increase in volume, assuming spherical micelles), and in micelle aggregation number from 79 to 125 (an increase by a factor of more than 1.5) in the latter case. It is not unreasonable to link this known substantial change in micelle behaviour to the reduction in C_{MWNT} we observe. The increase in micelle size indicates an increased affinity of surfactant molecules for one another, which may make it more difficult to individualise surfactant-functionalised MWNTs. It is also known that addition of salt to a solution of **Triton X-100** (or other non-ionic surfactants) reduces the cloud point of the solution, or conversely, moves the system closer to its cloud point.[186] At the cloud point, the surfactant becomes immiscible with water. It follows that if the surfactant is brought closer to its cloud point by addition of salt it becomes less hydrophilic (in agreement with the formation of larger micelles discussed above), which would reduce its ability to act as a dispersant. In the case of our work, this would result in a reduced C_{MWNT}. Attempts to exploit the change in surfactant behaviour at the cloud point by varying temperature will be discussed in more detail in Chapters 4 and 5.

3.3.4: NaCl Solutions: Linker-Free and Amide Linker Surfactants

Linker-free surfactants **PBA-G1(ONa)$_3$** and **PBA-G2(ONa)$_9$** both showed very significant reductions in C_{MWNT} when tested in 0.6 M NaCl rather than Millipore water. C_{MWNT} for **PBA-G1(ONa)$_3$** fell from 86 ± 2 to 4 ± 0 mg L^{-1} (26% to 1%) and for **PBA-G2(ONa)$_9$** fell from 76 ± 1 to 18 ± 0 mg L^{-1} (23% to 5%). Clearly the presence of (at least sodium and chloride) ions is unfavourable for producing MWNT dispersions using these surfactants. This can be explained by considering the ionic screening effect of the dissolved electrolyte. The term ionic screening is used here to mean the extent to which the effective charge of ionic groups

belonging to surfactants is reduced by surrounding ions, and as such is related to the Debye length, κ^{-1}, of the medium in which the surfactant is dissolved. A lower Debye length implies higher ionic screening. If the anionic moieties of a surfactant head group are screened its ability to disperse CNTs through coulombic repulsions will be reduced. This may be mitigated against to an extent, as ionic screening will also reduce the volume occupied by a head group due to coulomb interactions, allowing for improved surface coverage (i.e. lower A_{surf}) compared to that in Millipore water. It appears that in these cases the screening effect of 0.6 M NaCl is sufficient to overcome any benefit from reduced A_{surf}. The opposite effect was observed by the Hirsch group, who saw an increase in C_{MWNT} when ionic strength was increased from 0.005 M to 0.09 M.[183] It follows that the weaker screening at these levels does not overcome the beneficial effect of reduced A_{surf}.

As the dispersions in Millipore water were prepared using surfactants in salt form with no additional ions present due to excess base or buffer solutions, the effect of ions other than surfactant molecules and their counter ions is negligible, associated with only the very low levels of dissociated water molecules. This means that there is essentially no ionic screening and functionalised MWNTs repel one another strongly over long distances, resulting in successful dispersion of MWNTs despite a high A_{surf}. In salt solutions the range of this repulsive interaction will be considerably reduced by ionic screening, somewhat inhibiting MWNT dispersion and individualisation, while allowing for increased A_{surf} which may counteract this effect. These two scenarios are illustrated in Figure 3.12. The effect of ionic screening can be linked to the Debye length, κ^{-1}, of the medium, which indicates the distance over which the effect of a charge is felt. A shorter Debye length therefore represents increased ionic screening. Ignoring the effect of surfactants (which we use at much lower concentrations than the electrolyte), the Debye length, in nm, can be calculated for a range of electrolytes using the equations[187] below:

$$\kappa^{-1} = \frac{0.304}{\sqrt{[MX]}} \quad \text{(for 1:1 electrolytes } M^+X^-\text{)}$$

$$\kappa^{-1} = \frac{0.176}{\sqrt{[MX_2]}} \; or \; \frac{0.176}{\sqrt{[M_2X]}} \quad \text{(for 1:2 or 2:1 electrolytes } M^{2+}X^-{}_2 \text{ or } M^+{}_2X^{2-}\text{)}$$

$$\kappa^{-1} = \frac{0.152}{\sqrt{[MX]}} \quad \text{(for 2:2 electrolytes } M^{2+}X^{2-}\text{)}$$

These allow the Debye length of deionised water to be calculated as 961 nm and that of 0.6 M NaCl as 0.392 nm, i.e. a reduction of more than 3 orders of magnitude, implying a significant increase in ionic screening. On this basis it is unsurprising that the addition of 0.6 M NaCl can significantly inhibit MWNT dispersion. The higher C_{MWNT} obtained for **PBA-G2(ONa)$_9$** in

comparison to **PBA-G1(ONa)$_3$** reflects the higher charge on the G2 head group. As the G2 head group includes 9 carboxylate moieties, it is less adversely affected by ionic screening than the G1 head group, which includes only 3 carboxylate moieties. Although the G2 head group is sterically bulkier than the G1 head group we do not believe that this would increase A_{surf} significantly. A_{surf} for **PBA-G2(ONa)$_9$** would have to be three times that of **PBA-G1(ONa)$_3$** for the overall charge on a **PBA-G2(ONa)$_9$**-functionalised MWNT to be as low as on a **PBA-G1(ONa)$_3$**-functionalised MWNT. The higher MWNT charge density for the G2 surfactant results in higher C_{MWNT}.

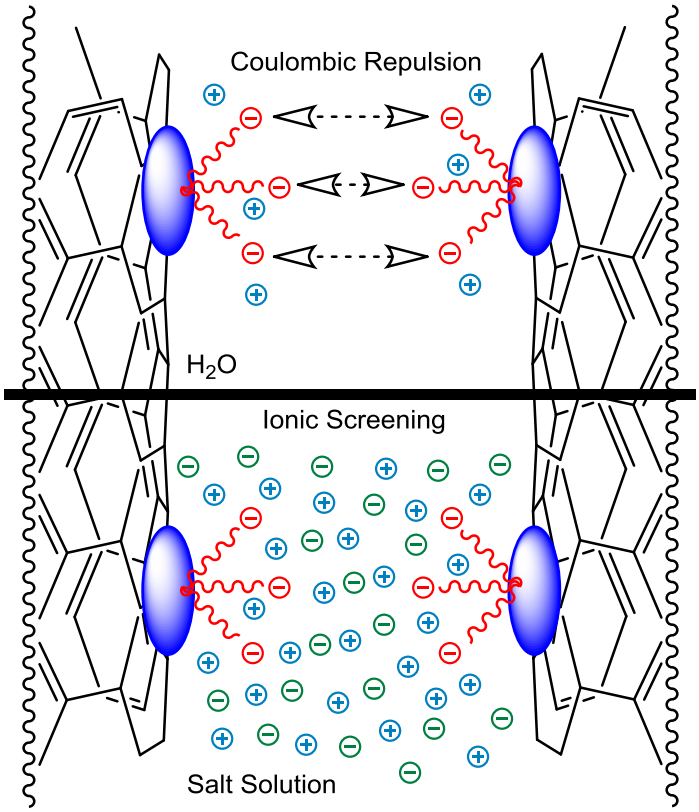

Figure 3.12: The addition of a salt to the surfactant solution used to disperse MWNTs significantly reduces the effect of coulombic repulsion between functionalised MWNTs due to ionic screening effects. This is illustrated above using a linker-free G1 surfactant and a simple 1:1 electrolyte in which the cation is the same as the surfactant's counter-ion. For clarity a SWNT is used to represent a MWNT surface. Not to scale.

In contrast to the linker-free surfactants, reasonable levels of MWNT dispersion could be achieved with the amide linker surfactants in 0.6 M NaCl. C_{MWNT} ranged from 54 ± 4 mg L^{-1} (16%) for **PBA-C6-G1(ONa)$_3$** to 78 mg L^{-1} (23%) for **PBA-(C6)$_2$-G2(ONa)$_9$**, approaching the levels obtained for commercial surfactants in Millipore water. These results for the amide linker surfactants contrast with those in Millipore water, in which the linker-free surfactants generally gave higher C_{MWNT} than the corresponding amide linker species. As we have seen

that 0.6 M has a negative effect on ionic head groups it appears that the linker unit plays a key role in facilitating MWNT dispersion in the presence of NaCl. For the G1 series it can be seen that adding one C6 linker results in a significant increase in C_{MWNT} compared to the linker-free analogue (54 ± 4 *vs.* 4 ± 0 mg L^{-1} (16% *vs.* 1%)), and the addition of a second C6 linker increases C_{MWNT} further (76 ± 6 mg L^{-1} (23%)), by around half as much as the addition of the first linker. For **PBA-(C6)$_2$-G1(ONa)$_3$**, C_{MWNT} in 0.6 M NaCl and Millipore water are within error of one another. The G2 series follows the same trend, with a large increase in C_{MWNT} when the surfactant with a single C6 linker is compared to the linker-free species (66 ± 6 *vs.* 18 ± 0 mg L^{-1} (20% *vs.* 5%)), and a smaller increase in the case of the surfactant with two C6 linkers (78 mg L^{-1} (23%)). In this case, C_{MWNT} in 0.6 M NaCl is slightly less than, but within error of, that obtained in Millipore water for **PBA-C6-G2(ONa)$_9$** but is lower than the Millipore water result in the case of **PBA-(C6)$_2$-G2(ONa)$_3$** (although results for this species are less reliable as they represent a single experiment only under both conditions).

The difference in the trends observed in Millipore water and 0.6 M NaCl imply that one or both of the following interactions are occurring: i) amide oxygen atoms are interacting with sodium ions; or ii) amide 'N-H' moieties are interacting with chloride ions. We note that hydrogen bonding could play a similar but weaker role in Millipore water, however, its effect is expected to be significantly disrupted in the presence of salt, and the results in Millipore water do not indicate that amide linker addition is favourable. We propose that these ion-dipole interactions increase the hydrophilicity of a functionalised MWNT surface, facilitating dispersion. This could be due to the attraction of ions towards the MWNT surface increasing the charge density in this space, and may also involve the spheres of hydration associated with the attracted ions which could help to 'wet' the area around the MWNT surface. Either or both of these effects would serve to screen the hydrophobicity of the MWNT surface.

Although an amide bond is present in the linker-free species, it is rather sterically hindered by the quaternary centre of the head group and its proximity to the MWNT surface due to the short distance between it and the pyrene anchor. This appears to reduce the effectiveness of any favourable interactions with salt for these species, resulting in the low C_{MWNT} obtained in 0.6 M NaCl. This observation may also help to explain the smaller increase in C_{MWNT} between species with one and two linkers compared to that between linker-free species and those with one linker. Compared to the rather hindered amide bond of linker-free species, the two amides are much more available to interact with salt, as each is sterically shielded on one side

only. Hence the effect of adding the C6 linker is closer to the addition of two amide moieties. Addition of a second linker adds only one more amide; hence the increase in C_{MWNT} is lower than when two linkers were made fully available. These proposed interactions are illustrated in Figure 3.13.

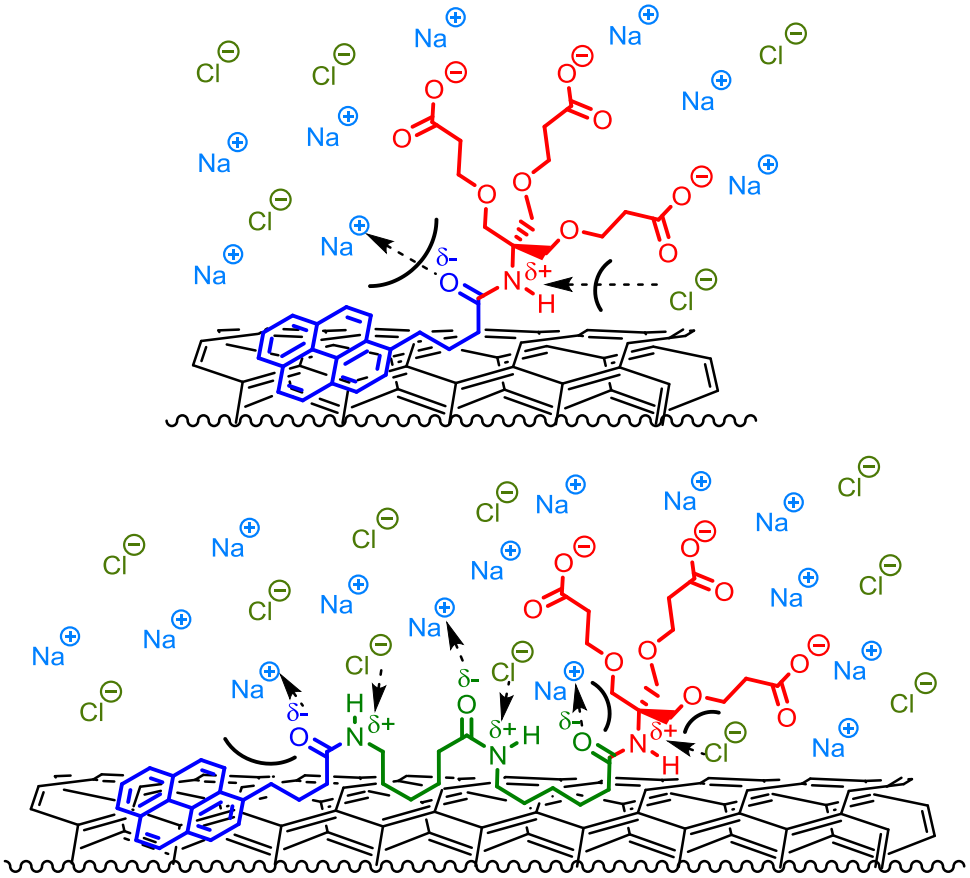

Figure 3.13: Illustration of possible interactions occurring between NaCl solution and MWNTs functionalised with **PBA-G1(ONa)$_3$** (top) or **PBA-(C6)$_2$-G1(ONa)$_3$** (bottom). The favoured orientation of the linker is unknown; here it is suggested that it lies along the MWNT surface due to the presence of hydrophobic alkyl units, with the amide moieties directed into the water. For clarity a SWNT is shown to represent a MWNT surface.

The increase in C_{MWNT} on addition of the first linker is very similar for both series, around 50 mg L^{-1}. This suggests that in 0.6 M NaCl the differing head groups provide a 'base level' of C_{MWNT} and the addition of the linker makes a further contribution, an observation supported by the trends observed below for the ether linker surfactants. The increase in C_{MWNT} upon addition of a second linker shows more variation. Data for additional members of each series would be needed to attempt to quantify any trends associated with linker length.

3.3.5: NaCl Solutions: Ether Linker Surfactants

Like the amide linker surfactants, the ether linker species afforded at least reasonable levels of C_{MWNT} in 0.6 M NaCl, relative to typical levels for commercial surfactants in Millipore water. Both the G0 and G1 series show an increase in C_{MWNT} with linker length, paralleling the trends observed for both amide linker series in 0.6 M NaCl and for the G0 ether linker series in Millipore water. Unlike the amide linker series, where the highest levels of C_{MWNT} in 0.6 M NaCl were comparable to those obtained in Millipore water, for some ether linker surfactants C_{MWNT} is higher in 0.6 M NaCl. For the G0 series this is observed only for **PyrB-PEG12-CH_2COONa**, which gave the highest C_{MWNT} of any of the materials discussed in this chapter under any conditions, 165 ± 22 mg L^{-1} (49%). The G0 surfactants with shorter OEG linkers, **PyrB-PEG2-CH_2COONa** and **PyrB-PEG4-CH_2COONa**, both perform significantly worse in 0.6 M NaCl, giving C_{MWNT} levels considerably lower than those obtained in Millipore water. The other member of the series, **PyrB-PEG6-CH_2COONa**, gives a level much closer to that obtained previously in Millipore water. The G1 series includes examples of a surfactant which performs worse in 0.6 M NaCl than in Millipore water (**PyrB-PEG2-CH_2COG1(ONa)$_3$**), one which performs slightly better (**PyrB-PEG4-CH_2COG1(ONa)$_3$**) and a third which shows a considerable improvement (**PyrB-PEG6-CH_2COG1(ONa)$_3$**). The latter gives the second highest C_{MWNT} reported in this Chapter, 154 ± 7 mg L^{-1} (46%). Unlike in Millipore water, the G1 surfactants consistently outperform their G0 analogues. This mirrors the results for the amide linker species in 0.6 M NaCl, where G2 surfactants tended to give higher C_{MWNT} than the analogous G1 species, and can be explained in the same way: the presence of three anionic carboxylate moieties in a G1 head group means it is less adversely affected by ionic screening than a simple monocarboxylate G0 head group.

These trends indicate an interaction between ether oxygen atoms and dissolved cations which increases the hydrophilicity of functionalised MWNTs. Interactions between dissolved ions and the amide bond to the G1 head group are also possible in the case of G1 surfactants. Figure 3.14 illustrates these proposed interactions.

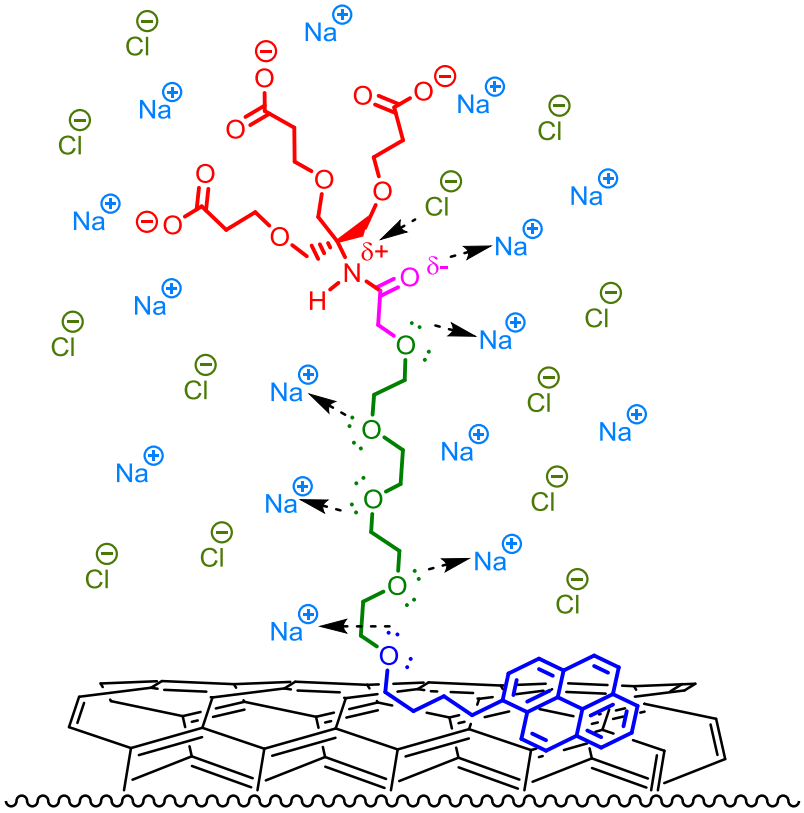

Figure 3.14: Illustration of possible interactions occurring between NaCl solution and MWNTs functionalised with **PyrB-PEG4-CH$_2$COG1(ONa)$_3$**. The favoured orientation of the linker is unknown; here it is suggested that it projects into the aqueous medium due to its hydrophilicity. For clarity a SWNT is shown to represent a MWNT surface.

A linear relationship is seen between C_{MWNT} in 0.6 M NaCl and linker length for both series. The number of ether moieties available to interact with dissolved ions will be used as a measure of linker length (this value is one more than the number of PEG repeat units in the linker chain). For each series the linear trend can be observed for surfactants with PEG2, PEG4 and PEG6 linkers. The measured C_{MWNT} in 0.6 M NaCl for these G0 materials (**PyrB-PEG2-CH$_2$COONa**, **PyrB-PEG4-CH$_2$COONa** and **PyrB-PEG6-CH$_2$COONa**) fit the formula $C_{MWNT} = 20m - 13$, where m represents the number of ether moieties able to interact with salt, well. In the case of the G1 surfactants (**PyrB-PEG2-CH$_2$COG1(ONa)$_3$**, **PyrB-PEG4-CH$_2$COG1(ONa)$_3$** and **PyrB-PEG6-CH$_2$COG1(ONa)$_3$**) the formula $C_{MWNT} = 20m + 14$ fits the results. The formulae are compared to the experimental data in Figure 3.15. Notably both series follow a trend of the same gradient, indicating that changes to the linker have the same effect in both cases. These trends may not extrapolate beyond m = 7; the result for **PyrB-PEG12-CH$_2$COONa** is indicative of a change in behaviour at some point beyond this for at least the G0 series. Unlike in Millipore water, in 0.6 M NaCl **PyrB-PEG12-CH$_2$COONa** gives a higher C_{MWNT} than its shorter-linker analogues. This further indicates that favourable interactions occur between the OEG linker and dissolved ions, but

makes it difficult to determine whether the optimal linker length under these conditions is longer or shorter than PEG12 without further results. It also suggests that the combination of an OEG linker and anionic carboxylate group is important, as **Triton X-100**, which has a similar (average 9.5 repeat units) PEG chain but a non-ionic head group gives much lower C_{MWNT} in 0.6 M NaCl than Millipore water.

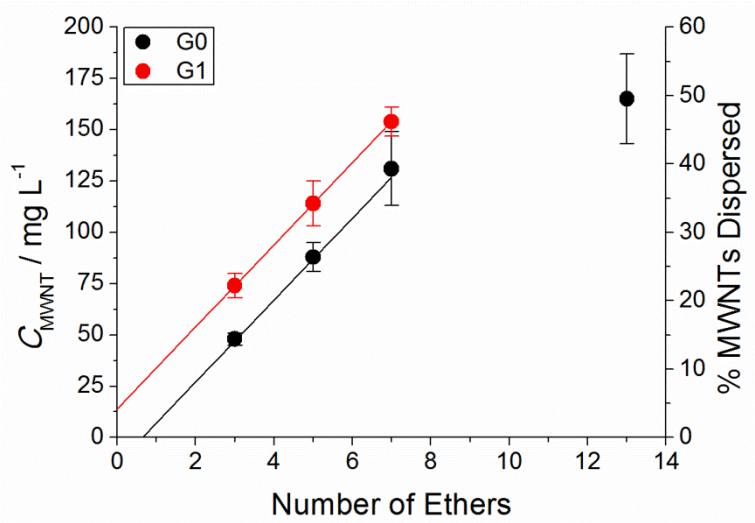

Figure 3.15: C_{MWNT} of dispersions obtained using 1 mM solutions of ether linker surfactants with G1 and G2 head groups in 0.6 M NaCl. Error bars are the standard deviation of 3 results.

To explain these trends a model is proposed in which C_{MWNT} in 0.6 M NaCl for PyrB-anchored surfactants is influenced by two factors: one relating to the head group of the surfactant and another relating to the linker. The intercept represents the contribution of the head group to C_{MWNT} and is larger for species where the head group has higher charge and is less significantly affected by ionic screening. It also represents the C_{MWNT} expected for a linker-free surfactant. The gradient represents the increase in C_{MWNT} due to the addition of linkers, and relates to the positive effect of interactions between ether oxygen atoms and sodium cations.

It can be concluded that for at least anionic surfactants incorporating an anchor derived from **PyrBOH** and a linker of m-1 PEG repeat units (i.e. m ether moieties in the anchor linker ensemble), for values of m up to at least 7, C_{MWNT} in 0.6 M NaCl using 1 mM surfactant solutions can be predicted by the formula:

$$C_{MWNT} \approx 20m + G$$

Where m is the number of ether moieties available to interact with salt and G is a constant for a given head group (-13 for G0 and +14 for G1). Changing the concentration of NaCl would be expected to affect both the gradient and intercept, as both values are influenced by

surfactant-salt interactions. The effect of other salts is examined below. Alterations to the anchor group may also have an influence, possibly causing changes to *G*.

In the case of the G1 series *G* includes the effect of the amide moiety, which should have the same effect in all cases as its environment does not significantly change. The exception is the linker-free surfactant **PBA-G1(ONa)$_3$** (m = 0); we proposed above that steric effects hinder interactions between its amide moiety and dissolved ions. This is reflected in a discrepancy between the value predicted by the formula above and the observed C_{MWNT} for **PBA-G1(ONa)$_3$**. The difference between the observed value of 4 ± 0 mg L^{-1} and the predicted value of 14 mg L^{-1} does not, however, appear to relate quantitatively to the trends in C_{MWNT} observed for the amide linker surfactants. *G* is larger for species which are less affected by ionic screening; the negative *G* for the GO series indicates that NaCl has a substantial adverse impact on this head group. It also suggests that 1 mM **SPB** would not disperse MWNTs in 0.6 M NaCl. The fact that the low solubility of **SPB** in this medium means a 1 mM solution cannot be produced supports this prediction.

3.3.6: Other Salts: Results

Selected surfactants were tested for their ability to disperse MWNTs in the presence of other salts. The effect of 0.6 M KCl and 0.3 M $CaCl_2$ on linker-free and amide linker materials was investigated using the G1 surfactants. For the ether linker surfactants the effect of these salts was examined using **PyrB-PEG6-CH$_2$COONa** and that of a wider range of salts using **PyrB-PEG6-CH$_2$COG1(ONa)$_3$**. The results for the linker-free and amide linker surfactants are shown in Figure 3.16 and Table 3.03, and those for the ether linker surfactants in Figure 3.17 and Table 3.04. The small error associated with ε is not included in the data.

Table 3.03: C_{MWNT} obtained using 1 mM solutions of G1 linker-free and amide linker surfactants in 0.6 M KCl and 0.3 M $CaCl_2$. Errors are the standard deviation of 3 results.

	0.6 M KCl			0.3 M $CaCl_2$		
Surfactant	**C_{MWNT} / mg L^{-1}**	**Error (σ) / mg L^{-1}**	**% MWNTs Dispersed**	**C_{MWNT} / mg L^{-1}**	**Error (σ) / mg L^{-1}**	**% MWNTs Dispersed**
PBA-G1(ONa)$_3$	17	4	5	0	0	0
PBA-C6-G1(ONa)$_3$	81	10	24	0	0	0
PBA-(C6)$_2$-G1(ONa)$_3$	91	4	27	-	-	-

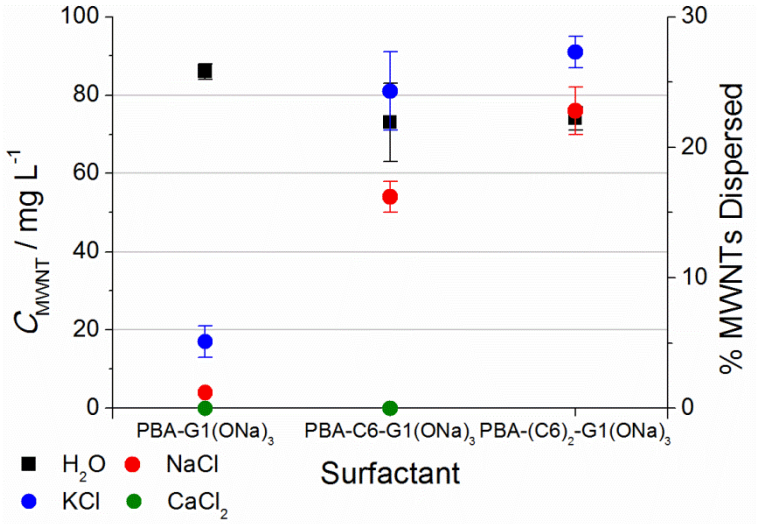

Figure 3.16: C_{MWNT} obtained using 1 mM solutions of G1 linker-free and amide linker surfactants in Millipore water and various salt solutions. Error bars are the standard deviation of 3 results.

Table 3.04: C_{MWNT} obtained using 1 mM solutions of selected ether linker surfactants in various salt solutions. Errors are the standard deviation of 3 results.

Surfactant	Salt Solution	C_{MWNT} / mg L^{-1}	Error (σ) / mg L^{-1}	% MWNTs Dispersed
PyrB-PEG6-CH$_2$COONa	0.6 M KCl	130	1	39
PyrB-PEG6-CH$_2$COONa	0.3 M CaCl$_2$	12	1	4
PyrB-PEG6-CH$_2$COG1(ONa)$_3$	0.6 M KCl	144	8	43
PyrB-PEG6-CH$_2$COG1(ONa)$_3$	0.3 M CaCl$_2$	3	1	1
PyrB-PEG6-CH$_2$COG1(ONa)$_3$	0.6 M NaI	130	2	39
PyrB-PEG6-CH$_2$COG1(ONa)$_3$	0.6 M KI	133	6	40
PyrB-PEG6-CH$_2$COG1(ONa)$_3$	0.3 M NaCl + 0.15 M CaCl$_2$	14	0	4

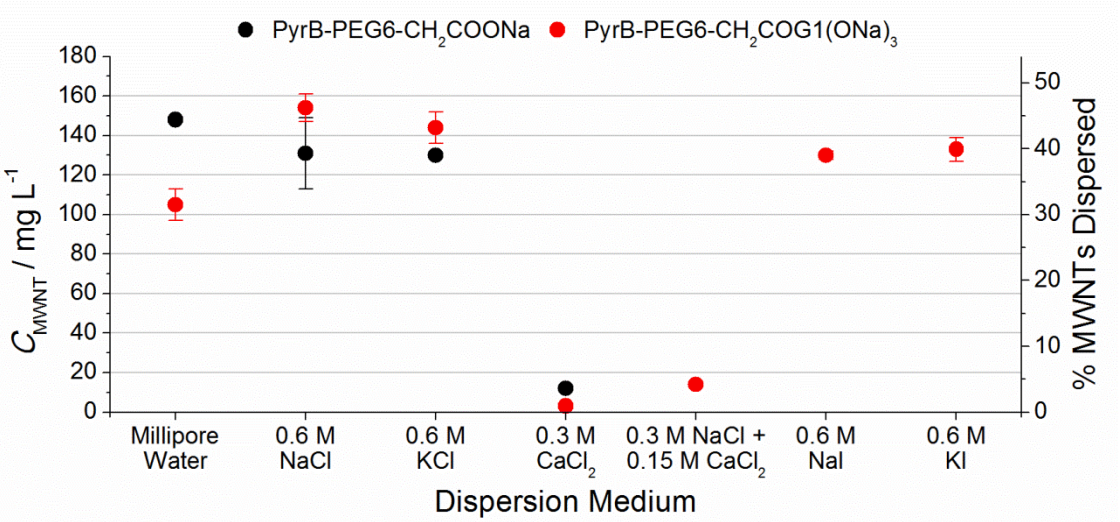

Figure 3.17: C_{MWNT} obtained using 1 mM solutions of selected ether linker surfactants in Millipore water and various salt solutions. Error bars are the standard deviation of 3 results.

3.3.7: Other Salts: Linker-Free and Amide Linker Surfactants

C_{MWNT} for linker-free **PBA-G1(ONa)$_3$** in 0.6 M KCl is significantly lower than in Millipore water (17 ± 4 mg L^{-1} *vs.* 86 ± 4 mg L^{-1} (5% *vs.* 26%)). This effect is similar to that of 0.6 M NaCl, although C_{MWNT} is higher in 0.6 M KCl. The two amide linker surfactants both give a higher C_{MWNT} in 0.6 M KCl than in either Millipore water or 0.6 M NaCl. The overall trend along the series is similar to that in 0.6 M NaCl: a large increase in C_{MWNT} upon addition of the first C6 linker followed by a smaller increase upon addition of the second. The magnitudes of these increases are similar for both salts. These results fit our previous hypotheses well. The ionic screening effect should be the same for both 0.6 M NaCl and KCl as equimolar solutions of 1:1 electrolytes have the same Debye length. Amides are known to interact slightly more favourably with potassium ions than with sodium ions due to their lower hydration enthalpy.[188,189] These stronger interactions explain the observed increase in C_{MWNT} in KCl. It appears that the cumulative effect of these slightly more favourable interactions with many amide groups induces a reasonably large change in C_{MWNT}. The increase in C_{MWNT} for **PBA-G1(ONa)$_3$** in 0.6 M KCl relative to 0.6 M NaCl indicates that its amide moiety is not completely sterically hindered, but that it is still sufficiently shielded to prevent ion-dipole interactions from overcoming the effect of ionic screening.

Attempts to disperse MWNTs in 0.3 M $CaCl_2$ using both **PBA-G1(ONa)$_3$** and **PBA-C6-G1(ONa)$_3$** resulted in no observable dispersion. We propose three factors which may contribute to this behaviour. Firstly, this medium has a slightly reduced Debye length compared to 0.6 M NaCl and KCl (0.321 nm *vs.* 0.392 nm) which would result in an increased ionic screening effect. Secondly, the formation of insoluble calcium salts of anionic surfactants is well known, as seen in the formation of soap scum with hard water.[190,191] While it was possible to produce 1 mM surfactant solutions in this medium without observing precipitate formation, conversion of the sodium salts to calcium salts would be expected based on the large excess of calcium ions in solution. Chelation of carboxylate groups to calcium ions could reduce the efficacy of our surfactants as MWNT dispersants. Finally, the hydration enthalpy of calcium ions is considerably larger than that of sodium and potassium ions, making cation-amide interactions much less favourable.

3.3.8: Other Salts: Ether Linker Surfactants

In 0.6 M KCl both **PyrB-PEG6-CH_2COONa** and **PyrB-PEG6-CH_2COG1(ONa)$_3$** give C_{MWNT} within error of that in 0.6 M NaCl, with a larger discrepancy in the latter case. This suggests that the two cations have essentially the same effect on ether linker surfactants, unlike amide linker surfactants. As discussed above, the ionic screening effect of the two salt solutions should be the same. This leads us to conclude that the interaction between ether oxygen atoms and alkali metal cations is not affected by hydration enthalpy to the same extent as that between amide oxygen atoms and cations.

The effect of calcium ions on the ether linker surfactants is almost as dramatic as that on amide linker surfactants. For both **PyrB-PEG6-CH_2COONa** and **PyrB-PEG6-CH_2COG1(ONa)$_3$**, however, it was possible to achieve dispersion of a small quantity of MWNTs. C_{MWNT} was 12 ± 1 mg L^{-1} (4%) and 3 ± 1 mg L^{-1} (1%) respectively. These are very low levels compared to Millipore water, 0.6M NaCl or 0.6 M KCl. To see if the negative effect of calcium ions could be overcome we investigated the ability of **PyrB-PEG6-CH_2COG1(ONa)$_3$** to disperse MWNTs in a mixed solution of NaCl and $CaCl_2$. Compared to Millipore water, this surfactant shows a higher C_{MWNT} in 0.6 M NaCl (by a factor of *ca.* 1.5) and a much lower C_{MWNT} in 0.3 M $CaCl_2$ (by a factor of *ca.* 35). A solution that was 0.3 M in NaCl and 0.15 M in $CaCl_2$ was used to maintain the overall 0.6 M 'concentration' of positive charge and 0.6 M concentration of chloride. The resulting C_{MWNT} of 14 ± 0 mg L^{-1} (4%) represented a small improvement compared to 0.3 M $CaCl_2$, but was still very low. As C_{MWNT} remains low under these conditions we propose that the formation of poorly soluble calcium carboxylate chelates is the main reason for the negative effect of calcium ions. We expect that using a much higher proportion of sodium ions could allow higher dispersion levels to be reached by shifting equilibrium in favour of sodium carboxylates, but have not investigated this further.

The effect of changing the anion was investigated by preparing MWNT dispersions in solutions of **PyrB-PEG6-CH_2COG1(ONa)$_3$** in 0.6 M NaI and KI. The ionic strength of these solutions should be the same as the analogous chloride salts, meaning the effect of ionic screening should be the same and any changes relate solely to the change in cation. As observed above, the choice of alkali metal cation had no significant effect on C_{MWNT}. The change from chloride to iodide resulted in a small decrease in C_{MWNT} in both cases, although the results for the potassium salts were within error. As anions should not interact significantly with the OEG linker we propose that this relates to differing interactions between the head group amide and the two cations. This could be confirmed by investigating

the effect of iodide on amide linker or G0 ether linker surfactants. The former would be expected to give lower C_{MWNT} when chloride is replaced by iodide; the latter would be expected to show no change.

3.4: Stimulus Response Tests

The previous section indicated that MWNT dispersions in our surfactants were sensitive to the presence of ions. We were keen to investigate whether the dispersions would respond to other stimuli. Sensitivity to pH was possible in all of our surfactants due to the presence of carboxylate moieties. At low pH these should be converted to less hydrophilic carboxylic acids, which could impact on the stability of the dispersions. The addition of acid to alter the pH of a dispersion would result in the formation of sodium salts, therefore we investigated this effect using surfactants which were shown (in Section 3.3) to have little sensitivity to NaCl, **PyrB-PEG6-CH_2COONa** and **PBA-(C6)$_2$-G1(ONa)$_3$**. This allows us to be confident that any response observed relates to the change in pH, not the presence of NaCl. We tested dispersions of MWNTs formed using these surfactants in both Millipore water and 0.6 M NaCl for a pH response.

Neat MWNT-surfactant dispersions prepared using our standard method were divided into three 0.5 ml aliquots. Two of these were treated with 25 μL of 1 M HCl solution (the third was used as a control) and the samples were left overnight under ambient conditions. This is an excess of acid compared to the surfactant carboxylate groups (*ca.* 50 or 17 equivalents for G0 or G1 surfactants, respectively) which ensures the dispersion is at an acidic pH. The addition of acid means the dispersion volume is increased by 5%, but dilution has no effect on dispersion stability. In all cases this resulted in the formation of a black precipitate in the acid-treated samples, with no change to the untreated control sample. One of the acid-treated samples was then treated with 25 μL of 1 M NaOH to neutralise added acid (again increasing the dispersion volume by 5% relative to the initial 0.5 ml). Gentle agitation of the base-treated sample by swirling for only 2 s was sufficient to re-disperse the precipitate, which remained stable for more than 1 week. When the remaining acid-treated samples dispersed using **PyrB-PEG6-CH_2COONa** were treated in the same way it was possible to re-suspend the precipitate; however it re-formed within *ca.* 90 min. We also observed that addition of an equivalent amount of 1 M HCl to a solution of **PyrB-PEG6-CH_2COONa** in Millipore water caused the solution to become cloudy. Phase separation occurred slowly over *ca.* 7 h. This surfactant is therefore insoluble in acidic media (this was exploited in the purification of G0

acids by acid-base workup). Representative images are shown in Figure 3.18. We are yet to test the sensitivity of this response to lower acid concentrations.

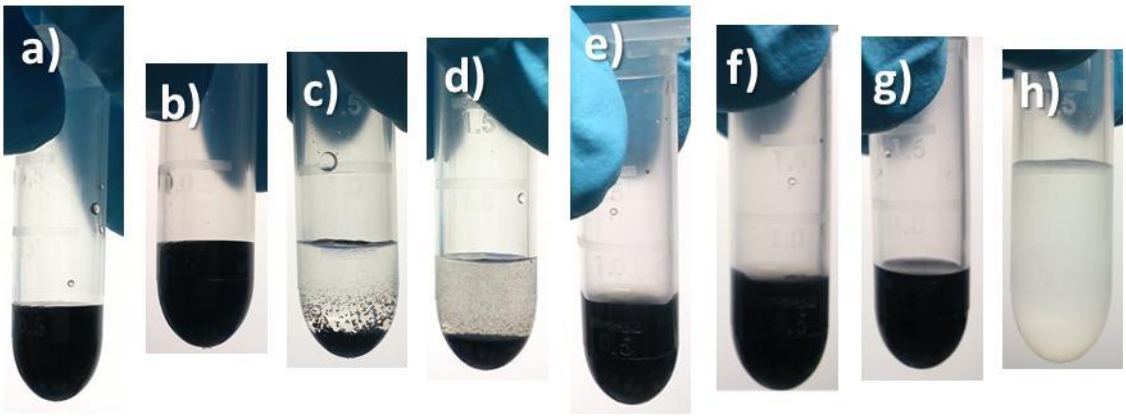

Figure 3.18: Images of MWNT dispersions and surfactant solution at various stages of the acid and base treatment process: a) MWNTs dispersed in 1 mM **PyrB-PEG6-CH$_2$COONa** in Millipore water, **A**; b) MWNTs dispersed in 1 mM **PyrB-PEG6-CH$_2$COONa** in 0.6 M NaCl, **B**; c) acid-treated **B** after standing overnight under ambient conditions; d) acid-treated **A** 1.5 h after re-suspending the precipitate which formed on standing overnight by gentle agitation; e) acid-treated **A** 1.5 h after base treatment and gentle agitation, **E**; f) **E** after a further 5 h; g) acid-treated **B** 6.5 h after base treatment and gentle agitation; h) 1 mM **PyrB-PEG6-CH$_2$COONa** in Millipore water after addition of HCl.

The significance of these results is that a *reversible* response has been induced in dispersions of MWNTs in our surfactants. We rationalise the observed behaviour as follows: addition of acid converts the carboxylate moieties into carboxylic acids, eliminating their ionic character. This means there is no longer any coulombic repulsion between functionalised MWNTs. Furthermore, the acid form of the surfactants is insoluble in acidic, aqueous media. The functionalised MWNTs are therefore hydrophobic, causing them to aggregate and precipitate due to hydrophobic interactions. The ease with which a stable dispersion can be re-formed following neutralisation is indicative that the surfactant remains bound to the MWNT surface throughout the process. If precipitation occurred due to stripping of the surfactant the unfunctionalised MWNTs would be expected to re-form bundles which would require ultrasonication to re-disperse. Treatment with base converts the carboxylic acids back to carboxylate salts, restoring their ionic character. This in turn means that the functionalised MWNTs again repel one another through coulombic interactions and are sufficiently hydrophilic to be dispersed in an aqueous medium. Re-dispersion is facile as the precipitated functionalised MWNTs are much more weakly bound than pristine MWNT bundles. This mechanism is illustrated in Figure 3.19. Our results are comparable with those reported by Ikeda *et al.* for SWNTs dispersed in basic solution using folic acid.[118]

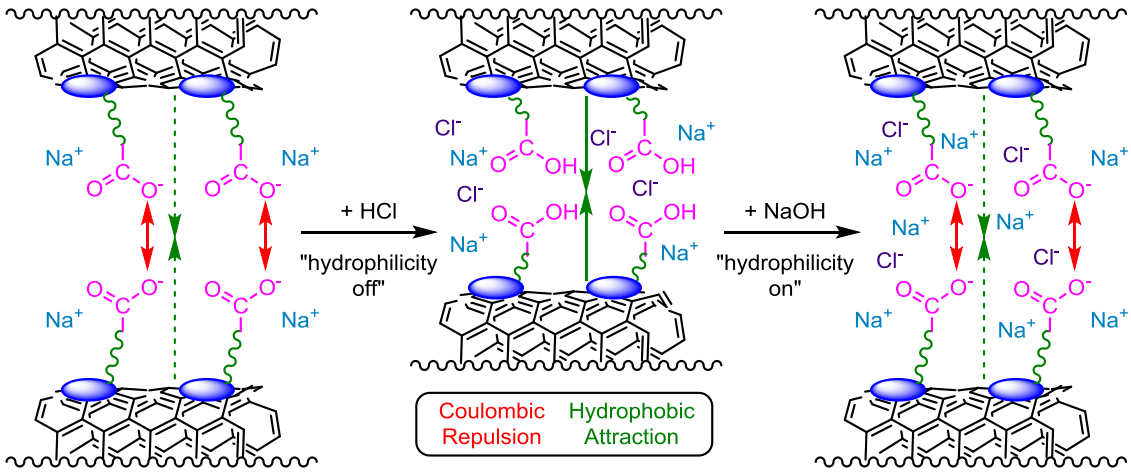

Figure 3.19: Proposed mechanism of acid-base triggered reversible dispersion of MWNTs For clarity a SWNT is shown to represent a MWNT surface, and a monocarboxylate surfactant is shown.

We were also interested in testing for a temperature response. In initial investigations, aliquots of selected dispersions were diluted tenfold with Millipore water or 0.6 M NaCl and examined using UV-visible spectroscopy at different temperatures (as for the determination of C_{MWNT}, dilution was required to achieve suitable levels of absorption). For these experiments the solutions were diluted with water, rather than the parent surfactant solution, to maintain the same MWNT:surfactant ratio as the parent dispersions. Dilution using the parent surfactant solution would increase the amount of surfactant available, which could affect possible equilibrium processes, for example if heating could strip surfactant molecules from the MWNT surface. Surfactant stripping on heating was observed by Ikeda *et al.* for folic acid stabilised SWNT dispersions in basic solution.[118] We hoped that this would be avoided by our use of pyrene anchors. To correct for any temperature response in the surfactant, the absorbance of a 0.1 mM surfactant solution at the same temperature was subtracted from that of the dispersion (although the surfactants displayed no observable absorbance at the relevant wavelength, 500 nm, within the studied temperature range). The incompatibility of the integrating sphere and temperature controller spectrometer accessories mean that the C_{MWNT} values obtained using this method differ slightly from those expected based on the results in Sections 3.2 and 3.3. Samples were heated from 20 to 80 °C in 10 °C increments and equilibrated for 5 min at each temperature before recording their absorption spectra. C_{MWNT} was calculated using the corrected absorbance at 500 nm and the previously calculated value of ε. No significant response was observed for any of the materials tested within the range 20-80 °C, as shown in Figure 3.20. This was the case across the examined spectral range of 190-1100 nm. Additionally, no precipitate could be seen at any point when samples were inspected by eye. Dispersions in the G1 surfactants were also examined using UV-visible transmittance (not shown). At 500 nm this was found to be equal

to zero at all temperatures for all surfactants tested. Clearly these materials do not display a temperature response between 20 and 80 °C, at least on the timescale of these experiments.

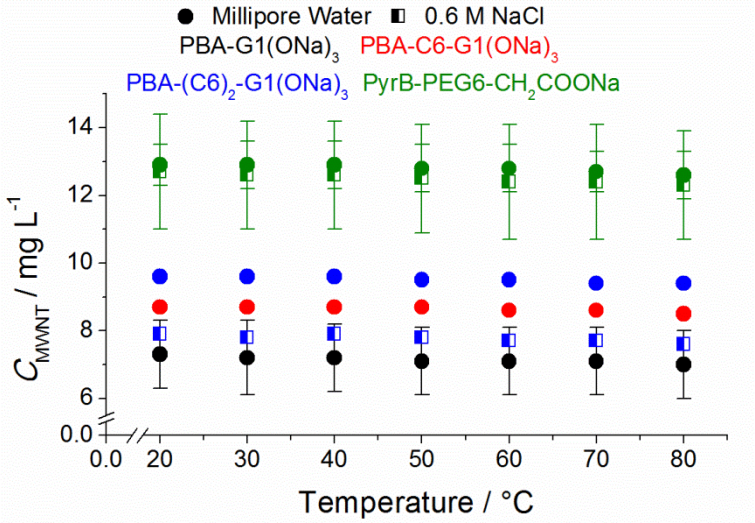

Figure 3.20: The effect of heating diluted MWNT dispersions in selected surfactants in Millipore water and 0.6 M NaCl. Where shown, error bars are the standard deviation of three results, otherwise the data represents a single experiment.

Undiluted dispersions of MWNTs in 1 mM **PyrB-PEG12-CH$_2$COONa** in both Millipore water and 0.6 M NaCl were similarly investigated by using 1 mm cuvettes rather than the 10 mm cuvettes used in all previous experiments (this has the same effect on absorbance as a tenfold dilution). As above, the absorbance of the parent surfactant solution was subtracted from that of the dispersion to account for any temperature response in the surfactant, and used to calculate C_{MWNT}. Again, no significant temperature response was observed in either case (Figure 3.21), and no visible precipitate could be seen. Holding the dispersions at 60 °C resulted in a small increase in absorbance, and hence C_{MWNT}, which is attributed to evaporation of water as no MWNT feedstock was available. Some loss of water can be seen in the images shown in Figure 3.21.

No further temperature response tests were conducted on MWNT dispersions formed using the anionic surfactants. We were subsequently able to demonstrate a temperature response using non-ionic surfactants (Chapters 4 and 5).

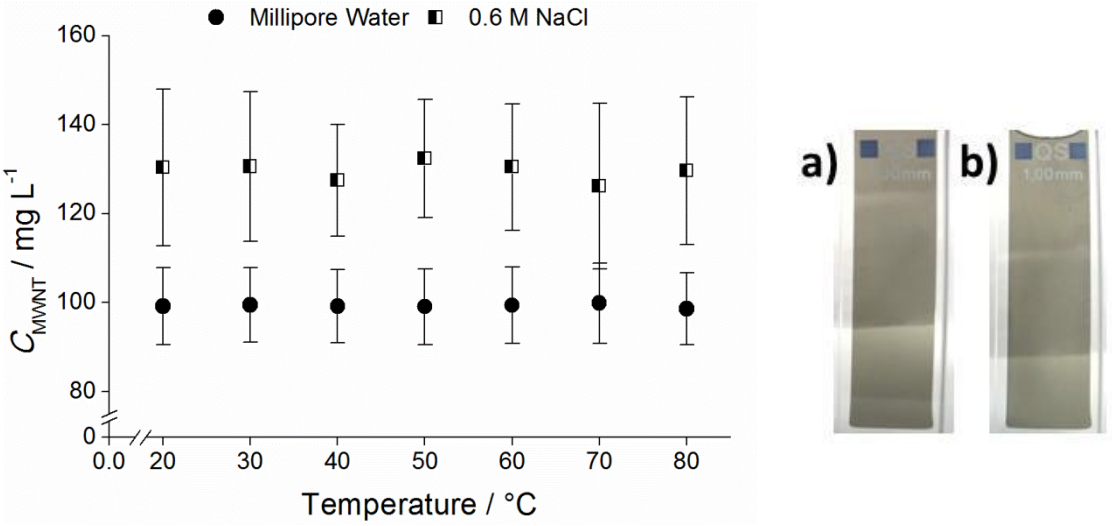

Figure 3.21: Left: The effect of heating MWNT dispersions in **PyrB-PEG12-CH$_2$COONa** in Millipore water and 0.6 M NaCl. Error bars are the standard deviation of three results. Right: MWNTs dispersed in **PyrB-PEG12-CH$_2$COONa** in Millipore water in a 1 mm cuvette: a) before heating; b) after heating from 20 to 80 °C, then at 60 °C overnight and cooling to 20 °C.

3.5: Conclusions

The ability of the ether linker surfactants synthesised in Chapter 2 to disperse MWNTs in aqueous media, including salt solutions, has been examined. In Millipore water the ether linker surfactants disperse MWNTs at least as well as commonly used commercial anionic surfactants under our standard conditions. They are also more effective than comparable linker-free and amide linker surfactants. The ability to disperse MWNTs was related to the charge density of functionalised MWNTs which is linked to the surface area occupied by each surfactant molecule. These properties are affected by the ionic strength of the dispersion medium: increased ionic strength reduces the range of coulombic repulsion, reducing the dispersive effect of surface charge but also allowing for increased surface coverage.[183] A combination of these factors and interactions between dissolved ions and the linker group means that surfactants can show increased, decreased or similar levels of MWNT dispersion in 0.6 M NaCl solution relative to Millipore water. These are dependent on surfactant structure; for example a longer OEG linker results in improved MWNT dispersion in 0.6 M NaCl. We examined the effect of other salts; KCl was found to have a similar effect to NaCl for ether linker surfactants, but resulted in higher dispersion concentrations for amide linker surfactants. $CaCl_2$ resulted in very low dispersion levels for all of the materials tested, which we propose is due to the formation of poorly soluble calcium carboxylates. We were also able to demonstrate a pH response in MWNT dispersions in both ether linker and amide linker surfactants. Addition of HCl resulted in precipitation of MWNTs which could be reversed by

addition of an equivalent quantity of NaOH. We were unable to observe a temperature response in any of the investigated dispersions.

Chapter 4: Synthesis of Non-Ionic Surfactants

This chapter describes the synthesis of two series of non-ionic surfactants fitting our Anchor-Linker-Head architecture. These species were designed to be responsive to temperature and potentially other stimuli. We describe the synthesis of surfactants with crown ether based head groups, followed by the synthesis of surfactants with podand based head groups which were designed to overcome some of the shortcomings of the crown ether compounds. The temperature responsive properties of both series of surfactants and their ability to disperse MWNTs and exfoliate graphene are discussed in Chapter 5.

4.1: Rationale

In the MWNT dispersion studies discussed in Chapter 3, one interesting observation was that under our conditions the commercial non-ionic surfactant **Triton X-100** afforded a significantly higher C_{MWNT} than any of the commercial ionic surfactants, and in Millipore water performed comparably with the best of our novel materials. This suggested that non-ionic variants of our ALH surfactants could show improved performance as dispersants for carbonaceous materials. Non-ionic surfactants disperse these materials through a different mechanism to ionic surfactants, coating the surface of the material in hydrophilic moieties which render it miscible with water, and using this hydrophilicity alongside steric bulk to break up CNT bundles, or exfoliate graphitic layers, when a stimulus such as ultrasonication is applied.[184]

Non-ionic surfactants offer a further advantage in comparison to ionic surfactants: a clear mechanism for a temperature response. The cloud point behaviour of **Triton X-100** was discussed in Section 3.3.3. This phenomenon can be influenced by changes in temperature or the presence of additives such as salts or water-immiscible hydrocarbons.[192,193] Surfactant concentration can also have an effect, but this is insignificant below *ca.* 10 wt%.[194] When induced thermally, the clouding occurs at the lower critical solution temperature (LCST), defined by IUPAC as the 'critical temperature below which a mixture is miscible,'[195] clarified by the statement 'below the LCST … a single phase exists for all compositions.' LCST behaviour is known for many commercial non-ionic surfactants, including **Triton X-100** (LCST = 65 °C), **Triton X-114** (LCST = 23 °C), **TWEEN® 20** (LCST = 76 °C) and **TWEEN® 80** (LCST = 65 °C).[196] Many other non-ionic PEG-functionalised materials have an LCST.[192] For these compounds the LCST transition is caused by the disruption of hydrogen bonding

interactions between PEG and water.[193] The phenomenon is entropy driven; the level of disorder in water is increased by minimising interactions with the solute.[197] This property is not exclusive to PEGylated materials; for example polymers and co-polymers of *N*-isopropylacrylamide show LCST behaviour.[197-199] They have attracted interest in areas such as drug delivery as their LCST is close to body temperature, and have been used to prepare responsive CNT and GO dispersions as discussed in Section 1.6.[108,111] The structurally similar isobutylamide moiety has been used to functionalise the periphery of poly(amidoamine) (PAMAM) dendrimers and render them thermosensitive.[200] Short OEGs have also been used at the periphery of PAMAM dendrimers to impart LCST behaviour.[201] We chose to develop PEG-based surfactants, building on the methodology developed in Chapter 2, rather than working with an alternative temperature responsive functionality.

The alcohols **PyrB-PEG4** and **PyrB-PEG6**, which were intermediates in the synthesis of anionic surfactants, were not sufficiently soluble in water to use in our MWNT dispersion studies. More hydrophilic materials were clearly required. The hydrophobic pyrene anchor plays a key role in the binding of our surfactants to graphitic surfaces, so it was undesirable to replace this with a less hydrophobic anchor. We therefore investigated suitable hydrophilic, non-ionic head groups which could be attached to an anchor-linker ensemble to afford non-ionic surfactants fitting our ALH architecture. A general target structure is shown in Figure 4.01. Simpler **PyrB-PEGn** or **PyrM-PEGn** materials with n > 6 were also considered, but investigation of the effect of linker length would have been complicated as few suitable monodisperse OEGs are available. Additionally, poor SWNT dispersing ability has previously been observed for an analogous perylene-based surfactant.[89]

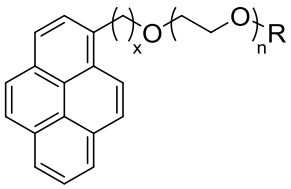

Figure 4.01: The general structures of targeted non-ionic surfactants. R represents a non-ionic, hydrophilic moiety.

4.2: Surfactants with a Crown Ether Head Group

Our first candidate head group was a crown ether moiety. Crown ethers of different sizes are known to selectively bind different cations[202] and therefore could potentially be used to incorporate both temperature responsive behaviour and ion sensitivity into a surfactant. As

various functionalised crown ethers can be sourced commercially they also served as a convenient way of testing non-ionic surfactants fitting the targeted structure. 2-Aminomethyl-15-crown-5, **51**, was coupled to **PyrB-PEG4-CH$_2$COOH** under our standard amide coupling conditions to afford **PyrB-PEG4-CH$_2$CO(15-c-5)** in 79% yield (Scheme 4.01). Purification by column chromatography required multiple purifications using highly polar eluents. By subsequently switching to an automated reversed-phase purification system **PyrB-PEG4-CH$_2$CO(15-c-5)** was isolated much more conveniently, albeit with a slightly lower yield of 72%. The cation binding ability of the material was demonstrated by high resolution mass spectrometry, which showed adducts of H^+, NH_4^+, Na^+ and K^+ (Figure 4.02).

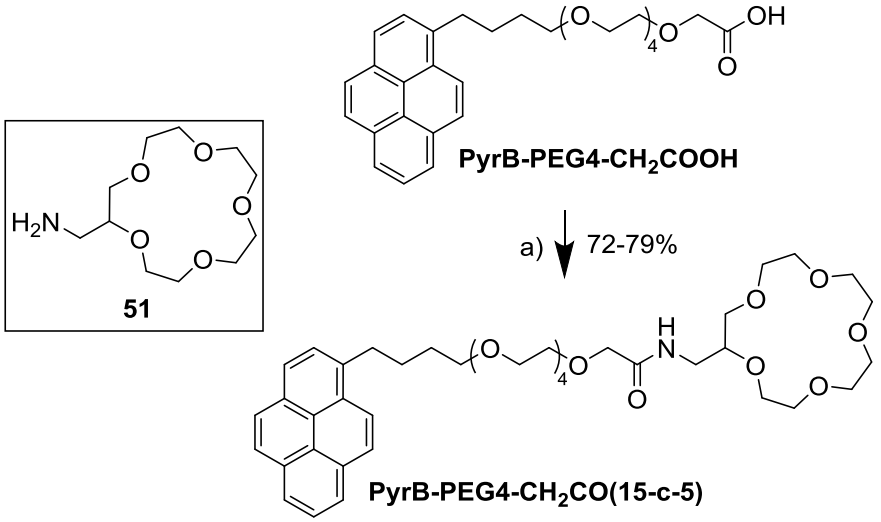

Scheme 4.01: Reagents and conditions: a) i. DIPEA, TBTU, DCM, RT, 15 min, ii. **51**, RT, 72h.

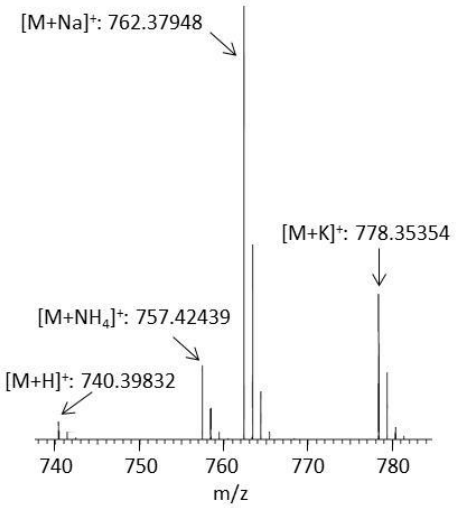

Figure 4.02: HRMS (ES^+) data for **PyrB-PEG4-CH$_2$CO(15-c-5)** showing multiple cation adducts.

PyrB-PEG4-CH$_2$CO(15-c-5) gave extremely promising results in terms of MWNT dispersing ability and temperature responsive behaviour, which are detailed in Chapter 5. This

prompted the development of analogues, to examine structure-property relationships. To simplify the synthesis of further surfactants we returned to the use of PyrM anchors as compatibility with *tert*-butyl ester deprotection conditions was no longer required. This allowed the synthesis of new surfactants of general structure **PyrM-PEGn-CH_2CO(15-c-5)** from **PyrMOH** in only 4 sequential steps. The synthesis of **PyrM-PEG6-CH_2COOH** was described in Section 2.3. We used the same route to isolate the PEG4 analogue, **PyrM-PEG4-CH_2COOH** (Scheme 4.02 and Table 4.01). Ag_2O-mediated monosubstitution of **PEG4** with a PyrM moiety required a shorter reaction time than for **PEG6** to minimise formation of the *bis*-substituted by-product. The yield of **PyrM-PEG4** was lower than that of **PyrM-PEG6** (60% *vs.* 80%); this is similar to the trend observed for monotosylation of OEGs in Section 2.4. Reaction of **PyrM-PEG4** with bromoacetic acid (**40**) afforded **PyrM-PEG4-CH_2COOH** in 88% yield. In this case the yield is higher for the PEG4 rather than the PEG6 compound, following the trend observed for the **PyrB-PEGn-CH_2COOH** series in Section 2.4. This fits our hypothesis that for longer OEG linkers the alkoxide intermediate is sterically shielded due to interactions between its sodium counter-ion and the oxygen atoms of the OEG.

The two acids were each coupled to **51** using our standard conditions (Scheme 4.02 and Table 4.01). In this case the advantage of automated reversed-phase chromatography was much clearer; attempted purification of **PyrM-PEG6-CH_2CO(15-c-5)** by manual normal-phase chromatography resulted in an isolated yield of only 17% after multiple purifications, whereas the automated reversed-phase system gave an isolated yield of 80%. **PyrM-PEG4-CH_2CO(15-c-5)** was isolated using this method in 54% yield. The yields for the two amide couplings were comparable to the analogous reactions between **PyrB-PEGn-CH_2COOH** acids and G1 dendron **14** in Section 2.4. The overall yields of the two surfactants from **PyrMOH** are 48% and 27% for **PyrM-PEG6-CH_2CO(15-c-5)** and **PyrM-PEG4-CH_2CO(15-c-5)** respectively. Both compare favourably with **PyrB-PEG4-CH_2CO(15-c-5)**, which has an overall yield from **PEG4** of 23% when reversed-phase purification is used for the final step.

Examination of temperature responsive behaviour in these surfactants and their use in the preparation of dispersions is discussed in Chapter 5.

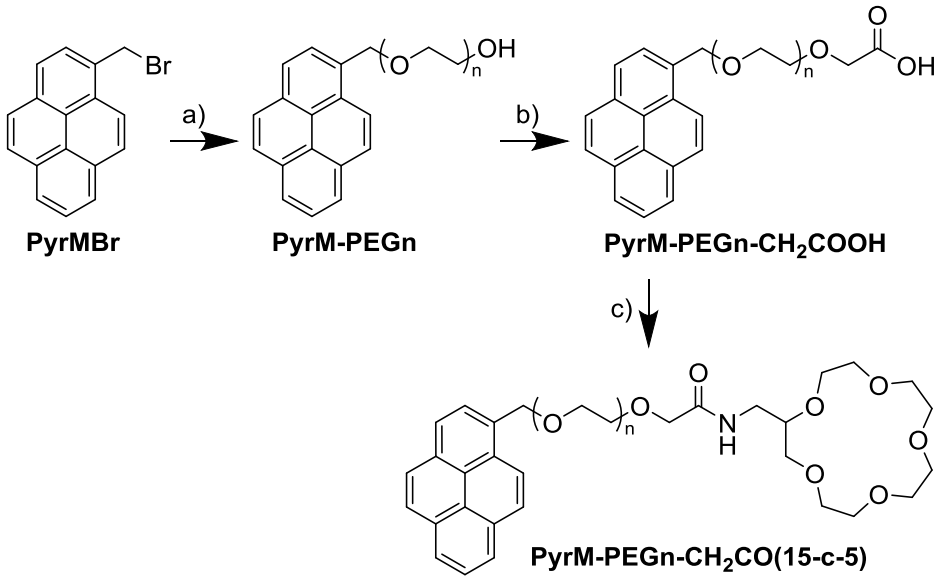

Scheme 4.02: Reagents and conditions: a) **PEGn**, Ag_2O, KI, DCM, RT, 45 min – 3 h; b) i. NaH, THF, 40 °C, 1 – 2 h, ii. **40**, 40 °C, 16 h; c) i. DIPEA, TBTU, DCM, RT, 15 min, ii. **51**, RT, 60 h. Yields are given in Table 4.01.

Table 4.01: Yields and reaction times for the reactions in Scheme 4.02.

	Monosubstitution (a)		Addition of Terminal Acid (b)	Amide Coupling (c)
OEG	**Reaction Time**	**% Yield**	**% Yield**	**% Yield**
PEG4	45 min	60	88	54
PEG6	3 h	80	79	80

4.3: Alternatives to Crown Ethers

4.3.1: Use of Podands

We show in Chapter 5 that ALH surfactants with a head group including a 15-crown-5 moiety can form temperature responsive MWNT dispersions. However, suitably functionalised crown ethers are very expensive and are unlikely to be suitable for any large scale applications. This meant it was desirable to develop surfactants with less costly, alternative head groups which retained these responsive properties. We therefore investigated analogues with a podand moiety – effectively 'cutting open' the crown ether to form two OEG arms, as illustrated in Figure 4.03. A podand is a species with two or more arms capable of chelating ions; these arms are often derived from OEGs and in certain conformations can resemble crown ethers. Short, functionalised OEGs suitable for the synthesis of podands are much cheaper reagents than functionalised crown ethers. Due to their structural similarities, the use of podand head groups was not expected to significantly affect the hydrophilicity of surfactants compared to crown ether analogues. Another anticipated advantage of podand

head groups was a reduced sensitivity to cations due to their decreased level of preorganisation compared to crown ethers (we show in Chapter 5 that for crown ether surfactants, dispersing MWNTs in 0.6 M NaCl gives a lower C_{MWNT} than in Millipore water).

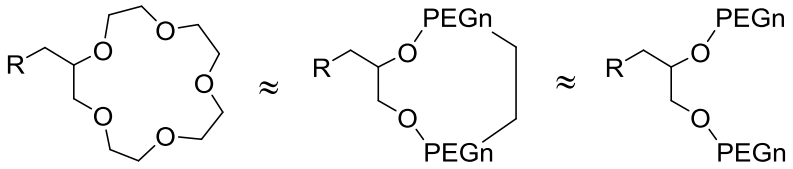

Figure 4.03: The investigation of podand head groups (right) was prompted by their structural similarity to a 'cut open' crown ether (left).

4.3.2: Podands Derived from Glycerol

One approach to surfactants with branched, podand head groups was to use an all-ether architecture based on OEGs and glycerol, **52**. This is illustrated in the retrosynthesis in Figure 4.04, in which the previously described 'anchor-linker' combinations **PyrB-PEGn** and **PyrM-PEGn** are used as precursors. A linear synthesis was planned in which a terminal glycerol moiety would be added to these compounds and subsequently functionalised with further OEG moieties to give a surfactant with a podand head group. The planned functionalisation of **PyrM-PEGn** or **PyrB-PEGn** with glycerol required suitable activation of one of the alcohol moieties used to form the ether bond. Protection of the remaining glycerol alcohol moieties was also desirable to minimise possible side reactions. Solketal, **53**, and tosylated solketal, **54** (Figure 4.04) were suitable glycerol derivatives for this approach.

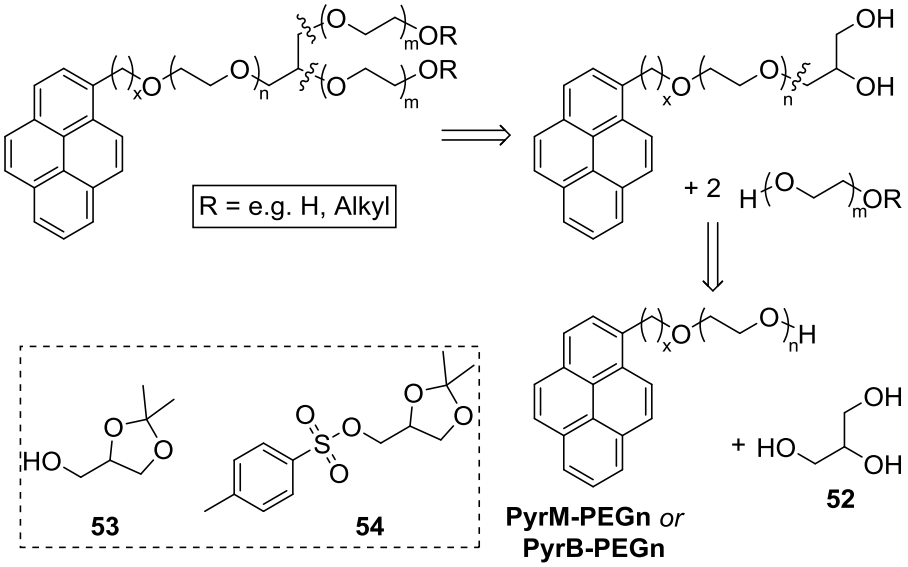

Figure 4.04: Retrosynthetic approach to an 'all-ether' podand surfactant derived from an 'anchor-linker' intermediate, glycerol (**52**) and OEGs. Suitable activation and protection of alcohol moieties would also be required, e.g. by using solketal, **53**, or its tosylate, **54**.

To test the viability of the route, **54** was first used in a Williamson ether synthesis with **PyrBOH** (Scheme 4.03) under conditions adapted from Section 2.4 (where **Ts-PEGn-THP** was the activated alcohol). This reaction yielded a small quantity (15%) of the targeted ether **PyrB-g(ⁱPr)** alongside dipyrenebutyl ether, **PyrB₂O**, and tosylated **PyrBOH** (**PyrBOTs**) which were isolated in 21% and 13% yields, respectively (although the latter was not fully purified). These by-products were not isolated in our previous ether syntheses, linking them to the use of **54**. Their presence suggests that the tosyl group of **54** was transferred to **PyrBOH** and the activated product then reacted with further **PyrBOH** to form **PyrB₂O**. This indicates a reaction pathway similar to that exploited by Sach *et al.* in the synthesis of aryl ethers from sulphonated phenols and aliphatic alcohols.[203] An S_N2 reaction cannot occur at an aromatic centre; instead the aryl ether is formed *via* transfer of the sulphonyl group to the aliphatic alcohol. An S_N2 reaction between the phenoxide and the aliphatic sulphonate intermediates yields the aryl ether. We attempted to improve the yield of **PyrB-g(ⁱPr)** by altering reagent stoichiometries. This was unsuccessful, resulting in either inseparable mixtures or the isolation of unreacted starting material (Table 4.02). Quantitative deprotection of the small isolated quantity of **PyrB-g(ⁱPr)** to give **PyrB-g(OH)₂** was achieved based on literature conditions using Amberlyst-15 ion-exchange resin (Scheme 4.03).[204,205]

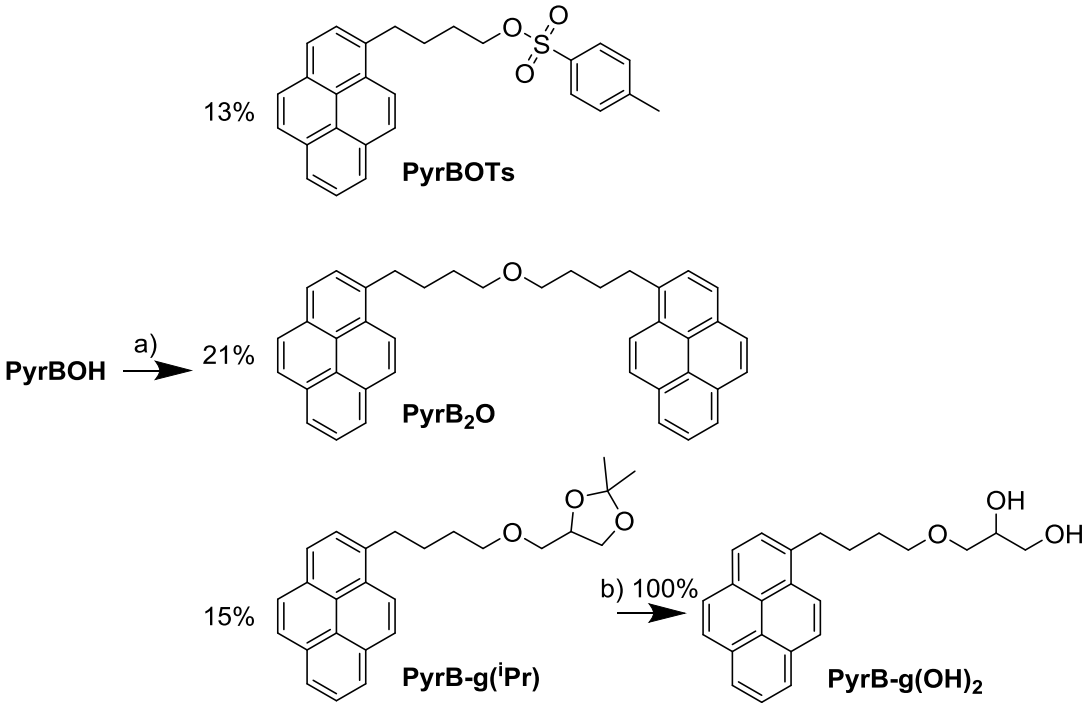

Scheme 4.03: Reagents and conditions: a) i. NaH, THF, 67 °C, 1 h, ii. **54,** 67°C, 17 h; b) Amberlyst-15, EtOH, 80 °C, 3 h.

Table 4.02: Attempted syntheses of **PyrB-g(ⁱPr)**

Equivalents of PyrBOH	Equivalents of 54	Equivalents of NaH	Result of Reaction
1.02	1	5	Various products (see Scheme 4.03)
1	1.2	5	Inseparable mixture
1	1.2	1.5	Recovered *ca.* 50% of starting materials. No product isolated.

It was hoped that an improved yield might be obtained if PEGylated species rather than **PyrBOH** were used in an ether synthesis with **54**. In this case slightly milder conditions, based on those used in the reactions between **40** and **PyrB-PEGn** or **PyrM-PEGn**, were used. Disappointingly an attempted reaction between **PyrB-PEG4** and **54** returned only starting materials (Scheme 4.04). This suggested low reactivity of **54**, and so we turned our attentions to a route using **53**. This required activation of the terminal alcohol of the anchor-linker intermediate, which was achieved for both **PyrM-PEG4** and **PyrM-PEG6** in near-quantitative yield by mesylation (Scheme 4.05). The reaction between **PyrM-PEG4-Ms** and **53** proceeded in a reasonable 55-57% yield at *ca.* 200 mg scale under two sets of conditions (Scheme 4.05 and Table 4.03). However, scale up of the reaction to *ca.* 650 mg scale gave a lower yield of 44%, suggesting that isolation of **PyrM-PEG4-g(ⁱPr)** in larger quantities may prove difficult. Varying the quantity and type of base used may have helped to optimise the reaction. Deprotection of **PyrM-PEG4-g(ⁱPr)** using Amberlyst-15 was facile, giving **PyrM-PEG4-g(OH)$_2$** in quantitative yield (Scheme 4.05).

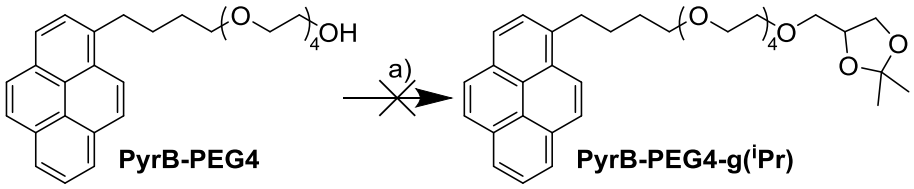

Scheme 4.04: Reagents and conditions: a) i. NaH, THF, 40 °C, 2 h, ii. **54**, 40 °C, 21 h.

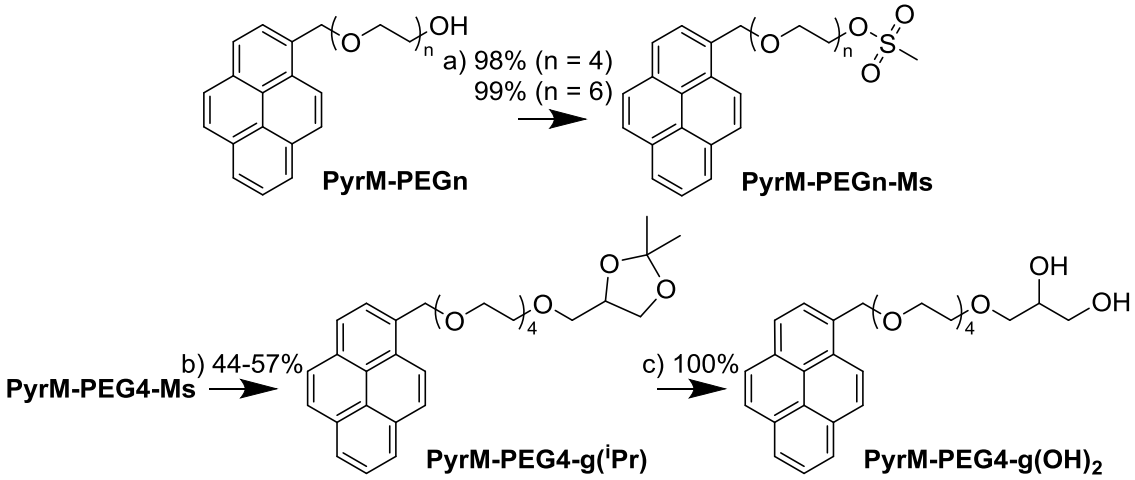

Scheme 4.05: Reagents and conditions: a) i. NEt_3, DCM, 0 °C, 10 min, ii. MsCl, 0 °C – RT, 16 h; b) i. NaH, THF, 40 or 67 °C, 1 – 2 h, ii. **53**, 40 or 67 °C, 18 – 24 h; c. Amberlyst-15, EtOH, 80 °C, 3.5 h.

Table 4.03: Syntheses of **PyrM-PEG4-g(^{i}Pr)**

Mass of PyrM-PEG4-Ms / mg	Equivalents of 53	Equivalents of NaH	Reaction Temperature / °C	% Yield
221	1.5	4.5	67	55
665	1.5	4.5	67	44
210	1.5	4.5	40	57

The low yield in the larger-scale synthesis of **PyrM-PEG4-g(^{i}Pr)** was particularly undesirable as further synthetic steps were required to convert this intermediate into a podand surfactant. The double ether synthesis needed to functionalise **PyrM-PEG4-g(OH)$_2$** with OEGs was anticipated to also be low yielding. With a view to possible future scale up it was preferable to minimise low yielding reactions involving costly pyrene-functionalised species. This led us to consider a more convergent synthesis of podand surfactants.

4.3.3: Synthesis of Podand Surfactants by Amide Coupling

In Chapter 2 we prepared surfactants with dendritic head groups by synthesising a head group precursor (**14**) and then attaching it to an anchor-linker ensemble. The synthesis of crown ether surfactants used a similar approach, which is here applied to the synthesis of podand surfactants. Incorporating a head group as the final step of surfactant synthesis would also facilitate the combination of different linker and head groups. Although precedent exists for the synthesis of PEG-functionalised glycerols,[206] their attachment to **PyrM-PEGn** alcohols could result in similar problems with yield and reproducibility to those observed in Section 4.3.2. We therefore returned to the use of amide couplings to incorporate head groups as this was successful for both G1 (Section 2.4) and crown ether head groups (Section 4.2). The required reagents were the previously synthesised acids of structure **PyrM-PEGn-CH$_2$COOH** and an amine-functionalised podand. Secondary amines functionalised with two OEG moieties have been used previously in the synthesis of aza-crown ethers.[207,208] Using literature conditions the secondary amine **HN(PEG2)$_2$** was prepared from 2-(2-aminoethoxy)ethanol, **55** and 2-(2-chloroethoxy)ethanol, **56**, in 72% yield, comparable to the reported 79% (Scheme 4.06).[208] Subsequent amide coupling between **HN(PEG2)$_2$** and **PyrM-PEG4-CH$_2$COOH**, and purification using reversed-phase chromatography afforded our first surfactant with a podand head group, **PyrM-PEG4-CH$_2$CON(PEG2)$_2$**, in 50% yield (Scheme 4.06).

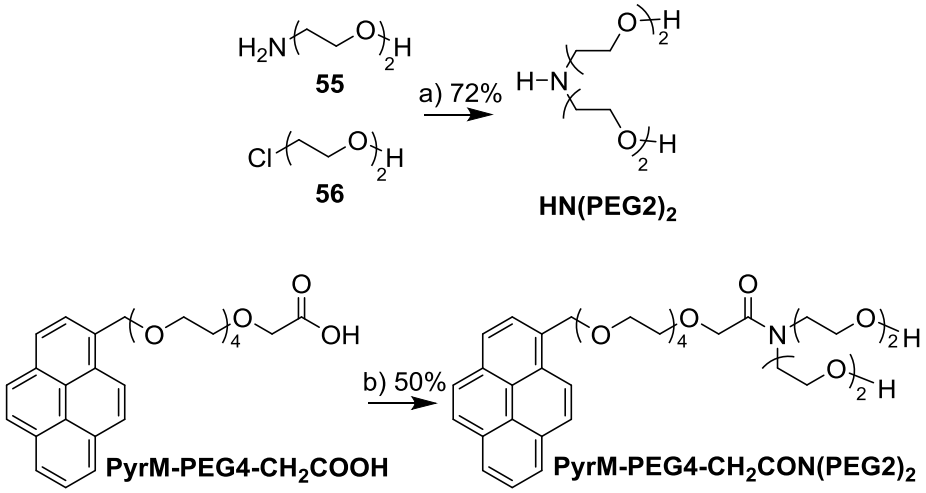

Scheme 4.06: Reagents and conditions: a) Na_2CO_3, toluene, 110 °C, 96 h; b) i. DIPEA, TBTU, DCM, RT, 15 min, ii. **HN(PEG2)$_2$**, RT, 72 h.

We show in Chapter 5 that **PyrM-PEG4-CH$_2$CON(PEG2)$_2$** does not exhibit a temperature response. Based on this result we chose not to synthesise the PEG6 linker analogue, as other results showed that LCST increased with linker length. Comparing **PyrM-PEG4-CH$_2$CON(PEG2)$_2$** to **PyrM-PEG4-CH$_2$CO(15-c-5)**, its closest analogue among the crown ether surfactants with LCSTs, there are two key structural variations which may explain their differing properties: the change from crown ether to podand and the use of a tertiary rather than secondary amide. Simply switching from a crown ether to a podand head group is unlikely to cause this contrasting behaviour as both surfactants contain similar numbers of OEG moieties which should favour LCST behaviour. However, the alcohol-terminated podand head group of **PyrM-PEG4-CH$_2$CON(PEG2)$_2$** may render this surfactant too hydrophilic to display LCST behaviour. The crown ether surfactants should be somewhat less hydrophilic as they contain only ether moieties and an amide. Alternatively, the use of a tertiary amide may alter e.g. hydrogen bonding interactions within the surfactant molecule and change its properties.

To better understand the structural requirements of temperature responsive surfactants we developed an approach to new podand head group precursors which closely resembled **51**. These were derived from (±)-3-amino-1,2-propanediol, **APD** (Figure 4.05) and for synthetic convenience were designed such that **APD** was substituted with two identical ethers. Head group precursors **APD(PEG2)$_2$** and **APD(PEG2Me)$_2$** are conceptually related to aminomethyl crown ethers **51** and **57** as shown in Figure 4.05. Isolation of surfactants incorporating these podands would enable tests to see whether the lack of LCST behaviour exhibited by **PyrM-PEG4-CH$_2$CON(PEG2)$_2$** is associated with its terminal alcohols or its tertiary amide.

The structural similarity between **APD** and glycerol means that the proposed head groups closely resemble those targeted in Section 4.3.2 but the presence of the amine moiety should allow for a more convenient synthesis.

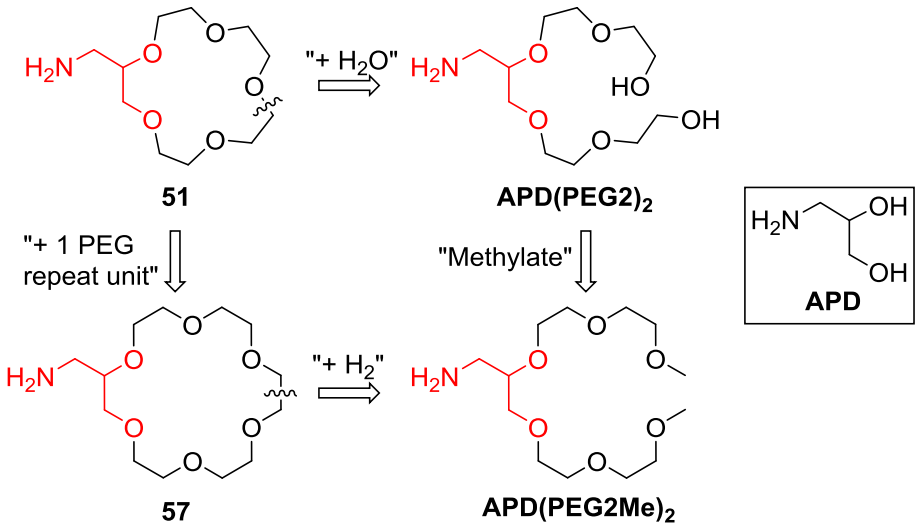

Figure 4.05: Conceptual relationships between functionalised crown ethers and candidate podand analogues. In each species the moiety which can be derived from **APD** is highlighted in red.

To our knowledge the functionalisation of **APD** with OEG ethers has not been reported, but literature precedent exists for the functionalisation of **APD** with aliphatic ethers. Kokotos *et al.* synthesised compounds of this type as intermediates in work on lipase inhibitors.[209] They used *tert*-butoxycarbonyl (Boc) protected, enantiopure **APD** in a biphasic Williamson ether synthesis reaction with various alkyl bromides, followed by deprotection of the amine to give **APD** diethers of structure **58** (Scheme 4.07).

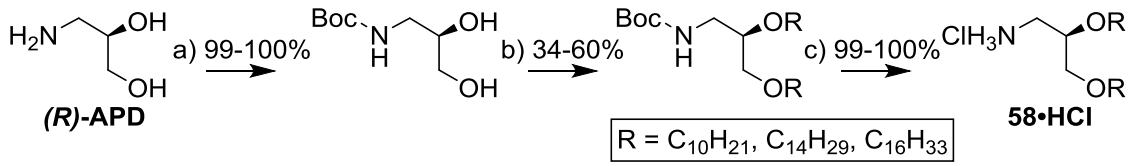

Scheme 4.07: Synthesis of **APD** diethers reported by Kokotos *et al.*[209] Only the *R*-enantiomer is shown. Reagents and conditions: a) Boc_2O, NEt_3, MeOH, 40-50 °C – RT, 40 min; b) RBr, Bu_4NHSO_4, $NaOH_{(aq)}$, Benzene, 50-60 °C, 6 h; c) $HCl_{(aq)}$, THF, RT, 1 h.

A subsequent publication by Hurley *et al.* on the synthesis of enantiopure synthetic lipids uses **APD** functionalised with aliphatic ethers, including unsaturated substituents.[210] In their route **APD** is protected as benzyl imine **59** before Williamson ether synthesis reactions with various aliphatic mesylates. Deprotection affords the **APD** diether, **58** (Scheme 4.08). This convenient route allows for isolation of **58** from **APD** with no intermediate purifications.

Hurley *et al.* state that Boc protection of **APD** is unsuitable for this route as when sodium hydride is the base an intramolecular reaction can occur between an alkoxide and the protected amine. They avoid the biphasic conditions used by Kokotos *et al.* as mesylates are incompatible with basic, aqueous conditions. Yields for *bis*-tetradecyl substituted **APD** (**58**, R = $C_{14}H_{29}$) were comparable to those reported by Kokotos *et al.*, around 50% for both the (*R)*- and *(S)*-enantiomers.

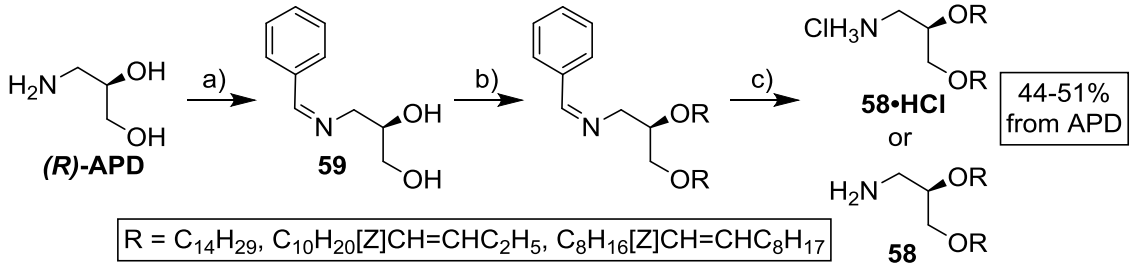

Scheme 4.08: Synthesis of **APD** diethers reported by Hurley *et al.*[210] Only the *R*-enantiomer is shown. Reagents and conditions: a) PhCHO, Na_2SO_4, DCM, MeOH, RT, 18 h; b) MsOR, NaH, THF, reflux, 72 h; c) $HCl_{(aq)}$, EtOH, RT, 6 h.

As racemic **51** had been used in the synthesis of the crown ether surfactants we selected racemic **APD** for the synthesis of the podand head groups. In Section 4.3.2 we found that mesylation of PEG derivatives was facile and near-quantitative. Therefore we chose to base our synthesis of **APD** derivatives on the route used by Hurley *et al.* and exploit mesylated OEGs where possible. However, chloride **56** is commercially available and so was a more convenient OEG starting material for the synthesis of **APD(PEG2)$_2$**. To prevent any side reactions **56** was protected as its THP ether, **60**, using the conditions for the protection of monotosylated OEGs from Section 2.4 (Scheme 4.09). The yield of **60** was somewhat lower than that previously achieved for the analogous tosylates. **APD** functionalisation was then attempted using the conditions of Hurley *et al.* with **60** in place of the aliphatic mesylates (Scheme 4.09).[210] As in the literature, the crude imine intermediate **59** was used immediately in the following ether synthesis step; isolation of a white solid from the first step was taken as sufficient evidence for its formation. The THP and benzyl imine protecting groups are both labile under acidic conditions, so we hoped to conduct both deprotections in a single synthetic step and isolate **APD(PEG2)$_2$** directly. However, we were unable to isolate **APD(PEG2)$_2$** or any protected derivatives following acid-base workup*. It is unclear whether **APD(PEG2)$_2$** or the THP-protected intermediate formed during the reaction. Further investigations have not been conducted as subsequent results indicated that surfactants with this head group would be too hydrophilic to show an LCST response (See Chapter 5).

* As **APD(PEG2)$_2$** is expected to be rather hydrophilic we also inspected the basified aqueous layer by removing the solvent and triturating the solid (mainly NaCl) obtained with various organic solvents.

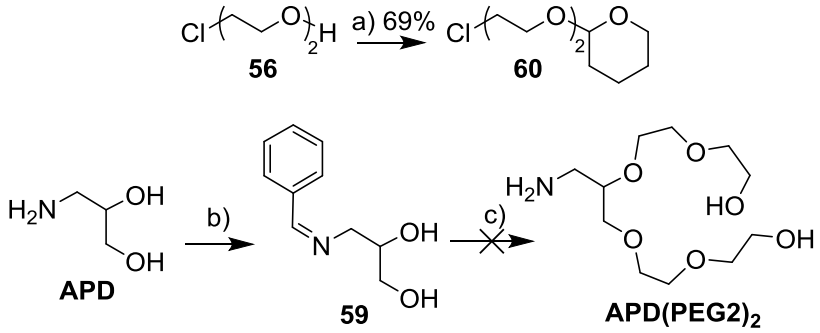

Scheme 4.09: Reagents and conditions: a) pyridinium *p*-toluenesulphonate, dihydropyran, DCM, 40 °C, 19 h; b) i. Na_2SO_4, DCM, MeOH, RT, 30 min, ii. PhCHO, RT, 18 h; c) i. NaH, THF, RT, 3 h, ii. **60**, 67 °C, 17 h, iii. $HCl_{(aq)}$, EtOH, 2.5 h.

In contrast, the synthesis of **APD(PEG2Me)$_2$** was successful. Surfactants where this podand was used as a head group (see below) showed an LCST response (see Chapter 5). To see if structural changes to the head group would tune the LCST we investigated analogues with different terminal alkyl groups and OEG lengths, with the general structure **APD(PEGmR)$_2$**. We attempted the synthesis of variants where R = Me, Et or ^{n}Bu, and m = 2 or 3. These all used OEG monoethers (**PEGm-R**) as a starting material; these are particularly desirable precursors as they are readily and cheaply available. As expected, mesylation of **PEGm-R** to give **Ms-PEGm-R** gave very high yields in all cases (Scheme 4.10 and Table 4.04). Functionalisation of **APD** with mesylates where R = Me or Et, and m = 2 or 3 was achieved using the conditions of Hurley *et al.* (Scheme 4.10 and Table 4.04).[210] **APD(PEGmR)$_2$** was obtained in yields of 22-40%. By modifying the reported work up procedure it was possible to isolate the product in high purity by using only acid-base workup, avoiding column chromatography. No monosubstituted **APD** was isolated in any case.

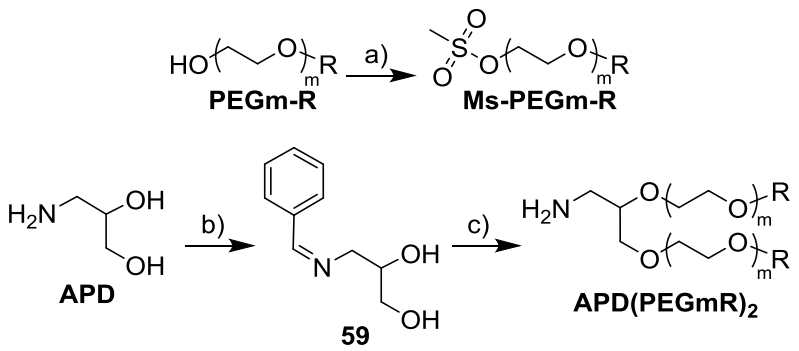

Scheme 4.10: Reagents and conditions: a) i. NEt_3, DCM, 0 °C, 10 min, ii. MsCl, 0 °C – RT, 18 h; b) i. Na_2SO_4, DCM, MeOH, RT, 30 min, ii. PhCHO, RT, 18 h; c) i. NaH, THF, RT, 3 h, ii. **Ms-PEGm-R**, 67 °C, 17 h, iii. $HCl_{(aq)}$, EtOH, 2.5 h. Yields are given in Table 4.04.

Table 4.04: Summary of yields from syntheses of **APD(PEGmR)$_2$** in Scheme 4.10.

m	R	% Yield of Mesylation (a)	% Yield of APD functionalisation (b, c)
2	Me	97	38
2	Et	94	40
2	^{n}Bu	100	0
3	Me	100	26
3	Et	100	22

The yields of **APD(PEG2Me)$_2$** and **APD(PEG2Et)$_2$** from **APD** were comparable to the 44-51% yields reported for aliphatic analogues.[210] We were therefore surprised to find that **APD(PEG2^{n}Bu)$_2$** could not be isolated. In this case, most of the **Ms-PEG2-^{n}Bu** starting material was recovered from an organic layer retained during acid-base workup. ^{1}H NMR spectroscopic analysis suggested that this was contaminated with another similar material, which was suspected to be the result of demesylation to give **PEG2-^{n}Bu** or dimerisation to give **^{n}Bu-PEG4-^{n}Bu** (Figure 4.06). Referenced to the singlet peak of the methyl moiety in the mesyl group, the integrals of the peaks in the alkyl region (associated with the *n*-butyl group) are each too large by a factor of *ca.* 1.4 (Figure 4.06). Peaks in the ether region (*ca.* 3.5 ppm) are distorted and have larger integrals than expected, sufficient to account for the remaining methylene protons in either of the suspected impurities. The integrals of the peaks at *ca.* 3.8 and 4.4 ppm are unchanged, indicating that the impurity does not contain an electron-withdrawing mesyl group. **^{n}Bu-PEG4-^{n}Bu** was considered more likely as there was no clear hydroxyl peak in the ^{1}H NMR spectrum. This was confirmed by LCMS data which showed the presence of two major species. The first fitted previously obtained data for **Ms-PEG2-^{n}Bu** and the second gave peaks at m/z = 307.1 and 329.4, corresponding to protonated and sodiated **^{n}Bu-PEG4-^{n}Bu**.

Confident that imine intermediate **59** was formed in the first stage of the reaction, we postulated there was a problem with alkoxide formation in the subsequent ether synthesis reaction. This would explain the large quantity of unreacted **Ms-PEG2-^{n}Bu**. The functionalisation of **APD** with **Ms-PEG2-^{n}Bu** was therefore repeated with a higher temperature in the alkoxide formation step. This reaction gave similar results to the previous attempt; none of the targeted material was isolated and most of the mesylate was recovered, contaminated with a similar, small quantity of dimer. It appears that there is a problem with the reactivity of **Ms-PEG2-^{n}Bu.** We tentatively suggest that the more amphiphilic nature of **Ms-PEG2-^{n}Bu** may allow the formation of supramolecular assemblies which hinder the mesyl groups. While we can find no precedent for such behaviour in compounds similar to **Ms-PEG2-^{n}Bu**, we note that the formation of inverse micelles in THF has been described previously for some carboxylic acids.[211,212]

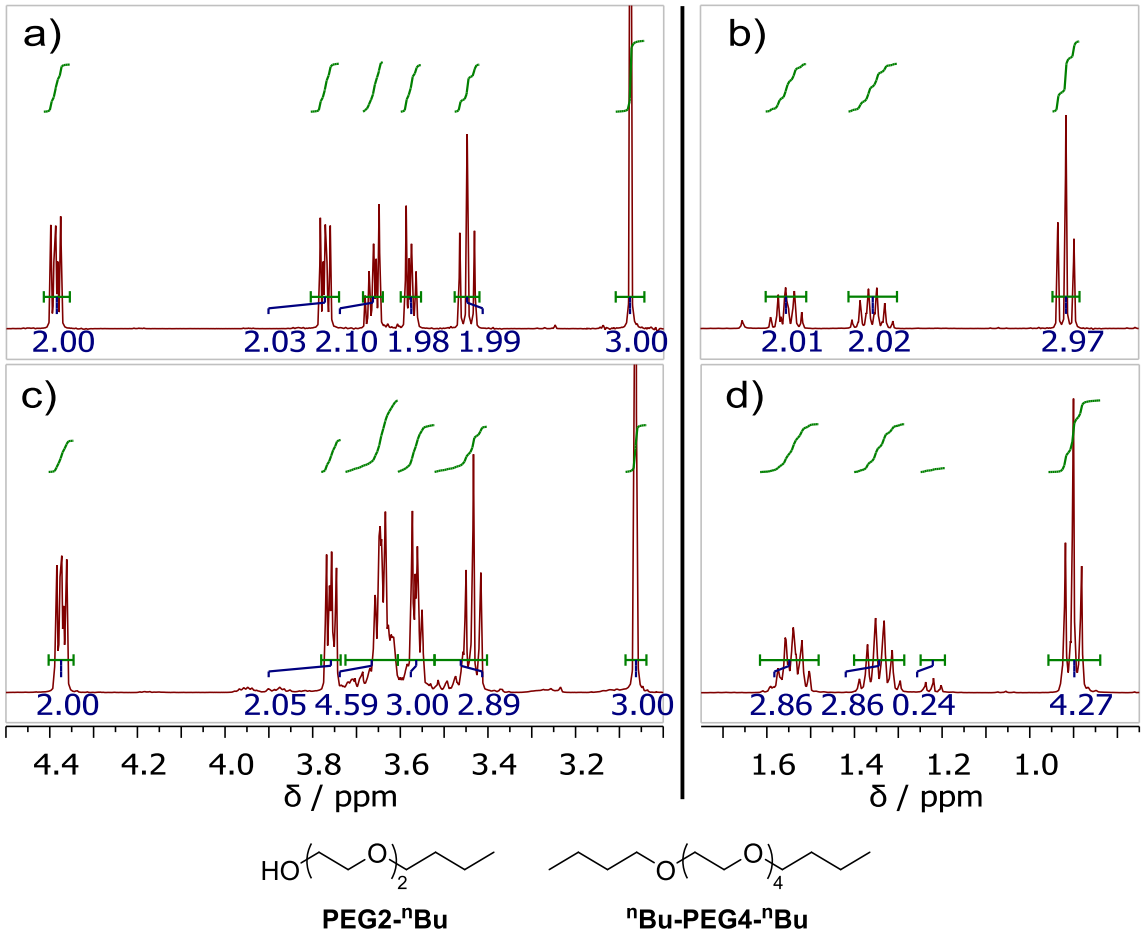

Figure 4.06: Top: Areas of ^{1}H NMR spectra of pure and recovered, contaminated **Ms-PEG2-^{n}Bu**: a) ether region, pure **Ms-PEG2-^{n}Bu**; b) alkyl region, pure **Ms-PEG2-^{n}Bu**; c) ether region, contaminated **Ms-PEG2-^{n}Bu**; d) alkyl region, contaminated **Ms-PEG2-^{n}Bu**. Bottom: Structures of suspected impurities.

The yields of **APD(PEG3Me)$_2$** and **APD(PEG3Et)$_2$** were somewhat lower than the analogous reactions using PEG2 species. We also encountered poor reproducibility for these reactions. In one instance the reaction with **Ms-PEG3-Me** failed entirely; none of the material obtained could be characterised. One synthesis of **APD(PEG3Et)$_2$** gave a yield of only 11%, although in this case it was possible to recover a large quantity of unreacted **Ms-PEG3-Et**. Similarly to the failed syntheses of **APD(PEG2^{n}Bu)$_2$**, ^{1}H NMR spectroscopy indicated that this recovered starting material was contaminated with a small amount of dimerised by-product. We have yet to attempt any optimisation of these reactions, and anticipate that improved yields and reproducibility could be achieved for all of the isolated products.

Isolation of a series of 8 podand surfactants of general structure **PyrM-PEGn-CH$_2$CO[APD(PEGmR)$_2$]** *via* amide couplings between the **APD(PEGmR)$_2$** amines (R = Me, Et; m = 2, 3) and the **PyrM-PEGn-CH$_2$COOH** acids (n = 4, 6) was facile

(Scheme 4.11 and Table 4.05). As for the crown ether surfactants, purification relied on reversed-phase chromatography. Yields were comparable to our previous amide couplings and ranged from 49-77%, averaging *ca.* 60%.

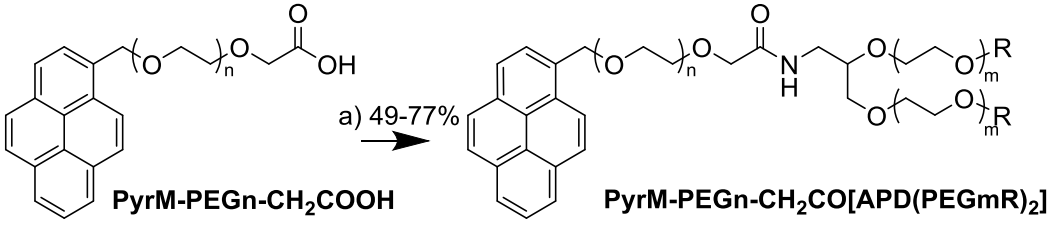

Scheme 4.11: Reagents and conditions: a) i. DIPEA, TBTU, DCM, RT, 15 min, ii. **APD(PEGmR)$_2$**, RT, 17-72 h. Yields are given in Table 4.05.

Table 4.05: Summary of yields of **PyrM-PEGn-CH$_2$CO[APD(PEGmR)$_2$]** *via* amide couplings between **APD(PEGmR)$_2$** and **PyrM-PEGn-CH$_2$COOH**.

n	m	R	% Yield
4	2	Me	59
4	2	Et	60
6	2	Me	63
6	2	Et	58
4	3	Me	61
4	3	Et	49
6	3	Me	77
6	3	Et	57

Interestingly, the ^{1}H NMR spectra of the crown ether and APD-derived podand surfactants in $CDCl_3$ all show a small coupling ($J \sim$ 1-2 Hz) between the methylene protons adjacent to the amide carbonyl, giving a doublet (examples are shown Figure 4.07a-c). This appears to be a geminal coupling attributable to the presence of the chiral APD moiety, despite the distance (5 bonds) between these groups. This is supported by the COSY spectra of **PyrB-PEG4-CH$_2$CO(15-c-5)** and **PyrM-PEG6-CH$_2$CO(15-c-5)** (not shown), which show no correlation between this doublet peak and any other peak. Additionally, for related species with achiral head groups (e.g. **PyrB-PEG6-CH$_2$COG1(O^{t}Bu)$_3$** and **PyrM-PEG4-CH$_2$CON(PEG2)$_2$**) these protons give a singlet peak (Figure 4.07d-e). The effect of the chiral centre on these protons may be enhanced by a possible hydrogen bonding interaction between the amide N-H moiety and the ether oxygen adjacent to the methylene group. In the ^{1}H NMR spectrum of **PyrB-PEG4-CH$_2$CO(15-c-5)** in D_2O the peak associated with this group is a singlet (Figure 4.07f), which may indicate that this proposed hydrogen bonding interaction has been disrupted. This does not confirm the role of hydrogen bonding as in D_2O many other peaks broaden sufficiently that their multiplicity cannot be seen (*cf.* Figure 2.08).

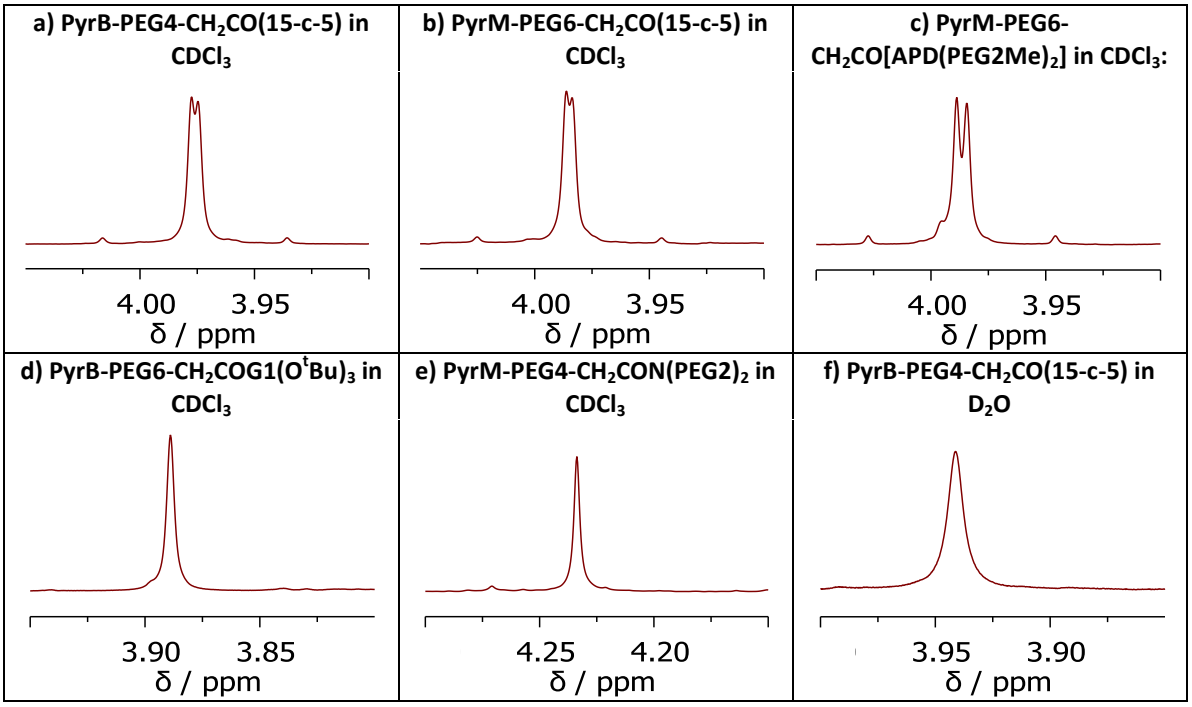

Figure 4.07: The ^{1}H NMR peak associated with the methylene protons adjacent to the amide carbonyl of some ALH surfactants and a surfactant precursor.

4.4: Conclusions

We have added 12 non-ionic species to our library of ALH surfactants. These include a series of 3 surfactants with amide-linked crown ether head groups: **PyrB-PEG4-CH_2CO(15-c-5)**, **PyrM-PEG4-CH_2CO(15-c-5)** and **PyrM-PEG6-CH_2CO(15-c-5)**. The functionalised crown ethers used in their synthesis are too expensive for large scale applications, so podand surfactants were developed as an alternative. Glycerol based podands were deemed unsuitable due to poor yields and reproducibility. We instead developed amide based podands; firstly **PyrM-PEG4-CH_2CON(PEG2)$_2$** and then 8 surfactants of general structure **PyrM-PEGn-CH_2CO[APD(PEGmR)$_2$]** (n = 4, 6; m = 2, 3; R = Me, Et). All of the surfactants are isolated *via* amide coupling between a head group precursor and an anchor-linker ensemble. This flexible approach could be readily adapted to further anchor, linker or head groups.

Chapter 5: Non-Ionic Surfactants: Temperature Response and MWNT Dispersion

In this chapter we examine the temperature responsive behaviour of the non-ionic surfactants synthesised in Chapter 4 using turbidimetry and dynamic light scattering (DLS). We examine the relationship between surfactant structure and temperature response and use this to develop methods to predict the behaviour of further materials. The use of responsive surfactants to produce responsive MWNT dispersions is examined.

5.1: LCST Measurements

5.1.1: Methods

The non-ionic surfactants synthesised in Chapter 4 were designed in the expectation they would exhibit an LCST response in aqueous solution. Their structures are summarised in Appendix 1. As a qualitative test for LCST we immersed a 0.2 wt% aqueous surfactant solution in a heated water bath and slowly increased its temperature until clouding was observed. The temperature at which clouding occurred was used as a guideline in subsequent measurements; this simple method has previously been used as a quantitative means of determining LCST.[194] Three common, quantitative approaches used to measure LCST are turbidimetry, dynamic light scattering (DLS) and differential scanning calorimetry (DSC).[108,109,199-201,213] We measured the LCST of our surfactants using turbidimetry and DLS. We could not achieve sufficient sensitivity in DSC measurements to detect a response.

Turbidimetric methods are based on the clouding that occurs when a solution is heated beyond its LCST. This clouding is caused by precipitation of the now-immiscible solute. The formation of solute aggregates means that the transmittance of the suspension sharply decreases across the entire UV-visible region. By monitoring a wavelength at which the transmittance is high at low temperatures it is possible to observe a sharp transition between high and low transmittance. The LCST is defined as either the onset of this transition[214-216] or the mid-point of this transition (i.e. the temperature at which transmittance is the average of its maximum and minimum values).[199,200,217] We used the latter definition which meant it was important to use a surfactant concentration at which the mid-point of the transition could be correctly identified. If a solution was too concentrated it was not possible to correctly define

the end point; the opacity of the clouding solutions was sufficient to give a transmittance of zero before the process was complete. If the solution was too dilute no, or only very little, transmittance change was observed. We determined the LCST of our surfactants at concentrations at which the minimum transmittance value was close to, but more than, zero, which varied between compounds. In a typical experiment, the surfactant solution was heated from 20 °C to 80 °C and its transmittance recorded at intervals. Closer intervals were used around the previously approximated LCST. At each interval the solution was equilibrated for *ca.* 2 min prior to measurement*. The transmittance at 550 nm was used to determine the LCST, although comparable results were obtained at other wavelengths.

To verify the results of the turbidimety study DLS was also used to measure the LCSTs of the surfactants. These studies were conducted by Dr Benjamin Robinson and Ms Claire Tinker-Mills at Lancaster University (Physics Department). DLS studies show an LCST response as a distinct and rapid increase in the average hydrodynamic diameter of suspended particles. Below the LCST small micelles formed from surfactants should be detectable, whereas above the LCST aggregate formation results in much larger particle sizes. As in the turbidimetry study we will define the LCST as the mid-point of the transition in particle size. 1 mM surfactant solutions in Millipore water were analysed at a range of temperatures to determine at what point aggregate formation occurred. One advantage of this method is that all of the surfactants were analysed at the same concentration, improving the comparability of the data.

5.1.2: Results

The results of the turbidimetry and DLS studies are shown in Figures 5.01, 5.02 and 5.03. Characteristic, sharp LCST transitions are shown in the turbidimetric data; these allowed us to determine LCSTs to an accuracy of ±0.5 °C. In some cases an increase in transmittance was observed after the LCST transition which we attribute to phase separation. In the DLS study the transition between small and large particles was not always sharp. In these cases a larger error was assigned which accounted for the beginning and end of the transition; otherwise an error of ±0.5 °C could be assigned. Below the LCST, the DLS studies indicated that the surfactants formed micelles with average diameters between 3 and 6 nm (depending on the surfactants). Most surfactants also showed a small number (<1%) of larger features with diameters on the order of 100 nm (still much smaller than the large aggregates observed

* The samples were equilibrated at each temperature as our equipment did not allow for use of a constant heating rate.

above the LCST). These have not yet been examined further, but are expected to be larger self-assembled structures, possibly vesicles. Neither the small or large features are detected above the LCST. When both are present we consider only the small features to calculate the mean particle diameter shown in Figures 5.01, 5.02 and 5.03. The LCSTs calculated using these data are shown in Table 5.01 alongside the values approximated by visual inspection.

Table 5.01: LCSTs of crown ether and podand surfactants as determined by visual inspection, turbidimetry and DLS.

	LCST / °C		
Surfactant	**Approximated Visually**[a]	**Turbidimetry**[b]	**DLS**[b]
PyrB-PEG4-CH_2CO(15-c-5)	50-60[c]	58.0 (±0.5)	62.5 (±2.5)
PyrM-PEG4-CH_2CO(15-c-5)	60	61.5 (±0.5)	59.5 (±0.5)
PyrM-PEG6-CH_2CO(15-c-5)	70	70.0 (±0.5)	71.5 (±0.5)
PyrM-PEG4-$CH_2CON(PEG2)_2$	>90	>80	n/a[d]
PyrM-PEG4-$CH_2CO[APD(PEG2Me)_2]$	71	69.0 (±0.5)	71.5 (±0.5)
PyrM-PEG6-$CH_2CO[APD(PEG2Me)_2]$	82	77.0 (±0.5)	78.0 (±1.0)
PyrM-PEG4-$CH_2CO[APD(PEG2Et)_2]$	42	42.0 (±0.5)	46.0 (±4.0)
PyrM-PEG6-$CH_2CO[APD(PEG2Et)_2]$	49	48.0 (±0.5)	48.5 (±0.5)
PyrM-PEG4-$CH_2CO[APD(PEG3Me)_2]$	76	75.5 (±0.5)	81.5 (±0.5)
PyrM-PEG6-$CH_2CO[APD(PEG3Me)_2]$	84	85.5 (±0.5)	>90
PyrM-PEG4-$CH_2CO[APD(PEG3Et)_2]$	49	49.0 (±0.5)	53.0 (±2.0)
PyrM-PEG6-$CH_2CO[APD(PEG3Et)_2]$	58	59.5 (±0.5)	57.5 (±0.5)

[a] to nearest 1 °C; [b] to nearest 0.5 °C; [c] approximated as described in Section 5.2.2; [d] not measured

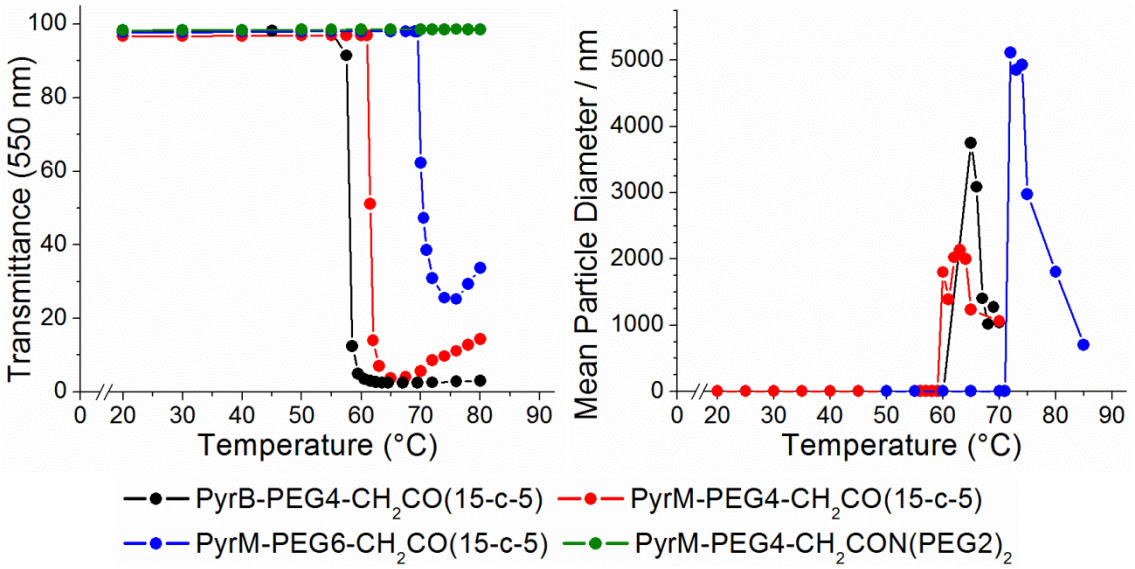

Figure 5.01: Left: Transmittance of aqueous solutions of **PyrB-PEG4-CH_2CO(15-c-5)** (0.54 mM, 0.04 wt%), **PyrM-PEG4-CH_2CO(15-c-5)** (1.43 mM, 0.1 wt%), **PyrM-PEG6-CH_2CO(15-c-5)** (1.27 mM, 0.1 wt%) and **PyrM-PEG4-$CH_2CON(PEG2)_2$** (1.56 mM, 0.1 wt%) at 550 nm over a range of temperatures. Right: Variation in mean particle diameter in 1 mM surfactant solutions upon heating as determined by DLS.

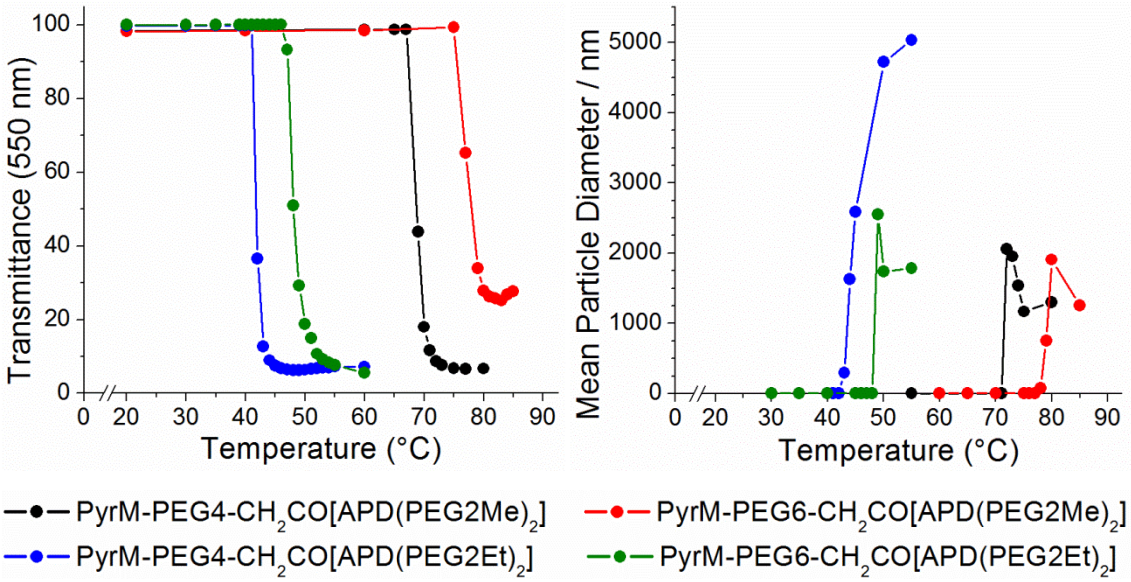

Figure 5.02: Left: Transmittance of aqueous solutions of **PyrM-PEG4-CH₂CO[APD(PEG2Me)₂]** (1.01 mM, 0.075 wt%), **PyrM-PEG6-CH₂CO[APD(PEG2Me)₂]** (0.90 mM, 0.075 wt%), **PyrM-PEG4-CH₂CO[APD(PEG2Et)₂]** (0.65 mM, 0.05 wt%) and **PyrM-PEG6-CH₂CO[APD(PEG2Et)₂]** (0.58 mM, 0.05 wt%) at 550 nm over a range of temperatures. Right: Variation in mean particle diameter in 1 mM surfactant solutions upon heating as determined by DLS.

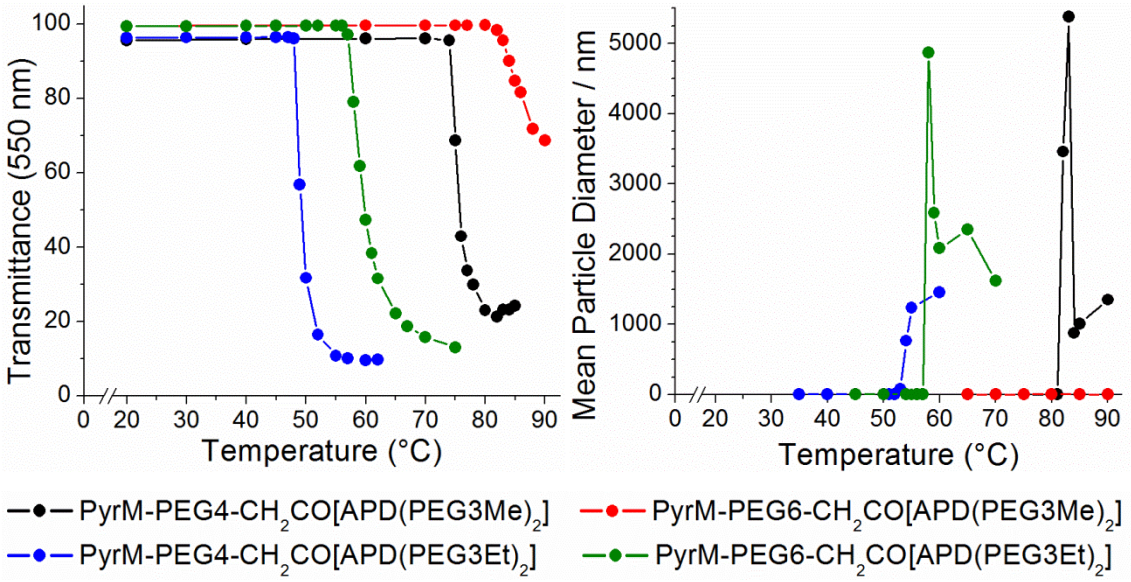

Figure 5.03: Left: Transmittance of aqueous solutions of **PyrM-PEG4-CH₂CO[APD(PEG3Me)₂]** (0.90 mM, 0.075 wt%), **PyrM-PEG6-CH₂CO[APD(PEG3Me)₂]** (0.82 mM, 0.075 wt%), **PyrM-PEG4-CH₂CO[APD(PEG3Et)₂]** (0.58 mM, 0.05 wt%) and **PyrM-PEG6-CH₂CO[APD(PEG3Et)₂]** (0.53 mM 0.05 wt%) at 550 nm over a range of temperatures. Right: Variation in mean particle diameter in 1 mM surfactant solutions upon heating as determined by DLS.

There is good agreement between the methods used. The largest discrepancy between results is 6 °C for **PyrM-PEG4-CH₂CO[APD(PEG3Me)₂]**. This is in agreement with previous studies which show that LCSTs calculated using turbidimetry and DLS are typically within ≤5 °C of

one another.[214-219] The LCSTs determined by DLS are mainly higher than those determined turbidimetrically. The observed variation between methods does not appear to relate to differences in surfactant concentration, indicating that in the range studied (*ca.* 0.5 – 3 mM across the three techniques) concentration has no significant effect on LCST. To confirm that we were observing a true, reversible LCST transition further qualitative tests were conducted. Samples repeatedly heated above and then cooled below their LCST clouded and cleared as expected each time. This process could be repeated in excess of 10 times. Figure 5.04 shows aqueous solutions of **PyrM-PEG4-CH_2CO[APD(PEG2Et)$_2$]**, **PyrM-PEG6-CH_2CO[APD(PEG3Et)$_2$]** and **PyrM-PEG4-CH_2CO(15-c-5)** above and below their LCSTs

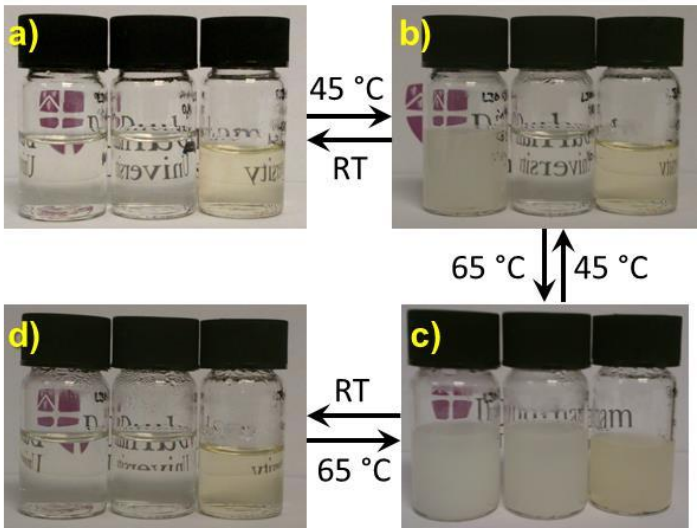

Figure 5.04: Photographs of aqueous solutions of **PyrM-PEG4-CH_2CO[APD(PEG2Et)$_2$]** (left), **PyrM-PEG6-CH_2CO[APD(PEG3Et)$_2$]** (centre) and **PyrM-PEG4-CH_2CO(15-c-5)** (right): a) under ambient conditions, b) after heating to 45 °C, c) after heating to 65 °C, d) after the heated samples have cooled under ambient conditions.

All of the tested surfactants except **PyrM-PEG4-$CH_2CON(PEG2)_2$** showed an LCST response in the qualitative and turbidimetric studies. The DLS experiments failed to detect an LCST response for **PyrM-PEG6-CH_2CO[APD(PEG3Me)$_2$]**. The LCST of this compound was calculated as 85.5 ± 0.5 °C by turbidimetry, although the observed transition was less sharp than for the other surfactants. This is the highest LCST of the materials investigated and is near the upper limit of the studied temperature range, which could explain why the transition proved difficult to observe in the quantitative studies.

5.1.3: Structure-Property Relationships

The LCSTs* of the non-ionic surfactants relate to their structure and hydrophilicity. In general, the more hydrophilic a surfactant, the higher its LCST. These relationships are summarised by three principal observations:

1) LCST increases with PEG chain length

Longer OEG chains make a surfactant more hydrophilic. For all five pairs of surfactants which are identical apart from their linker, the LCST of the PEG6 analogue is higher than the PEG4 surfactant (for all measurement techniques). The average difference in LCST between analogues is 8.6 °C and ranges from 6 °C to 10.5 °C for the APD(PEG2Et)$_2$ and APD(PEG3Et)$_2$ head groups, respectively. The change from an APD(PEG2R)$_2$ to an APD(PEG3R)$_2$ head group also adds two PEG repeat units to the surfactant. This has a similar effect, on average increasing the LCST by 8.4 °C and ranging from 6.5 °C to 11.5 °C for R = Me with PEG4 linkers and R = Et with PEG6 linkers, respectively. The similarity in these effects suggests that altering the position of the PEG units within the surfactant structure has minimal effect on the LCST. This is demonstrated by surfactants of general structure **PyrM-PEG4-CH$_2$CO[APD(PEG3R)$_2$]** and **PyrM-PEG6-CH$_2$CO[APD(PEG2R)$_2$]** which, for a given R group, are structural isomers differing only in the relative location of their PEG repeat units. Both the R = Me and R = Et pairings have near-identical LCSTs (within 1.5 °C). Overall, the addition of two PEG repeat units in any position gives a mean LCST increase of 8.5 °C, or 4.25 °C per PEG repeat unit (the LCSTs measured using other techniques give slightly lower values but show the same trend).

2) The head group has a significant effect on LCST

The APD(PEG2Et)$_2$ head group is less hydrophilic than the APD(PEG2Me)$_2$ head group as it has longer terminal alkyl chains. The hydrophilicity of the (15-c-5) head group should lie between that of the two APD(PEG2R)$_2$ head groups (based on HLB contributions – see Section 5.1.4 and Appendix 2). Terminal alcohol groups mean that the N(PEG2)$_2$ head group is the most hydrophilic of those studied. As the effect of adding PEG repeat units to the head group has been accounted for above, the effect of APD(PEG3R)$_2$ head groups can be considered equivalent to their PEG2 analogues. When the anchor and linker are identical, a change of head group from APD(PEGmMe)$_2$ to APD(PEGmEt)$_2$ lowers the LCST by 27.1 °C on average. The magnitude of this change is surprising given that the surfactant structures differ

* Unless otherwise stated this section will refer to the LCSTs which were determined turbidimetrically, as these have the smallest experimental error.

by only two methylene groups. The reduction in LCST when an APD(PEG2Me)$_2$ head group is replaced by a (15-c-5) head group is smaller, 7.25 °C on average (in this case, slightly larger values are observed using the LCSTs determined by other methods). The N(PEG2)$_2$ head group causes a large increase in LCST relative to the others studied, such that it is beyond the investigated temperature range.

3) Changes to the anchor group have a less significant effect on LCST than those to the head group

The surfactants **PyrB-PEG4-CH$_2$CO(15-c-5)** and **PyrM-PEG4-CH$_2$CO(15-c-5)** differ only in the alkyl unit between the pyrene moiety and the first ether group. Changing from a PyrB anchor group to a PyrM anchor group results in a 3.5 °C increase in LCST*. The structural change is the addition of three methylene groups, but the observed effect is considerably smaller than that seen when only two methylene groups are added to a podand head group (i.e. R = Me to R = Et). This was not anticipated as the decrease in surfactant hydrophilicity (at least based on HLB – see Section 5.1.4 and Appendix 2) should be larger in the former case. However, when considered in terms of micelle assembly the observation is reasonable. It appears that changes to the moieties which are within the hydrophobic core are less significant than changes to the hydrophilicity of moieties which are preferentially located at the periphery of the micelle. This observation is currently limited to a single example and requires further investigation.

5.1.4: Predicting LCST

Using the above data we attempted to develop a means to predict the LCST of structurally related surfactants to guide future synthetic work. We initially considered a method based on hydrophilic-lipophilic balance (HLB). HLB is commonly used as a guide when selecting a surfactant for industrial or commercial applications. It was originally developed by Griffin for use in the cosmetic industry,[220,221] and fits on a scale from 0-20 (for non-ionic surfactants), with higher values indicating higher hydrophilicity. Although HLB values can be calculated experimentally, this is much less common than using estimates based on either Griffin's or Davies' method. Griffin's method for non-ionic surfactants is based solely on molecular weight,[221] whereas Davies' method accounts for structural groups within a surfactant based on empirical data.[222] Due to the complex structures of our surfactants we used Davies'

* The DLS results disagree, giving an LCST decrease of 3 °C. However, the experimental error associated with the LCST of **PyrB-PEG4-CH$_2$CO(15-c-5)** is large (± 2.5 °) using this method.

method in which different functional groups within a surfactant contribute to HLB based on their hydrophilicity or lipophilicity.

Table 5.02 shows the (turbidimetric) LCSTs of the non-ionic surfactants together with their HLB values calculated using Davies' method[222] and some empirically assigned structural parameters (see below). Tables of HLB group contributions are widely available online,[223] but do not include values for all functional groups. The HLB values in Table 5.02 include some assumptions for HLB contributions based on those of similar functional groups for which values are available. Details of how the values were calculated can be found in Appendix 2.

Table 5.02: LCSTs, HLB values and empirical structural parameters of the crown ether and podand surfactants

Surfactant	LCST / °C	HLB	A	p	H
PyrB-PEG4-CH_2CO(15-c-5)	58.0 (±0.5)	10.435	4	7	24.9
PyrM-PEG4-CH_2CO(15-c-5)	61.5 (±0.5)	11.86	1	7	24.9
PyrM-PEG6-CH_2CO(15-c-5)	70.0 (±0.5)	12.52	1	9	24.9
PyrM-PEG4-CH_2CO[APD(PEG2Me)$_2$]	69.0 (±0.5)	12.19	1	8	27.1
PyrM-PEG6-CH_2CO[APD(PEG2Me)$_2$]	77.0 (±0.5)	12.85	1	10	27.1
PyrM-PEG4-CH_2CO[APD(PEG2Et)$_2$]	42.0 (±0.5)	11.24	1	8	0
PyrM-PEG6-CH_2CO[APD(PEG2Et)$_2$]	48.0 (±0.5)	11.90	1	10	0
PyrM-PEG4-CH_2CO[APD(PEG3Me)$_2$]	75.5 (±0.5)	12.85	1	10	27.1
PyrM-PEG6-CH_2CO[APD(PEG3Me)$_2$]	85.5 (±0.5)	13.51	1	12	27.1
PyrM-PEG4-CH_2CO[APD(PEG3Et)$_2$]	49.0 (±0.5)	11.90	1	10	0
PyrM-PEG6-CH_2CO[APD(PEG3Et)$_2$]	59.5 (±0.5)	12.56	1	12	0
PyrM-PEG4-$CH_2CON(PEG2)_2$	n/a	13.23	-	-	-

The HLB values of the surfactants with LCSTs lie between *ca*. 10.5 and 13.5, with most in the region of 11-13. **PyrM-PEG4-$CH_2CON(PEG2)_2$**, which does not have an LCST (at least below 90 °C) has an HLB of 13.23, which shows that HLB alone cannot definitively show whether a surfactant has an LCST. We suggest the guideline that ALH surfactants with an HLB between 11 and 13 are likely to have an LCST. At higher values an LCST is less likely; such compounds may be too hydrophilic. A precise lower limit is difficult to determine without further data. We suggest that an HLB below 10 is unlikely to result in a surfactant with an LCST significantly above room temperature. The presence of an amide moiety, which has a substantial HLB contribution of +9.6, could be key to obtaining ALH surfactants with LCST behaviour without needing to incorporate much longer PEG chains in linkers and head groups. This agrees with the poor water solubility observed for simple **PyrB-PEGn** alcohols (Section 4.1). It also suggests that the glycerol-based 'all-ether' podands targeted in Section 4.3.2 would likely have had very low LCSTs if OEGs similar to those in the APD-based podands had been used. The presence of terminal alcohol moieties may have counteracted

this, but this would have further increased synthetic complexity. Similarly, a sodium carboxylate moiety has a large HLB contribution of +19.1, meaning our anionic surfactants (Chapters 2 and 3) all have HLB values above 18. Our observations suggest this is too hydrophilic to give LCST behaviour, in agreement with the studies in Section 3.4. The combination of an amide and either a 15-crown-5 moiety or podand with alkyl-terminated short OEG arms affords materials with ideal hydrophilicity: sufficient to be readily soluble in water, but not so high that they do not possess an LCST.

The HLB values for the crown and podand surfactants are compared with their LCSTs in Figure 5.05. LCST tends to increase with HLB, but there are several exceptions, most noticeably **PyrB-PEG4-CH_2CO(15-c-5)**. We noted above that changes to the hydrophilicity of the anchor appear to have a smaller effect than would be expected. This could explain why the HLB approach fails to account for such changes correctly. If this species is discounted, and only the PyrM anchored surfactants are considered, some linear correlation can be seen between HLB and LCST (R^2 = 0.813). From the regression line we obtain a predictive formula based on HLB:

$$LCST \approx 20HLB - 182 \pm 10$$

where the error is based on the agreement with the experimental data.

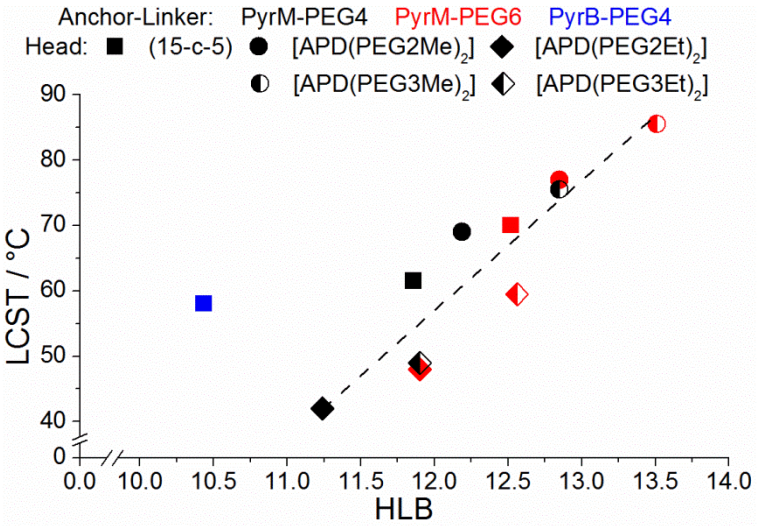

Figure 5.05: Comparison of HLB with LCST for the crown ether and podand surfactants which exhibit LCST behaviour. Surfactants with the same head group are shown with the same marker shape and those with the same anchor and linker in the same colour. The dashed line is a linear fitting of the data for PyrM-anchored materials.

The formula is consistent with the above guidelines, predicting LCSTs of *ca.* 38 ± 10 °C and 78 ± 10 °C for HLBs of 11 and 13, respectively. The predicted LCST for

PyrM-PEG4-CH_2CON(PEG2)$_2$ is 83 ± 10 °C, which does not disagree with the observed absence of LCST below 90 °C. The margin of error is not unreasonable given the considerable number of approximations associated with HLB values. We suggest that this formula could guide the selection of new head groups. It is potentially applicable to any surfactant with a head group attached to a PyrM-PEGn anchor-linker ensemble *via* amide coupling. It could be used to determine whether a new surfactant is likely to show LCST and give a rough approximation of this temperature.

In addition to analysing LCST trends in terms of HLB we were keen to relate LCST more directly to molecular structure. Previous studies have shown relationships between structure and LCST for materials containing a PEG moiety.[192-194,224] These are typically simpler molecules than our surfactants, such as monoalkylated OEGs. Huibers *et al.* showed a linear relationship between the logarithm of the number of PEG repeat units in a monoalkylated OEG and its LCST based on literature data for 62 materials.[192] Terms relating to other structural features, such as branching within the alkyl chain, are also included. Schott describes a linear equation involving the reciprocal of the LCST and the "effective degree of ethoxylation," i.e. the number of additional PEG repeat units beyond the minimum required to impart solubility in ice-cold water.[194] The study used a mixture of literature LCST values and experimental data, and included monoalkylated OEGs and OEGs monosubstituted with *para*-alkylated phenols (the latter group includes members of the Triton X surfactant family). Schott's method was subsequently refined by Kim and Kim to account for polydisperse PEG chains.[193] Based on a series of PEG8 derivatives, Berthod *et al.* describe a linear relationship between alkyl chain length and LCST for monoalkylated OEGs,[224] along with a more general relationship in which the LCST is proportional to the square root of the number of PEG repeat units, and also dependent on the alkyl chain length.

Based on these precedents and the relationships discussed in Section 5.1.3 we examined the relationship between the total number of PEG repeat units in our surfactants (i.e. those in both the linker and head groups), p, and their LCST. The value p was defined as shown in Figure 5.06 and included those in the OEG linker and any complete repeat units in the head group that did not include part of the APD moiety (to ensure the remainder of the head group was considered equally in all cases). Hence p = n + 3 for surfactants of general structure **PyrM-PEGn-CH_2CO(15-c-5)** (or **PyrB-PEGn-CH_2CO(15-c-5)**), and p = n + 2m for those of general structure **PyrM-PEGn-CH_2CO[APD(PEGmR)$_2$]**, as shown in Table 5.02 above.

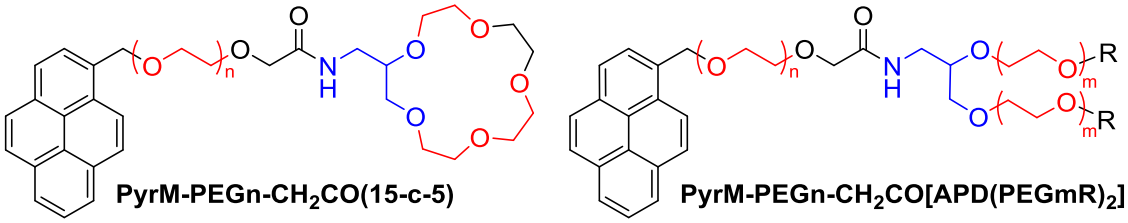

Figure 5.06: The total number of PEG repeat units in a surfactant, *p*, was defined by counting the units highlighted in red for crown ether (left) and podand (right) surfactants, respectively. For consistency no part of the APD moiety (highlighted in blue) was included in this count.

A simple plot of LCST against p (not shown) does not indicate a clear overall trend linking these values. However, by making empirical corrections based on the effects of head and anchor groups observed in Section 5.1.3 the data were fitted to a straight line. Making minor refinements to the empirical parameters improved correlation slightly, giving the relationship:

$$LCST = 4.30p + H - 1.17A + 7.8$$

The prefactor of 4.30 agrees with the observed average LCST increase of 4.25 °C per PEG repeat unit. The parameter H was derived empirically from the differences in LCST between surfactants which are identical apart from their head group. APD(PEGmEt)$_2$ head groups (which give the lowest observed LCSTs) were assigned H = 0 and the other head groups were referenced to this value. The values used are given in Table 5.02 above. Based on the work of Berthod *et al.* we have suggested that increasing the alkyl chain length in the anchor will have a negative, linear effect on LCST.[224] The parameter A is simply the number of methylene units in this alkyl chain (Table 5.02). Alternatively, each anchor group could have been assigned an empirical parameter as for the head groups. Figure 5.07 is a plot of p against LCST corrected for H and A. Linear regression analysis gives:

$$LCST - H + 1.17A = (4.30 \pm 0.17)p + (7.8 \pm 1.6)$$

$$R^2 = 0.984$$

from which the predictive equation above was derived. It is interesting that we find a direct linear relationship between p and the LCST for our surfactants, in contrast with the more complex relationships described for monoalkylated OEGs. The more elaborate structure of our surfactants is presumably responsible for this difference, which may be attributable to the large, hydrophobic, aromatic pyrene moiety, the bulkier, hydrophilic crown and podand head groups, or a combination of the two.

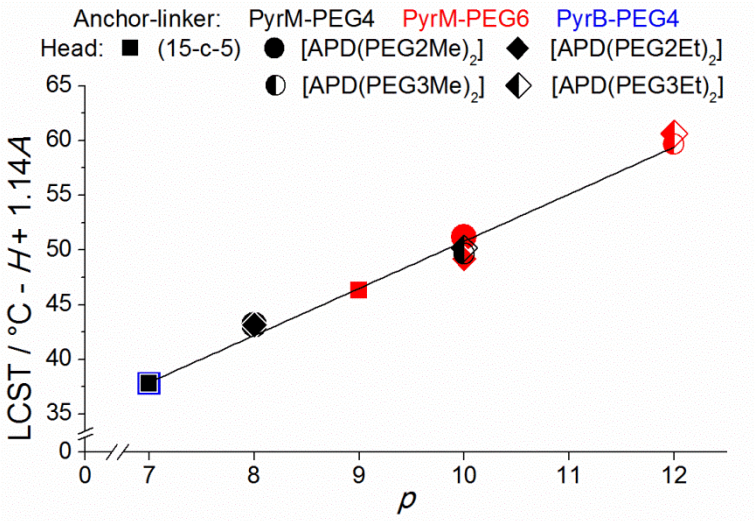

Figure 5.07: Comparison of total number of PEG repeat units, *p*, with an LCST corrected for the influence of anchor and head groups for the crown ether and podand surfactants which exhibit LCST behaviour. Surfactants with the same head group are shown with the same marker shape and those with the same anchor and linker in the same colour.

The experimental LCSTs agree with the values produced by the formula within 2 °C, much better agreement than the HLB method. Compared to the HLB method this formula is limited in the surfactants for which predictions can be made, as *H* values for any new head groups are unknown. To further refine this method the synthesis of surfactants with alternative alkyl chains in the anchor unit or other head groups would be of interest.

The structural and HLB predictive methods were applied to a range of podand surfactants including some for which synthesis had been unsuccessful (Chapter 4). All fitted the general structure **PyrM-PEGn-CH_2CO[APD(PEGmR)$_2$]** (see Figure 5.06 above), and are summarised with their predicted LCST values in Table 5.03. Predictions made using the structural method include assumptions to estimate appropriate *H* values. For R groups other than methyl and ethyl we have postulated a linear change in LCST with alkyl chain length. This is based on the work of Li *et al.* who observed a near-linear relationship between LCST and the ratio of ethyl- and propyl-substituted PEG2 moieties at the periphery of PAMAM dendrons,[201] suggesting that increasing alkylation has a negative linear effect on LCST. We have extended this assumption to predictions for hydroxy-terminated podands, but this may not fully account for their hydrophilicity.

Table 5.03: Predicted LCSTs for podand surfactants of structure **PyrM-PEGn-CH_2CO[APD(PEGmR)$_2$]** based on the structural and HLB predictive methods.

			Structural Prediction				HLB Prediction	
n	**m**	**R**	***p***	***H***	***A***	**Predicted LCST[a] / °C**	**HLB**	**Predicted LCST[b] / °C**
2	2	Me	6	27.1	1	59.5	11.53	49 ± 10
2	2	Et	6	0	1	32.5	10.58	30 ± 10
8	3	Me	14	27.1	1	94.0	14.17	101 ± 10
8	3	Et	14	0	1	67.0	13.22	82 ± 10
4	2	H	8	54.2[c]	1	95.0[d]	14.38	106 ± 10
6	2	H	10	54.2[c]	1	104.0[d]	15.04	119 ± 10
4	2	Pr	8	-27.1[c]	1	14.0	10.29	24 ± 10
4	3	Pr	10	-27.1[c]	1	22.5[e]	10.95	37 ± 10[e]
6	3	Pr	12	-27.1[c]	1	31.0	11.61	50 ± 10
4	2	^{n}Bu	8	-54.2[c]	1	-13.0	9.34	5 ± 10
4	3	^{n}Bu	10	-54.2[c]	1	-4.5[e]	10.00	18 ± 10[e]
6	3	^{n}Bu	12	-54.2[c]	1	4.0	10.66	31 ± 10
12	3	^{n}Bu	18	-54.2[c]	1	30.0	12.64	71 ± 10

[a] to nearest 0.5 °C; [b] to nearest 1 °C; [c] assuming the number of methylene units in the head group has a linear contribution; [d] values may be underestimates if the *H* value does not correctly account for the hydrophilicity of terminal alcohols; [e] the same prediction is made for the n = 6, m = 2 structural isomer.

Both predictive methods suggest similar trends in LCST for the candidate surfactants and indicate that simple structural modifications should allow the LCST to be tuned within the liquid range of water at atmospheric pressure. Small changes to the linker of the isolated podand surfactants would cover a range from *ca.* 30 °C to *ca.* 100 °C. Predictions for new R groups using both methods expectedly show that the most hydrophilic materials, those with terminal alcohols, will have the highest LCSTs. Assuming an *H* value of 54.2, LCSTs of 95.0 and 104.0 °C for n = 4 and 6 surfactants, respectively, are predicted by the structural method. We consider 95 °C to be too high a temperature to easily investigate or exploit the LCST transition. A predicted value above 100 °C indicates no LCST behaviour (at least at atmospheric pressure[224]). The HLB method predicts LCSTs above 100 °C for both alcohol-terminated podands. Both methods show that these materials are not relevant targets. A similar argument can be made for the *n*-butyl analogues with PEG4 or PEG6 linkers, for which both methods predict low LCSTs; in some cases below 0 °C (this implies that they would be water immiscible, at least at atmospheric pressure). There is a possibility that a longer PEG12 linker would increase the LCST to a reasonable temperature, but the predicted value differs greatly between the two methods. Propyl analogues may also not have an LCST significantly higher than room temperature.

5.2: MWNT Dispersion Studies

5.2.1: Results and Discussion

Investigation of the dispersion of MWNTs using the non-ionic surfactants has been more limited than for the anionic surfactants as more attention has been paid to their use in graphite exfoliation (Chapter 6). However, we have investigated MWNT dispersions prepared using two non-ionic surfactants, **PyrB-PEG4-CH_2CO(15-c-5)** and **PyrM-PEG4-CH_2CO[APD(PEG2Et)$_2$]**. MWNT dispersions were prepared using our standard conditions (Section 3.1). The data for **PyrM-PEG4-CH_2CO[APD(PEG2Et)$_2$]** in 0.6 M NaCl was collected by Dr Daniel Welsh. The results of MWNT dispersion studies in Millipore deionised water and 0.6 M NaCl are shown in Figure 5.08 and Table 5.04. Selected results from Chapter 3 are included in Figure 5.08 for comparison. As in Chapter 3, the percentage of MWNTs dispersed is relative to the maximum possible value under the conditions used, 333.333 mg L^{-1}. Reproducibility was similar to the previous studies, and as before the small error in ε was discounted. The stability of dispersions in non-ionic surfactants was comparable to those in anionic surfactants.

Table 5.04: C_{MWNT} in 1 mM non-ionic surfactant solutions in Millipore water and 0.6 M NaCl. Errors are the standard deviation of 3 results.

	Millipore Water			0.6 M NaCl		
Surfactant	**C_{MWNT} / mg L^{-1}**	**Error (σ) / mg L^{-1}**	**% MWNTs Dispersed**	**C_{MWNT} / mg L^{-1}**	**Error (σ) / mg L^{-1}**	**% MWNTs Dispersed**
PyrB-PEG4-CH_2CO(15-c-5)	202	8	61	66	7	20
PyrM-PEG4-CH_2CO[APD(PEG2Et)$_2$]	168	5	50	41	6	12

As hypothesised, in Millipore water both non-ionic surfactants gave the C_{MWNT} higher than observed under any conditions for anionic or reference surfactants. **PyrB-PEG4-CH_2CO(15-c-5)** gave the highest C_{MWNT}: 202 ± 8 mg L^{-1} (61%). The highest C_{MWNT} for an anionic surfactant in Millipore water was 148 ± 1 mg L^{-1} (44%) using **PyrB-PEG6-CH_2COONa**. Similarly to **Triton X-100**, a significant reduction in C_{MWNT} was observed when the non-ionic surfactants were tested in 0.6 M NaCl; in this case NaCl had an even more profound negative impact, reducing C_{MWNT} by a factor of three and four, respectively, for **PyrB-PEG4-CH_2CO(15-c-5)** and **PyrM-PEG4-CH_2CO[APD(PEG2Et)$_2$]** (rather than a factor of two for **Triton X-100**). As discussed in Section 3.3.3, the addition of NaCl moves an aqueous solution of a non-ionic surfactant closer to its cloud point, reducing its hydrophilicity and therefore its ability to disperse carbonaceous material. In the absence of an ionic head group any favourable interactions between dissolved cations and the OEG

moieties appear to be insufficient to overcome this effect. The enhanced negative impact of 0.6 M NaCl on our non-ionic surfactants in comparison to **Triton X-100** could be due to the ability of crown ethers and podands to coordinate cations. The 15-crown-5 moiety in **PyrB-PEG4-CH$_2$CO(15-c-5)** is complementary to sodium cations and its binding may be further strengthened if the linker OEG also contributes, allowing the surfactant to bind ions like a lariat ether[202] (Figure 5.09) Similar binding could occur with **PyrM-PEG4-CH$_2$CO[APD(PEG2Et)$_2$]**, although it has lower preorganisation. This complexation would favour ether oxygen atoms directed towards the bound cation and away from the bulk solution, hindering additional interactions between the OEG oxygen atoms and other dissolved cations.

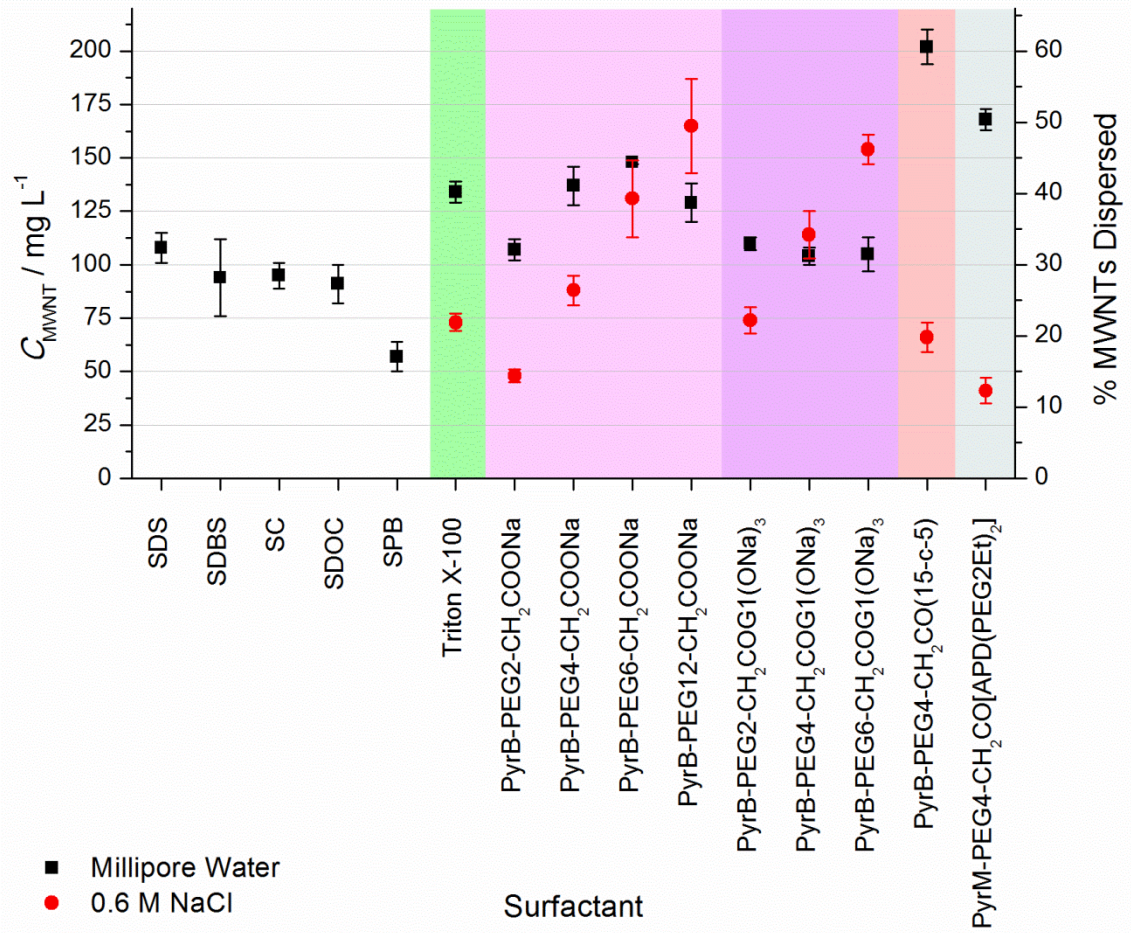

Figure 5.08: C_{MWNT} in a range of 1 mM surfactant solutions in Millipore water and 0.6 M NaCl. Error bars are the standard deviation of 3 results except for **SDS**, **SDBS**, **SC**, **SDOC** and **SPB**, which are from 6 results. Colours indicate surfactant groups: white - reference anionic; green – reference non-ionic; pink – ether linker G0; purple – ether linker G1; red – crown ether; grey – podand.

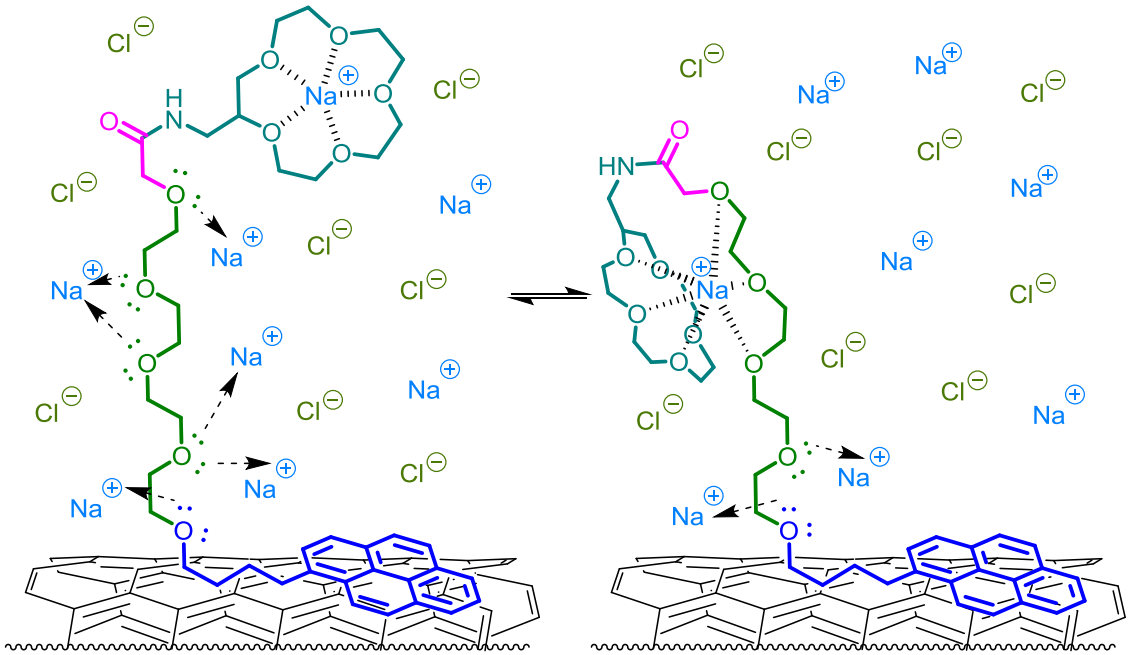

Figure 5.09: The crown ether moiety of **PyrB-PEG4-CH$_2$CO(15-c-5)** can complex sodium ions. The ether linker may contribute further to binding such that the surfactant acts like a lariat ether. The favoured orientation of the linker is unknown; here it is suggested that it projects into the aqueous medium due to its hydrophilicity. For clarity a SWNT is used to represent a MWNT surface.

5.2.2: Temperature Response Tests

The MWNT dispersions in **PyrB-PEG4-CH$_2$CO(15-c-5)** were tested for a temperature response using the method for undiluted dispersions from Section 3.4. Spectral changes were observed for both the dispersion and parent surfactant solution above the LCST of the surfactant. The samples were held overnight at a temperature above that where spectral changes were observed to examine any further changes. Further spectra were recorded after cooling back to 20 °C. Figure 5.10 shows UV-visible absorption spectra using 1 mM **PyrB-PEG4-CH$_2$CO(15-c-5)** in both Millipore water and 0.6 M NaCl; for each set of conditions data is shown for representative surfactant and dispersion samples. Observations were consistent across a triplicate set of samples in all cases.

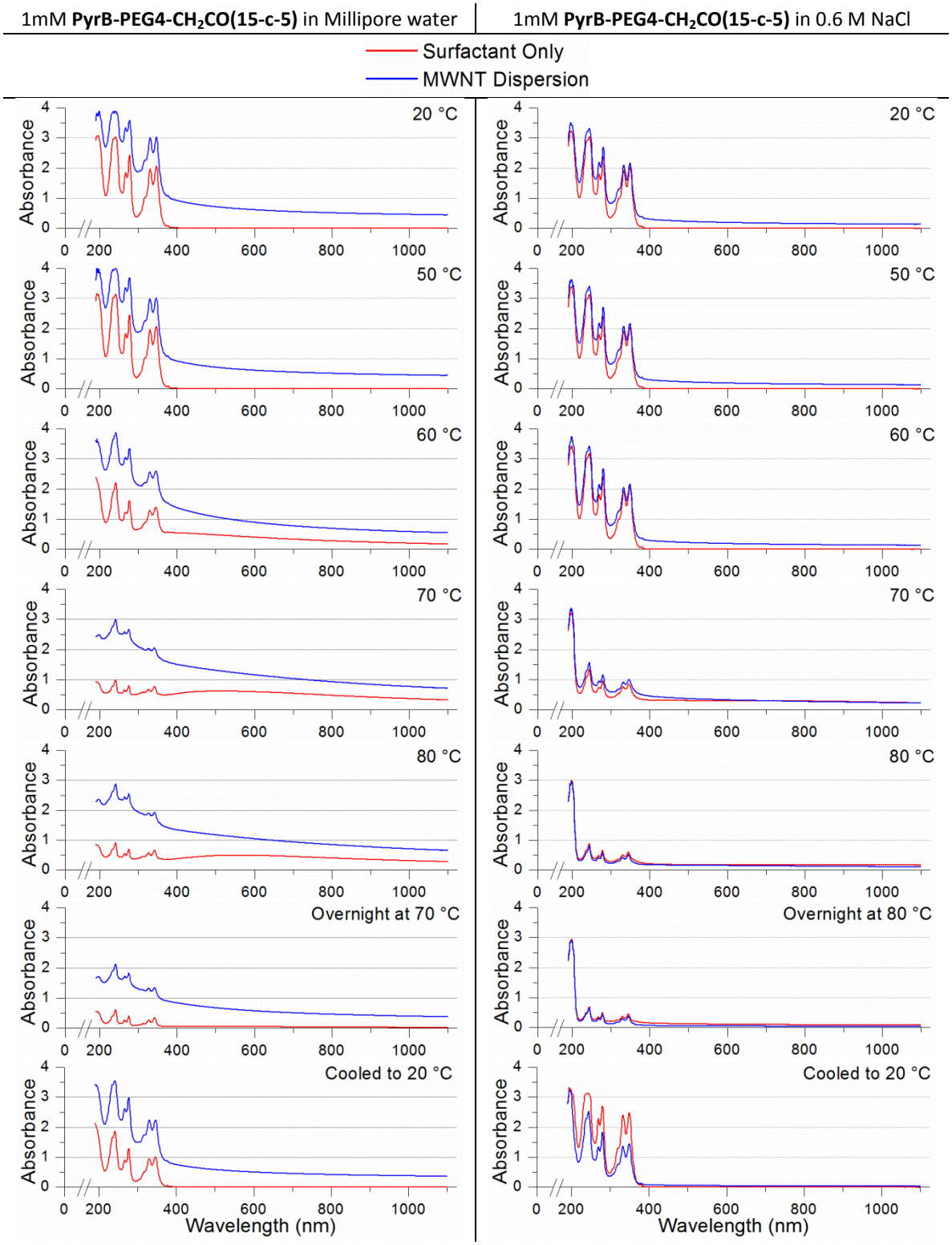

Figure 5.10: Representative spectra of parent surfactant solutions and MWNT dispersions in 1 mM **PyrB-PEG4-CH$_2$CO(15-c-5)** in Millipore water and 0.6 M NaCl at various temperatures.

As the surfactant solutions are heated the absorbance peaks below *ca.* 400 nm (which relate to the pyrene moiety) decrease in magnitude. Their absorbance increases upon cooling, although in Millipore water they remain somewhat below their original intensity.

Additionally the development of a broad absorbance across the spectral range, characteristic of clouding above the LCST, can be observed as the solutions are heated. The temperature at which this effect is first observed is 60 °C for the aqueous solution (in agreement with the turbidimetric LCST, 58 °C) and 70 °C for the solution in 0.6 M NaCl. This behaviour is counterintuitive: the presence of a salt should lower the LCST of the solution by reducing the hydrophilicity of the surfactant. We suggest that ionic character imparted by cation binding may allow for miscibility with water at higher temperatures despite the concurrent reduction in hydrophilicity. The broad absorbance was no longer observed after the solutions had been heated overnight. We reason that complete phase separation has occurred after this time.

In the case of the MWNT dispersions the decrease in pyrene absorbance can also be seen upon heating. Again this increases upon cooling, but to below its original level. The presence of dispersed MWNTs means that a broad absorbance is observed even at the beginning of the experiment, however, growth in this absorbance due to the surfactant clouding can still be detected above the LCST. This indicates that not all surfactant is bound to the surface of MWNTs. The overlapping absorbance due to LCST meant that C_{MWNT} could not be determined based on UV-visible absorption data. After heating overnight the broad absorbance has lower intensity than at the beginning of the experiment, indicating that in addition to phase separation of aggregated surfactant there is a reduction in C_{MWNT}, i.e. thermally induced precipitation of dispersed MWNTs has occurred. The spectral change is particularly noticeable in the dispersion in 0.6 M NaCl, where the absorbance is near zero above *ca.* 400 nm. The precipitated MWNTs could be observed by eye. For the dispersion in 0.6 M NaCl some precipitation was visible after only 15 min at 80 °C. NaCl therefore appears to accelerate this precipitation, although it leads to a lower C_{MWNT} in the initial dispersion. The change in absorbance due to MWNTs was not reversed upon cooling, and similarly the precipitated MWNTs did not visibly re-disperse.

Although simply cooling did not reverse the precipitation of MWNTs, it was possible to re-disperse them with only mild agitation. Inverting a sample repeatedly over a period of 1 min significantly increased the absorbance associated with MWNTs. Absorbance spectra before and after this process are shown in Figure 5.11. In the case of the dispersion in 0.6 M NaCl the absorbance was slightly (*ca.* 1%) higher than before any heating, indicating that essentially all of the MWNTs were re-dispersed. The small increase in absorbance is attributed to evaporation of a small quantity of water during the heating cycle. For the aqueous dispersion the absorbance due to MWNTs was around 90% of its original value following the inversions,

showing that the majority of MWNTs had been re-dispersed. The absorbance peaks related to pyrene had also now returned to their original levels. In an attempt to re-disperse any remaining MWNTs the samples were bath sonicated for 1 minute and then subjected to a further 1 minute of gentle inversions. These are considerably milder conditions than those used initially to prepare the dispersions. Following this treatment no significant spectral changes were observed for the dispersion in 0.6 M NaCl, suggesting that the earlier inversions were sufficient to re-disperse all of the precipitated MWNTs. The dispersion in Millipore water now had an absorption *ca.* 2% higher than the original sample, suggesting complete re-dispersion had been achieved (again the absorption increase is attributed to water loss) The re-dispersed samples were kept under ambient conditions for several days and showed no significant visual or spectral changes in this time. This indicates that following precipitation and re-dispersion the dispersions remain stable. *This is, to the best of our knowledge, the first example of the reversible thermal precipitation of CNTs using a small molecule dispersant* (rather than thermoresponsive polymers[109,113]) *without harsh re-processing* (e.g. extended ultrasonication[118]).

To further qualitatively investigate this phenomenon MWNT dispersions were heated in a water bath; precipitation was observed after only 15 min at 85 °C for MWNTs dispersed in 0.6 M NaCl using 1 mM **PyrB-PEG4-CH_2CO(15-c-5)** or **PyrM-PEG4-CH_2CO[APD(PEG2Et)$_2$]**. Aqueous solutions responded much more slowly; after heating for 14 h at 70 °C and a further 5 hours at 85 °C only limited precipitation could be seen. The precipitate from both 0.6 M NaCl dispersions was stable for several hours after cooling and could easily be re-dispersed by shaking the sample (Figure 5.12). The re-dispersed MWNTs were re-precipitated by re-heating. The resulting precipitate could also be re-dispersed by shaking. Re-dispersed MWNTs in 1 mM **PyrB-PEG4-CH_2CO(15-c-5)** in 0.6 M NaCl were stable (i.e. no visible precipitate formed) for more than 2 weeks after four thermal precipitation and re-dispersion cycles. *This shows that for this surfactant only very gentle agitation is needed to re-form a stable dispersion after thermal precipitation*. Re-dispersed MWNTs in 1 mM **PyrM-PEG4-CH_2CO[APD(PEG2Et)$_2$]** in 0.6 M NaCl were less stable and precipitated within 1.5 days following two thermal precipitation and re-dispersion cycles. This suggests that at least partial stripping of this surfactant from the MWNT surface occurs during the thermal precipitation process.

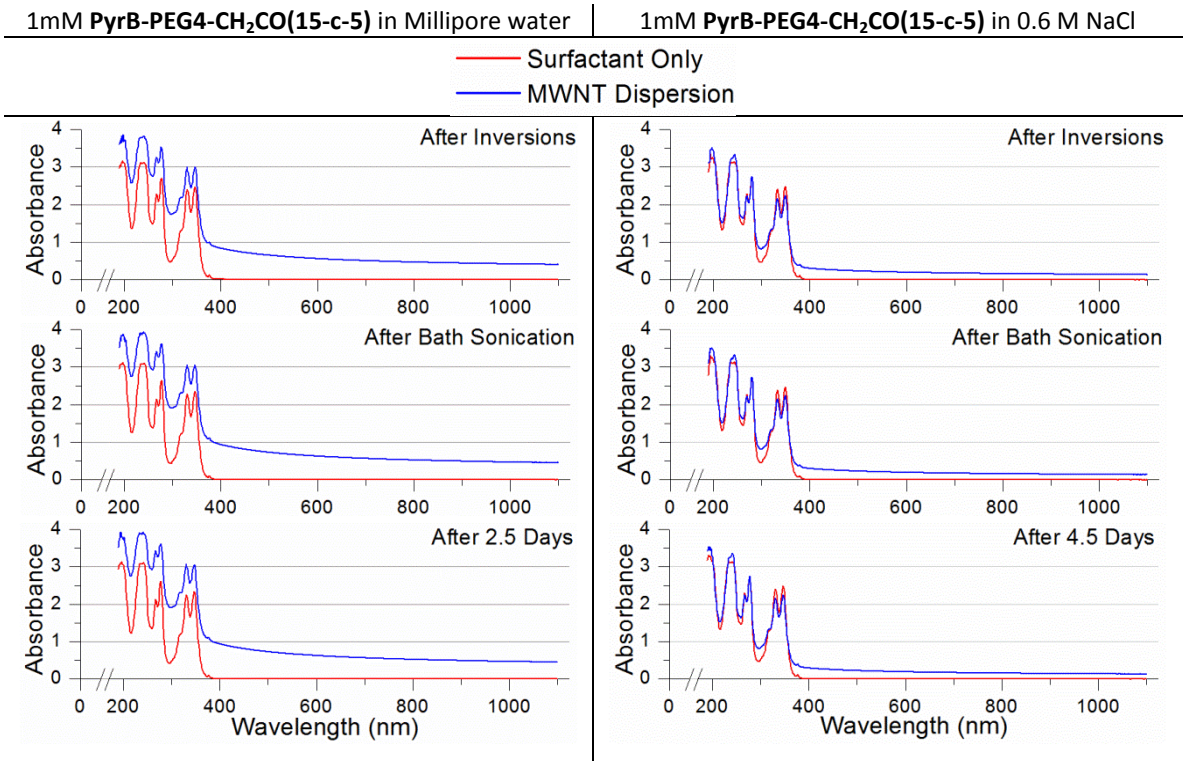

Figure 5.11: Representative spectra of parent surfactant solutions and MWNT dispersions in 1 mM **PyrB-PEG4-CH$_2$CO(15-c-5)** in Millipore water and 0.6 M NaCl after a heating cycle, subjected to various conditions to afford re-dispersion.

Figure 5.12: A MWNT dispersion in 1 mM **PyrB-PEG4-CH$_2$CO(15-c-5)** in 0.6 M NaCl before heating (left), after heating (centre) and after cooling and shaking (right).

We attribute the reversible thermally induced precipitation of MWNTs dispersed using non-ionic ALH surfactants to two key features. i) The LCST transition allows the hydrophilic moieties at the periphery of functionalised MWNTs to be switched "off," becoming hydrophobic. Re-aggregation occurs through hydrophobic effects, which are enhanced in the presence of NaCl. ii) The strongly-binding pyrene anchor unit ensures that the surfactant remains bound to the MWNT surface during aggregation. This prevents the aggregated MWNTs from re-forming π-stacked bundles. Upon cooling the surfactants are switched back "on" and regain their hydrophilic character. As there are no strong attractive interactions between the aggregated, functionalised MWNTs, re-dispersion is facile.

5.3: Conclusions

The LCSTs of the non-ionic surfactants synthesised in Chapter 4 have been determined by visual inspection, turbidimetry and DLS measurements. Agreement between the three methods is good. The LCSTs have been used to develop two methods to predict the LCST of additional ALH surfactants: one based on HLB and one based on empirically derived structural parameters. Two of the surfactants, **PyrB-PEG4-CH_2CO(15-c-5)** and **PyrM-PEG4-CH_2CO[APD(PEG2Et)$_2$]**, have been shown to effectively disperse MWNTs, giving higher C_{MWNT} than any of our anionic surfactants in Millipore water. MWNTs dispersed using these surfactants can be thermally precipitated; this effect is enhanced if the dispersions are prepared in 0.6 M NaCl. The precipitated MWNTs can be re-dispersed using much gentler methods than those initially used to prepare the dispersion. For **PyrB-PEG4-CH_2CO(15-c-5)** the dispersion shows good stability even after four thermal precipitation and re-dispersion cycles. To our knowledge this is the first time gently reversible thermal precipitation of MWNTs has been achieved using a small molecule dispersant.

Chapter 6: Exfoliation of Graphite Using Anionic and Non-Ionic Surfactants

This chapter describes an ongoing study in which members of the anionic and non-ionic surfactant series are applied to the exfoliation of graphite. Investigation of a temperature response in dispersions is discussed.

6.1: Graphite Exfoliation

6.1.1: Methodology

The ability of surfactants to exfoliate graphite and form stable dispersions was assessed using methodology based on our MWNT dispersion studies (Chapters 3 and 5). To ensure all data were comparable the same batch of graphite* was used throughout our study. To obtain reasonable levels of dispersion, several alterations to the procedure used for MWNTs were required. These included a larger feedstock of the material to be dispersed, longer sonication time and lower centrifugal force (full details are given in the experimental section). Preliminary TEM studies on dispersions prepared in **SDOC** (not shown) indicated that the dispersed material contains graphitic flakes of up to 20 layers. We will use the term exfoliated graphite (EG) to describe this heterogeneous mixture of graphene, MLG and graphite nanoflakes.[48] Spectroscopic studies were conducted as for MWNT dispersions, using ten-fold dilutions of the EG dispersions. An extinction coefficient, ε, was required for EG in order to determine the concentration of the dispersions, C_{EG}. Previously reported ε values for 'graphene' dispersions (which generally contain a mixture of at least graphene and MLG) range from 13.90 to 66.00 ml mg^{-1} cm^{-1} at 660 nm.[46,65] Intermediate values of *ca.* 24-38 ml mg^{-1} cm^{-1} are common.[103,181,225,226] An attempt to calculate ε in our laboratory using a filtration method based on that reported by Das *et al.*[227] gave what appeared to be an erroneously low value of 2.7 ± 1.4 ml mg^{-1} cm^{-1} at 660 nm. This differs from reported values by an order of magnitude and has a large experimental error. We hope to establish a more representative value by using the precipitation method[94] used to determine ε for MWNTs in Section 3.1. In this Chapter we will adopt the convention used by Seo *et al.* and use the largest reported value of ε (66.00 ml mg^{-1} cm^{-1} at 660 nm[65]) to establish a minimum value for C_{EG}.[228] The maximum possible C_{EG} under the conditions used is 5000 mg L^{-1}. Further optimisation of

* Asbury Carbons, grade 4827

the conditions has not yet been investigated. In particular, studies in the literature often use much longer sonication times to ensure EG that consists mainly of graphene and FLG is obtained.

The structures of the surfactants used to exfoliate graphite are summarised in Appendix 1. As in our MWNT dispersion study, commercial surfactants were used as a reference. Four of these (**SDS**, **SDBS**, **SDOC** and **Triton X-100**) were also used in that study, while the fifth, sodium taurodeoxycholate, **STDOC**, was chosen as it has been shown to be efficient at graphene exfoliation.[103] Selections of our anionic and non-ionic surfactants were used to prepare EG dispersions. The anionic species were linker-free surfactant **PBA-G1(ONa)$_3$**, amide linker surfactants **PBA-C6-G1(ONa)$_3$** and **PBA-(C6)$_2$-G1(ONa)$_3$**, and ether linker surfactant **PyrB-PEG6-CH$_2$COG1(ONa)$_3$**. The non-ionic species were the crown ether surfactants **PyrB-PEG4-CH$_2$CO(15-c-5)** and **PyrM-PEG4-CH$_2$CO(15-c-5)**, and the podand surfactants **PyrM-PEG4-CH$_2$CO[APD(PEG2Me)$_2$]**, **PyrM-PEG4-CH$_2$CO[APD(PEG2Et)$_2$]**, **PyrM-PEG6-CH$_2$CO[APD(PEG2Me)$_2$]** and **PyrM-PEG6-CH$_2$CO[APD(PEG2Et)$_2$]**.

6.1.2: Results

Table 6.01: C_{EG} in a range of 1 mM aqueous surfactant solutions. Errors are the standard deviation of 3 results except for **SDBS** which is from 4 results. % graphite dispersed is relative to the maximum value possible in the conditions used, 5000 mg L^{-1}.

	Millipore Water			0.6 M NaCl		
Surfactant	**C_{EG} / mg L^{-1}**	**Error (σ) / mg L^{-1}**	**% Graphite Dispersed**	**C_{EG} / mg L^{-1}**	**Error (σ) / mg L^{-1}**	**% Graphite Dispersed**
SDS	70	3	1	-	-	-
SDBS	93	20	2	-	-	-
SDOC	72	3	1	-	-	-
STDOC	76	1	2	-	-	-
Triton X-100	-	-	-	1	0	0.02
PBA-G1(ONa)$_3$	91	4	2	0	0	0
PBA-C6-G1(ONa)$_3$	83	5	2	11	2	0.22
PBA-(C6)$_2$G1(ONa)$_3$	81	4	2	20	2	0.4
PyrB-PEG6-CH$_2$COG1(ONa)$_3$	75	2	2	35	2	0.7
PyrB-PEG4-CH$_2$CO(15-c-5)	52	1	1	-	-	-
PyrM-PEG4-CH$_2$CO(15-c-5)	39	1	1	1	0	0.02
PyrM-PEG4-CH$_2$CO[APD(PEG2Me)$_2$]	60	0	1	1	1	0.02
PyrM-PEG4-CH$_2$CO[APD(PEG2Et)$_2$]	53	3	1	-	-	-
PyrM-PEG6-CH$_2$CO[APD(PEG2Me)$_2$]	72	2	1	-	-	-
PyrM-PEG6-CH$_2$CO[APD(PEG2Et)$_2$]	76	2	2	-	-	-

Figure 6.01 and Table 6.01 show the results of graphene exfoliation in Millipore water and 0.6 M NaCl conducted in our laboratory by Dr Daniel Welsh. C_{EG} represents a minimum value

based on ε = 66.00 ml mg^{-1} cm^{-1} at 660 nm.[65] Any trends will still hold if a different extinction coefficient is found to be more appropriate as all results will be scaled up or down equivalently. Reproducibility was generally good, although as in the MWNT study the results in **SDBS** had a large standard deviation. The dispersions showed no signs of instability under ambient conditions over several months.

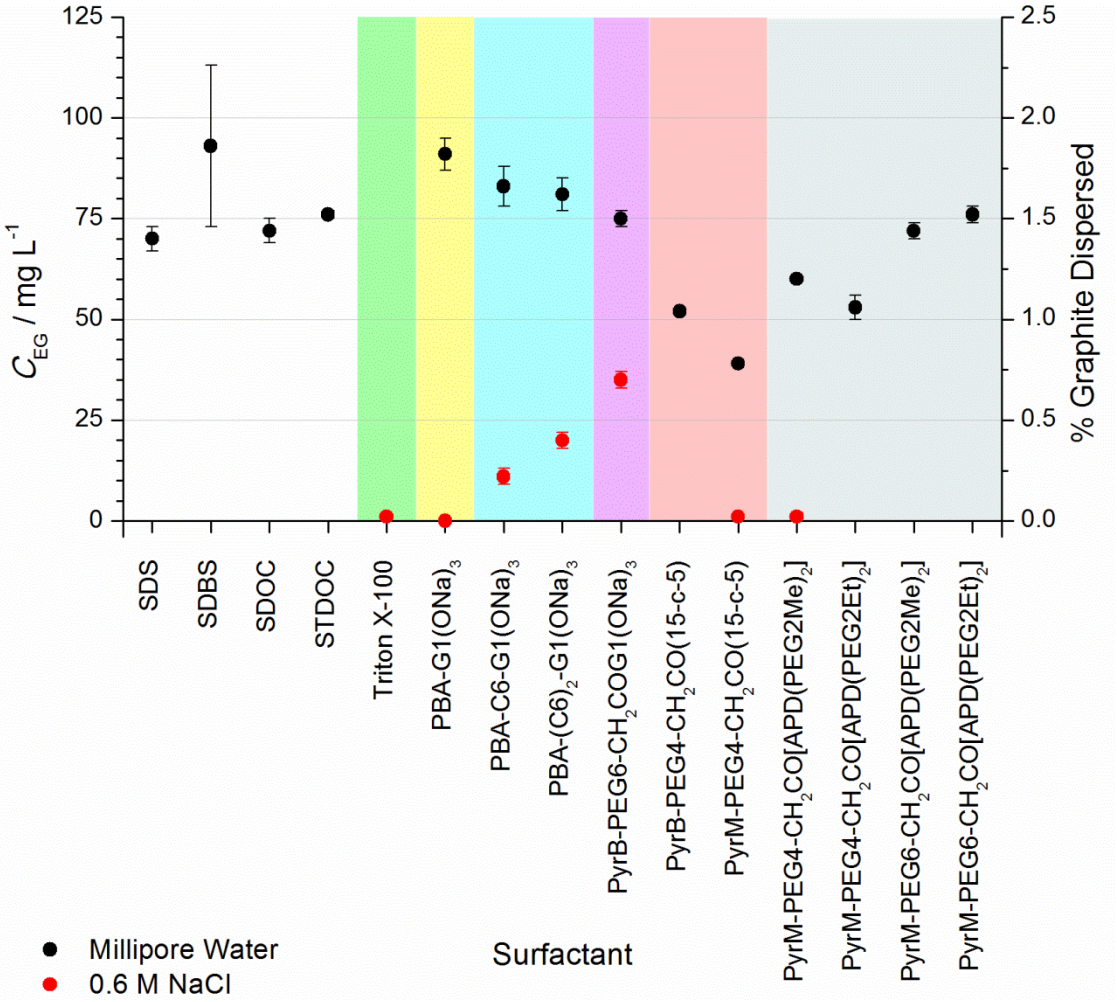

Figure 6.01: Minimum C_{EG} in a range of 1 mM surfactant solutions in Millipore water and 0.6 M NaCl. Error bars are the standard deviation of 3 results except for **SDBS** which is from 4 results. Colours indicate surfactant groups: white - reference anionic; green – reference non-ionic; yellow – linker-free G1; light blue – amide linker G1; purple – ether linker G1; red – crown ether; grey – podand.

6.1.3: Anionic Surfactants

Little variation could be seen in C_{EG} obtained using the commercial surfactants **SDS**, **SDOC** or **STDOC** in Millipore water. **SDBS** gives a slightly higher C_{EG} although it has a large experimental error. These results disagree with those reported by Sun *et al.* who found **STDOC** to give much more concentrated dispersions than **SDS**,[103] although they used much

longer sonication times. Guardia *et al.* report that these surfactants all give reasonably similar concentrations of graphene and FLG.[102] The small variation between commercial anionic surfactants is similar to that observed for MWNT dispersions in Chapter 3.

In Millipore water our anionic surfactants all gave C_{EG} comparable to the commercial materials. In contrast to the MWNT dispersions studies, linker-free **PBA-G1(ONa)$_3$** and amide linker surfactants **PBA-C6-G1(ONa)$_3$** and **PBA-(C6)$_2$-G1(ONa)$_3$** give higher C_{EG} than the ether linker surfactant **PyrB-PEG6-CH$_2$COG1(ONa)$_3$**. We had expected to observe trends in EG dispersion ability which would mirror those with MWNTs, so we were initially surprised to see that the addition of hydrophilic PEG linker had a negative effect compared to linker-free and amide linker species. The amide linker surfactants also gave lower C_{EG} than **PBA-G1(ONa)$_3$**. The presence of a linker may hinder the exfoliation process as intercalation of graphite with bulkier surfactants will be less favourable. This effect is much more significant for graphene exfoliation than MWNT dispersion due to the much larger surface area between graphene layers than bundled MWNTs. Hence the least bulky G1 surfactant, **PBA-G1(ONa)$_3$**, gives the highest C_{EG}.

Trends in C_{EG} for the anionic surfactants in 0.6 M NaCl resemble those in C_{MWNT} much more closely. No EG was observed when **PBA-G1(ONa)$_3$** was used under these conditions, whereas the addition of linkers gave low levels of C_{EG}. As with MWNTs the ether linker species **PyrB-PEG6-CH$_2$COG1(ONa)$_3$** was the best of those tested. However, in 0.6 M NaCl C_{EG} was only half that obtained in Millipore water, in contrast to the significant increase in C_{MWNT} observed using this surfactant in 0.6 M NaCl. Including the linker-free species it can be seen that sequential addition of C6 linkers results in a linear increase in C_{EG}, providing further evidence for the key role of linker units in the presence of salts.

6.1.4: Non-Ionic Surfactants

Our non-ionic surfactants are generally less effective at exfoliating graphite in Millipore water than our anionic surfactants. The best of those tested, **PyrM-PEG6-CH$_2$CO[APD(PEG2Et)$_2$]** gives a comparable C_{EG} to the worst of the tested anionic species, **PyrB-PEG6-CH$_2$COG1(ONa)$_3$**. This highlights the differences between MWNT dispersion and graphite exfoliation, as excellent results were achieved using non-ionic surfactants to disperse MWNTs. Crown ether surfactants are less effective at graphite exfoliation than analogous podands. Results for surfactants with a PyrM-PEG4 anchor-linker ensemble show

an increase in C_{EG} as the head group is changed from 15-c-5 to APD(PEG2Et)$_2$ to APD(PEG2Me)$_2$. PyrM-PEG6 surfactants show the opposite trend for the two podand head groups, with the APD(PEG2Et)$_2$ species giving a slightly higher C_{EG}. For both podand head groups the surfactants with longer PEG6 linkers are better dispersants. The poorer exfoliation ability of the crown ether surfactants could relate to steric bulk; the 15-c-5 head group is limited in the conformations it can adopt, whereas the podand head groups are much more flexible. This should allow podand surfactants to intercalate into graphite more easily than crown ether surfactants. Further results are required to fully understand the differing effect of the terminal alkyl units of podand surfactants when different linker units are used. There may be a delicate balance between hydrophilicity and hydrophobicity which impacts on surfactant performance. Another interesting observation is that the PyrB-anchored crown ether surfactant gives a higher C_{EG} than its PyrM-anchored analogue. We relate this to an increased affinity for the graphitic surface due to a higher number of hydrophobic methylene groups. This may facilitate intercalation of the surfactant into graphite despite a concomitant slight increase in steric bulk.

Attempted exfoliation of graphite using our non-ionic surfactants in 0.6 M NaCl resulted in negligible levels of dispersion. **Triton X-100** gave equivalent results under these conditions, indicating that this relates to the non-ionic nature of the surfactants. 0.6 M NaCl was observed to have a significant negative effect on C_{MWNT} for non-ionic surfactants, which is enhanced in the case of EG. The addition of a salt increases the strength of hydrophobic effects and also reduces the hydrophilicity of the OEG moieties in the non-ionic surfactants. This will make it much more difficult for these surfactants to stabilise dispersed EG, particularly if surface coverage is incomplete. The larger surface area of EG than MWNTs means this is much more likely. This effect is less critical for anionic surfactants, which retain a level of coulombic repulsion even in the presence of salts. We demonstrated the destabilising effect of salts by adding a small quantity of solid NaCl to an aqueous dispersion of EG in **PyrM-PEG4-CH$_2$CO[APD(PEG2Et)$_2$]**. This resulted in rapid, irreversible flocculation and precipitation of EG, confirming that the negative effect of salt relates to the stability of surfactant-functionalised EG, not the initial exfoliation process.

6.2: Temperature Studies

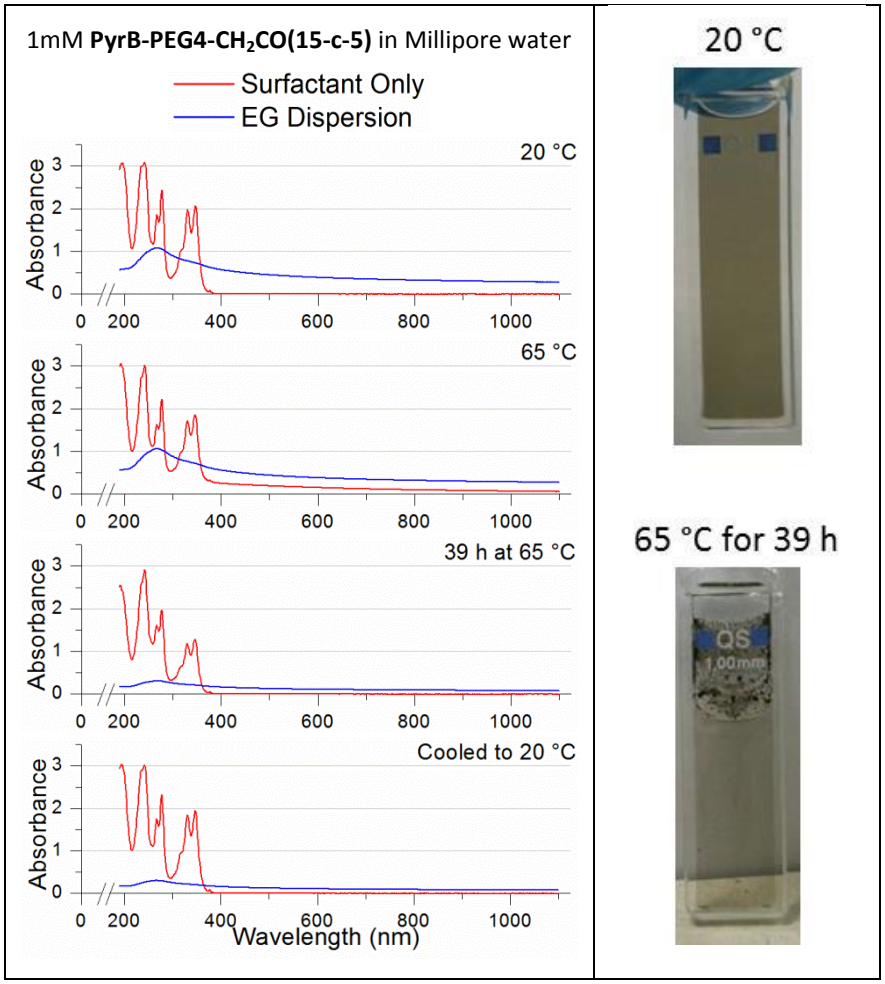

Figure 6.02: Left: Spectra of the parent surfactant solution and an EG dispersion in 1 mM **PyrB-PEG4-CH$_2$CO(15-c-5)** in Millipore water at various points in the temperature study. Right: Photographs of the EG dispersion in a 1 mm cuvette initially (top) and after heating at 65 °C for 39 h (bottom).

We showed in Section 5.2.2 that MWNTs dispersed in our temperature responsive non-ionic surfactants could be reversibly thermally precipitated. We conducted a similar spectroscopic study on an aqueous dispersion of EG in 1 mM **PyrB-PEG4-CH$_2$CO(15-c-5)**. The low C_{EG} given by our non-ionic surfactants in 0.6 M NaCl meant the study could not be conducted in this medium, in which thermal precipitation of MWNTs was most easily and quickly observed. Spectroscopic evidence of comparable behaviour in aqueous dispersions of EG to that observed for MWNTs is shown in Figure 6.02. In the dispersion spectra no clear peaks associated with pyrene can be seen and an initial broad absorbance increase is not seen when the dispersion is heated above the LCST. This suggests that no free surfactant is present, i.e. all of the surfactant added during processing is strongly bound to graphitic surfaces. Our

observations were complicated by the formation of deposits of precipitated EG on the cuvette walls, just above the solvent level, rather than at its base (Figure 6.02). Further experiments are required to confirm that this effect is definitely attributable to thermal precipitation and not due to evaporation of water from the sample. Attempts to re-disperse the precipitated material had limited success, even after bath sonication. We hope that these difficulties can be overcome by using a larger sample of dispersion in a bigger vessel.

6.3: Conclusions

We have shown that surfactants from both our anionic and non-ionic series are effective at exfoliating graphite, performing similarly to commercial surfactants in Millipore water under the conditions used. Exfoliation of graphite is more difficult in the presence of 0.6 M NaCl, but as for dispersions of MWNTs, C_{EG} in this medium can be improved by using anionic surfactants with linkers which can interact favourably with dissolved ions. Non-ionic surfactants perform particularly poorly in 0.6 M NaCl; we attribute this to a combination of their reduced hydrophilicity and the increased strength of hydrophobic interactions in the presence of salts. Preliminary evidence of thermal precipitation of EG dispersed using our non-ionic surfactants has been obtained.

Chapter 7: Experimental Procedures

7.1: General Methods

Unless otherwise stated reactions were conducted under an argon atmosphere which was dried by passage through a column of phosphorus pentoxide. All commercial chemicals were used without further purification. Anhydrous solvents were dried through an HPLC column on an Innovative Technology Inc. solvent purification system. Normal-phase column chromatography was carried out using 40-60 μm mesh silica or a Biotage One Isolera automated purification system fitted with a Biotage SNAP KP-Sil silica cartridge. Reversed-phase chromatography was carried out using a Biotage Isolera One automated purification system fitted with a Biotage SNAP KP-C18-HS silica cartridge. Analytical thin layer chromatography was performed on pre-coated plates of silica gel (Merck, silica gel 60F254), visualization was made using ultraviolet light (254 nm or 365 nm), potassium permanganate TLC stain, or cerium molybdate TLC stain (stains were prepared following standard procedures).

NMR spectra were recorded on a Bruker Avance-400 spectrometer. Chemical shifts are reported in ppm relative to $CHCl_3$ as internal reference which was set to 7.27 ppm for ^{1}H NMR spectroscopy and 77.23 ppm for ^{13}C NMR spectroscopy. Melting points were determined in open-ended capillaries using a Stuart SMP40 automatic melting point apparatus at a ramping rate of 2 °C/min. ESI mass spectra were measured using a TQD mass spectrometer equipped with an Acquity UPLC (Waters Ltd, UK). ASAP mass spectra were measured using a Xevo QToF mass spectrometer (Waters Ltd, UK) equipped with an Agilent 7890 GC (Agilent Technologies UK Ltd, UK). Exact mass spectra (HRMS) were measured using a LCT Premier XE mass spectrometer equipped with an Acquity UPLC (Waters Ltd, UK) (4 d.p. data) or a LTQ FT mass spectrometer equipped with a Surveyor HPLC (Thermo-Finnigan Corporation) (5 d.p. data). For the TQD, Xevo QToF and LCT Premier XE mass spectrometers MS data was processed using MassLynx 4.1. Exact mass measurements utilised a lock-mass correction to provide < 3 mDa precision. Exact mass measurement used Elemental Composition version 4.0 embedded within MassLynx 4.1 (Waters Ltd, UK). For the LTQ FT mass spectrometer MS data was processed using QualBrowser version 2.0. UV-visible spectroscopic measurements used a Thermo Evolution 220 UV-visible spectrometer with an integrating sphere (ISA220) or Smart Peltier 8-Cell Changer accessory, using the supplied Thermo INSIGHT software. Regression analysis of experimental data was conducted using OriginPro 8.

7.2: Synthetic Procedures

This section will begin by describing general procedures used in the synthesis of series of analogous compounds. Details specific to the synthesis of individual compounds can be found subsequently, together with analytical data.

7.2.1: General Synthetic Procedures

Monosubstitution of OEGs with PyrM groups:
The OEG (1 eq.) was added dropwise over 10 min to a vigorously stirred dispersion of Ag_2O (1.5 eq.) and KI (0.4 eq.) in anhydrous DCM (*ca.* 25 ml / 1 g PyrMBr). PyrMBr (1 eq.) in anhydrous DCM (*ca.* 25 ml / 1 g PyrMBr) was then added dropwise over 20 min to the stirred reaction. After stirring at room temperature for 45 min - 3 h the reaction mixture was filtered through celite to remove inorganic species. The solvent was removed *in vacuo* to afford a crude oil which was purified using column chromatography.

Addition of terminal acid:
A solution of PyrB-PEGn or PyrM-PEGn (1 eq.) in anhydrous THF was added dropwise to a vigorously stirred dispersion of NaH (13 eq.) in anhydrous THF and stirred at 40 °C for 1-2 h. Bromoacetic acid (1.2 or 1.5 eq.) was then carefully added and the reaction was stirred at 40 °C for a further 16-20 h. After this time the reaction was allowed to cool to room temperature then carefully quenched with water. The THF was then removed under vacuum. Brine was added to the aqueous solution which was extracted three times with ethyl acetate (N.B. the two layers separate very slowly). The aqueous layer was then acidified to pH 1 using 1 M HCl and extracted three times with ethyl acetate. These organic layers were combined and dried over Na_2SO_4 which was then removed by filtration. The solvent was removed *in vacuo* and excess bromoacetic acid removed by distillation under vacuum using a Kugelrohr (typically 120 °C, *ca.* 1 mbar for 30-45 min) to leave pure product.

Amide Coupling:
The carboxylic acid (1 eq.) was dissolved in anhydrous DCM. *N,N*-diisopropylethylamine (DIPEA) (2 eq. per carboxylic acid moiety) and *N,N,N',N'*-tetramethyl-O-(benzotriazol-1-yl)uronium tetrafluoroborate (TBTU) (1 eq. per

carboxylic acid moiety) were added and the solution* was stirred for 15 min. The amide (1 eq. per carboxylic acid moiety) in anhydrous DCM was added dropwise to the stirred solution and the solution was then stirred for at least 17 h (longer reaction times did not appear to affect yields). In cases where the amide was purified using normal-phase chromatography, the mixture was then extracted three times with saturated $NaHCO_3$, three times with 1 M $NaHSO_4$ and twice with water (2 × 25 ml). The residual tetramethylurea by-product was removed by distillation under vacuum and the residue further purified by column chromatography. In cases where the amide was purified by reversed-phase chromatography the solvent was then removed *in vacuo* and the residue purified using a Biotage Isolera One purification system fitted with a reversed-phase silica cartridge.

Deprotection of *tert*-Butyl Esters:

The ester was dissolved in formic acid and stirred overnight at room temperature. The formic acid was removed under vacuum to afford the product with no further purification.

Monotosylation of OEGs:

Based on a literature procedure,[154] Ag_2O (1.5 eq.), KI (0.2 eq.) and tosyl chloride (1.1 eq.) were dispersed in anhydrous DCM and stirred vigorously at 0 °C. The OEG (1 eq.) was added to the cooled mixture. After stirring at 0 °C for 15 - 60 min (dependant on the OEG) the reaction mixture was filtered through celite to remove inorganic species. The solvent was removed *in vacuo* to afford a crude oil which was purified using column chromatography.

THP-protection of monotosylated OEGs:

Based on a literature procedure,[155] **Ts-PEGn** (1 eq.) was dissolved in anhydrous DCM and stirred at room temperature. Pyridinium *p*-toluenesulphonate (0.2 eq.) was added to the stirred mixture followed by 3,4-dihydro-2H-pyran (1.5 eq.) and the reaction was stirred at 40 °C for 20 h. After cooling to room temperature the reaction mixture was concentrated under vacuum then poured into ice-water and extracted twice with DCM. The organic layers were combined and washed with water and brine before drying over $MgSO_4$, which was removed by filtration. Removal of the solvent *in vacuo* afforded the crude material which was purified by column chromatography.

* In some cases this solution was cooled to 0 °C at this point, then allowed to warm slowly to room temperature after addition of the amine.

Synthesis of OEGs monosubstituted with PyrB groups:

Based on a literature procedure,[174] sodium hydride (5 eq.) was dispersed in anhydrous THF and stirred vigorously at room temperature. A solution of **PyrBOH** (1 eq.) in THF was carefully added dropwise to the stirred solution which was then heated to 67 °C for 1-2 h. The reaction was then allowed to cool slightly such that reflux was no longer occurring. A solution of **Ts-PEGn-THP** (1.2 eq.) in THF was then added dropwise and the reaction then stirred at 67 °C for 18 h. The reaction was then allowed to cool to room temperature before the solvent was removed under vacuum. The residue was dissolved in $CHCl_3$ and any insoluble materials were removed by filtration and washed thoroughly with $CHCl_3$. The combined filtrate was dried *in vacuo* then redissolved in a 10% solution of conc. HCl in THF which was stirred at room temperature for 18 h. The solution was concentrated *in vacuo* and treated with brine before extracting four times with DCM. The combined organic layers were dried over $MgSO_4$ which was then removed by filtration. Removal of the solvent *in vacuo* afforded the crude material which was purified by column chromatography.

Formation of Sodium Carboxylates:

These reactions were not conducted under argon. The mono- or tricarboxylic acid (1 eq.) was dissolved in methanol and stirred at room temperature. The solution was treated with 1.0000 M $NaOH_{(aq)}$ (exactly 1 eq. per carboxylic acid moiety) then stirred at room temperature for 30 min. The solvent was removed *in vacuo* and the residue was dissolved in distilled water which was lyophilised to give the product with no further purification. The highly hygroscopic products were stored under vacuum.

Deprotection of Isopropylidene Acetals

Amberlyst-15 ion exchange beads were added to a solution of the acetal in EtOH and the mixture stirred at reflux for 3 h. After cooling the beads were removed by filtration and the filtrate dried *in vacuo* to afford the product with no further purification.

Mesylation:

Triethylamine (1.1 eq.) was added to a stirred solution of the alcohol precursor (1 eq.) in anhydrous DCM and cooled to 0 °C. After stirring at this temperature for 10 min, mesyl chloride (1.1. eq.) in anhydrous DCM was added dropwise to the stirred, cooled solution over 10 min. Following this addition the reaction was stirred for a further 16-20 h and allowed to warm slowly to room temperature. The solution was then extracted twice with saturated $NaHCO_{3(aq)}$ solution, twice with water, and once with brine. The organic layer was dried over

$MgSO_4$ which was then removed by filtration. Removal of the solvent *in vacuo* afforded the product with no further purification.

APD Di-ether Formation:

This method was adapted from a published procedure.[210] Step 1) Na_2SO_4 (5 eq.) was dispersed in a 10:1 mixture of anhydrous DCM and anhydrous MeOH at room temperature. (±)-3-Amino-1,2-propanediol (1 eq.) was added and the mixture stirred for 30 min. After this time benzaldehyde (1 eq.) was added and the reaction was stirred for 18 h. Na_2SO_4 was then removed by filtration and the solvent was removed from the filtrate *in vacuo* to afford crude imine **59** as a white solid which was used with no additional purification. Step 2) The imine was dissolved in anhydrous THF and added dropwise over 10 min to a dispersion of NaH (5 eq.) in anhydrous THF at room temperature (N.B. effervescence), then stirred for 3 h. A solution of mesylate (3 eq.) in anhydrous THF was then added and the reaction heated at reflux for 17 h. After cooling to room temperature the reaction was carefully quenched with water and extracted with ethyl acetate (3 × 100 ml). The organic layers were combined and dried over $MgSO_4$ which was removed by filtration. Removal of the solvent *in vacuo* afforded crude, protected intermediate. Step 3) The crude material was dissolved in a mixture of conc. HCl, water and ethanol (1:1:2) and stirred at room temperature for 2.5 h. The reaction was then extracted with DCM (3 × 75 ml). The aqueous layer was basified to *ca.* pH 14 using 5 M NaOH then extracted with DCM (3 × 50 ml). The organic layers were combined and dried over $MgSO_4$ which was then removed by filtration. Removal of the solvent *in vacuo* afforded highly pure product without further purification.

7.2.2: Synthesis and Characterisation

1-Bromomethylpyrene, PyrMBr

Based on a literature procedure,[135] phosphorus tribromide (1.00 ml, 10.6 mmol, 0.40 eq.) was added to a stirred solution of 1-pyrenemethanol (6.18 g, 26.6 mmol, 1 eq.) in anhydrous toluene (300 ml) at room temperature. The reaction was stirred at reflux for 19 h. After cooling to room temperature, ether (300 ml) was added to the reaction mixture which was then extracted with water (3 × 200 ml). The organic layer was dried over $MgSO_4$ which was then removed by filtration. Evaporation of the solvent afforded **PyrMBr** as a yellow solid without any further purification (7.39 g, 94%), mp 139.9-141.8 °C, lit[135] 140-142 °C; ^{1}H NMR (400 MHz, $CDCl_3$) δ 8.36 (d, *J* = 9.2 Hz, 1H), 8.26 – 8.18 (m, 3H), 8.11 – 8.05 (m, 2H), 8.05 - 7.96 (m, 3H), 5.24 (s, 2H); ^{13}C NMR (101 MHz, $CDCl_3$) δ 132.1, 131.4, 131.0, 130.8,

129.3, 128.4, 128.2, 127.9, 127.5, 126.5, 125.8, 125.8, 125.3, 125.0, 124.8, 123.0, 32.4; MS-ASAP$^+$ *m/z*: 297.0 $[M+H]^+$, 296.0 $[M]^{+\cdot}$, 295.0 $[M+H]^+$, 294.0 $[M]^{+\cdot}$, 216.1 $[PyrM]^+$, 215.0 $[PyrM]^{+\cdot}$; HRMS-ASAP$^+$ *m/z*: $[M]^{+\cdot}$ calculated for $C_{17}H_{11}Br$, 294.0044; found, 294.0053.

4-Benzyloxybutanoic acid, 19

Benzyl bromide (500 mg, 2.92 mmol, 4 eq.) and γ-butyrolactone (63 mg, 0.73 mmol, 1 eq.) were dissolved in toluene (5 ml). Freshly crushed 85% KOH (207 mg, 3.14 mmol, 4.3 eq.) was added to the stirred solution which was then heated to 110 °C and stirred at reflux for 90 h. After cooling to room temperature, the mixture was extracted with water (20 ml) and ether (10 ml) before further extractions with ether (2 × 20 ml). The aqueous layer was cooled to 0 °C and acidified using 3 M H_2SO_4 (2.5 ml). Extraction with DCM (3 × 10 ml) and evaporation of the solvent from the organic layer yielded crude **19** (23 mg, 16%), ^{1}H NMR (400 MHz, $CDCl_3$) δ 7.38 – 7.28 (m, 5H), 4.53 (s, 2H), 3.55 (t, *J* = 6.1 Hz, 2H), 2.51 (t, *J* = 7.3 Hz, 2H), 2.02 - 1.92 (m, 2H), c.f. lit[229].

1-Pyrenecarboxylic acid, 22

This compound was isolated as a by-product of an attempted ether synthesis. 1-pyrenemethanol (250 mg, 1.08 mmol, 1 eq.) was added to a stirred dispersion of NaH (336 mg, 14.00 mmol, 13 eq.) in anhydrous THF (15 ml) and stirred at 40 °C for 2 h. 6-Bromohexanoic acid (525 mg, 2.69 mmol, 2.5 eq.) was then added and stirring at 40 °C was continued for a further 24 h. The reaction was allowed to cool and left to stir at room temperature for 40 h. After removal of the THF the residue was treated with ethyl acetate (30 ml) before careful addition of water (30 ml, dropwise at first). The mixture was then extracted with ethyl acetate (3 × 30 ml). The aqueous layer was acidified to pH1 using 5 M HCl which afforded a yellow precipitate. Extraction with ethyl acetate (3 × 20 ml), removal of solvent and recrystallisation from chloroform yielded **22** as a yellow, crystalline solid (104 mg, 39%), mp 270.6-272.7, lit[230] 274°C; ^{1}H NMR (400 MHz, DMSO-*d6*) δ 13.33 (s, 1H), 9.24 (d, *J* = 9.4 Hz, 1H), 8.62 (d, *J* = 8.1 Hz, 1H), 8.46 – 8.11 (m, 7H); ^{13}C NMR (101 MHz, DMSO-*d6*) δ 169.0, 133.5, 130.5, 130.0, 129.8, 129.4, 129.1, 128.4, 127.1, 126.6, 126.4, 126.1, 124.6, 124.43, 124.39, 123.9, 123.4; MS-ASAP$^+$ *m/z*: 247.3 $[M+H]^+$, 246.2 $[M]^{+\cdot}$, 229.2 $[M-OH]^{+\cdot}$; HRMS-ASAP$^+$ *m/z*: $[M]^{+\cdot}$ calculated for $C_{17}H_{11}O_2$, 247.0759; found, 247.0770.

***tert*-Butyl-3-(1-pyrenemethyloxy)propanoate, 30**

1-Pyrenemethanol (1.00 g, 4.31 mmol, 1 eq.) was dissolved in DMSO (2 ml) and cooled to 15 °C using a xylene/liquid nitrogen bath. 2.15 M NaOH (0.2 ml, 0.1 eq.) was added to this

stirred solution. *tert*-Butyl acrylate (0.76 ml, 5.18 mmol, 1.2 eq.) was then added dropwise over 15 min. The reaction was left to stir and warm to room temperature over 20 h before removing the solvents under vacuum. The crude material was purified by column chromatography (silica, DCM) which afforded **30** as a pale yellow solid (1.33 g, 86%), mp 75.8-76.9 °C; ^{1}H NMR (400 MHz, $CDCl_3$) δ 8.38 (d, *J* = 9.2 Hz, 1H), 8.23 – 8.11 (m, 4H), 8.09 – 7.99 (m, 4H), 5.25 (s, 2H), 3.90 (t, *J* = 6.4 Hz, 2H), 2.61 (t, *J* = 6.4 Hz, 2H), 1.47 (s, 9H); ^{13}C NMR (101 MHz, $CDCl_3$) δ 171.16, 131.59, 131.53, 131.49, 131.08, 129.59, 127.90, 127.62, 127.6, 127.1, 126.1, 125.39, 125.37, 125.2, 125.0, 124.7, 123.7, 80.8, 72.0, 66.4, 36.7, 28.3; MS-ES$^+$ *m/z*: 743.4 $[2M+Na]^+$, 383.3 $[M+Na]^+$, 215.2 $[PyrM]^+$; HRMS-ES$^+$ *m/z*: $[M+Na]^+$ calculated for $C_{24}H_{24}O_3Na$, 383.1623; found, 383.1606; Anal. Calcd for $C_{24}H_{24}O_3$: C, 79.97, H, 6.71, N, 0.00. Found C, 79.86, H, 6.65, N, 0.00.

3-(1-pyrenemethyloxy)propan-1-ol, 31

A solution of **30** (995 mg, 2.76 mmol, 1 eq.) in anhydrous THF (7 ml) was added dropwise over 20 min to a dispersion of $LiAlH_4$ (210 mg, 5.53 mmol, 2 eq.) in anhydrous THF (7 ml) which was kept at 0 °C throughout the addition. The reaction was left to stir and allowed to warm to room temperature* over 22 h, then quenched by addition of water (1.5 ml), 2 M NaOH (1.5 ml) and further water (1.5 ml). The THF was removed *in vacuo* and the residue was extracted with DCM (3 × 15 ml). Addition of a small quantity of brine facilitated the extraction. The organic layers were combined and dried over Na_2SO_4 which was then removed by filtration. After removal of the solvent, the crude material was purified using column chromatography (silica, DCM with 0 - 3% MeOH) which afforded **31** as a brown oil (661 mg, 82%), ^{1}H NMR (400 MHz, $CDCl_3$) δ 8.37 (d, *J* = 9.2 Hz, 1H), 8.25 – 8.14 (m, 4H), 8.11 - 8.00 (m, 4H), 5.26 (s, 2H), 3.84 – 3.75 (m, 4H), 2.13 (t, *J* = 5.4 Hz, 1H), 1.97 – 1.86 (m, 2H); ^{13}C NMR (101 MHz, $CDCl_3$) δ 131.6, 131.4, 131.3, 131.00, 129.6, 128.1, 127.7, 127.6, 127.2, 126.2, 125.5, 125.2, 124.9, 124.7, 123.4, 72.1, 69.5, 62.1, 32.5; MS-ES$^+$ *m/z*: 603.3 $[2M+Na]^+$, 313.5 $[M+Na]^+$, 215.2 $[C_{17}H_{11}]^+$; HRMS-ES$^+$ *m/z*: $[M+Na]^+$ calculated for $C_{24}H_{24}O_3Na$, 313.1204; found, 313.1213.

6-(*tert*-Butyldimethylsilyloxy)-hexan-1-ol, 36

1,6-hexanediol (5.00 g, 42.3 mmol, 1 eq.) was added to a vigorously stirred dispersion of NaH (1.02 g, 42.5 mmol, 1 eq.) in anhydrous THF (80 ml) and stirred at room temperature for 1 h. *tert*-Butyldimethylsilyl chloride (6.38 g, 42.3 mmol, 1 eq.) was then added and the reaction stirred at room temperature for 90 min. The reaction mixture was then poured into ether

* RT was only *ca.* 15°C during the course of this reaction.

(200 ml) and washed with 10% $K_2CO_{3(aq)}$ (100 ml) and brine (125 ml) before drying the organic layer over Na_2SO_4 which was then removed by filtration. After removal of the solvent, the crude material was purified using column chromatography (silica, ethyl acetate) to afford **36** as a very pale yellow oil (4.10 g, 42%), ^{1}H NMR (400 MHz, $CDCl_3$) δ 3.65 (t, *J* = 6.6 Hz, 2H), 3.62 (t, *J* = 6.5 Hz, 2H), 1.63 – 1.50 (m, 4H), 1.44 – 1.32 (m, 4H), 1.25 (s, 1H), 0.90 (s, 9H), 0.05 (s, 6H); ^{13}C NMR (101 MHz, $CDCl_3$) δ 63.4, 63.2, 33.0, 26.2, 25.9, 25.8, 18.6, -5.0; MS-ES$^+$ *m/z*: 255.3 $[M+Na]^+$, 233.3 $[M+H]^+$; HRMS-ES$^+$ *m/z*: $[M+Na]^+$ calculated for $C_{12}H_{28}O_2SiNa$, 255.1756; found, 255.1750, $[M+H]^+$ calculated for $C_{12}H_{29}O_2Si$ 233.1937; found 233.1929.

1,6-bis-(*tert*-Butyldimethylsilyloxy)-hexane, 38

Using the conditions for the synthesis of **36** at 5.6 mmol scale, in addition to **36** (540 mg, 41%) **38** was isolated as a very pale yellow oil (180 mg, 19%), ^{1}H NMR (400 MHz, $CDCl_3$) δ 3.61 (t, *J* = 6.6 Hz, 4H), 1.56 – 1.49 (m, 4H), 1.36 – 1.31 (m, 4H), 0.90 (s, 18H), 0.05 (s, 12H); ^{13}C NMR (101 MHz, $CDCl_3$) δ 63.5, 33.1, 26.2, 25.9, 18.6, -5.0; MS-ES$^+$ *m/z*: 369.3 $[M+Na]^+$, 215.3[M-OTBDMS]$^+$; HRMS-ES$^+$ *m/z*: $[M+Na]^+$ calculated for $C_{18}H_{42}O_2Si_2Na$, 369.26155; found, 369.26180.

6-(1-pyrenemethyloxy)-1-hexyloxy-*tert*-butyldimethylsilane, 39

36 (390 mg, 1.7 mmol, 2 eq.) in anhydrous THF (5 ml) was added to a vigorously stirred dispersion of NaH (270 mg, 11 mmol, 13 eq.) in anhydrous THF (10 ml) and stirred at 40 °C for 2 h. PyrMBr (250 mg, 0.85 mmol, 1 eq.) was then added the reaction stirred at 40 °C for 16 h at which point TLC indicated the reaction was complete. The reaction was allowed to cool to room temperature before removing the solvent *in vacuo*. The residue was dissolved in ethyl acetate (50 ml) and carefully treated with water (50 ml). The aqueous layer was extracted with additional ethyl acetate (50 ml) and the organic layers were combined and dried over Na_2SO_4 which was then removed by filtration. After removal of the solvent, the crude material was purified using column chromatography (silica, 1:1 – 2:1 DCM/hexane) to afford **39** as a yellow solid (210 mg, 55%), mp 58.0-58.6 °C; ^{1}H NMR (400 MHz, $CDCl_3$) δ 8.39 (d, *J* = 9.2 Hz, 1H), 8.24 – 8.19 (m, 2H), 8.18 – 8.14 (m, 2H), 8.11 – 8.00 (m, 4H), 5.22 (s, 2H), 3.64 (t, *J* = 6.6 Hz, 4H), 1.79 – 1.70 (m, 2H), 1.64 – 1.52 (m, 2H), 1.51 – 1.35 (m, 4H), 0.99 (s, 9H), 0.13 (s, 6H); ^{13}C NMR (101 MHz, $CDCl_3$) δ 132.0, 131.4, 131.3, 131.0, 129.4, 127.7, 127.6, 127.4, 126.9, 126.0, 125.28, 125.26, 125.1, 124.9, 124.6, 123.6, 71.6, 70.7, 63.4, 33.0, 30.1, 26.3, 26.2, 25.9, 18.6, -5.1; MS-ES$^+$ *m/z*: 469.4 $[M+Na]^+$, 215.2 $[PyrM]^+$; HRMS-ES$^+$ *m/z*: $[M+Na]^+$ calculated for $C_{29}H_{38}O_2NaSi$, 469.2539; found, 469.2540.

PyrM-PEG6

This reaction was conducted using the general procedure for monosubstitution of OEGs with PyrM groups. The following reagents were used in the stated quantities: PEG6 (0.85 ml, 3.38 mmol, 1 eq.), Ag_2O (1180 mg, 5.09 mmol, 1.5 eq.), KI (225 mg, 1.36 mmol, 0.4 eq.), PyrMBr (1000 mg, 3.39 mmol, 1 eq.) and DCM (50 ml). Once the addition of **PyrMBr** was complete, the reaction was stirred for a further 3 h. **PyrM-PEG6** was isolated using column chromatography (silica, 4:1 EtOAc/acetone – 1:1 EtOAc/acetone) as a yellow oil (1340 mg, 80%), ^{1}H NMR (400 MHz, $CDCl_3$) δ 8.42 (d, *J* = 9.2 Hz, 1H), 8.24 – 8.18 (m, 2H), 8.18 – 8.13 (m, 2H), 8.09 – 7.99 (m, 4H), 5.30 (s, 2H), 3.80 – 3.75 (m, 2H), 3.75 – 3.54 (m, 22H), 2.51 (t, *J* = 6.2 Hz, 1H); ^{13}C NMR (101 MHz, $CDCl_3$) δ 131.6, 131.5, 131.4, 131.0, 129.6, 127.8, 127.60, 127.58, 127.3, 126.1, 125.38, 125.37, 125.1, 124.9, 124.7, 123.8, 72.7, 72.0, 70.9, 70.84, 70.80, 70.78, 70.76, 70.75, 70.72, 70.70, 70.5, 69.7, 61.9; MS-ASAP$^+$ *m/z*: 497.2 $[M+H]^+$, 496.2 $[M]^{+\cdot}$, 215.1 $[PyrM]^{+\cdot}$; HRMS-ASAP$^+$ *m/z*: $[M]^{+\cdot}$ calculated for $C_{29}H_{36}O_7$, 496.2461; found, 496.2450.

PyrM-PEG6-PyrM

Hexaethylene glycol (0.44 ml, 1.75 mmol, 2.7 eq.) was added to a stirred dispersion of NaH (201 mg, 8.38 mmol, 13 eq.) in anhydrous THF (10 ml) and stirred at 40 °C for 2 h. **PyrMBr** (190 mg, 0.644 mmol, 1 eq.) was then added and stirring at 40 °C was continued for a further 2 h, at which point **PyrMBr** was no longer visible by TLC. Treatment with hexane (25 ml) afforded a sticky brown solid which could be removed from the yellow solution by filtration. The filtrate was dried *in vacuo* and purified by column chromatography (silica, ethyl acetate) to afford **PyrM-PEG6-PyrM** as a yellow-brown oil (43 mg, 19%), ^{1}H NMR (400 MHz, $CDCl_3$) δ 8.39 (d, *J* = 9.2 Hz, 2H), 8.26 – 8.11 (m, 8H), 8.11 – 7.92 (m, 8H), 5.26 (s, 4H), 3.79 – 3.53 (m, 24H); ^{13}C NMR (101 MHz, $CDCl_3$) δ 131.7, 131.47, 131.46, 131.0, 129.6, 127.8, 127.60, 127.56, 127.2, 126.1, 125.38, 125.36, 125.1, 124.9, 124.7, 123.7, 77.6, 77.2, 76.9, 72.0, 70.9, 70.84, 70.79, 70.76, 70.74, 69.8; MS-ASAP$^+$ *m/z*: 711.3 $[M+H]^+$, 710.3 $[M]^{+\cdot}$, 496.3 $[M+H\text{-}C_{17}H_{11}]^+$, 495.3 $[M\text{-}PyrM]^{+\cdot}$, 215.3 $[PyrM]^{+\cdot}$; HRMS-ASAP$^+$ *m/z*: $[M]^{+\cdot}$ calculated for $C_{46}H_{46}O_7$, 710.3244; found, 710.3234.

PyrM-PEG6-CH_2COOH

Route A: From **PyrM-PEG6**

This reaction was conducted using the general procedure for addition of a terminal acid group. The following reagents were used in the stated quantities: **PyrM-PEG6** (913 mg, 1.84 mmol, 1 eq.), NaH (574 mg, 23.9 mmol, 13 eq.), bromoacetic acid (307 mg, 2.21 mmol,

1.2 eq.) and THF (40 ml). **PyrM-PEG6-CH_2COOH** was obtained as a yellow-brown oil (804 mg, 79%), ^{1}H NMR (400 MHz, $CDCl_3$) δ 8.41 (d, *J* = 9.2 Hz, 1H), 8.20 (t, *J* = 7.4 Hz, 2H), 8.17 – 8.12 (m, 2H), 8.07 – 7.99 (m, 4H), 5.29 (s, 2H), 4.14 (s, 2H), 3.79 – 3.75 (m, 2H), 3.74 - 3.57 (m, 22H); ^{13}C NMR (101 MHz, $CDCl_3$) δ 172.0, 131.4, 131.3, 131.2, 130.8, 129.4, 127.7, 127.4, 127.1, 125.9, 125.2, 124.9, 124.7, 124.5, 123.6, 71.8, 71.4, 70.6, 70.5, 70.44, 70.36, 70.3, 69.5, 68.9; MS-ASAP$^+$ *m/z*: 554.2 $[M]^{+\cdot}$, 496.2 $[M\text{-}CH_2COOH]^{+\cdot}$, 215.1 $[PyrM]^{+\cdot}$; HRMS-ASAP$^+$ *m/z*: $[M]^{+\cdot}$ calculated for $C_{31}H_{38}O_9$, 554.2516; found, 554.2506.

Route B: From **PyrM-PEG6-CH_2COOMe**

This reaction was not conducted under argon. 1M $LiOH_{(aq)}$ (2.5 ml, 2.5 mmol) was added dropwise over 30 min to a stirred, room temperature solution of **PyrM-PEG6-CH_2COOMe** (130 mg, 0.23 mmol) in MeCN (2.5 ml). The mixture was stirred vigorously for 10 min then diluted with additional water (2.5 ml). The mixture was then acidified to pH 2 using 10% aqueous HCl and extracted with ethyl acetate (3 × 5 ml). The organic layers were combined and dried over $MgSO_4$, which was then removed by filtration. After removal of the solvent, **PyrM-PEG6-CH_2COOH** was isolated as a yellow oil without any further purification (112 mg, 88%). Spectral data agreed with that obtained for Route A.

PyrM-PEG6-CH_2COOMe

A solution of KO^{t}Bu (100 mg, 0.89 mmol, 2 eq.) in anhydrous THF (1 ml) was added dropwise over 10 min to a stirred solution of **PyrM-PEG6** (220 mg, 0.44 mmol, 1 eq.) in anhydrous THF at 0 °C. After 30 min methyl bromoacetate (0.05 ml, 0.53 mmol, 1.2 eq.) was added dropwise over 10 min and the reaction stirred at 0 °C for a further 2 h, then stirred for a further 17 h while allowing the reaction to warm slowly to room temperature. The solvent and excess methyl bromoacetate were removed under vacuum and the crude residue was purified using column chromatography (silica, 3:1 – 1:1 ethyl acetate/acetone) to afford **PyrM-PEG6-CH_2COOMe** as a yellow oil (136 mg, 54%), ^{1}H NMR (400 MHz, $CDCl_3$) δ 8.42 (d, *J* = 9.2 Hz, 1H), 8.23 – 8.18 (m, 2H), 8.18 – 8.13 (m, 2H), 8.09 – 7.99 (m, 4H), 5.30 (s, 2H), 4.16 (s, 2H), 3.81 – 3.58 (m, 27H); MS-ASAP$^+$ *m/z*: 568.3 $[M]^{+\cdot}$, 496.2 $[PyrM\text{-}PEG6]^{+\cdot}$, 338.3 $[M+H\text{-}PyrMO]^+$, 216.1 $[PyrM+H]^+$ 215.1 $[PyrM]^{+\cdot}$; HRMS-ASAP$^+$ *m/z*: $[M]^{+\cdot}$ calculated for $C_{32}H_{40}O_9$, 568.2672; found, 568.2689.

Tris(3-tert-butoxy-3-oxopropoxy)aminomethane, 14

This compound was synthesised according to a literature procedure.[123] A solution of tris(hydroxymethyl)aminomethane (1.22g, 10 mmol, 1 eq.) in DMSO which had been stored over molecular sieves (2 ml) was stirred at 15 °C using a xylene/liquid nitrogen bath. 5 M

sodium hydroxide (0.2 ml, 1 mmol, 0.1 eq.) was added to this stirred solution. *tert*-Butyl acrylate (5.0 ml, 34 mmol, 3.4 eq.) was then added dropwise over 50 min. The reaction was left to stir and warm to room temperature over 48 h before removing the solvents under vacuum. The crude material was purified by column chromatography (silica, 2:1 EtOAc/hexane - EtOAc) to give **14** as a pale yellow oil (2.42 g, 48%), ^{1}H NMR (400 MHz, $CDCl_3$) δ 3.64 (t, *J* = 6.4 Hz, 6H), 3.31 (s, 6H), 2.45 (t, *J* = 6.4 Hz, 6H), 1.44 (s, 27H); ^{13}C NMR (101 MHz, $CDCl_3$) δ 171.1, 80.6, 73.1, 67.4, 56.2, 36.6, 28.3.

PyrM-PEG6-CH_2COG1(O^{t}Bu)$_3$

This reaction was conducted using the general procedure for amide coupling reactions. The following reagents were used in the stated quantities: **PyrM-PEG6-CH_2COOH** (194 mg, 0.35 mmol, 1 eq.), DIPEA (0.12 ml, 0.69 mmol, 2 eq.), TBTU (112 mg, 0.35 mmol, 1 eq.), **G1(O^{t}Bu)$_3$**/(023) (177 mg, 0.35 mmol, 1 eq.) and DCM (10 ml). This reaction was initially ice cooled and stirred for 72 h. The crude product was purified using extractions and column chromatography (silica, DCM with 0-5% MeOH) to yield **PyrM-PEG6-CH_2COG1(O^{t}Bu)** as a yellow oil of ≥90% purity as determined by ^{1}H NMR (139 mg, ~38%), ^{1}H NMR (400 MHz, $CDCl_3$) δ 8.41 (d, *J* = 9.2 Hz, 1H), 8.23 – 8.17 (m, 2H), 8.17 – 8.11 (m, 2H), 8.08 – 7.98 (m, 4H), 6.75 (bs, 1H), 5.29 (s, 2H), 3.88 (s, 2H), 3.78 – 3.74 (m, 2H), 3.74 – 3.68 (m, 9H), 3.68 – 3.55 (m, 27H), 2.45 (t, *J* = 6.5 Hz, 7H), 1.44 (s, 30H); ^{13}C NMR (101 MHz, $CDCl_3$) δ 170.9, 169.7, 131.6, 131.5, 131.4, 131.0, 129.6, 127.8, 127.59, 127.57, 127.3, 126.1, 125.4, 125.1, 124.9, 124.6, 123.8, 80.6, 72.0, 71.1, 70.94, 70.92, 70.83, 70.79, 70.75, 70.73, 70.70, 70.6, 69.7, 69.2, 67.2, 59.6, 53.6, 36.4, 28.3; MS-ASAP$^+$ *m/z*: 1042.6 $[M+H]^+$, 1041.6 $[M]^{+\cdot}$, 506.3 [**G1(O^{t}Bu)$_3$**/(023)+H]$^+$, 496.2 [PyrM-PEG6]$^{+\cdot}$, 215.1 [PyrM]$^{+\cdot}$; HRMS-ESI$^+$ *m/z*: $[M+H]^+$ calculated for $C_{56}H_{84}NO_{17}$, 1042.57338; found, 1042.57284.

1-Pyrenebutanol, PyrBOH

1-Pyrenebutyric acid (2.88 g, 10 mmol, 1 eq.) was dissolved in anhydrous THF (20 ml) and stirred at room temperature. 1 M borane THF complex solution in THF (20 ml, 20 mmol, 2 eq.) was added dropwise to the stirred solution over 15 min and the solution stirred at room temperature for 3 days. After this time the reaction was quenched by careful addition of 1 M HCl (30 ml) and then concentrated *in vacuo*. The aqueous residue was extracted with DCM (2 × 30 ml). The combined organic layers were washed with 2M NaOH (2 × 30 ml) and brine (2 × 30 ml) then dried over Na_2SO_4 which was removed by filtration. After removal of the solvent, **PyrBOH** was isolated with no further purification as a yellow solid (2.72 g, 99%), mp 72.5-74.5 °C; ^{1}H NMR (400 MHz, $CDCl_3$) δ 8.28 (d, *J* = 9.3 Hz, 1H), 8.20 – 8.14 (m, 2H), 8.14

– 8.08 (m, 2H), 8.06 – 7.97 (m, 3H), 7.87 (d, *J* = 7.8 Hz, 1H), 3.71 (t, *J* = 6.5 Hz, 2H), 3.38 (t, *J* = 7.6 Hz, 2H), 2.01 – 1.89 (m, 2H), 1.81 – 1.69 (m, 2H), 1.35 (bs, 1H); ^{13}C NMR (101 MHz, $CDCl_3$) δ 136.9, 131.6, 131.1, 130.0, 128.8, 127.7, 127.44, 127.42, 126.8, 126.0, 125.3, 125.2, 125.1, 125.0, 124.9, 123.6, 63.0, 33.4, 32.9, 28.2; MS-ES$^+$ *m/z*: 297.2 $[M+Na]^+$; HRMS-ES$^+$ *m/z*: $[M+Na]^+$ calculated for $C_{20}H_{19}O$, 275.1436; found, 275.1430.

***tert*-Butyl-3-(1-pyrenebutyloxy)propanoate, 48**

1-Pyrenebutanol (230 mg, 0.84 mmol, 1 eq.) was dissolved in DMSO (2 ml) and cooled to 15 °C using a xylene/liquid nitrogen bath. 0.42 M NaOH (0.2 ml, 0.1 eq.) was added to the stirred solution. *tert*-Butyl acrylate (0.15 ml, 1.02 mmol, 1.2 eq.) was then added dropwise over 10 min. The reaction was left to stir and warm to room temperature over 20 h before removing the solvents under vacuum. The crude material was purified using a Biotage Isolera One purification system (Silica, 25-100% DCM in hexane) which afforded **48** as a pale yellow solid (213 mg, 63%), mp 80.2-81.3 °C; ^{1}H NMR (400 MHz, $CDCl_3$) δ 8.29 (d, *J* = 9.3 Hz, 1H), 8.21 – 8.13 (m, 2H), 8.14 – 8.07 (m, 2H), 8.07 – 7.96 (m, 3H), 7.88 (d, *J* = 7.8 Hz, 1H), 3.67 (t, *J* = 6.5 Hz, 2H), 3.52 (t, *J* = 6.5 Hz, 2H), 3.37 (t, *J* = 7.8 Hz, 2H), 2.50 (t, *J* = 6.5 Hz, 2H), 1.98 - 1.88 (m, 2H), 1.80 – 1.71 (m, 2H), 1.42 (s, 9H); ^{13}C NMR (101 MHz, $CDCl_3$) δ 171.2, 137.1, 131.6, 131.1, 130.0, 128.8, 127.7, 127.5, 127.4, 126.7, 125.9, 125.3, 125.2, 124.97, 124.96, 124.8, 123.7, 80.7, 71.1, 66.7, 36.6, 33.5, 29.9, 28.6, 28.3.

3-(1-pyrenebutyloxy)propanoic acid, 49

This reaction was conducted using the general procedure for deprotection of *tert*-butyl esters. The following reagents were used in the stated quantities: **48** (126 mg, 0.31 mmol) and formic acid (5 ml). **49** was obtained as a pale yellow solid (0.94 mg, 88%), ^{1}H NMR (400 MHz, DMSO-*d6*) δ 12.21 (bs, 1H), 8.31 – 8.25 (m, 1H), 8.25 – 8.19 (m, 2H), 8.19 – 8.11 (m, 2H), 8.11 – 8.04 (m, 2H), 8.04 – 7.98 (m, 1H), 7.86 (d, *J* = 7.8 Hz, 1H), 3.56 (t, *J* = 6.2 Hz, 2H), 3.37 (t, *J* = 6.3 Hz, 2H), 3.24 (t, *J* = 7.6 Hz, 2H), 2.45 (t, *J* = 6.2 Hz, 2H), 1.82 – 1.65 (m, 2H), 1.65 – 1.49 (m, 2H); ^{13}C NMR (101 MHz, DMSO-*d6*) δ 172.7, 136.9, 130.9, 130.4, 129.2, 128.1, 127.44, 127.38, 127.1, 126.4, 126.1, 124.9, 124.7, 124.3, 124.2, 123.5, 69.9, 65.9, 34.8, 32.3, 29.0, 28.1;

1-(4-Bromo)butylpyrene, PyrBBr

Based on a literature procedure[173] **PyrBOH** (500 mg, 1.82 mmol, 1 eq.), CBr_4 (755 mg, 2.28 mmol, 1.25 eq.) and K_2CO_3 (378 mg, 2.73 mmol, 1.5 eq.) were stirred in anhydrous DCM (10 ml) at 0 °C. A solution of PPh_3 (598 mg, 2.28 mmol, 1.25 eq.) in anhydrous DCM (5 ml)

was added dropwise to the stirred solution over 15 min and the stirred solution was allowed to warm to room temperature overnight. After this time solids were removed by filtration and the filtrate dried *in vacuo*. The residue was purified using a Biotage Isolera One purification system (Silica, 2-20% ethyl acetate in hexane) which afforded **PyrBBr** as a pale yellow solid (508 mg, 83%), ^{1}H NMR (400 MHz, $CDCl_3$) δ 8.28 (d, *J* = 9.3 Hz, 1H), 8.21 - 8.15 (m, 2H), 8.13 (d, *J* = 8.5 Hz, 2H), 8.08 – 7.97 (m, 3H), 7.87 (d, *J* = 7.8 Hz, 1H), 3.48 (t, *J* = 6.3 Hz, 2H), 3.38 (t, *J* = 7.0 Hz, 2H), 2.08 – 1.99 (m, 4H); ^{13}C NMR (101 MHz, $CDCl_3$) δ 136.3, 131.6, 131.1, 130.1, 128.8, 127.7, 127.6, 127.4, 126.9, 126.1, 125.3, 125.2, 125.1, 125.02, 124.96, 123.4, 33.8, 32.9, 32.8, 30.4.

Bn-PEG6

Based on a literature procedure[155] Ag_2O (2.42 g, 10.44 mmol, 1.5 eq.) and KI (0.46 g, 2.78 mmol, 0.4 eq.) were dispersed in anhydrous DCM (50 ml) and stirred vigorously at room temperature. PEG6 (1.75 ml, 6.96 mmol, 1 eq.) was added dropwise to the stirred mixture followed by dropwise addition of benzyl bromide (0.91 ml, 7.65 mmol, 1.1 eq.) over 10 min. After stirring at room temperature for 2 h the reaction mixture was filtered through celite to remove inorganic species. The solvent was removed *in vacuo* to afford a crude oil which was purified using column chromatography (silica, ethyl acetate – 2:1 ethyl acetate/acetone) to give Bn-PEG6 as a pale yellow oil (2.15 g, 83%), ^{1}H NMR (400 MHz, $CDCl_3$) δ 7.38 – 7.27 (m, 5H), 4.57 (s, 2H), 3.74 – 3.59 (m, 24H), 2.59 (bs, 1H); ^{13}C NMR (101 MHz, $CDCl_3$) δ 138.6, 128.6, 127.9, 127.8, 73.5, 72.7, 70.89, 70.87, 70.85, 70.84, 70.84, 70.81, 70.6, 69.7, 62.0.

PyrB-PEG6-Bn and 1-(but-3-eneyl)pyrene, 50

A solution of KO^{t}Bu (133 mg, 1.19 mmol, 2 eq.) in anhydrous THF (1.2 ml) was added dropwise over 15 min to a stirred solution of **Bn-PEG6** (221 mg, 0.59 mmol, 1 eq.) in anhydrous THF (10 ml) at 0 °C. After 45 min a solution of **PyrBBr** (200 mg, 0.59 mmol, 1 eq.) in anhydrous THF (10 ml) was added dropwise over 10 min. The reaction was then allowed to warm to room temperature while stirring overnight. After this time the solution was concentrated *in vacuo* and the residue dissolved in DCM (10 ml) and extracted with water (10 ml). The aqueous layer was acidified with 5 M HCl and extracted with DCM (2 × 15 ml). All of the organic layers were then combined and dried over Na_2SO_4, which was removed by filtration before removing the solvent under vacuum. The residue was purified using a Biotage Isolera One purification system (Silica, 3:1 hexane/DCM – DCM – DCM with 5% MeOH) to afford **50** as a yellow oil (85 mg, 56%),^{1}H NMR (400 MHz, $CDCl_3$) δ 8.30 (d, *J* = 9.3 Hz, 1H), 8.21 – 8.15 (m, 2H), 8.15 – 8.10 (m, 2H), 8.08 – 7.97 (m, 3H), 7.89

(d, *J* = 7.8 Hz, 1H), 6.02 (ddt, *J* = 16.9, 10.2, 6.6 Hz, 1H), 5.19 – 5.11 (m, 1H), 5.10 – 5.02 (m, 2H), 3.51 – 3.42 (m, 3H), 2.68 – 2.58 (m, 2H). Further purification of other fractions by column chromatography (silica, DCM – DCM with 3% MeOH) gave **PyrB-PEG6-Bn** as a yellow oil (103 mg, 28%), ^{1}H NMR (400 MHz, $CDCl_3$) δ 8.29 (d, *J* = 9.2 Hz, 1H), 8.20 – 8.13 (m, 2H), 8.13 – 8.08 (m, 2H), 8.07 – 7.96 (m, 3H), 7.87 (d, *J* = 7.8 Hz, 1H), 7.39 – 7.27 (m, 5H), 4.57 (s, 2H), 3.71 – 3.56 (m, 24H), 3.54 (t, *J* = 6.5 Hz, 2H), 3.37 (t, *J* = 7.7 Hz, 2H), 1.99 – 1.88 (m, 2H), 1.84 – 1.74 (m, 2H); ^{13}C NMR (101 MHz, $CDCl_3$) δ 138.4, 137.0, 131.5, 131.0, 129.9, 128.7, 128.5, 127.9, 127.7, 127.6, 127.4, 127.3, 126.7, 125.9, 125.18, 125.15, 124.92, 124.90, 124.8, 123.6, 73.3, 71.3, 70.74, 70.73, 70.69, 70.68, 70.67, 70.65, 70.3, 69.5, 33.4, 29.8, 28.5.

Ts-PEG2

This reaction was conducted using the general procedure for monotosylation of OEGs. The following reagents were used in the stated quantities: Ag_2O (1.100 g, 47.5 mmol, 1.5 eq.), KI (1.050 g, 6.3 mmol, 0.2 eq.), TsCl (6.630 g, 34.8 mmol, 1.1 eq.), PEG2 (3.0 ml, 31.6 mmol, 1 eq.) and DCM (300 ml). The reaction was stirred for 30 min following the addition of PEG2. **Ts-PEG2** was isolated using column chromatography (silica, EtOAc) as a pale yellow oil (4400 mg, 53%),^{1}H NMR (400 MHz, $CDCl_3$) δ 7.78 (d, *J* = 8.4 Hz, 2H), 7.32 (d, *J* = 8.4 Hz, 2H), 4.19 – 4.15 (m, 2H), 3.69 – 3.62 (m, 4H), 3.53 – 3.49 (m, 2H), 2.43 (s, 3H), 2.41 (s, 1H); ^{13}C NMR (101 MHz, $CDCl_3$) δ 145.1, 133.0, 130.0, 128.0, 72.6, 69.4, 68.6, 61.7, 21.7; MS-ES$^+$ *m/z*: 283.4 $[M+Na]^+$, 261.5 $[M+H]^+$; HRMS-ES$^+$ *m/z*: $[M+Na]^+$ calculated for $C_{11}H_{16}O_5SNa$, 283.0616; found, 283.0624.

Ts-PEG4

This reaction was conducted using the general procedure for monotosylation of OEGs. The following reagents were used in the stated quantities: Ag_2O (6040 mg, 26.1 mmol, 1.5 eq.), KI (577 mg, 3.5 mmol, 0.2 eq.), TsCl (3640 mg, 19.1 mmol, 1.1 eq.), PEG4 (3.0 ml, 17.4 mmol, 1 eq.) and DCM (170 ml). The reaction was stirred for 15 min following the addition of PEG4. **Ts-PEG4** was isolated using column chromatography (silica, EtOAc – 3:1 EtOAc/acetone) as a pale yellow oil (3760 mg, 62%), ^{1}H NMR (400 MHz, $CDCl_3$) δ 7.78 (d, *J* = 8.3 Hz, 2H), 7.33 (d, *J* = 8.3 Hz, 2H), 4.16 – 4.12 (m, 2H), 3.71 – 3.65 (m, 4H), 3.65 – 3.60 (m, 4H), 3.60 – 3.55 (m, 6H), 2.57 (bs, 1H), 2.43 (s, 3H); ^{13}C NMR (101 MHz, $CDCl_3$) δ 145.0, 133.2, 130.0, 128.1, 72.6, 70.9, 70.8, 70.6, 70.5, 69.4, 68.8, 61.9, 21.8; MS-ASAP$^+$ *m/z*: 349.1 $[M+H]^+$, 199.0 $[TsOCH_2CH_2]^+$; HRMS-ES$^+$ *m/z*: $[M+Na]^+$ calculated for $C_{15}H_{24}O_7SNa$, 371.11349; found, 371.11358.

Ts-PEG6

This reaction was conducted using the general procedure for monotosylation of OEGs. The following reagents were used in the stated quantities: Ag_2O (2765 mg, 11.93 mmol, 1.5 eq.), KI (264 mg, 1.59 mmol, 0.2 eq.), TsCl (1668 mg, 8.75 mmol, 1.1 eq.), PEG6 (2.0 ml, 7.96 mmol, 1 eq.) and DCM (80 ml). The reaction was stirred for 15 min following the addition of PEG6. **Ts-PEG6** was isolated using column chromatography (silica, 4:1 EtOAc/acetone) as a pale yellow oil (3030 mg, 87%),^{1}H NMR (400 MHz, $CDCl_3$) δ 7.80 (d, *J* = 8.3 Hz, 2H), 7.34 (d, *J* = 8.3 Hz, 2H), 4.18 – 4.13 (m, 2H), 3.70 – 3.56 (m, 22H), 2.58 (bs, 1H), 2.45 (s, 3H); ^{13}C NMR (101 MHz, $CDCl_3$) δ 145.0, 133.2, 130.0, 128.2, 72.7, 70.9, 70.80, 70.76, 70.75, 70.73, 70.70, 70.5, 69.4, 68.9, 61.9, 21.8; MS-ES$^+$ *m/z*: 459.8 $[M+Na]^+$; HRMS-ES$^+$ *m/z*: $[M+Na]^+$ calculated for $C_{19}H_{32}O_9SNa$, 459.1665; found, 459.1659.

Ts-PEG12

This reaction was conducted using the general procedure for monotosylation of OEGs. The following reagents were used in the stated quantities: Ag_2O (700 mg, 3.02 mmol, 1.5 eq.), KI (70 mg, 0.42 mmol, 0.2 eq.), TsCl (422 mg, 2.21 mmol, 1.1 eq.), PEG12 (1100 mg, 2.01 mmol, 1 eq.) and DCM (20 ml). The reaction was stirred for 1 h following the addition of PEG12. **Ts-PEG12** was isolated using column chromatography (silica, acetone) as a yellow oil (710 mg, 50%),^{1}H NMR (400 MHz, $CDCl_3$) δ 7.78 (d, *J* = 8.4 Hz, 2H), 7.33 (d, *J* = 8.4 Hz, 2H), 4.16 – 4.12 (m, 2H), 3.80 – 3.43 (m, 46H), 2.67 (bs, 1H), 2.43 (s, 3H); ^{13}C NMR (101 MHz, $CDCl_3$) δ 145.0, 133.3, 130.0, 128.2, 72.8, 71.0, 70.81, 70.76, 70.74, 70.73, 70.71, 70.5, 69.4, 68.9, 61.9, 21.8; MS-ES$^+$ *m/z*: 723.5 $[M+Na]^+$, 701.5 $[M+H]^+$; HRMS-ES$^+$ *m/z*: $[M+Na]^+$ calculated for $C_{31}H_{56}O_{15}SNa$, 723.3238; found, 723.3239.

Ts-PEG2-THP

This reaction was conducted using the general procedure for THP protection of monotosylated OEGs. The following reagents were used in the stated quantities: **Ts-PEG2** (980 mg, 3.76 mmol, 1 eq.), pyridinium *p*-toluenesulphonate (190 mg, 0.76 mmol, 0.2 eq.), dihydropyran (0.51 ml, 5.59 mmol, 1.5 eq.) and DCM (25 ml). **Ts-PEG2-THP** was isolated using column chromatography (silica, 1:1 hexane/EtOAc – EtOAc) as a pale yellow oil (1150 mg, 89%), ^{1}H NMR (400 MHz, $CDCl_3$) δ 7.81 (d, *J* = 8.3 Hz, 2H), 7.35 (d, *J* = 8.3 Hz, 2H), 4.63 – 4.56 (m, 1H), 4.20 – 4.15 (m, 2H), 3.89 – 3.78 (m, 2H), 3.74 – 3.69 (m, 2H), 3.64 – 3.59 (m, 2H), 3.57 – 3.46 (m, 2H), 2.45 (s, 3H), 1.87 – 1.77 (m, 1H), 1.77 – 1.65 (m, 2H), 1.63 – 1.47 (m, 4H); ^{13}C NMR (101 MHz, $CDCl_3$) δ 145.0, 133.3, 130.0, 128.2, 99.2, 70.9, 69.5, 68.9, 66.8,

62.5, 30.8, 25.6, 21.9, 19.7; MS-ES$^+$ *m/z*: 367.4 $[M+Na]^+$; HRMS-ES$^+$ *m/z*: $[M+Na]^+$ calculated for $C_{16}H_{24}O_6SNa$, 367.1191; found, 367.1222.

Ts-PEG4-THP

This reaction was conducted using the general procedure for THP protection of monotosylated OEGs. The following reagents were used in the stated quantities: **Ts-PEG4** (3.74 g, 10.7 mmol, 1 eq.), pyridinium *p*-toluenesulphonate (0.54 g, 2.15 mmol, 0.2 eq.), dihydropyran (1.47 ml, 16.1 mmol, 1.5 eq.) and DCM (100 ml). **Ts-PEG4-THP** was isolated using column chromatography (silica, EtOAc) as a yellow oil (4.46 g, 96%), ^{1}H NMR (400 MHz, $CDCl_3$) δ 7.80 (d, *J* = 8.4 Hz, 2H), 7.34 (d, *J* = 8.4 Hz, 2H), 4.62 (dd, *J* = 4.3, 3.0 Hz, 1H), 4.18 - 4.14 (m, 2H), 3.90 – 3.82 (m, 2H), 3.71 – 3.56 (m, 13H), 3.54 – 3.46 (m, 1H), 2.45 (s, 3H), 1.89 – 1.77 (m, 1H), 1.76 – 1.67 (m, 1H), 1.64 – 1.46 (m, 4H); ^{13}C NMR (101 MHz, $CDCl_3$) δ 144.9, 133.3, 130.0, 128.2, 99.2, 71.0, 70.9, 70.80, 70.75, 70.75, 69.4, 68.9, 66.9, 62.4, 30.8, 25.6, 21.8, 19.7; MS-ES$^+$ *m/z*: 455.2 $[M+Na]^+$, 349.1 $[Ts\text{-}PEG4+H]^+$; HRMS-ES$^+$ *m/z*: $[M+Na]^+$ calculated for $C_{20}H_{32}O_8SNa$, 455.1716; found, 455.1728.

Ts-PEG6-THP

This reaction was conducted using the general procedure for THP protection of monotosylated OEGs. The following reagents were used in the stated quantities: **Ts-PEG6** (1.80 g, 4.12 mmol, 1 eq.), pyridinium *p*-toluenesulphonate (0.21 g, 0.84 mmol, 0.2 eq.), dihydropyran (0.56 ml, 6.14 mmol, 1.5 eq.) and DCM (50 ml). **Ts-PEG6-THP** was isolated using column chromatography (silica, EtOAc) as a yellow oil (1.95 g, 91%), ^{1}H NMR (400 MHz, $CDCl_3$) δ 7.78 (d, *J* = 8.4 Hz, 2H), 7.34 (d, *J* = 8.4 Hz, 1H), 4.63 – 4.55 (m, 1H), 4.17 – 4.11 (m, 2H), 3.89 – 3.77 (m, 2H), 3.69 – 3.52 (m, 21H), 3.52 – 3.43 (m, 1H), 2.43 (s, 3H), 1.87 - 1.74 (m, 1H), 1.74 – 1.63 (m, 1H), 1.62 – 1.43 (m, 4H); ^{13}C NMR (101 MHz, $CDCl_3$) δ 145.0, 133.2, 130.0, 128.2, 99.1, 70.9, 70.8, 70.74, 70.70, 70.69, 69.4, 68.9, 66.8, 62.4, 30.8, 25.6, 21.8, 19.7; MS-ES$^+$ *m/z*: 543.6 $[M+Na]^+$; HRMS-ES$^+$ *m/z*: $[M+Na]^+$ calculated for $C_{24}H_{40}O_{10}SNa$, 543.2240; found, 543.2244.

Ts-PEG12-THP

This reaction was conducted using the general procedure for THP protection of monotosylated OEGs. The following reagents were used in the stated quantities: **Ts-PEG12** (705 mg, 1.01 mmol, 1 eq.), pyridinium *p*-toluenesulphonate (51 mg, 0.20 mmol, 0.2 eq.), dihydropyran (0.14 ml, 1.53 mmol, 1.5 eq.) and DCM (20 ml). **Ts-PEG12-THP** was isolated using column chromatography (silica, EtOAc – 5:1 acetone/EtOAc) as a yellow oil (650 mg,

82%), ^{1}H NMR (400 MHz, $CDCl_3$) δ 7.80 (d, *J* = 8.3 Hz, 2H), 7.34 (d, *J* = 8.3 Hz, 2H), 4.65 – 4.61 (m, 1H), 4.18 – 4.14 (m, 2H), 3.90 – 3.83 (m, 2H), 3.74 – 3.57 (m, 45H), 3.55 – 3.44 (m, 1H), 2.45 (s, 3H), 1.89 – 1.78 (m, 1H), 1.76 – 1.67 (m, 1H), 1.65 – 1.46 (m, 4H); ^{13}C NMR (101 MHz, $CDCl_3$) δ 145.0, 133.2, 130.0, 128.2, 99.1, 70.9, 70.80, 70.79, 70.77, 70.73, 70.72, 69.4, 68.9, 66.8, 62.4, 30.8, 25.6, 21.8, 19.7; MS-ES$^+$ *m/z*: 807.5 $[M+Na]^+$; HRMS-ES$^+$ *m/z*: $[M+Na]^+$ calculated for $C_{36}H_{64}O_{16}SNa$, 807.3813; found, 807.3829.

PyrB-PEG2

This reaction was conducted using the general procedure for the Synthesis of OEGs monosubstituted with PyrB groups. The following reagents were used in the stated quantities: NaH (311 mg, 12.96 mmol, 5 eq.), **PyrBOH** (711 mg, 2.59 mmol, 1 eq.), **Ts-PEG2-THP** (1070 mg, 3.11 mmol, 1.2 eq.), THF (20 ml) and conc. HCl (7 ml) in THF (63 ml). **PyrB-PEG2** was isolated following column chromatography (silica, EtOAc) as a yellow oil (505 mg, 54%), ^{1}H NMR (400 MHz, $CDCl_3$) δ 8.29 (d, *J* = 9.3 Hz, 1H), 8.20 – 8.14 (m, 2H), 8.14 – 8.09 (m, 2H), 8.06 – 7.96 (m, 3H), 7.88 (d, *J* = 7.8 Hz, 1H), 3.75 – 3.70 (m, 2H), 3.69 – 3.64 (m, 2H), 3.63 – 3.57 (m, 4H), 3.54 (t, *J* = 6.6 Hz, 2H), 3.38 (t, *J* = 7.7 Hz, 2H), 2.49 (bs, 1H), 1.99 – 1.89 (m, 2H), 1.84 – 1.75 (m, 2H); ^{13}C NMR (101 MHz, $CDCl_3$) δ 137.0, 131.7, 131.1, 130.0, 128.8, 127.7, 127.5, 127.4, 126.8, 126.0, 125.31, 125.26, 125.02, 124.99, 124.9, 123.6, 72.7, 71.5, 70.7, 70.5, 62.1, 33.5, 29.9, 28.6; MS-ASAP$^+$ *m/z*: 363.2 $[M+H]^+$, 362.2 $[M]^{+\cdot}$, 258.1 $[PyrB+H]^+$, 257.1 $[PyrB]^{+\cdot}$; HRMS-ASAP$^+$ *m/z*: $[M]^{+\cdot}$ calculated for $C_{24}H_{26}O_3$, 362.1882; found, 362.1872.

PyrB-PEG4

This reaction was conducted using the general procedure for the Synthesis of OEGs monosubstituted with PyrB groups. The following reagents were used in the stated quantities: NaH (289 mg, 12.04 mmol, 5 eq.), **PyrBOH** (661 mg, 2.41 mmol, 1 eq.), **Ts-PEG4-THP** (1250 mg, 2.89 mmol, 1.2 eq.), THF (16 ml) and conc. HCl (6 ml) in THF (54 ml). **PyrB-PEG4** was isolated following column chromatography (silica, EtOAc – 4:1 EtOAc/acetone) as a yellow oil (632 mg, 58%), ^{1}H NMR (400 MHz, $CDCl_3$) δ 8.29 (d, *J* = 9.2 Hz, 1H), 8.20 – 8.14 (m, 2H), 8.14 – 8.08 (m, 2H), 8.06 – 7.96 (m, 3H), 7.88 (d, *J* = 7.8 Hz, 1H), 3.74 – 3.50 (m, 18H), 3.38 (t, *J* = 7.7 Hz, 2H), 2.56 (bs, 1H), 1.98 – 1.89 (m, 2H), 1.85 – 1.72 (m, 2H); ^{13}C NMR (101 MHz, $CDCl_3$) δ 137.0, 131.6, 131.0, 129.9, 128.7, 127.6, 127.4, 127.3, 126.6, 125.9, 125.20, 125.16, 124.92, 124.90, 124.8, 123.6, 72.7, 71.4, 70.70, 70.68, 70.65, 70.4, 70.3, 61.8, 33.4, 29.8, 28.5; MS-ASAP$^+$ *m/z*: 451.2 $[M+H]^+$, 450.2 $[M]^{+\cdot}$; HRMS-ASAP$^+$ *m/z*: $[M]^{+\cdot}$ calculated for $C_{28}H_{34}O_5$, 450.2406; found, 450.2408.

PyrB-PEG6

This reaction was conducted using the general procedure for the Synthesis of OEGs monosubstituted with PyrB groups. The following reagents were used in the stated quantities: NaH (0.60 g, 25.00 mmol, 5 eq.), **PyrBOH** (1.36 g, 4.96 mmol, 1 eq.), **Ts-PEG6-THP** (3.10 g, 5.95 mmol, 1.2 eq.), THF (48 ml) and conc. HCl (20 ml) in THF (180 ml). **PyrB-PEG6** was isolated following column chromatography (silica, EtOAc – 1:1 EtOAc/acetone) as a yellow-brown oil (1.76 g, 66%), ^{1}H NMR (400 MHz, $CDCl_3$) δ 8.28 (d, *J* = 9.2 Hz, 1H), 8.20 - 8.13 (m, 2H), 8.13 – 8.07 (m, 2H), 8.06 – 7.96 (m, 3H), 7.87 (d, *J* = 7.8 Hz, 1H), 3.75 - 3.69 (m, 2H), 3.69 – 3.56 (m, 22H), 3.53 (t, *J* = 6.5 Hz, 2H), 3.37 (t, *J* = 7.7 Hz, 2H), 2.58 (bs, 1H), 1.98 – 1.88 (m, 2H), 1.84 – 1.72 (m, 2H); ^{13}C NMR (101 MHz, $CDCl_3$) δ 137.1, 131.6, 131.1, 130.0, 128.8, 127.7, 127.5, 127.4, 126.7, 126.0, 125.29, 125.25, 125.00, 124.98, 124.8, 123.7, 72.7, 71.4, 70.83, 70.80, 70.78, 70.76, 70.7, 70.6, 70.4, 62.0, 33.5, 29.9, 28.6; MS-ASAP^{+} *m/z*: 539.3 $[M+H]^{+}$, 538.3 $[M]^{+\cdot}$; HRMS-ASAP^{+} *m/z*: $[M]^{+\cdot}$ calculated for $C_{32}H_{42}O_7$, 538.2931; found 538.2927.

PyrB-PEG12

This reaction was conducted using the general procedure for the Synthesis of OEGs monosubstituted with PyrB groups. The following reagents were used in the stated quantities: NaH (82 mg, 3.42 mmol, 5 eq.), **PyrBOH** (188 mg, 0.69 mmol, 1 eq.), **Ts-PEG12-THP** (644 mg, 0.82 mmol, 1.2 eq.), THF (8 ml) and conc. HCl (3 ml) in THF (27 ml). **PyrB-PEG12** was isolated following column chromatography (silica, EtOAc – 1:1 EtOAc/acetone) as a yellow oil (275 mg, 50%), ^{1}H NMR (400 MHz, $CDCl_3$) δ 8.28 (d, *J* = 9.3 Hz, 1H), 8.19 – 8.13 (m, 2H), 8.12 – 8.07 (m, 2H), 8.05 – 7.94 (m, 3H), 7.86 (d, *J* = 7.8 Hz, 1H), 3.74 – 3.70 (m, 2H), 3.69 – 3.56 (m, 46H), 3.53 (t, *J* = 6.5 Hz, 2H), 3.36 (t, *J* = 7.7 Hz, 2H), 2.70 (bs, 1H), 1.97 – 1.87 (m, 2H), 1.82 – 1.73 (m, 2H); ^{13}C NMR (101 MHz, $CDCl_3$) δ 137.0, 131.6, 131.1, 129.9, 128.8, 127.7, 127.4, 127.3, 126.7, 125.9, 125.22, 125.18, 125.0, 124.9, 124.8, 123.6, 72.6, 71.4, 70.8, 70.73, 70.70, 70.5, 70.3, 61.9, 33.5, 29.9, 28.6; MS-ES^{+} *m/z*: 825.6 $[M+Na]^{+}$, 803.6 $[M+H]^{+}$; HRMS-ES^{+} *m/z*: $[M+Na]^{+}$ calculated for $C_{44}H_{66}O_{13}Na$, 825.4401; found 825.4438.

PyrB-PEG2-CH_2COOH

This reaction was conducted using the general procedure for addition of a terminal acid group. The following reagents were used in the stated quantities: **PyrB-PEG2** (475 mg, 1.31 mmol, 1 eq.), NaH (409 mg, 17.04 mmol, 13 eq.), bromoacetic acid (219 mg, 1.58 mmol, 1.2 eq.) and THF (25 ml). **PyrB-PEG2-CH_2COOH** was obtained as a brown oil (509 mg, 92%),

^{1}H NMR (400 MHz, $CDCl_3$) δ 8.29 (d, *J* = 9.3 Hz, 1H), 8.19 – 8.14 (m, 2H), 8.13 – 8.09 (m, 2H), 8.06 – 7.96 (m, 3H), 7.88 (d, *J* = 7.8 Hz, 1H), 4.12 (s, 2H), 3.71 – 3.63 (m, 6H), 3.61 – 3.57 (m, 2H), 3.54 (t, *J* = 6.6 Hz, 2H), 3.37 (t, *J* = 7.7 Hz, 2H), 1.98 – 1.89 (m, 2H), 1.83 – 1.74 (m, 2H); ^{13}C NMR (101 MHz, $CDCl_3$) δ 172.5, 137.0, 131.7, 131.1, 130.0, 128.8, 127.7, 127.5, 127.4, 126.7, 126.0, 125.30, 125.25, 125.02, 125.00, 124.9, 123.7, 71.7, 71.5, 71.0, 70.2, 70.1, 69.0, 33.5, 29.8, 28.6; MS-ASAP^{+} *m/z*: 421.2 $[M+H]^{+}$, 420.2 $[M]^{+\cdot}$, 376.2 $[M-CO_2]^{+\cdot}$, 258.1 $[PyrB+H]^{+}$, 257.1 $[PyrB]^{+\cdot}$; HRMS-ASAP^{+} (*m/z*): $[M]^{+\cdot}$ calculated for $C_{26}H_{28}O_5$, 420.1937; found, 420.1921.

PyrB-PEG4-CH_2COOH

This reaction was conducted using the general procedure for addition of a terminal acid group. The following reagents were used in the stated quantities: **PyrB-PEG4** (518 mg, 1.15 mmol, 1 eq.), NaH (359 mg, 14.96 mmol, 13 eq.), bromoacetic acid (240 mg, 1.73 mmol, 1.5 eq.) and THF (20 ml). **PyrB-PEG4-CH_2COOH** was obtained as a yellow-brown oil (535 mg, 91%), ^{1}H NMR (400 MHz, $CDCl_3$) δ 8.28 (d, *J* = 9.3 Hz, 1H), 8.19 – 8.13 (m, 2H), 8.13 – 8.08 (m, 2H), 8.06 – 7.95 (m, 3H), 7.87 (d, *J* = 7.8 Hz, 1H), 4.12 (s, 2H), 3.69 – 3.56 (m, 16H), 3.54 (t, *J* = 6.5 Hz, 2H), 3.36 (t, *J* = 7.7 Hz, 2H), 1.98 – 1.87 (m, 2H), 1.83 – 1.73 (m, 2H); ^{13}C NMR (101 MHz, $CDCl_3$) δ 172.5, 137.1, 131.6, 131.1, 129.9, 128.8, 127.7, 127.5, 127.3, 126.7, 126.0, 125.3, 125.2, 124.97, 124.96, 124.8, 123.7, 71.5, 71.4, 70.81, 70.75, 70.7, 70.6, 70.5, 70.2, 69.1, 33.5, 29.8, 28.6; MS-ASAP^{+} *m/z*: 509.2 $[M+H]^{+}$, 508.2 $[M]^{+\cdot}$, 464.2 $[M-CO_2]^{+\cdot}$, 257.1 $[PyrB]^{+\cdot}$; HRMS-ASAP^{+} (*m/z*): $[M]^{+\cdot}$ calculated for $C_{30}H_{36}O_7$, 508.2461; found, 508.2475.

PyrB-PEG6-CH_2COOH

This reaction was conducted using the general procedure for addition of a terminal acid group. The following reagents were used in the stated quantities: **PyrB-PEG6** (1.60 g, 2.97 mmol, 1 eq.), NaH (0.93 g, 38.75 mmol, 13 eq.), bromoacetic acid (0.50 g, 3.60 mmol, 1.2 eq.) and THF (65 ml). **PyrB-PEG6-CH_2COOH** was obtained as a yellow-brown oil (1.24 g, 70%), ^{1}H NMR (400 MHz, $CDCl_3$) δ 9.45 (bs, 1H), 8.27 (d, *J* = 9.3 Hz, 1H), 8.18 – 8.12 (m, 2H), 8.12 – 8.07 (m, 2H), 8.05 – 7.95 (m, 3H), 7.86 (d, *J* = 7.8 Hz, 1H), 4.14 (s, 2H), 3.72 – 3.67 (m, 2H), 3.67 – 3.55 (m, 22H), 3.53 (t, *J* = 6.5 Hz, 2H), 3.36 (t, *J* = 7.7 Hz, 2H), 1.97 – 1.87 (m, 2H), 1.82 – 1.73 (m, 2H); ^{13}C NMR (101 MHz, $CDCl_3$) δ 171.9, 137.1, 131.7, 131.1, 130.0, 128.8, 127.7, 127.5, 127.4, 126.7, 126.0, 125.29, 125.25, 125.00, 124.99, 124.9, 123.7, 71.5, 71.4, 70.82, 70.79, 70.77, 70.75, 70.71, 70.68, 70.66, 70.61, 70.58, 70.5, 70.3, 69.3, 33.5, 29.9, 28.6; MS-ASAP^{+} *m/z*: 597.3 $[M+H]^{+}$, 596.3 $[M]^{+\cdot}$, 257.1 $[PyrB]^{+\cdot}$; HRMS-ASAP^{+} *m/z*: $[M+Na]^{+}$ calculated for $C_{34}H_{44}O_9$, 596.2985; found, 596.2987.

PyrB-PEG12-CH_2COOH

This reaction was conducted using the general procedure for addition of a terminal acid group. The following reagents were used in the stated quantities: **PyrB-PEG12** (275 mg, 0.34 mmol, 1 eq.), NaH (107 mg, 4.46 mmol, 13 eq.), bromoacetic acid (57 mg, 0.41 mmol, 1.2 eq.) and THF (15 ml). **PyrB-PEG12-CH_2COOH** was obtained as a brown oil (161 mg, 55%), ^{1}H NMR (400 MHz, $CDCl_3$) δ 8.29 (d, *J* = 9.3 Hz, 1H), 8.19 – 8.14 (m, 2H), 8.13 – 8.08 (m, 2H), 8.06 – 7.96 (m, 3H), 7.87 (d, *J* = 7.8 Hz, 1H), 4.17 (s, 2H), 3.78 – 3.72 (m, 2H), 3.72 - 3.51 (m, 48H), 3.37 (t, *J* = 7.8 Hz, 2H), 1.98 – 1.88 (m, 2H), 1.83 – 1.74 (m, 2H); ^{13}C NMR (101 MHz, $CDCl_3$) δ 172.0, 137.1, 131.7, 131.1, 130.0, 128.8, 127.7, 127.5, 127.4, 126.7, 126.0, 125.29, 125.25, 125.01, 124.99, 124.9, 123.7, 71.6, 71.5, 70.89, 70.86, 70.82, 70.80, 70.76, 70.75, 70.73, 70.71, 70.66, 70.6, 70.4, 69.2, 33.5, 29.9, 28.6; MS-ES$^+$ *m/z*: 883.6 $[M+Na]^+$, 453.5 $[M+2Na]^{2+}$; HRMS-ASAP$^+$ *m/z*: $[M+Na]^+$ calculated for $C_{46}H_{68}O_{15}Na$, 883.4456; found, 883.4493.

PyrB-PEG2-CH_2COG1(O^{t}Bu)$_3$

This reaction was conducted using the general procedure for amide coupling reactions. The following reagents were used in the stated quantities: **PyrB-PEG2-CH_2COOH** (402 mg, 0.96 mmol, 1 eq.), DIPEA (0.33 ml, 1.89 mmol, 2 eq.), TBTU (307 mg, 0.96 mmol, 1 eq.), **G1(O^{t}Bu)$_3$**/(023) (483 mg, 0.96 mmol, 1 eq.) and DCM (10 ml). This reaction was initially ice cooled and stirred for 22 h. The crude product was purified using extractions and column chromatography (silica, EtOAc) to yield **PyrB-PEG2-CH_2COG1(O^{t}Bu)** as a yellow oil (468 mg, 54%), ^{1}H NMR (400 MHz, $CDCl_3$) δ 8.29 (d, *J* = 9.3 Hz, 1H), 8.19 – 8.14 (m, 2H), 8.13 – 8.08 (m, 2H), 8.07 – 7.96 (m, 3H), 7.88 (d, *J* = 7.8 Hz, 1H), 6.75 (s, 1H), 3.88 (s, 2H), 3.71 (s, 6H), 3.68 – 3.61 (m, 12H), 3.61 – 3.57 (m, 2H), 3.54 (t, *J* = 6.6 Hz, 2H), 3.38 (t, *J* = 7.7 Hz, 2H), 2.44 (t, *J* = 6.5 Hz, 6H), 1.98 – 1.88 (m, 2H), 1.83 – 1.74 (m, 2H), 1.44 (s, 27H); ^{13}C NMR (101 MHz, $CDCl_3$) δ 170.9, 169.7, 137.0, 131.6, 131.1, 130.0, 128.8, 127.7, 127.5, 127.4, 126.8, 126.0, 125.29, 125.24, 125.03, 124.99, 124.9, 123.7, 80.6, 71.5, 71.2, 71.0, 70.9, 70.6, 70.4, 69.2, 67.3, 59.7, 36.5, 33.5, 29.9, 28.6, 28.3; MS-ES$^+$ *m/z*: 930.6 $[M+Na]^+$, 908.6 $[M+H]^+$; HRMS-ES$^+$ *m/z*: $[M+Na]^+$ calculated for $C_{51}H_{73}NO_{13}Na$, 930.4980; found, 930.5010.

PyrB-PEG4-CH_2COG1(O^{t}Bu)$_3$

This reaction was conducted using the general procedure for amide coupling reactions. The following reagents were used in the stated quantities: **PyrB-PEG4-CH_2COOH** (640 mg, 1.27 mmol, 1 eq.), DIPEA (0.44 ml, 2.53 mmol, 2 eq.), TBTU (407 mg, 1.27 mmol, 1 eq.), **G1(O^{t}Bu)$_3$**/(023) (640 mg, 1.27 mmol, 1 eq.) and DCM (20 ml). This reaction was initially ice

cooled and stirred for 72 h. The crude product was purified using extractions and column chromatography (silica, EtOAc) to yield **PyrB-PEG4-CH_2COG1(O^{t}Bu)** as a yellow oil (679 mg, 54%), ^{1}H NMR (400 MHz, $CDCl_3$) δ 8.29 (d, *J* = 9.2 Hz, 1H), 8.20 – 8.14 (m, 2H), 8.14 – 8.07 (m, 2H), 8.06 – 7.96 (m, 3H), 7.87 (d, *J* = 7.7 Hz, 1H), 6.75 (s, 1H), 3.88 (s, 2H), 3.72 (s, 6H), 3.69 – 3.56 (m, 22H), 3.54 (t, *J* = 6.5 Hz, 2H), 3.37 (t, *J* = 7.8 Hz, 2H), 2.45 (t, *J* = 6.5 Hz, 6H), 2.00 – 1.87 (m, 2H), 1.83 – 1.74 (m, 2H); ^{13}C NMR (101 MHz, $CDCl_3$) δ 170.9, 169.7, 137.1, 131.6, 131.1, 130.0, 128.8, 127.7, 127.5, 127.4, 126.7, 126.0, 125.28, 125.24, 125.01, 124.98, 124.8, 123.7, 80.6, 71.5, 71.2, 71.0, 70.83, 70.82, 70.81, 70.79, 70.77, 70.6, 70.4, 69.2, 67.3, 59.7, 36.5, 33.5, 29.9, 28.6, 28.3; MS-ASAP$^+$ *m/z*: 996.5 $[M+H]^+$, 995.5 $[M]^{+\cdot}$, 508.2 $[PyrB\text{-}PEG4\text{-}CH_2CONH_3]^+$, 507.2 $[PyrB\text{-}PEG4\text{-}CH_2CONH_2]^{+\cdot}$, 450.2 $[PyrB\text{-}PEG4]^{+\cdot}$; HRMS-ASAP$^+$ *m/z*: $[M+H]^+$ calculated for $C_{55}H_{82}NO_{15}$, 996.5684; found, 996.5644.

PyrB-PEG6-CH_2COG1(O^{t}Bu)$_3$

This reaction was conducted using the general procedure for amide coupling reactions. The following reagents were used in the stated quantities: **PyrB-PEG6-CH_2COOH** (670 mg, 1.12 mmol, 1 eq.), DIPEA (0.39 ml, 2.24 mmol, 2 eq.), TBTU (361 mg, 1.12 mmol, 1 eq.), **G1(O^{t}Bu)$_3$**/(023) (568 mg, 1.12 mmol, 1 eq.) and DCM (20 ml). This reaction was initially ice cooled and stirred for 72 h. The crude product was purified using extractions and column chromatography (silica, 3:1 EtOAc/acetone) to yield **PyrB-PEG6-CH_2COG1(O^{t}Bu)** as a yellow oil (946 mg, 78%), ^{1}H NMR (400 MHz, $CDCl_3$) δ 8.28 (d, *J* = 9.2 Hz, 1H), 8.18 – 8.13 (m, 2H), 8.13 – 8.08 (m, 2H), 8.05 – 7.96 (m, 3H), 7.87 (d, *J* = 7.7 Hz, 1H), 6.75 (s, 1H), 3.89 (s, 2H), 3.72 (s, 6H), 3.69 – 3.55 (m, 30H), 3.53 (t, *J* = 6.5 Hz, 2H), 3.37 (t, *J* = 7.8 Hz, 2H), 2.45 (t, *J* = 6.5 Hz, 6H), 1.97 – 1.88 (m, 2H), 1.82 – 1.73 (m, 2H), 1.45 (s, 27H); ^{13}C NMR (101 MHz, $CDCl_3$) δ 170.8, 169.7, 137.0, 131.6, 131.1, 130.0, 128.8, 127.7, 127.5, 127.3, 126.7, 126.0, 125.3, 125.2, 124.98, 124.95, 124.8, 123.7, 80.6, 71.4, 71.2, 71.0, 70.82, 70.81, 70.78, 70.76, 70.73, 70.72, 70.6, 70.4, 69.2, 67.3, 59.7, 36.5, 33.5, 29.9, 28.6, 28.3; MS-ES$^+$ *m/z*: 1106.5 $[M+Na]^+$, 1084.3 $[M+H]^+$; HRMS-ES$^+$ *m/z*: $[M+H]^+$ calculated for $C_{59}H_{90}NO_{17}$, 1084.6209; found, 1084.6212.

PyrB-PEG2-CH_2COG1(OH)$_3$

This reaction was conducted using the general procedure for deprotection of *tert*-butyl esters. The following reagents were used in the stated quantities: **PyrB-PEG2-CH_2COG1(O^{t}Bu)$_3$** (266 mg, 0.29 mmol) and formic acid (5 ml). **PyrB-PEG2-CH_2COG1(OH)$_3$** was obtained as a yellow oil (217 mg, 100%), ^{1}H NMR (400 MHz, CD_3OD) δ 8.33 (d, *J* = 9.3 Hz, 1H), 8.22 – 8.15 (m, 2H), 8.13 (d, *J* = 8.8 Hz, 2H), 8.07 – 7.96 (m, 3H), 7.90 (d, *J* = 7.8 Hz, 1H), 7.04 (s, 1H), 3.83 (s, 2H), 3.66 (s, 6H), 3.64 – 3.60 (m, 10H),

3.60 – 3.52 (m, 6H), 3.38 (t, *J* = 7.7 Hz, 2H), 2.47 (t, *J* = 6.1 Hz, 6H), 1.99 – 1.87 (m, 2H), 1.82 - 1.70 (m, 2H); ^{13}C NMR (101 MHz, CD_3OD) δ 175.3, 172.2, 138.3, 132.9, 132.4, 131.2, 129.9, 128.6, 128.5, 128.3, 127.6, 127.0, 126.3, 126.2, 125.92, 125.89, 125.8, 124.6, 72.1, 71.9, 71.6, 71.5, 71.4, 71.1, 70.0, 68.1, 61.1, 35.8, 34.1, 30.7, 29.7; MS-ES$^-$ *m/z*: 738.4 $[M-H]^-$; HRMS-ES$^-$ *m/z*: $[M-H]^-$ calculated for $C_{39}H_{48}NO_{13}$, 738.3126; found, 738.3134.

PyrB-PEG4-CH_2COG1(OH)$_3$

This reaction was conducted using the general procedure for deprotection of *tert*-butyl esters. The following reagents were used in the stated quantities: **PyrB-PEG4-CH_2COG1(O^{t}Bu)$_3$** (228 mg, 0.23 mmol) and formic acid (5 ml). **PyrB-PEG4-CH_2COG1(OH)$_3$** was obtained as a yellow oil (190 mg, 100%), ^{1}H NMR (400 MHz, CD_3OD) δ 8.33 (d, *J* = 9.3 Hz, 1H), 8.22 – 8.15 (m, 2H), 8.12 (d, *J* = 8.4 Hz, 2H), 8.08 – 7.96 (m, 3H), 7.89 (d, *J* = 7.8 Hz, 1H), 7.04 (s, 1H), 3.83 (s, 2H), 3.68 (s, 6H), 3.65 (t, *J* = 6.1 Hz, 6H), 3.62 – 3.45 (m, 18H), 3.37 (t, *J* = 7.8 Hz, 2H), 2.49 (t, *J* = 6.1 Hz, 6H), 1.98 – 1.87 (m, 2H), 1.80 - 1.70 (m, 2H); ^{13}C NMR (101 MHz, CD_3OD) δ 175.3, 172.2, 138.3, 132.9, 132.3, 131.2, 129.9, 128.6, 128.5, 128.2, 127.6, 127.0, 126.24, 126.17, 125.93, 125.90, 125.8, 124.6, 72.1, 71.8, 71.53, 71.47, 71.42, 71.40, 71.3, 71.2, 70.0, 68.1, 61.1, 35.8, 34.2, 30.7, 29.7; MS-ES$^+$ *m/z*: 850.5 $[M+Na]^+$; HRMS-ES$^+$ *m/z*: $[M+Na]^+$ calculated for $C_{43}H_{57}NO_{15}Na$, 850.3626; found, 850.3618.

PyrB-PEG6-CH_2COG1(OH)$_3$

This reaction was conducted using the general procedure for deprotection of *tert*-butyl esters. The following reagents were used in the stated quantities: **PyrB-PEG6-CH_2COG1(O^{t}Bu)$_3$** (946 mg, 0.87 mmol) and formic acid (15 ml). **PyrB-PEG6-CH_2COG1(OH)$_3$** was obtained as a yellow oil (800 mg, 100%), ^{1}H NMR (400 MHz, CD_3OD) δ 8.34 (d, *J* = 9.3 Hz, 1H), 8.22 – 8.16 (m, 2H), 8.13 (d, *J* = 8.7 Hz, 2H), 8.08 – 7.97 (m, 3H), 7.90 (d, *J* = 7.8 Hz, 1H), 7.06 (s, 1H), 3.86 (s, 2H), 3.69 (s, 6H), 3.66 (t, *J* = 6.1 Hz, 6H), 3.62 – 3.58 (m, 6H), 3.58 – 3.43 (m, 20H), 3.38 (t, *J* = 7.8 Hz, 2H), 2.50 (t, *J* = 6.1 Hz, 6H), 1.98 - 1.88 (m, 2H), 1.80 – 1.71 (m, 2H); ^{13}C NMR (101 MHz, CD_3OD) δ 175.2, 172.2, 138.3, 132.9, 132.3, 131.2, 129.9, 128.6, 128.5, 128.2, 127.6, 127.0, 126.24, 126.18, 125.92, 125.89, 125.8, 124.6, 72.1, 71.9, 71.56, 71.55, 71.48, 71.47, 71.46, 71.45, 71.44, 71.42, 71.37, 71.2, 70.0, 68.1, 61.1, 35.8, 34.1, 30.7, 29.7; MS-ES$^-$ *m/z*: 914.5 $[M-H]^-$; HRMS-ES$^-$ *m/z*: $[M-H]^-$ calculated for $C_{47}H_{64}NO_{17}$, 914.4174; found, 914.4193.

PyrB-PEG2-CH_2COONa

This reaction was conducted using the general procedure for formation of sodium carboxylates. The following reagents were used in the stated quantities: **PyrB-PEG2-CH_2COOH** (91 mg, 0.216 mmol, 1 eq.), methanol (5 ml) and 1.0000 M $NaOH_{(aq)}$ (0.216 ml, 1 eq.). **PyrB-PEG2-CH_2COONa** was obtained as a pale yellow hygroscopic solid (96 mg, 100%), ^{1}H NMR (400 MHz, D_2O) δ 7.39 (d, *J* = 6.2 Hz, 1H), 7.29 – 7.16 (m, 4H), 7.13 (t, *J* = 8.8 Hz, 2H), 7.01 (d, *J* = 8.8 Hz, 1H), 6.87 (d, *J* = 7.5 Hz, 1H), 3.73 (s, 2H), 3.24 – 3.18 (m, 2H), 3.08 – 3.03 (m, 2H), 2.83 (bs, 2H), 2.61 (bs, 2H), 2.40 (bs, 2H), 2.26 (bs, 2H), 0.80 (bs, 4H).

PyrB-PEG4-CH_2COONa

This reaction was conducted using the general procedure for formation of sodium carboxylates. The following reagents were used in the stated quantities: **PyrB-PEG4-CH_2COOH** (510 mg, 1.003 mmol, 1 eq.), methanol (15 ml) and 1.0000 M $NaOH_{(aq)}$ (1.003 ml, 1 eq.). **PyrB-PEG4-CH_2COONa** was obtained as a sticky brown hygroscopic solid (532 mg, 100%), ^{1}H NMR (400 MHz, D_2O) δ 7.42 (d, *J* = 4.9 Hz, 1H), 7.34 (d, *J* = 9.2 Hz, 1H), 7.31 – 7.22 (m, 3H), 7.19 (d, *J* = 9.1 Hz, 2H), 7.10 (d, *J* = 8.5 Hz, 1H), 6.96 (d, *J* = 7.5 Hz, 1H), 3.83 (s, 2H), 3.46 – 3.39 (m, 2H), 3.36 – 3.29 (m, 2H), 3.23 – 3.18 (m, 2H), 3.18 – 3.07 (m, 6H), 3.07 – 3.01 (m, 2H), 2.93 – 2.85 (m, 2H), 2.64 (bs, 2H), 2.39 (bs, 2H), 0.98 (bs, 4H).

PyrB-PEG6-CH_2COONa

This reaction was conducted using the general procedure for formation of sodium carboxylates. The following reagents were used in the stated quantities: **PyrB-PEG6-CH_2COOH** (513 mg, 0.860 mmol, 1 eq.), methanol (10 ml) and 1.0000 M $NaOH_{(aq)}$ (0.860 ml, 1 eq.). **PyrB-PEG6-CH_2COONa** was obtained as a sticky brown hygroscopic solid (532 mg, 100%), ^{1}H NMR (400 MHz, D_2O) δ 7.46 (d, *J* = 7.1 Hz, 1H), 7.40 – 7.26 (m, 4H), 7.25 - 7.13 (m, 3H), 7.00 (d, *J* = 7.8 Hz, 1H), 3.88 (s, 2H), 3.56 – 3.51 (m, 2H), 3.51 – 3.46 (m, 2H), 3.42 – 3.36 (m, 2H), 3.36 – 3.31 (m, 2H), 3.31 – 3.24 (m, 4H), 3.24 – 3.17 (m, 8H), 3.17 – 3.11 (m, 2H), 3.02 – 2.95 (m, 2H), 2.73 (bs, 2H), 2.44 (bs, 2H), 1.04 (bs, 4H).

PyrB-PEG12-CH_2COONa

This reaction was conducted using the general procedure for formation of sodium carboxylates. The following reagents were used in the stated quantities: **PyrB-PEG12-CH_2COOH** (158 mg, 0.184 mmol, 1 eq.), methanol (5 ml) and 1.0000 M $NaOH_{(aq)}$ (0.184 ml, 1 eq.). **PyrB-PEG12-CH_2COONa** was obtained as a sticky brown hygroscopic solid

(162 mg, 100%), ^{1}H NMR (400 MHz, D_2O) δ 7.55 – 7.15 (m, 8H), 7.05 (d, *J* = 7.5 Hz, 1H), 3.92 (s, 2H), 3.72 – 3.66 (m, 2H), 3.66 – 3.26 (m, 42H), 3.23 (bs, 2H), 3.08 (bs, 2H), 2.82 (bs, 2H), 2.50 (bs, 2H), 1.11 (bs, 4H).

PyrB-PEG2-CH_2COG1(ONa)$_3$

This reaction was conducted using the general procedure for formation of sodium carboxylates. The following reagents were used in the stated quantities: **PyrB-PEG2-CH_2COG1(OH)$_3$** (202 mg, 0.273 mmol, 1 eq.), methanol (5 ml) and 1.0000 M $NaOH_{(aq)}$ (0.819 ml, 3 eq.). **PyrB-PEG2-CH_2COG1(ONa)$_3$** was obtained as a hygroscopic yellow solid (220 mg, 100%), ^{1}H NMR (400 MHz, D_2O) δ 8.06 (d, *J* = 7.5 Hz, 1H), 8.01 (d, *J* = 7.6 Hz, 1H), 7.92 (d, *J* = 7.6 Hz, 1H), 7.90 – 7.82 (m, 4H), 7.78 (d, *J* = 9.3 Hz, 1H), 7.57 (d, *J* = 7.8 Hz, 1H), 3.68 (s, 2H), 3.49 (t, *J* = 6.9 Hz, 6H), 3.39 (s, 6H), 3.37 – 3.22 (m, 10H), 2.95 (t, *J* = 7.1 Hz, 2H), 2.31 (t, *J* = 6.9 Hz, 6H), 1.60 – 1.41 (m, 4H).

PyrB-PEG4-CH_2COG1(ONa)$_3$

This reaction was conducted using the general procedure for formation of sodium carboxylates. The following reagents were used in the stated quantities: **PyrB-PEG4-CH_2COG1(OH)$_3$** (180 mg, 0.217 mmol, 1 eq.), methanol (5 ml) and 1.0000 M $NaOH_{(aq)}$ (0.651 ml, 3 eq.). **PyrB-PEG4-CH_2COG1(ONa)$_3$** was obtained as a hygroscopic yellow solid (194 mg, 100%), ^{1}H NMR (400 MHz, D_2O) δ 7.67 – 7.60 (m, 2H), 7.55 (d, *J* = 7.4 Hz, 1H), 7.53 – 7.40 (m, 4H), 7.37 (d, *J* = 9.3 Hz, 1H), 7.15 (d, *J* = 7.9 Hz, 1H), 3.80 (s, 2H), 3.70 – 3.55 (m, 12H), 3.36 – 3.28 (m, 2H), 3.26 – 3.21 (m, 2H), 3.19 – 3.03 (m, 10H), 3.02 – 2.96 (m, 2H), 2.82 (bs, 2H), 2.56 (bs, 2H), 2.39 (t, *J* = 6.7 Hz, 6H), 1.14 (bs, 4H).

PyrB-PEG6-CH_2COG1(ONa)$_3$

This reaction was conducted using the general procedure for formation of sodium carboxylates. The following reagents were used in the stated quantities: **PyrB-PEG6-CH_2COG1(OH)$_3$** (753 mg, 0.822 mmol, 1 eq.), methanol (10 ml) and 1.0000 M $NaOH_{(aq)}$ (2.466 ml, 3 eq.). **PyrB-PEG6-CH_2COG1(ONa)$_3$** was obtained as a hygroscopic yellow solid (807 mg, 100%), ^{1}H NMR (400 MHz, D_2O) δ 7.63 – 7.53 (m, 2H), 7.53 – 7.44 (m, 2H), 7.44 – 7.30 (m, 4H), 7.12 (d, *J* = 7.8 Hz, 1H), 3.91 (s, 2H), 3.75 – 3.61 (m, 12H), 3.54 - 3.49 (m, 2H), 3.49 – 3.43 (m, 2H), 3.42 – 3.36 (m, 2H), 3.36 – 3.29 (m, 2H), 3.29 – 3.24 (m, 2H), 3.24 – 3.05 (m, 12H), 3.04 – 2.96 (m, 2H), 2.81 (bs, 2H), 2.54 (bs, 2H), 2.42 (t, *J* = 6.7 Hz, 6H), 1.12 (bs, 4H).

PyrB-PEG4-CH_2CO(15-c-5)

This reaction was conducted using the general procedure for amide coupling reactions. The following reagents were used in the stated quantities: **PyrB-PEG4-CH_2COOH** (533 mg, 1.05 mmol, 1 eq.), DIPEA (0.37 ml, 2.12 mmol, 2 eq.), TBTU (336 mg, 1.05 mmol, 1 eq.), 2-aminomethyl-15-crown-5 (0.23 ml, 1.05 mmol, 1 eq.) and DCM (20 ml). This reaction was stirred at RT for 72 h. The crude material was purified using a Biotage Isolera One purification system (reversed phase with C18 silica, 9:1 H_2O/MeOH - MeOH) to yield **PyrB-PEG4-CH_2CO(15-c-5)** as a yellow oil (560 mg, 72%), ^{1}H NMR (400 MHz, $CDCl_3$) δ 8.29 (d, *J* = 9.3 Hz, 1H), 8.19 – 8.13 (m, 2H), 8.13 – 8.08 (m, 2H), 8.06 – 7.96 (m, 3H), 7.87 (d, *J* = 7.8 Hz, 1H), 7.10 (t, *J* = 6.1 Hz, 1H), 3.98 (d, *J* = 1.2 Hz, 2H), 3.80 – 3.75 (m, 2H), 3.72 - 3.50 (m, 36H), 3.37 (t, *J* = 7.8 Hz, 2H), 3.33 – 3.25 (m, 1H), 1.98 – 1.89 (m, 2H), 1.83 - 1.74 (m, 2H); ^{1}H NMR (400 MHz, D_2O) δ 7.46 (d, *J* = 7.8 Hz, 2H), 7.40 – 7.10 (m, 6H), 7.06 (d, *J* = 7.4 Hz, 1H), 3.94 (s, 2H), 3.75 – 3.16 (m, 35H), 3.09 (bs, 2H), 2.83 (bs, 2H), 2.51 (bs, 2H), 1.14 (bs, 4H); ^{13}C NMR (101 MHz, $CDCl_3$) δ 170.1, 137.1, 131.6, 131.1, 130.0, 128.8, 127.7, 127.5, 127.4, 126.7, 126.0, 125.3, 125.2, 125.01, 124.97, 124.8, 123.7, 78.2, 72.2, 71.4, 71.2, 71.14, 71.09, 71.05, 70.82, 70.79, 70.77, 70.72, 70.69, 70.66, 70.5, 70.4, 70.2, 40.4, 33.5, 29.9, 28.6; MS-ES$^+$ *m/z*: 762.2 $[M+Na]^+$, 392.7 $[M+2Na]^{2+}$; HRMS-ES$^+$ (*m/z*): $[M+H]^+$ calculated for $C_{41}H_{58}NO_{11}$, 740.40044; found, 740.39832.

A smaller scale reaction using 178 mg **PyrB-PEG4-CH_2COOH** was purified directly (i.e. no extractions were performed on the crude material) by column chromatography (silica, DCM with 5% MeOH and 5% $NH_{3(aq)}$ (35 wt%) – DCM with 20% MeOH and 5% $NH_{3(aq)}$ (35 wt%)) to yield **PyrB-PEG4-CH_2CO(15-c-5)** as a yellow oil (205 mg, 79%). Spectral data agreed with that above.

PyrM-PEG4

This reaction was conducted based on the general procedure for monosubstitution of OEGs with PyrM groups. The following reagents were used in the stated quantities: PEG4 (0.72 ml, 4.17 mmol, 1 eq.), Ag_2O (1440 mg, 6.21 mmol, 1.5 eq.), KI (276 mg, 1.66 mmol, 0.4 eq.), **PyrMBr** (1230 mg, 4.17 mmol, 1 eq.) and DCM (50 ml). Once the addition of **PyrMBr** was complete, the reaction was stirred for a further 45 min. **PyrM-PEG4** was isolated using column chromatography (silica, EtOAc – 1:1 EtOAc/acetone) as a yellow oil (1020 mg, 60%),^{1}H NMR (400 MHz, $CDCl_3$) δ 8.41 (d, *J* = 9.2 Hz, 1H), 8.23 – 8.17 (m, 2H), 8.17 – 8.12 (m, 2H), 8.09 – 7.98 (m, 4H), 5.29 (s, 2H), 3.79 – 3.74 (m, 2H), 3.74 – 3.71 (m, 2H), 3.71 – 3.65 (m, 6H), 3.62 (s, 4H), 3.58 – 3.53 (m, 2H), 2.60 (bs, 1H); ^{13}C NMR (101 MHz, $CDCl_3$) δ 131.6, 131.5, 131.4, 131.0, 129.6, 127.8, 127.58, 127.57, 127.3, 126.1, 125.4, 125.1, 124.9, 124.6,

123.7, 72.6, 72.0, 70.9, 70.80, 70.77, 70.75, 70.5, 69.7, 61.9; MS-ES$^+$ *m/z*: 431.1 $[M+Na]^+$; HRMS-ES$^+$ *m/z*: $[M+Na]^+$ calculated for $C_{25}H_{28}O_5Na$, 431.1834; found, 431.1845.

PyrM-PEG4-CH_2COOH

This reaction was conducted using the general procedure for addition of a terminal acid group. The following reagents were used in the stated quantities: **PyrM-PEG4** (764 mg, 1.87 mmol, 1 eq.), NaH (584 mg, 24.3 mmol, 13 eq.), bromoacetic acid (390 mg, 2.81 mmol, 1.5 eq.) and THF (30 ml). **PyrM-PEG4-CH_2COOH** was obtained as a yellow-brown oil (771 mg, 88%), ^{1}H NMR (400 MHz, $CDCl_3$) δ 9.02 (bs, 1H), 8.40 (d, *J* = 9.2 Hz, 1H), 8.22 – 8.17 (m, 2H), 8.17 - 8.11 (m, 2H), 8.08 – 7.98 (m, 4H), 5.29 (s, 2H), 4.11 (s, 2H), 3.81 – 3.75 (m, 2H), 3.75 - 3.70 (m, 2H), 3.70 – 3.62 (m, 7H), 3.62 – 3.56 (m, 5H); ^{13}C NMR (101 MHz, $CDCl_3$) δ 172.6, 131.5, 131.4, 131.0, 129.6, 127.8, 127.6, 127.3, 126.1, 125.38, 125.37, 125.1, 124.9, 124.6, 123.7, 72.0, 71.5, 70.9, 70.83, 70.78, 70.6, 70.5, 70.4, 69.6, 69.1; MS-ES- *m/z*: 932.2 $[2M-H]^-$, 465.2 $[M-H]^-$; HRMS-ES$^-$ *m/z*: $[M-H]^-$ calculated for $C_{27}H_{29}O_7$, 465.1913; found, 465.1943.

PyrM-PEG4-CH_2CO(15-c-5)

This reaction was conducted using the general procedure for amide coupling reactions. The following reagents were used in the stated quantities: **PyrM-PEG4-CH_2COOH** (276 mg, 0.59 mmol, 1 eq.), DIPEA (0.21 ml, 1.21 mmol, 2 eq.), TBTU (190 mg, 0.59 mmol, 1 eq.), 2-aminomethyl-15-crown-5 (0.13 ml, 0.59 mmol, 1 eq.) and DCM (10 ml). This reaction was stirred at RT for 60 h. The crude material was purified using a Biotage Isolera One purification system (reversed phase with C18 silica, 9:1 H_2O/MeOH - MeOH) to yield **PyrM-PEG4-CH_2CO(15-c-5)** as a yellow oil (223 mg, 54%), ^{1}H NMR (400 MHz, $CDCl_3$) δ 8.41 (d, *J* = 9.2 Hz, 1H), 8.23 – 8.17 (m, 2H), 8.17 – 8.12 (m, 2H), 8.09 – 7.98 (m, 4H), 7.11 (t, *J* = 6.1 Hz, 1H), 5.29 (s, 2H), 3.96 (d, *J* = 1.4 Hz, 2H), 3.81 – 3.74 (m, 4H), 3.74 – 3.49 (m, 32H), 3.34 – 3.23 (m, 1H); ^{13}C NMR (101 MHz, $CDCl_3$) δ 170.1, 131.6, 131.5, 131.4, 131.0, 129.6, 127.9, 127.6, 127.3, 126.1, 125.4, 125.1, 124.9, 124.7, 123.8, 78.2, 72.2, 72.1, 71.2, 71.13, 71.05, 71.0, 70.94, 70.86, 70.80, 70.79, 70.77, 70.73, 70.66, 70.6, 70.5, 70.2, 69.7, 40.4; MS-ES$^+$ *m/z*: 719.9 $[M+Na]^+$; HRMS-ES$^+$ (*m/z*): $[M+Na]^+$ calculated for $C_{38}H_{51}NO_{11}Na$, 720.3360; found, 720.3355.

PyrM-PEG6-CH_2CO(15-c-5)

This reaction was conducted using the general procedure for amide coupling reactions. The following reagents were used in the stated quantities: **PyrM-PEG6-CH_2COOH** (379 mg, 0.68 mmol, 1 eq.), DIPEA (0.24 ml, 1.38 mmol, 2 eq.), TBTU (219 mg, 0.69 mmol, 1 eq.),

2-aminomethyl-15-crown-5 (0.15 ml, 0.68 mmol, 1 eq.) and DCM (15 ml). This reaction was stirred at RT for 60 h. The crude material was purified using a Biotage Isolera One purification system (reversed phase with C18 silica, 9:1 H_2O/MeOH - MeOH) to yield **PyrM-PEG6-CH_2CO(15-c-5)** as a yellow oil (426 mg, 80%), ^{1}H NMR (400 MHz, $CDCl_3$) δ 8.41 (d, *J* = 9.2 Hz, 1H), 8.23 – 8.17 (m, 2H), 8.17 – 8.13 (m, 2H), 8.09 – 7.99 (m, 4H), 7.11 (t, *J* = 5.7 Hz, 1H), 5.29 (s, 2H), 3.98 (d, *J* = 1.3 Hz, 2H), 3.80 – 3.75 (m, 4H), 3.74 – 3.51 (m, 40H); ^{13}C NMR (101 MHz, $CDCl_3$) δ 170.1, 131.6, 131.41, 131.37, 131.0, 129.5, 127.8, 127.6, 127.5, 127.2, 126.1, 125.3, 125.1, 124.8, 124.6, 123.7, 78.1, 72.1, 72.0, 71.12, 71.08, 71.0, 70.94, 70.87, 70.8, 70.73, 70.71, 70.68, 70.66, 70.64, 70.60, 70.56, 70.4, 70.2, 69.7, 40.3; MS-ES$^+$ *m/z*: 808.6 $[M+Na]^+$, 415.9 $[M+2Na]^{2+}$; HRMS-ES$^+$ (*m/z*): $[M+H]^+$ calculated for $C_{42}H_{60}NO_{13}$, 786.40592; found, 786.40667.

PyrB-g(^{i}Pr), PyrB$_2$O and PyrBOTs

Sodium hydride (214 mg, 8.92 mmol, 5 eq.) was dispersed in anhydrous THF (10 ml) and stirred vigorously at room temperature. A solution of **PyrBOH** (500 mg, 1.82 mmol, 1.02 eq.) in THF (5 ml) was carefully added dropwise to the stirred solution which was then heated at 67 °C for 1 h. The reaction was then allowed to cool slightly such that reflux was no longer occurring. A solution of 2,2-dimethyl-1,3-dioxolan-4-yl methyl *p*-toluenesulphonate (512 mg, 1.79 mmol, 1 eq.) in THF (5 ml) was then added dropwise and the reaction then stirred at 67 °C for 17 h. The reaction was then allowed to cool to room temperature before the solvent was removed under vacuum. The residue was dissolved in $CHCl_3$ and any insoluble materials were removed by filtration and washed thoroughly with $CHCl_3$. The combined filtrate was dried *in vacuo* then purified by column chromatography (Silica, DCM – DCM with 10% MeOH) to afford **PyrB$_2$O**, **PyrBOTs** and impure **PyrB-g(^{i}Pr)**. The latter was purified by further column chromatography (Silica, 4:1 hexane/EtOAc – 3:1 hexane / EtOAc) to afford **PyrB-g(^{i}Pr)** as a light brown solid (105 mg, 15%), ^{1}H NMR (400 MHz, $CDCl_3$) δ 8.29 (d, *J* = 9.2 Hz, 1H), 8.20 – 8.15 (m, 2H), 8.14 – 8.09 (m, 2H), 8.07 – 7.97 (m, 3H), 7.88 (d, *J* = 7.8 Hz, 1H), 4.32 – 4.24 (m, 1H), 4.06 (dd, *J* = 8.2, 6.4 Hz, 1H), 3.73 (dd, *J* = 8.2, 6.4 Hz, 1H), 3.61 – 3.49 (m, 3H), 3.45 – 3.40 (m, 1H), 3.37 (t, *J* = 7.7 Hz, 2H), 1.99 – 1.89 (m, 2H), 1.84 – 1.74 (m, 2H), 1.45 (s, 3H), 1.39 (s, 3H); ^{13}C NMR (101 MHz, $CDCl_3$) δ 136.9, 131.6, 131.1, 130.0, 128.8, 127.7, 127.43, 127.36, 126.7, 126.0, 125.3, 125.2, 125.01, 124.96, 124.8, 123.6, 109.6, 74.9, 72.1, 71.8, 67.1, 33.5, 29.8, 28.5, 27.0, 25.6;

PyrB$_2$O was isolated as a viscous yellow oil (100 mg, 21%), ^{1}H NMR (400 MHz, $CDCl_3$) δ 8.27 (d, *J* = 9.2 Hz, 2H), 8.18 – 8.14 (m, 2H), 8.13 – 7.96 (m, 12H), 7.85 (d, *J* = 7.8 Hz, 2H), 3.50 (t, *J* = 6.4 Hz, 4H), 3.37 (t, *J* = 7.8 Hz, 4H), 2.01 – 1.90 (m, 4H), 1.84 – 1.74 (m, 4H); ^{13}C NMR

(101 MHz, $CDCl_3$) δ 137.1, 131.6, 131.1, 129.9, 128.8, 127.7, 127.4, 127.3, 126.7, 125.9, 125.3, 125.2, 125.0, 124.8, 123.6, 70.9, 33.5, 30.0, 28.7; MS-ES$^+$ *m/z*: 553.8 $[M+Na]^+$.

PyrBOTs was isolated as a viscous yellow oil of sufficient purity to identify the product (99 mg, 13%), ^{1}H NMR (400 MHz, $CDCl_3$) δ 8.21 – 8.15 (m, 3H), 8.13 – 8.06 (m, 2H), 8.05 - 7.99 (m, 3H), 7.79 (d, *J* = 7.7 Hz, 1H), 7.76 (d, *J* = 8.3 Hz, 2H), 7.25 (d, *J* = 8.3 Hz, 2H), 4.09 (t, *J* = 6.1 Hz, 2H), 3.30 (t, *J* = 7.5 Hz, 2H), 2.36 (s, 3H), 1.96 – 1.85 (m, 2H), 1.85 – 1.74 (m, 2H); ^{13}C NMR (101 MHz, $CDCl_3$) δ 144.8, 136.0, 133.3, 131.6, 131.1, 130.1, 130.0, 128.8, 128.0, 127.7, 127.5, 127.4, 126.9, 126.1, 125.3, 125.2, 125.1, 125.0, 123.4, 70.6, 32.9, 29.0, 27.7, 21.7; MS-ES$^+$ *m/z*: 879.9 $[2M+Na]^+$, 451.6 $[M+Na]^+$.

PyrB-g(OH)$_2$

This reaction was conducted using the general procedure for deprotection of isopropylidene acetals. The following reagents were used in the stated quantities: Amberlyst-15 (20 mg), **PyrB-g(^{i}Pr)** (105 mg, 0.270 mmol), EtOH (20 ml). **PyrB-g(OH)$_2$** was obtained as a beige solid (95 mg, 100%), ^{1}H NMR (400 MHz, $CDCl_3$) δ 8.26 (d, *J* = 9.3 Hz, 1H), 8.19 – 8.14 (m, 2H), 8.14 - 8.08 (m, 2H), 8.06 – 7.96 (m, 3H), 7.86 (d, *J* = 7.8 Hz, 1H), 3.90 – 3.80 (m, 1H), 3.74 - 3.57 (m, 2H), 3.56 – 3.41 (m, 4H), 3.36 (t, *J* = 7.7 Hz, 2H), 2.76 (bs, 1H), 2.36 (bs, 1H), 1.97 – 1.86 (m, 2H), 1.81 – 1.70 (m, 2H); ^{13}C NMR (101 MHz, $CDCl_3$) δ 136.8, 131.6, 131.1, 130.0, 128.8, 127.7, 127.43, 127.42, 126.8, 126.0, 125.3, 125.2, 125.1, 125.0, 124.9, 123.5, 72.6, 71.7, 70.7, 64.4, 33.4, 29.8, 28.4; MS-ES$^+$ *m/z*: 371.7 $[M+Na]^+$; HRMS-ES$^+$ *m/z*: $[M+Na]^+$ calculated for $C_{23}H_{24}O_3Na$, 371.1623; found, 371.1645.

PyrM-PEG4-Ms

This reaction was conducted based on the general mesylation procedure above. Larger quantities of triethylamine and mesyl chloride were used than in the general procedure. The following reagents were used in the stated quantities: Triethylamine (1.10 ml, 7.89 mmol, 4.2 eq.), **PyrM-PEG4** (767 mg, 1.88 mmol, 1 eq.), mesyl chloride (0.61 ml, 7.89 mmol, 4.2 eq.) and DCM (50 ml). **PyrM-PEG4-Ms** was obtained as a yellow oil (899 mg, 98%), ^{1}H NMR (400 MHz, $CDCl_3$) δ 8.41 (d, *J* = 9.2 Hz, 1H), 8.23 – 8.17 (m, 2H), 8.17 – 8.13 (m, 2H), 8.08 - 7.99 (m, 4H), 5.29 (s, 2H), 4.33 – 4.28 (m, 2H), 3.80 – 3.74 (m, 2H), 3.74 – 3.69 (m, 2H), 3.69 – 3.61 (m, 6H), 3.61 – 3.55 (m, 4H), 3.01 (s, 3H); ^{13}C NMR (101 MHz, $CDCl_3$) δ 131.6, 131.5, 131.4, 131.0, 129.6, 127.8, 127.6, 127.3, 126.1, 125.40, 125.39, 125.1, 124.9, 124.7, 123.8, 72.0, 70.9, 70.84, 70.76, 70.7, 69.7, 69.4, 69.1, 37.8; MS-ES$^+$ *m/z*: 509.1 $[M+Na]^+$, 295.0 $[HO(CH_2CH_2O)_4MsNaH]^+$, 215.1 $[PyrM]^+$; HRMS-ES$^+$ (*m/z*): $[M+Na]^+$ calculated for $C_{26}H_{30}O_7NaS$, 509.1610; found, 509.1611.

PyrM-PEG6-Ms

This reaction was conducted based on the general mesylation procedure above. Larger quantities of triethylamine and mesyl chloride were used than in the general procedure. The following reagents were used in the stated quantities: Triethylamine (1.23 ml, 8.82 mmol, 4.2 eq.), **PyrM-PEG6** (1040 mg, 2.09 mmol, 1 eq.), mesyl chloride (0.68 ml, 8.79 mmol, 4.2 eq.) and DCM (50 ml). **PyrM-PEG6-Ms** was obtained as a yellow oil (1192 mg, 99%), ^{1}H NMR (400 MHz, $CDCl_3$) δ 8.41 (d, *J* = 9.2 Hz, 1H), 8.23 – 8.17 (m, 2H), 8.17 – 8.12 (m, 2H), 8.09 – 7.98 (m, 4H), 5.28 (s, 2H), 4.36 – 4.30 (m, 2H), 3.79 – 3.75 (m, 2H), 3.74 – 3.52 (m, 20H), 3.05 (s, 3H); ^{13}C NMR (101 MHz, $CDCl_3$) δ 131.6, 131.43, 131.39, 131.0, 129.6, 127.8, 127.58, 127.56, 127.2, 126.1, 125.4, 125.1, 124.9, 124.6, 123.7, 72.0, 70.9, 70.82, 70.77, 70.75, 70.72, 70.72, 70.68, 70.6, 69.7, 69.5, 69.1, 37.9; MS-ES$^+$ *m/z*: 597.1 $[M+Na]^+$, 361.1 $[HO(CH_2CH_2O)_6Ms+H]^+$, 317.1 $[HO(CH_2CH_2O)_5Ms+H]^+$, 215.1 $[PyrM]^+$; HRMS-ES$^+$ (*m/z*): $[M+Na]^+$ calculated for $C_{30}H_{38}O_9NaS$, 597.2134; found, 597.2143.

PyrM-PEG4-g(^{i}Pr)

Sodium hydride (47 mg, 1.96 mmol, 4.5 eq.) was dispersed in anhydrous THF (12 ml) and stirred vigorously at room temperature. Solketal (0.08 ml, 0.64 mmol, 1.5 eq.) was carefully added dropwise to the stirred solution which was then heated at 40 °C for 1 h. After this time a solution of **PyrM-PEG4-Ms** (210 mg, 0.43 mmol, 1 eq.) in THF (8 ml) was then added dropwise and the reaction then stirred at 40 °C for 16 h. The reaction was allowed to cool to room temperature and carefully quenched with H_2O (5 ml). The THF was removed *in vacuo* and DCM (30 ml) was added to the aqueous residue. The mixture was extracted with brine (3 × 30 ml) and the organic layer was dried over $MgSO_4$ which was then removed by filtration. After removal of the solvent, the crude material was purified using column chromatography (silica, EtOAc) to afford **PyrM-PEG4-g(^{i}Pr)** as a yellow oil (129 mg, 57%), ^{1}H NMR (400 MHz, $CDCl_3$) δ 8.41 (d, *J* = 9.2 Hz, 1H), 8.23 – 8.17 (m, 2H), 8.17 – 8.12 (m, 2H), 8.08 – 7.99 (m, 4H), 5.29 (s, 2H), 4.30 – 4.22 (m, 1H), 4.03 (dd, *J* = 8.3, 6.4 Hz, 1H), 3.80 – 3.75 (m, 2H), 3.75 – 3.70 (m, 3H), 3.70 – 3.65 (m, 4H), 3.65 – 3.57 (m, 8H), 3.57 – 3.51 (m, 1H), 3.49 – 3.42 (m, 1H), 1.42 (s, 3H), 1.36 (s, 3H); ^{13}C NMR (101 MHz, $CDCl_3$) δ 131.6, 131.5, 131.4, 131.0, 129.6, 127.8, 127.59, 127.57, 127.2, 126.1, 125.4, 125.1, 124.9, 124.6, 123.8, 109.5, 74.9, 72.5, 72.0, 71.1, 70.94, 70.85, 70.81, 70.78, 70.7, 69.7, 67.0, 27.0, 25.6; MS-ES$^+$ *m/z*: 545.0 $[M+Na]^+$, 540.0 $[M+NH_4]^+$, 215.0 $[PyrM]^+$; HRMS-ES$^+$ (*m/z*): $[M+Na]^+$ calculated for $C_{31}H_{38}O_7Na$, 545.2515; found, 545.2513.

PyrM-PEG4-g(OH)$_2$

This reaction was conducted using the general procedure for deprotection of isopropylidene acetals. The following reagents were used in the stated quantities: Amberlyst-15 (20 mg), **PyrM-PEG4-g(^{i}Pr)** (81 mg, 0.16 mmol), EtOH (20 ml). **PyrM-PEG4-g(OH)$_2$** was obtained as a yellow film (77 mg, 100%), ^{1}H NMR (400 MHz, $CDCl_3$) δ 8.39 (d, *J* = 9.2 Hz, 1H), 8.22 – 8.16 (m, 2H), 8.16 – 8.08 (m, 2H), 8.08 – 7.97 (m, 4H), 5.27 (s, 2H), 3.85 – 3.79 (m, 1H), 3.79 – 3.74 (m, 2H), 3.74 – 3.69 (m, 2H), 3.69 – 3.53 (m, 14H), 3.53 – 3.46 (m, 2H), 3.19 (bs, 2H); ^{13}C NMR (101 MHz, $CDCl_3$) δ 131.5, 131.43, 131.38, 131.0, 129.5, 127.8, 127.6, 127.5, 127.2, 126.1, 125.3, 125.1, 124.9, 124.6, 123.7, 73.0, 72.0, 70.9, 70.8, 70.71, 70.68, 70.64, 70.57, 69.7, 64.0; MS-ES$^+$ *m/z*: 505.0 $[M+Na]^+$, 291.1 $[HO(CH_2CH_2O)_4CH_2CH(OH)CH_2OH+Na]^+$, 215.0 $[PyrM]^+$; HRMS-ES$^+$ (*m/z*): $[M+Na]^+$ calculated for $C_{28}H_{34}O_7Na$, 505.2202; found, 505.2218.

HN(PEG2)$_2$

Based on a literature procedure,[208] a solution of 2-(2-chloroethoxy)ethanol (3.2 ml, 30 mmol, 1 eq.) in toluene (7.5 ml) was added dropwise to a stirred refluxing mixture of 2-(2-aminoethoxy)ethanol (12.0 ml, 120 mmol, 4 eq.) and Na_2CO_3 (3.5 g, 33 mmol 1.1 eq.) in toluene (75 ml) in a flask fitted with Dean-Stark apparatus. The reaction was heated at reflux for 4 days and then cooled to room temperature. Solids were removed by filtration and the residue washed with ether. The combined filtrates were concentrated *in vacuo* and the crude residue purified by distillation using a Kugelrohr. **HN(PEG2)$_2$** was isolated (195 °C, 0.5 mbar) as a yellow oil (4.16 g, 72%), ^{1}H NMR (400 MHz, $CDCl_3$) δ 3.80 (bs, 2H), 3.70 – 3.66 (m, 4H), 3.61 – 3.57 (m, 4H), 3.57 – 3.54 (m, 4H), 2.84 – 2.78 (m, 4H); ^{13}C NMR (101 MHz, $CDCl_3$) δ 72.9, 69.9, 61.8, 49.1; MS-ES$^+$ *m/z*: 216.0 $[M+Na]^+$, 194.7 $[M+H]^+$; HRMS-ES$^+$ (*m/z*): $[M+H]^+$ calculated for $C_8H_{20}NO_4$, 194.1392; found, 194.1374.

PyrM-PEG4-CH$_2$CON(PEG2)$_2$

This reaction was conducted using the general procedure for amide coupling reactions. The following reagents were used in the stated quantities: **PyrM-PEG4-CH$_2$COOH** (288 mg, 0.62 mmol, 1 eq.), DIPEA (0.22 ml, 1.26 mmol, 2 eq.), TBTU (198 mg, 0.62 mmol, 1 eq.), **HN(PEG2)$_2$** (119 mg, 0.62 mmol, 1 eq.) and DCM (15 ml). This reaction was stirred at RT for 72 h. The crude material was purified using a Biotage Isolera One purification system (reversed phase with C18 silica, 9:1 H_2O/MeOH – MeOH) to yield **PyrM-PEG4-CH$_2$CON(PEG2)$_2$** as a yellow oil (198 mg, 50%), ^{1}H NMR (400 MHz, $CDCl_3$) δ 8.38 (d, *J* = 9.2 Hz, 1H), 8.21 – 8.15 (m, 2H), 8.15 – 8.10 (m, 2H), 8.06 – 7.96 (m, 4H), 5.26 (s, 2H), 4.23 (s, 2H), 3.77 – 3.73 (m, 2H), 3.72 – 3.43 (m, 30H), 2.86 (bs, 3H); ^{13}C NMR (101 MHz,

$CDCl_3$) δ 170.3, 131.5, 131.4, 131.3, 130.9, 129.5, 127.8, 127.53, 127.52, 127.2, 126.1, 125.3, 125.0, 124.8, 124.6, 123.7, 72.8, 72.6, 71.9, 70.8, 70.74, 70.66, 70.65, 70.62, 70.62, 70.59, 70.4, 69.7, 69.5, 69.1, 61.8, 61.7, 48.2, 46.8; MS-ES$^+$ *m/z*: 664.0 $[M+Na]^+$; HRMS-ES$^+$ (*m/z*): $[M+H]^+$ calculated for $C_{35}H_{48}NO_{10}$, 642.3278; found, 642.3270.

2-(2-(2-chloroethoxy)ethoxy)tetrahydropyran, 60

This reaction was conducted by adapting the general procedure for THP protection of monotosylated OEGs. 2-(2-chloroethoxy)ethanol was used in place of a tosylated OEG. The following reagents were used in the stated quantities: 2-(2-chloroethoxy)ethanol (2 ml, 18.9 mmol, 1 eq.), pyridinium *p*-toluenesulphonate (0.95 g, 3.8 mmol, 0.2 eq.), dihydropyran (2.6 ml, 28.5 mmol, 1.5 eq.) and DCM (100 ml). **60** was isolated using column chromatography (silica, 4:1 Hexane/EtOAc) as a colourless oil (2,71 g, 69%),^{1}H NMR (400 MHz, $CDCl_3$) δ 4.68 – 4.59 (m, 1H), 3.91 – 3.82 (m, 2H), 3.82 – 3.72 (m, 2H), 3.72 – 3.66 (m, 2H), 3.66 – 3.57 (m, 3H), 3.53 – 3.46 (m, 1H), 1.90 – 1.76 (m, 1H), 1.76 – 1.66 (m, 1H), 1.65 – 1.44 (m, 4H); ^{13}C NMR (101 MHz, $CDCl_3$) δ 99.1, 71.5, 70.8, 66.8, 62.4, 42.9, 30.7, 25.6, 19.6; MS-ES$^+$ *m/z*: 231.0 $[M+Na]^+$; HRMS-ES$^+$ *m/z*: $[M+Na]^+$ calculated for $C_9H_{17}O_3ClNa$, 231.0764; found, 231.0765.

Ms-PEG2-Me

This reaction was conducted based on the general mesylation procedure above. Slightly larger quantities of triethylamine and mesyl chloride were used than in the general procedure. The following reagents were used in the stated quantities: triethylamine (4.27 ml, 30.6 mmol, 1.2 eq.), **PEG2-Me** (3.00 ml, 25.5 mmol, 1 eq.), mesyl chloride (2.37 ml, 30.6 mmol, 1.2 eq.) and DCM (200 ml). **Ms-PEG2-Me** was obtained as a yellow oil (4910 mg, 97%), ^{1}H NMR (400 MHz, $CDCl_3$) δ 4.39 – 4.34 (m, 2H), 3.78 – 3.73 (m, 2H), 3.67 – 3.62 (m, 2H), 3.55 – 3.51 (m, 2H), 3.35 (s, 3H), 3.05 (s, 3H); ^{13}C NMR (101 MHz, $CDCl_3$) δ 71.9, 70.7, 69.4, 69.2, 59.1, 37.8; MS-ES$^+$ *m/z*: 221.0 $[M+Na]^+$; HRMS-ES$^+$ (*m/z*): $[M+Na]^+$ calculated for $C_6H_{14}O_5NaS$, 221.0460; found, 221.0461.

Ms-PEG2-Et

This reaction was conducted using the general mesylation procedure above. The following reagents were used in the stated quantities: Triethylamine (5.71 ml, 40.9 mmol, 1.1 eq.), **PEG2-Et** (5.00 ml, 37.2 mmol, 1 eq.), mesyl chloride (3.17 ml, 41.0 mmol, 1.1 eq.) and DCM (150 ml). **Ms-PEG2-Et** was obtained as a yellow oil (7400 mg, 94%), ^{1}H NMR (400 MHz, $CDCl_3$) δ 4.42 – 4.36 (m, 2H), 3.80 – 3.75 (m, 2H), 3.69 – 3.64 (m, 2H), 3.62 – 3.57 (m, 2H),

3.52 (q, *J* = 7.0 Hz, 2H), 3.08 (s, 3H), 1.21 (t, *J* = 7.0 Hz, 3H); ^{13}C NMR (101 MHz, $CDCl_3$) δ 71.0, 69.9, 69.5, 69.2, 66.9, 37.9, 15.3; MS-ES$^+$ *m/z*: 235.4 $[M+Na]^+$, 213.0 $[M+H]^+$; HRMS-ES$^+$ (*m/z*): $[M+H]^+$ calculated for $C_7H_{17}O_5S$, 213.0797; found, 213.0791.

Ms-PEG2-^{n}Bu

This reaction was conducted using the general mesylation procedure above. The following reagents were used in the stated quantities: Triethylamine (4.57 ml, 32.8 mmol, 1.1 eq.), **PEG2-^{n}Bu** (5.00 ml, 29.8 mmol, 1 eq.), mesyl chloride (2.54 ml, 32.8 mmol, 1.1 eq.) and DCM (150 ml). **Ms-PEG2-^{n}Bu** was obtained as a yellow oil (7160 mg, 100%), ^{1}H NMR (400 MHz, $CDCl_3$) δ 4.41 – 4.36 (m, 2H), 3.81 – 3.74 (m, 2H), 3.69 – 3.64 (m, 2H), 3.60 – 3.55 (m, 2H), 3.45 (t, *J* = 6.7 Hz, 2H), 3.08 (s, 3H), 1.60 – 1.51 (m, 2H), 1.41 – 1.30 (m, 2H), 0.92 (t, *J* = 7.4 Hz, 3H); ^{13}C NMR (101 MHz, $CDCl_3$) δ 71.4, 70.9, 70.2, 69.5, 69.2, 37.9, 31.9, 19.5, 14.1; MS-ES$^+$ *m/z*: 263.2 $[M+Na]^+$; HRMS-ES$^+$ (*m/z*): $[M+H]^+$ calculated for $C_9H_{21}O_5S$, 241.1110; found, 241.1101.

Ms-PEG3-Me

This reaction was conducted using the general mesylation procedure above. The following reagents were used in the stated quantities: Triethylamine (4.79 ml, 34.3 mmol, 1.1 eq.), **PEG3-Me** (5.00 ml, 31.2 mmol, 1 eq.), mesyl chloride (2.66 ml, 34.4 mmol, 1.1 eq.) and DCM (150 ml). **Ms-PEG3-Me** was obtained as a pale yellow oil (7550 mg, 100%), ^{1}H NMR (400 MHz, $CDCl_3$) δ 4.38 – 4.32 (m, 2H), 3.78 – 3.71 (m, 2H), 3.68 – 3.58 (m, 6H), 3.54 – 3.48 (m, 2H), 3.34 (s, 3H), 3.05 (s, 3H); ^{13}C NMR (101 MHz, $CDCl_3$) δ 72.1, 70.8, 70.69, 70.67, 69.5, 69.2, 59.2, 37.8; MS-ES$^+$ *m/z*: 264.9 $[M+Na]^+$, 242.9 $[M+H]^+$; HRMS-ES$^+$ (*m/z*): $[M+H]^+$ calculated for $C_8H_{19}O_6S$, 243.0902; found, 243.0906.

Ms-PEG3-Et

This reaction was conducted using the general mesylation procedure above. The following reagents were used in the stated quantities: Triethylamine (4.39 ml, 31.5 mmol, 1.1 eq.), **PEG3-Et** (5.00 ml, 28.6 mmol, 1 eq.), mesyl chloride (2.44 ml, 31.5 mmol, 1.1 eq.) and DCM (150 ml). **Ms-PEG3-Et** was obtained as a pale yellow oil (7320 mg, 100%), ^{1}H NMR (400 MHz, $CDCl_3$) δ 4.38 – 4.33 (m, 2H), 3.76 – 3.72 (m, 2H), 3.68 – 3.59 (m, 6H), 3.58 – 3.53 (m, 2H), 3.49 (q, *J* = 7.0 Hz, 2H), 3.06 (s, 3H), 1.18 (t, *J* = 7.0 Hz, 3H); ^{13}C NMR (101 MHz, $CDCl_3$) δ 70.8, 70.7, 70.6, 69.9, 69.5, 69.1, 66.7, 37.8, 15.3; MS-ES$^+$ *m/z*: 278.4 $[M+Na]^+$, 256.9 $[M+H]^+$; HRMS-ES$^+$ (*m/z*): $[M+H]^+$ calculated for $C_9H_{21}O_6S$, 257.1059; found, 257.1064.

APD(PEG2Me)$_2$

This reaction was conducted using the general procedure for the synthesis of APD di-ethers. The following reagents were used in the stated quantities: Step 1) sodium sulphate (4580 mg, 32.2 mmol, 5 eq.), (±)-3-amino-1,2-propanediol (0.5 ml, 6.4 mmol, 1 eq.), benzaldehyde (0.65 ml, 6.4 mmol, 1 eq.) DCM (20 ml) and MeOH (2 ml); Step 2) NaH (774 mg, 32.2 mmol, 5 eq.), **Ms-PEG2-Me** (3835 mg, 19.3 mmol, 3 eq.) and THF (80 ml); Step 3) conc. HCl (25 ml), water (25 ml) and EtOH (50 ml). **APD(PEG2Me)$_2$** was obtained as a yellow oil (710 mg, 38%), ^{1}H NMR (400 MHz, $CDCl_3$) δ 3.83 – 3.66 (m, 2H), 3.66 – 3.58 (m, 10H), 3.56 – 3.43 (m, 7H), 3.39 – 3.32 (m, 6H), 2.89 – 2.68 (m, 2H), 2.00 (bs, 2H); ^{13}C NMR (101 MHz, $CDCl_3$) δ 80.5, 72.08, 72.06, 71.9, 70.96, 70.95, 70.72, 70.68, 70.6, 69.6, 59.2, 43.4; MS-ES$^+$ *m/z*: 296.6 $[M+H]^+$; HRMS-ES$^+$ (*m/z*): $[M+H]^+$ calculated for $C_{13}H_{30}NO_6$, 296.2073; found, 296.2057.

APD(PEG2Et)$_2$

This reaction was conducted using the general procedure for the synthesis of APD di-ethers. The following reagents were used in the stated quantities: Step 1) sodium sulphate (7785 mg, 55 mmol, 5 eq.), (±)-3-amino-1,2-propanediol (0.85 ml, 11 mmol, 1 eq.), benzaldehyde (1.11 ml, 11 mmol, 1 eq.) DCM (35 ml) and MeOH (3.5 ml); Step 2) NaH (1315 mg, 55 mmol, 5 eq.), **Ms-PEG2-Et** (6980 mg, 33 mmol, 3 eq.) and THF (140 ml); Step 3) conc. HCl (40 ml), water (40 ml) and EtOH (80 ml). **APD(PEG2Et)$_2$** was obtained as a yellow oil (1410 mg, 40%), ^{1}H NMR (400 MHz, $CDCl_3$) δ 3.84 – 3.67 (m, 2H), 3.67 – 3.60 (m, 10H), 3.60 – 3.42 (m, 11H), 2.89 – 2.69 (m, 2H), 1.81 (bs, 2H), 1.23 – 1.16 (m, 6H); ^{13}C NMR (101 MHz, $CDCl_3$) δ 80.7, 72.0, 71.0, 70.9, 70.81, 70.76, 70.02, 70.00, 69.7, 66.8, 43.6, 15.3; MS-ES$^+$ *m/z*: 324.8 $[M+H]^+$; HRMS-ES$^+$ (*m/z*): $[M+H]^+$ calculated for $C_{15}H_{34}NO_6$, 324.23806; found, 324.23784.

APD(PEG3Me)$_2$

This reaction was conducted using the general procedure for the synthesis of APD di-ethers. The following reagents were used in the stated quantities: Step 1) sodium sulphate (6411 mg, 45.1 mmol, 5 eq.), (±)-3-amino-1,2-propanediol (0.70 ml, 9.0 mmol, 1 eq.), benzaldehyde (0.92 ml, 9.1 mmol, 1 eq.) DCM (30 ml) and MeOH (3 ml); Step 2) NaH (1083 mg, 45.1 mmol, 5 eq.), **Ms-PEG3-Me** (6562 mg, 27.1 mmol, 3 eq.) and THF (120 ml); Step 3) conc. HCl (10 ml), water (10 ml) and EtOH (25 ml). **APD(PEG3Me)$_2$** was obtained as a yellow oil (902 mg, 26%), ^{1}H NMR (400 MHz, $CDCl_3$) δ 3.85 – 3.67 (m, 2H), 3.67 – 3.59 (m, 18H), 3.57 – 3.43 (m, 7H), 3.41 – 3.34 (m, 6H), 2.89 – 2.67 (m, 2H), 1.57 (bs, 2H); ^{13}C NMR (101 MHz, $CDCl_3$) δ 80.8, 72.1, 72.0, 71.03, 71.01, 70.83, 70.82, 70.80, 70.76, 70.7, 69.8, 59.2, 43.6; MS-ES$^+$ *m/z*: 384.1 $[M+H]^+$; HRMS-ES$^+$ (*m/z*): $[M+H]^+$ calculated for $C_{17}H_{38}NO_8$, 384.2597; found, 384.2585.

APD(PEG3Et)$_2$

This reaction was conducted using the general procedure for the synthesis of APD di-ethers. The following reagents were used in the stated quantities: Step 1) sodium sulphate (6411 mg, 45.1 mmol, 5 eq.), (±)-3-amino-1,2-propanediol (0.70 ml, 9.0 mmol, 1 eq.), benzaldehyde (0.92 ml, 9.1 mmol, 1 eq.) DCM (30 ml) and MeOH (3 ml); Step 2) NaH (1083 mg, 45.1 mmol, 5 eq.), **Ms-PEG3-Et** (6942 mg, 27.1 mmol, 3 eq.) and THF (120 ml); Step 3) conc. HCl (10 ml), water (10 ml) and EtOH (25 ml). **APD(PEG3Et)$_2$** was obtained as a yellow oil (833 mg, 22%), ^{1}H NMR (400 MHz, $CDCl_3$) δ 3.83 – 3.68 (m, 2H), 3.68 – 3.60 (m, 18H), 3.60 – 3.43 (m, 11H), 2.88 – 2.69 (m, 2H), 1.67 (bs, 2H), 1.37 (s, 2H), 1.20 (t, *J* = 7.0 Hz, 6H); ^{13}C NMR (101 MHz, $CDCl_3$) δ 80.8, 72.0, 71.0, 70.9, 70.8, 70.7, 70.0, 69.7, 66.8, 43.6, 15.3; MS-ES$^+$ *m/z*: 412.1 $[M+H]^+$; HRMS-ES$^+$ (*m/z*): $[M+H]^+$ calculated for $C_{19}H_{42}NO_8$, 412.2910; found, 412.2895.

PyrM-PEG4-CH$_2$CO[APD(PEG2Me)$_2$]

This reaction was conducted using the general procedure for amide coupling reactions. The following reagents were used in the stated quantities: **PyrM-PEG4-CH$_2$COOH** (400 mg, 0.86 mmol, 1 eq.), DIPEA (0.30 ml, 1.72 mmol, 2 eq.), TBTU (275 mg, 0.86 mmol, 1 eq.), **APD(PEG2Me)$_2$** (253 mg, 0.86 mmol, 1 eq.) and DCM (20 ml). This reaction was stirred at RT for 17 h. The crude material was purified using a Biotage Isolera One purification system (reversed phase with C18 silica, 9:1 H_2O/MeOH - MeOH) to yield **PyrM-PEG4-CH$_2$CO[APD(PEG2Me)$_2$]** as a yellow oil (376 mg, 59%), ^{1}H NMR (400 MHz, $CDCl_3$) δ 8.41 (d, *J* = 9.3 Hz, 1H), 8.24 – 8.17 (m, 2H), 8.17 – 8.12 (m, 2H), 8.09 – 7.97 (m, 4H), 7.11 (bs, 1H), 5.29 (s, 2H), 3.97 (d, *J* = 2.1 Hz, 2H), 3.81 – 3.74 (m, 3H), 3.74 – 3.56 (m, 27H), 3.56 – 3.48 (m, 6H), 3.37 (s, 3H), 3.36 (s, 3H), 3.35 – 3.28 (m, 1H); ^{13}C NMR (101 MHz, $CDCl_3$) δ 170.1, 131.6, 131.5, 131.4, 131.0, 129.6, 127.9, 127.6, 127.3, 126.2, 125.4, 125.1, 124.9, 124.7, 123.8, 77.8, 72.13, 72.11, 72.06, 72.0, 71.08, 71.06, 71.0, 70.94, 70.86, 70.81, 70.80, 70.77, 70.74, 70.72, 70.6, 70.5, 69.7, 69.6, 59.2, 59.2, 40.1; MS-ES$^+$ *m/z*: 765.8 $[M+Na]^+$ 394.6 $[M+2Na]^{2+}$; HRMS-ES$^+$ (*m/z*): $[M+H]^+$ calculated for $C_{40}H_{58}NO_{12}$, 744.3959; found, 744.3957.

PyrM-PEG4-CH$_2$CO[APD(PEG2Et)$_2$]

This reaction was conducted using the general procedure for amide coupling reactions. The following reagents were used in the stated quantities: **PyrM-PEG4-CH$_2$COOH** (442 mg, 0.95 mmol, 1 eq.), DIPEA (0.33 ml, 1.89 mmol, 2 eq.), TBTU (304 mg, 0.95 mmol, 1 eq.), **APD(PEG2Et)$_2$** (306 mg, 0.95 mmol, 1 eq.) and DCM (20 ml). This reaction was stirred at RT for 17 h. The crude material was purified using a Biotage Isolera One purification system

(reversed phase with C18 silica, 9:1 H_2O/MeOH - MeOH) to yield **PyrM-PEG4-CH_2CO[APD(PEG2Et)$_2$]** as a yellow oil (441 mg, 60%), ^{1}H NMR (400 MHz, $CDCl_3$) δ 8.39 (d, *J* = 9.2 Hz, 1H), 8.22 – 8.16 (m, 2H), 8.16 – 8.11 (m, 2H), 8.08 – 7.97 (m, 4H), 7.10 (t, *J* = 5.9 Hz, 1H), 5.28 (s, 2H), 3.96 (d, *J* = 1.8 Hz, 2H), 3.80 – 3.73 (m, 3H), 3.73 – 3.54 (m, 31H), 3.54 – 3.46 (m, 6H), 3.32 (dt, *J* = 13.8, 5.9 Hz, 1H), 1.38 – 1.01 (m, 6H); ^{13}C NMR (101 MHz, $CDCl_3$) δ 170.1, 131.6, 131.43, 131.38, 131.0, 129.5, 127.8, 127.6, 127.2, 126.1, 125.4, 125.1, 124.9, 124.6, 123.7, 77.7, 71.99, 71.97, 71.04, 71.01, 70.92, 70.89, 70.81, 70.76, 70.73, 70.67, 70.4, 69.96, 69.95, 69.7, 69.6, 66.8, 40.1, 15.3; MS-ES$^+$ *m/z*: 795.0 $[M+Na]^+$, 771.7 $[M+H]^+$, 408.5 $[M+2Na]^{2+}$; HRMS-ES$^+$ (*m/z*): $[M+H]^+$ calculated for $C_{42}H_{62}NO_{12}$, 772.4272; found, 772.4271.

PyrM-PEG6-CH_2CO[APD(PEG2Me)$_2$]

This reaction was conducted using the general procedure for amide coupling reactions. The following reagents were used in the stated quantities: **PyrM-PEG6-CH_2COOH** (400 mg, 0.72 mmol, 1 eq.), DIPEA (0.25 ml, 1.44 mmol, 2 eq.), TBTU (232 mg, 0.72 mmol, 1 eq.), **APD(PEG2Me)$_2$** (213 mg, 0.72 mmol, 1 eq.) and DCM (20 ml). This reaction was stirred at RT for 72 h. The crude material was purified using a Biotage Isolera One purification system (reversed phase with C18 silica, 9:1 H_2O/MeOH - MeOH) to yield **PyrM-PEG6-CH_2CO[APD(PEG2Me)$_2$]** as a yellow oil (379 mg, 63%), ^{1}H NMR (400 MHz, $CDCl_3$) δ 8.41 (d, *J* = 9.2 Hz, 1H), 8.23 – 8.17 (m, 2H), 8.17 – 8.10 (m, 2H), 8.08 – 7.98 (m, 4H), 7.10 (t, *J* = 5.7 Hz, 1H), 5.29 (s, 2H), 3.99 (d, *J* = 1.8 Hz, 2H), 3.82 – 3.75 (m, 3H), 3.74 – 3.49 (m, 41H), 3.37 (s, 3H), 3.36 (s, 3H), 3.36 – 3.28 (m, 1H); ^{13}C NMR (101 MHz, $CDCl_3$) δ 170.1, 131.6, 131.5, 131.4, 131.0, 129.6, 127.9, 127.60, 127.59, 127.3, 126.1, 125.4, 125.1, 124.9, 124.7, 123.8, 77.8, 72.13, 72.05, 72.0, 71.1, 71.0, 70.94, 70.85, 70.80, 70.77, 70.74, 70.72, 70.6, 70.5, 69.7, 69.6, 59.21, 59.20, 40.1; MS-ES$^+$ *m/z*: 854.1 $[M+Na]^+$, 438.6 $[M+2Na]^{2+}$, 215.0 $[PyrM]^+$; HRMS-ES$^+$ (*m/z*): $[M+H]^+$ calculated for $C_{44}H_{66}NO_{14}$, 832.4483; found, 832.4481.

PyrM-PEG6-CH_2CO[APD(PEG2Et)$_2$]

This reaction was conducted using the general procedure for amide coupling reactions. The following reagents were used in the stated quantities: **PyrM-PEG6-CH_2COOH** (647 mg, 1.17 mmol, 1 eq.), DIPEA (0.41 ml, 2.35 mmol, 2 eq.), TBTU (375 mg, 1.17 mmol, 1 eq.), **APD(PEG2Et)$_2$** (377 mg, 1.17 mmol, 1 eq.) and DCM (25 ml). This reaction was stirred at RT for 72 h. The crude material was purified using a Biotage Isolera One purification system (reversed phase with C18 silica, 9:1 H_2O/MeOH - MeOH) to yield **PyrM-PEG6-CH_2CO[APD(PEG2Et)$_2$]** as a yellow oil (586 mg, 58%), ^{1}H NMR (400 MHz,

$CDCl_3$) δ 8.41 (d, *J* = 9.2 Hz, 1H), 8.23 – 8.17 (m, 2H), 8.17 – 8.12 (m, 2H), 8.09 – 7.99 (m, 4H), 7.12 (t, *J* = 5.9 Hz, 1H), 5.29 (s, 2H), 3.99 (d, *J* = 1.8 Hz, 2H), 3.81 – 3.75 (m, 3H), 3.74 – 3.69 (m, 3H), 3.69 – 3.47 (m, 42H), 3.33 (dt, *J* = 13.7, 5.9 Hz, 1H), 1.24 – 1.17 (m, 6H); ^{13}C NMR (101 MHz, $CDCl_3$) δ 170.2, 131.6, 131.5, 131.4, 131.0, 129.6, 127.8, 127.59, 127.58, 127.3, 126.1, 125.4, 125.1, 124.9, 124.6, 123.7, 77.8, 72.02, 71.95, 71.1, 71.0, 70.94, 70.90, 70.81, 70.76, 70.73, 70.70, 70.68, 70.5, 69.97, 69.96, 69.7, 69.6, 66.8, 40.1, 15.3; MS-ES$^+$ *m/z*: 882.2 $[M+Na]^+$; HRMS-ES$^+$ (*m/z*): $[M+H]^+$ calculated for $C_{46}H_{70}NO_{14}$, 860.4796; found, 860.4787.

PyrM-PEG4-CH_2CO[APD(PEG3Me)$_2$]

This reaction was conducted using the general procedure for amide coupling reactions. The following reagents were used in the stated quantities: **PyrM-PEG4-CH_2COOH** (375 mg, 0.80 mmol, 1 eq.), DIPEA (0.28 ml, 1.61 mmol, 2 eq.), TBTU (258 mg, 0.80 mmol, 1 eq.), **APD(PEG3Me)$_2$** (308 mg, 0.80 mmol, 1 eq.) and DCM (20 ml). This reaction was stirred at RT for 72 h. The crude material was purified using a Biotage Isolera One purification system (reversed phase with C18 silica, 9:1 H_2O/MeOH - MeOH) to yield **PyrM-PEG4-CH_2CO[APD(PEG3Me)$_2$]** as a yellow oil (408 mg, 61%), ^{1}H NMR (400 MHz, $CDCl_3$) δ 8.40 (d, *J* = 9.2 Hz, 1H), 8.23 – 8.17 (m, 2H), 8.17 – 8.12 (m, 2H), 8.10 – 7.97 (m, 4H), 7.09 (t, *J* = 5.9 Hz, 1H), 5.28 (s, 2H), 3.96 (d, *J* = 2.1 Hz, 2H), 3.82 – 3.74 (m, 3H), 3.74 – 3.55 (m, 35H), 3.55 – 3.47 (m, 6H), 3.37 (s, 3H), 3.36 (s, 3H), 3.35 – 3.27 (m, 1H); ^{13}C NMR (101 MHz, $CDCl_3$) δ 170.1, 131.6, 131.5, 131.4, 131.0, 129.6, 127.8, 127.6, 127.2, 126.1, 125.4, 125.1, 124.9, 124.6, 123.7, 77.7, 72.1, 72.03, 72.01, 71.05, 71.04, 70.95, 70.92, 70.84, 70.78, 70.77, 70.75, 70.69, 70.5, 69.7, 69.6, 59.20, 59.19, 40.1; MS-ES$^+$ *m/z*: 855.1 $[M+Na]^+$, 833.1 $[M+H]^+$; HRMS-ES$^+$ (*m/z*): $[M+H]^+$ calculated for $C_{44}H_{66}NO_{14}$, 832.4483; found, 832.4486.

PyrM-PEG4-CH_2CO[APD(PEG3Et)$_2$]

This reaction was conducted using the general procedure for amide coupling reactions. The following reagents were used in the stated quantities: **PyrM-PEG4-CH_2COOH** (305 mg, 0.65 mmol, 1 eq.), DIPEA (0.23 ml, 1.32 mmol, 2 eq.), TBTU (210 mg, 0.65 mmol, 1 eq.), **APD(PEG3Et)$_2$** (269 mg, 0.65 mmol, 1 eq.) and DCM (15 ml). This reaction was stirred at RT for 72 h. The crude material was purified using a Biotage Isolera One purification system (reversed phase with C18 silica, 9:1 H_2O/MeOH - MeOH) to yield **PyrM-PEG4-CH_2CO[APD(PEG3Et)$_2$]** as a yellow oil (275 mg, 49%), ^{1}H NMR (400 MHz, $CDCl_3$) δ 8.40 (d, *J* = 9.2 Hz, 1H), 8.23 – 8.17 (m, 2H), 8.17 – 8.11 (m, 2H), 8.10 – 7.98 (m, 4H), 7.09 (t, *J* = 5.9 Hz, 1H), 5.28 (s, 2H), 3.96 (d, *J* = 2.1 Hz, 2H), 3.82 – 3.74 (m, 3H), 3.74 – 3.54 (m, 39H), 3.54 – 3.44 (m, 6H), 3.32 (dt, *J* = 13.8, 5.9 Hz, 1H), 1.24 – 1.16 (m, 6H); ^{13}C NMR

(101 MHz, $CDCl_3$) δ 170.1, 131.6, 131.5, 131.4, 131.0, 129.6, 127.8, 127.6, 127.2, 126.1, 125.4, 125.1, 124.9, 124.6, 123.7, 77.7, 72.03, 72.01, 71.01 71.0, 70.94, 70.92, 70.84, 70.75, 70.7, 70.5, 70.0, 69.7, 69.6, 66.8, 40.1, 15.4; MS-ES$^+$ *m/z*: 883.1 $[M+Na]^+$, 859.6 $[M+H]^+$, 452.6 $[M+2Na]^{2+}$; HRMS-ES$^+$ (*m/z*): $[M+H]^+$ calculated for $C_{46}H_{70}NO_{14}$, 860.4796; found, 860.4782.

PyrM-PEG6-CH_2CO[APD(PEG3Me)$_2$]

This reaction was conducted using the general procedure for amide coupling reactions. The following reagents were used in the stated quantities: **PyrM-PEG6-CH_2COOH** (448 mg, 0.81 mmol, 1 eq.), DIPEA (0.28 ml, 1.61 mmol, 2 eq.), TBTU (259 mg, 0.81 mmol, 1 eq.), **APD(PEG3Me)$_2$** (310 mg, 0.81 mmol, 1 eq.) and DCM (20 ml). This reaction was stirred at RT for 72 h. The crude material was purified using a Biotage Isolera One purification system (reversed phase with C18 silica, 9:1 H_2O/MeOH - MeOH) to yield **PyrM-PEG6-CH_2CO[APD(PEG3Me)$_2$]** as a yellow oil (573 mg, 77%), ^{1}H NMR (400 MHz, $CDCl_3$) δ 8.40 (d, *J* = 9.2 Hz, 1H), 8.22 – 8.16 (m, 2H), 8.16 – 8.10 (m, 2H), 8.07 – 7.97 (m, 4H), 7.10 (t, *J* = 6.0 Hz, 1H), 5.28 (s, 2H), 3.98 (d, *J* = 1.9 Hz, 2H), 3.80 – 3.73 (m, 3H), 3.73 – 3.56 (m, 43H), 3.56 – 3.48 (m, 6H), 3.37 (s, 3H), 3.36 (s, 3H), 3.35 – 3.28 (m, 1H); ^{13}C NMR (101 MHz, $CDCl_3$) δ 170.1, 131.6, 131.41, 131.37, 131.0, 129.5, 127.8, 127.6, 127.5, 127.2, 126.1, 125.3, 125.1, 124.9, 124.6, 123.7, 77.7, 72.1, 72.0, 71.0, 70.93, 70.90, 70.81, 70.76, 70.73, 70.70, 70.68, 70.67, 70.5, 69.7, 69.6, 59.2, 40.1; MS-ES$^+$ *m/z*: 943.2 $[M+Na]^+$, 920.1 $[M+H]^+$, 482.6 $[M+2Na]^{2+}$; HRMS-ES$^+$ (*m/z*): $[M+Na]^+$ calculated for $C_{48}H_{73}NO_{16}Na$, 942.4827; found, 942.4860.

PyrM-PEG6-CH_2CO[APD(PEG3Et)$_2$]

This reaction was conducted using the general procedure for amide coupling reactions. The following reagents were used in the stated quantities: **PyrM-PEG6-CH_2COOH** (350 mg, 0.63 mmol, 1 eq.), DIPEA (0.22 ml, 1.26 mmol, 2 eq.), TBTU (203 mg, 0.63 mmol, 1 eq.), **APD(PEG3Et)$_2$** (260 mg, 0.63 mmol, 1 eq.) and DCM (15 ml). This reaction was stirred at RT for 72 h. The crude material was purified using a Biotage Isolera One purification system (reversed phase with C18 silica, 9:1 H_2O/MeOH - MeOH) to yield **PyrM-PEG6-CH_2CO[APD(PEG3Et)$_2$]** as a yellow oil (338 mg, 57%), ^{1}H NMR (400 MHz, $CDCl_3$) δ 8.40 (d, *J* = 9.2 Hz, 1H), 8.23 – 8.17 (m, 2H), 8.17 – 8.11 (m, 2H), 8.09 – 7.97 (m, 4H), 7.10 (t, *J* = 5.9 Hz, 1H), 5.28 (s, 2H), 3.98 (d, *J* = 1.9 Hz, 2H), 3.80 – 3.74 (m, 3H), 3.74 – 3.55 (m, 47H), 3.55 – 3.47 (m, 6H), 3.32 (dt, *J* = 13.7, 5.9 Hz, 1H), 1.24 – 1.16 (m, 6H); ^{13}C NMR (101 MHz, $CDCl_3$) δ 170.1, 131.6, 131.44, 131.40, 131.0, 129.6, 127.8, 127.58, 127.56, 127.2, 126.1, 125.4, 125.1, 124.9, 124.6, 123.7, 77.7, 72.0, 71.1, 70.94, 70.92, 70.84, 70.78, 70.76,

70.73, 70.72, 70.71, 70.68, 70.5, 70.0, 69.7, 69.6, 66.8, 40.1, 15.4; MS-ES$^+$ *m/z*: 971.4 $[M+Na]^+$, 496.6 $[M+2Na]^{2+}$; HRMS-ES$^+$ (*m/z*): $[M+H]^+$ calculated for $C_{50}H_{78}NO_{16}$, 948.5321; found, 948.5336.

7.3: Analytical Procedures

Preparation of MWNT Dispersions

A solution of surfactant (3 ml, 1 mM in Millipore water or 0.6 M NaCl) was added to a 7 ml glass vial containing MWNTs (1 mg). The mixture was cooled over an ice-water bath and ultrasonicated using a Cole-Parmer 750-Watt ultrasonic homogeniser (1/8" tapered tip, 20% amplitude, 2 min with a 20 sec on/off pulse cycle), followed by sonication in a 13 L Bandelin Sonorex Digital Ultrasonic Bath (100% power) at RT for a further 2 min. 2 ml of the resulting dispersion was transferred to a 2 ml Eppendorf tube and centrifuged at 2500 *g* for 30 min (Hermle Z323). The supernatant dispersion was decanted and analysed.

Determination of MWNT Extinction Coefficient, ε

3 MWNT dispersions were prepared based on the above procedure, using 15 mg of MWNTs and 5 ml of 1 mM SDS in each case. Two 2 ml aliquots from each sample were subjected to our standard centrifugation conditions and the supernatants recombined to give *ca*. 3 ml of dispersion. Dilute dispersions for UV-visible spectroscopy were prepared by diluting aliquots with the parent SDS solution. Based on the method of Liu *et al.*[94] a further 1.7 ml was transferred to a 50 ml centrifuge tube and treated with 25 ml acetone to induce precipitation. The suspension was then centrifuged at 7000 *g* for 30 min (Hermle Z323) and the supernatant decanted. Acetone treatment (25 ml), centrifugation (7000 *g*, 30 min) and decanting of the supernatant was repeated twice. The residue was then suspended in the minimum amount of acetone and transferred to a pre-weighed vial. The solvent was removed by gentle heating on a hot plate and the residue further dried by heating overnight in an oven at *ca.* 70 °C. The mass of the dried sample was then used to determine the concentration of the dispersion. This allowed the concentration of serially diluted dispersions which were analysed using UV-visible spectroscopy to be calculated and used to calculate the extinction coefficient, ε.

Graphite Exfoliation

A solution of surfactant (3 ml, 1 mM in Millipore water or 0.6 M NaCl) was added to a 7 ml glass vial containing graphite (15 mg). The mixture was cooled over an ice-water bath and

ultrasonicated using a Cole-Parmer 750-Watt ultrasonic homogeniser (1/8" tapered tip, 20% amplitude, 15 min). 2 ml of the resulting dispersion was transferred to a 2 ml Eppendorf tube and centrifuged at 1280 *g* for 30 min (Hermle Z323). The supernatant dispersion was decanted and analysed.

UV-visible Spectroscopic Analysis of MWNT and EG Dispersions

A sample of dispersion was diluted 10-fold using the parent surfactant solution and its absorbance measured using a Thermo Evolution 220 UV-visible spectrometer fitted with an integrating sphere (ISA220), using the parent surfactant solution as a baseline. Typically, 3 samples were prepared and the mean absorbance at 500 nm (MWNTs) or 660 nm (EG) was used to calculate C_{MWNT} or C_{EG}, respectively, using the Beer-Lambert law.

TEM Imaging

Samples were prepared by dropping *ca.* 20 μL of MWNT dispersion onto a holey-carbon TEM grid (agar scientific) which was dried in air overnight. Images were obtained using a JEOL 2100F FEG TEM.

Temperature Response Tests on MWNT and EG Dispersions

Either: i) Aliquots (2-3 ml) of 0.1 mM surfactant solution and 10-fold diluted MWNT or EG dispersion (each in Millipore water or 0.6 M NaCl, dilutions made using this solvent) were transferred to a 10 mm path length cuvette; or ii) Aliquots (350 μl) of 1 mM surfactant solution and undiluted MWNT or EG dispersion were transferred to a 1 mm path length cuvette. Using a Thermo Evolution 220 UV-visible spectrometer fitted with a Smart Peltier 8-Cell Changer, the absorbance of each sample was measured at increasing temperatures, equilibrating for 5 min at each interval. In some cases the samples were held at a high temperature overnight and their absorbance measured after this time. The samples were then cooled to RT and their absorbance measured.

LCST Determination

Method A) Visual Inspection

Millipore water (5 ml) was added to surfactant (10 mg) which was allowed to dissolve fully. The solution was held in a water bath and warmed slowly from room temperature until clouding was observed. The water bath temperature at this point was used as an approximate LCST.

Method B) Turbidimietry

Surfactant solution (2.5 ml, 0.53-1.56 mM) was transferred to a 10 mm path length cuvette. Using a Thermo Evolution 220 UV-visible spectrometer fitted with a Smart Peltier 8-Cell Changer, the transmittance of each sample was measured at increasing temperatures, equilibrating for 2 min at each interval.

Method C) Dynamic Light Scattering

Surfactant solution (1 ml, 1 mM) in Millipore water was transferred to a glass cuvette and analysed by DLS (Malvern instruments, Zetasizer Nano ZS). Temperature was incremented, initially, in 5 °C steps to approximate the LCST, then a narrow range around this temperature was investigated using 1 °C steps. Equilibration time at each temperature was 2 min. All measurements were back scattered using a wavelength of light which was auto-optimised by the equipment. Initial data analysis was conducted using Spraytec analysis software (Malvern).

Appendix 1: Summary of Surfactant Structures

This Appendix is intended to be used as a reference in Chapters 3, 5 and 6. A separate copy is provided with the printed thesis. It includes the structures of the surfactants used to prepare MWNT and EG dispersions and for which LCST was measured. For ALH surfactants, the anchor group is coloured blue, the linker group green, and the head group red.

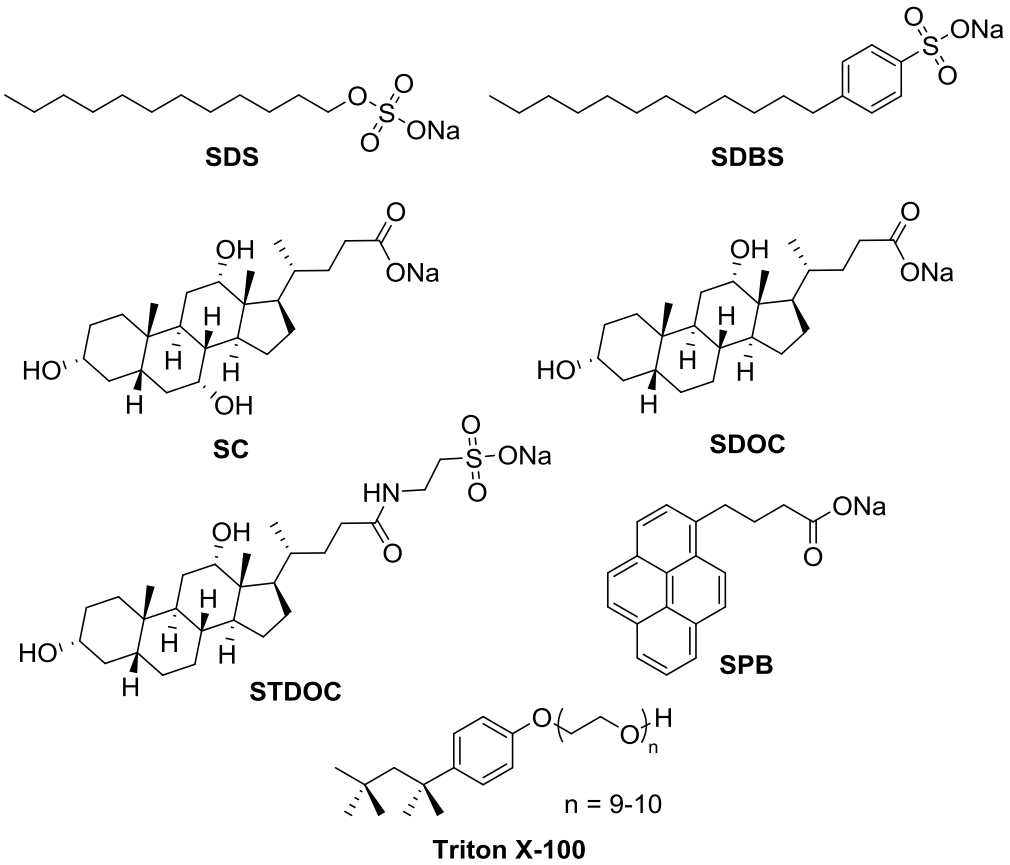

Figure A1: Structures of commercial surfactants and **SPB**, used for comparison in dispersion studies. **SC** and **SPB** were used in MWNT dispersion studies only. **STDOC** was used in graphite exfoliation studies only.

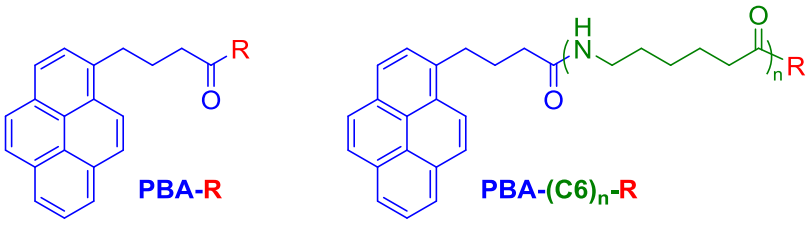

Linker-Free

Surfactant	R
PBA-G1(ONa)$_3$	G1(ONa)$_3$
PBA-H1(ONa)$_3$	H1(ONa)$_3$
PBA-G2(ONa)$_9$	G2(ONa)$_9$

Amide Linker

Surfactant	n	R
PBA-C6-G1(ONa)$_3$	1	G1(ONa)$_3$
PBA-C6-G2(ONa)$_9$	1	G2(ONa)$_9$
PBA-(C6)$_2$-G1(ONa)$_3$	2	G1(ONa)$_3$
PBA-(C6)$_2$-G2(ONa)$_9$	2	G2(ONa)$_9$

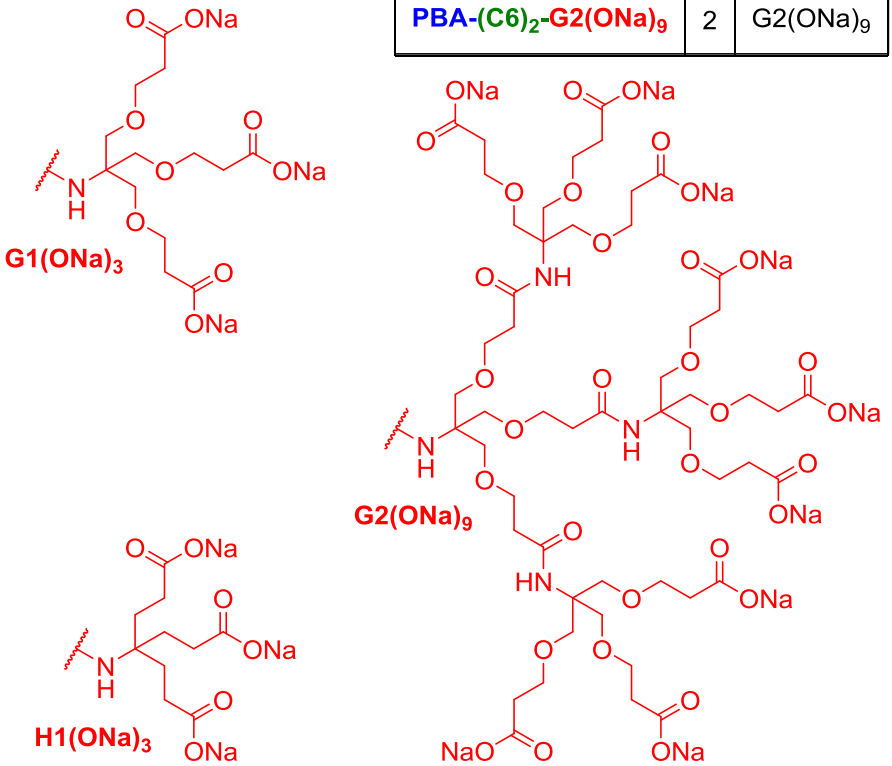

Figure A2: Summary of the structures of linker-free and amide linker surfactants synthesised by Dr Daniel Welsh which were compared to the ether linker surfactants in dispersion studies. All materials were used in MWNT dispersion studies. Only **PBA-G1(ONa)$_3$**, **PBA-C6-G1(ONa)$_3$** and **PBA-(C6)$_2$-G1(ONa)$_3$** were used in graphite exfoliation studies.

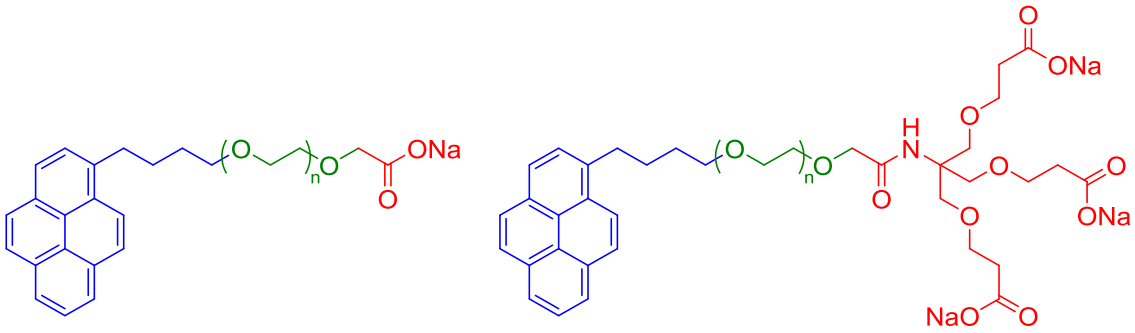

Figure A3: Structures of the anionic ether linker surfactants used in dispersion studies. All materials were used in MWNT dispersion studies. Only **PyrB-PEG6-CH_2COG1$(ONa)_3$** was used in graphite exfoliation studies.

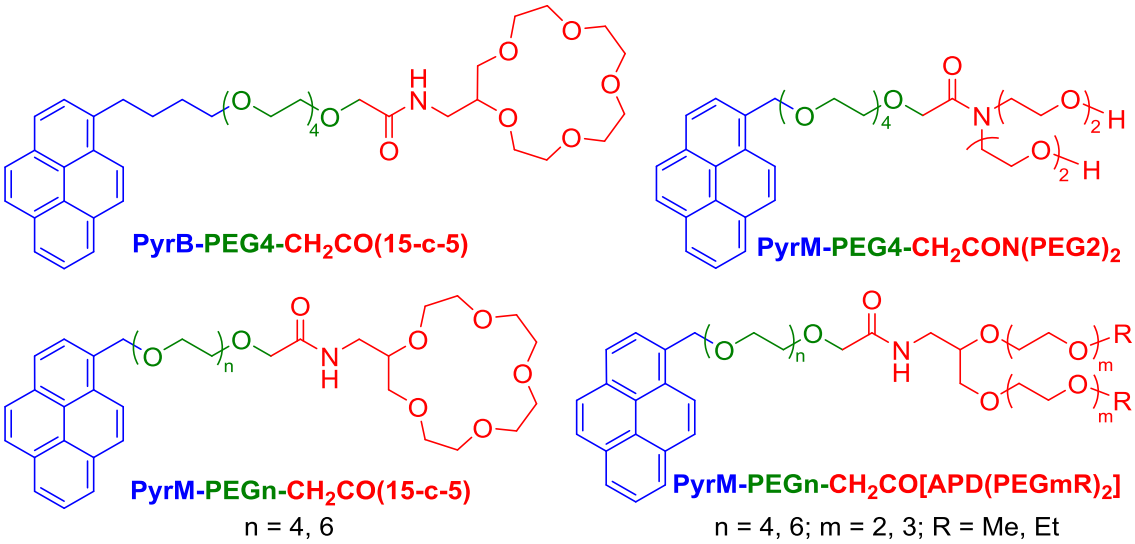

Figure A4: Structures of the non-ionic ether-linker surfactants used in the LCST studies. **PyrB-PEG4-CH_2CO(15-c-5)** and **PyrM-PEG4-CH_2CO[APD(PEG2Et)$_2$]** were used in MWNT dispersion studies. **PyrB-PEG4-CH_2CO(15-c-5)**, **PyrM-PEG4-CH_2CO(15-c-5)**, **PyrM-PEG4-CH_2CO[APD(PEG2Me)$_2$]**, **PyrM-PEG4-CH_2CO[APD(PEG2Et)$_2$]**, **PyrM-PEG6-CH_2CO[APD(PEG2Me)$_2$]** and **PyrM-PEG6-CH_2CO[APD(PEG2Et)$_2$]** were used in graphite exfoliation studies.

Appendix 2: Calculation of HLB Values for Non-Ionic Surfactants

To calculate HLB values by Davies' method[222] the following equation can be used:

$$\text{HLB} = mH_H - nH_L + 7$$

Where m is the number of (identical) hydrophilic groups in the molecule, H_H is the nominal HLB value of the hydrophilic groups, n is the number of (identical) hydrophobic (i.e. lipophilic) groups in the molecule and H_L is their nominal HLB value. The addition of 7 serves to bring values calculated using this method in line with those calculated using the Griffin method.[220,221]

To facilitate analysis of the effect of different anchor, linker and head groups on the HLB of our surfactants we have used an alternative calculation derived from Davies' method. We have calculated nominal HLB values for each of the different anchor, linker and head groups used in the crown ether and podand surfactants based on available data, assigning negative values to any hydrophobic portions of each group. By selecting the appropriate anchor, linker and head values the HLB of a surfactant is given by adding the nominal HLB values of each component to 7, i.e:

$$\text{HLB} = H_{Anchor} + H_{Linker} + H_{Head} + 7$$

The HLB contributions used to calculate the nominal HLB values and the assumptions made for functional groups not listed in available tables are summarised in Table A1, and the nominal HLB values calculated for various anchor, linker and head groups are shown in Table A2. For this purpose, the anchor is defined as the aromatic moiety and any alkyl substituent prior to the first ether oxygen. The linker is considered to include the first ether oxygen and all PEG repeat units between this and the first subsequent non-ethylene glycol moiety (usually a methylene unit between the last ethylene glycol oxygen and a carbonyl group). The head group is defined such that it includes the remainder of the molecule beyond the last linker PEG repeat unit (including any PEG repeat units in the head group). This usually includes the part of the surfactant derived from an amine and that derived from bromoacetic acid. Note that although the head group is hydrophilic, some moieties within it may be hydrophobic. These definitions are illustrated in Figure A5.

As an example, the surfactant **PyrM-PEG4-CH_2CO[APD(PEG2Me)$_2$]** is split into a PyrM anchor, PEG4 linker and CH_2CO[APD(PEG2Me)$_2$] head group. The PyrM anchor consists of 16 unsaturated or quaternary carbon atoms and one CH_2 moiety (each -0.475), totalling -8.075. A PEG4 linker includes the first ether oxygen (+1.3) and 4 ethylene oxide moieties (each

+0.33), totalling +2.62. The $CH_2CO[APD(PEG2Me)_2]$ head group includes a CH_2 moiety (-0.475), a secondary amide (+9.6), the remainder of an APD moiety (contributing -0.15 for the unit resembling propylene glycol and +1.3 for the additional ether oxygen), 4 ethylene oxide moieties (2 per PEG2 arm, each +0.33) and two methyl groups (each -0.475), totalling +10.645. This considers the moieties within the linker and head groups in the same way used when counting the total number of PEG units in a surfactant (see Figure 5.06). The HLB for **PyrM-PEG4-$CH_2CO[APD(PEG2Me)_2]$** is therefore given by:

$$\mathrm{HLB} = -8.075 + 2.62 + 10.645 + 7 = 12.19$$

Table A2: HLB contributions for functional groups taken from available tables[223] and assumed contributions for functional groups not listed in available tables.

Hydrophobic Moieties		
Group	**Reported HLB Contribution**	**Value Used**
Unsaturated carbon -CH=	0.475	-0.475
Alkyl -CH_2-	0.475	-0.475
Alkyl -CH_3	0.475	-0.475
Hydrophilic Moieties		
Group	**Reported HLB Contribution**	**Value Used**
PEG repeat unit -CH_2CH_2O-	0.33	0.33
Hydroxy-terminated PEG repeat unit -CH_2CH_2OH	0.95	0.95
Other Ether -O-	1.3	1.3
COONa	19.1	19.1
Unlisted Moieties		
Group	**Assumption Used**	**Value Used**
Quaternary carbon (aromatic or aliphatic)	Same contribution as all other carbons	-0.475
Secondary Amide -CONH-	Same contribution as primary amide	9.6
Tertiary Amide -CONH-	Same contribution as primary amide	9.6
APD-derived -CH_2CHCH_2- | O-	Same contribution as propylene glycol repeat unit -CH_2CHCH_2- | O-	-0.15

Table A2: Nominal HLB values for selected components of non-ionic surfactants discussed in Chapter 5.

Anchor	**Nominal HLB Value** (H_{Anchor})	**Linker**	**Nominal HLB Value** (H_{Linker})	**Head**	**Nominal HLB Value** (H_{Head})
PyrM	-8.075	**PEG2**	1.96	**CH_2CO(15-c-5)**	10.325
PyrB	-9.5	**PEG4**	2.62	**$CH_2CO[APD(PEG2Me)_2]$**	10.645
		PEG6	3.28	**$CH_2CO[APD(PEG2Et)_2]$**	9.695
		PEG12	5.26	**$CH_2CO[APD(PEG2^nBu)_2]$**	7.795
				$CH_2CO[APD(PEG3Me)_2]$	11.305
				$CH_2CO[APD(PEG3Et)_2]$	10.355
				$CH_2CO[APD(PEG3^nBu)_2]$	8.455
				$CH_2CON(PEG2)_2$	11.685

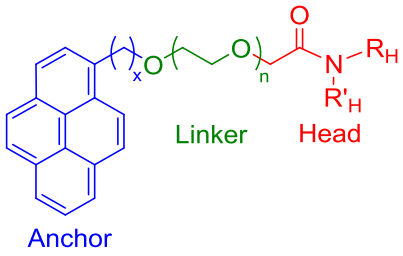

Figure A5: The means by which the anchor, linker and head groups are defined for the purpose of HLB calculations. For head groups derived from **APD** (including (15-c-5)) R_H represents the remainder of the crown or podand head group and R'_H = H. For **PyrM-PEG4-CH$_2$CON(PEG2)$_2$** R_H = R'_H = PEG2.

List of References

(1) Kroto, H. W.; Heath, J. R.; O'Brien, S. C.; Curl, R. F.; Smalley, R. E. *Nature* **1985**, *318*, 162.
(2) Iijima, S. *Nature* **1991**, *354*, 56.
(3) Iijima, S.; Ichihashi, T. *Nature* **1993**, *363*, 603.
(4) Bethune, D. S.; Klang, C. H.; de Vries, M. S.; Gorman, G.; Savoy, R.; Vazquez, J.; Beyers, R. *Nature* **1993**, *363*, 605.
(5) Novoselov, K. S.; Geim, A. K.; Morozov, S. V.; Jiang, D.; Zhang, Y.; Dubonos, S. V.; Grigorieva, I. V.; Firsov, A. A. *Science* **2004**, *306*, 666.
(6) Delgado, J. L.; Herranz, M. A.; Martin, N. *J. Mater. Chem.* **2008**, *18*, 1417.
(7) Ugarte, D. *Nature* **1992**, *359*, 707.
(8) Sano, N.; Wang, H.; Chhowalla, M.; Alexandrou, I.; Amaratunga, G. A. J. *Nature* **2001**, *414*, 506.
(9) Heath, J. R.; O'Brien, S. C.; Zhang, Q.; Liu, Y.; Curl, R. F.; Tittel, F. K.; Smalley, R. E. *J. Am. Chem. Soc.* **1985**, *107*, 7779.
(10) Popov, A. A.; Yang, S.; Dunsch, L. *Chem. Rev.* **2013**, *113*, 5989.
(11) Iijima, S.; Yudasaka, M.; Yamada, R.; Bandow, S.; Suenaga, K.; Kokai, F.; Takahashi, K. *Chem. Phys. Lett.* **1999**, *309*, 165.
(12) Hirsch, A. *Nat. Mater.* **2010**, *9*, 868.
(13) Schnorr, J. M.; Swager, T. M. *Chem. Mater.* **2011**, *23*, 646.
(14) Jia, X.; Campos-Delgado, J.; Terrones, M.; Meunier, V.; Dresselhaus, M. S. *Nanoscale* **2011**, *3*, 86.
(15) Monthioux, M.; Kuznetsov, V. L. *Carbon* **2006**, *44*, 1621.
(16) Saito, R.; Fujita, M.; Dresselhaus, G.; Dresselhaus, M. S. *Appl. Phys. Lett.* **1992**, *60*, 2204.
(17) Lu, X.; Chen, Z. *Chem. Rev.* **2005**, *105*, 3643.
(18) Wang, X.; Li, Q.; Xie, J.; Jin, Z.; Wang, J.; Li, Y.; Jiang, K.; Fan, S. *Nano Lett.* **2009**, *9*, 3137.
(19) Krupke, R.; Hennrich, F.; Löhneysen, H. v.; Kappes, M. M. *Science* **2003**, *301*, 344.
(20) Masheter, A. T.; Abiman, P.; Wildgoose, G. G.; Wong, E.; Xiao, L.; Rees, N. V.; Taylor, R.; Attard, G. A.; Baron, R.; Crossley, A.; Jones, J. H.; Compton, R. G. *J. Mater. Chem.* **2007**, *17*, 2616.
(21) He, C. N.; Zhao, N. Q.; Du, X. W.; Shi, C. S.; Li, J. J.; He, F. *Materials Science and Engineering: A* **2008**, *479*, 248.
(22) Benito, P.; Herrero, M.; Labajos, F. M.; Rives, V.; Royo, C.; Latorre, N.; Monzon, A. *Chem. Eng. J.* **2009**, *149*, 455.
(23) Collins, P. G.; Arnold, M. S.; Avouris, P. *Science* **2001**, *292*, 706.
(24) Coleman, J. N. *Adv. Funct. Mater.* **2009**, *19*, 3680.
(25) Hu, L.; Li, J.; Liu, J.; Grüner, G.; Marks, T. *Nanotechnology* **2010**, *21*, 155202.
(26) Park, S.; Vosguerichian, M.; Bao, Z. *Nanoscale* **2013**, *5*, 1727.
(27) Landi, B. J.; Ganter, M. J.; Cress, C. D.; DiLeo, R. A.; Raffaelle, R. P. *Energy & Environmental Science* **2009**, *2*, 638.
(28) Shulaker, M. M.; Hills, G.; Patil, N.; Wei, H.; Chen, H.-Y.; Wong, H. S. P.; Mitra, S. *Nature* **2013**, *501*, 526.
(29) Sun, H.; Xu, Z.; Gao, C. *Adv. Mater.* **2013**, *25*, 2554.
(30) Rutkin, A. Get an Olympic edge. *New Scientist* 15th Feb 2014 22.
(31) Poland, C. A.; Duffin, R.; Kinloch, I.; Maynard, A.; Wallace, W. A. H.; Seaton, A.; Stone, V.; Brown, S.; MacNee, W.; Donaldson, K. *Nat. Nanotechnol.* **2008**, *3*, 423.
(32) Ali-Boucetta, H.; Nunes, A.; Sainz, R.; Herrero, M. A.; Tian, B.; Prato, M.; Bianco, A.; Kostarelos, K. *Angew. Chem. Int. Ed.* **2013**, *52*, 2274.
(33) Liu, Y.; Zhao, Y.; Sun, B.; Chen, C. *Acc. Chem. Res.* **2012**, *46*, 702.
(34) Li, R.; Wang, X.; Ji, Z.; Sun, B.; Zhang, H.; Chang, C. H.; Lin, S.; Meng, H.; Liao, Y.-P.; Wang, M.; Li, Z.; Hwang, A. A.; Song, T.-B.; Xu, R.; Yang, Y.; Zink, J. I.; Nel, A. E.; Xia, T. *ACS Nano* **2013**, *7*, 2352.

(35) Petersen, E. J.; Zhang, L.; Mattison, N. T.; O'Carroll, D. M.; Whelton, A. J.; Uddin, N.; Nguyen, T.; Huang, Q.; Henry, T. B.; Holbrook, R. D.; Chen, K. L. *Environ. Sci. Technol.* **2011**, *45*, 9837.
(36) Rümmeli, M. H.; Ayala, P.; Pichler, T. In *Carbon Nanotubes and Related Structures*; Wiley-VCH Verlag GmbH & Co. KGaA: 2010, p 1.
(37) Nikolaev, P.; Bronikowski, M. J.; Bradley, R. K.; Rohmund, F.; Colbert, D. T.; Smith, K. A.; Smalley, R. E. *Chem. Phys. Lett.* **1999**, *313*, 91.
(38) Prasek, J.; Drbohlavova, J.; Chomoucka, J.; Hubalek, J.; Jasek, O.; Adam, V.; Kizek, R. *J. Mater. Chem.* **2011**, *21*, 15872.
(39) Cassell, A. M.; Raymakers, J. A.; Kong, J.; Dai, H. *J. Phys. Chem. B* **1999**, *103*, 6484.
(40) Dupuis, A.-C. *Prog. Mater Sci.* **2005**, *50*, 929.
(41) Journet, C.; Maser, W. K.; Bernier, P.; Loiseau, A.; de la Chapelle, M. L.; Lefrant, S.; Deniard, P.; Lee, R.; Fischer, J. E. *Nature* **1997**, *388*, 756.
(42) Thess, A.; Roland, L.; Nikolaev, P.; Dai, H.; Petit, P.; Robert, J.; Xu, C.; Lee, Y. H.; Seong Gon, K.; Rinzler, A. G.; Colbert, D. T.; Scuseria, G. E.; Tománek, D.; Fischer, J. E.; Smalley, R. E. *Science* **1996**, *273*, 483.
(43) McClure, J. W. *Physical Review* **1956**, *104*, 666.
(44) Dreyer, D. R.; Ruoff, R. S.; Bielawski, C. W. *Angew. Chem. Int. Ed.* **2010**, *49*, 9336.
(45) Edwards, R. S.; Coleman, K. S. *Nanoscale* **2013**, *5*, 38.
(46) Lotya, M.; Hernandez, Y.; King, P. J.; Smith, R. J.; Nicolosi, V.; Karlsson, L. S.; Blighe, F. M.; De, S.; Wang, Z.; McGovern, I. T.; Duesberg, G. S.; Coleman, J. N. *J. Am. Chem. Soc.* **2009**, *131*, 3611.
(47) Ciesielski, A.; Samori, P. *Chem. Soc. Rev.* **2014**, *43*, 381.
(48) Bianco, A.; Cheng, H.-M.; Enoki, T.; Gogotsi, Y.; Hurt, R. H.; Koratkar, N.; Kyotani, T.; Monthioux, M.; Park, C. R.; Tascon, J. M. D.; Zhang, J. *Carbon* **2013**, *65*, 1.
(49) Lee, C.; Wei, X.; Kysar, J. W.; Hone, J. *Science* **2008**, *321*, 385.
(50) Nair, R. R.; Blake, P.; Grigorenko, A. N.; Novoselov, K. S.; Booth, T. J.; Stauber, T.; Peres, N. M. R.; Geim, A. K. *Science* **2008**, *320*, 1308.
(51) Wang, X.; Zhi, L.; Mullen, K. *Nano Lett.* **2007**, *8*, 323.
(52) Ruoff, R. *Nat. Nano* **2008**, *3*, 10.
(53) Bianco, A. *Angew. Chem. Int. Ed.* **2013**, *52*, 4986.
(54) Seabra, A. B.; Paula, A. J.; de Lima, R.; Alves, O. L.; Durán, N. *Chem. Res. Toxicol.* **2014**, *27*, 159.
(55) Cai, M.; Thorpe, D.; Adamson, D. H.; Schniepp, H. C. *J. Mater. Chem.* **2012**, *22*, 24992.
(56) Jeon, I.-Y.; Choi, H.-J.; Jung, S.-M.; Seo, J.-M.; Kim, M.-J.; Dai, L.; Baek, J.-B. *J. Am. Chem. Soc.* **2013**, *135*, 1386.
(57) León, V.; Rodriguez, A. M.; Prieto, P.; Prato, M.; Vázquez, E. *ACS Nano* **2014**, *8*, 563.
(58) Wang, X.; Zhi, L.; Tsao, N.; Tomović, Ž.; Li, J.; Müllen, K. *Angew. Chem. Int. Ed.* **2008**, *47*, 2990.
(59) Pei, S.; Cheng, H.-M. *Carbon* **2012**, *50*, 3210.
(60) Hummers, W. S.; Offeman, R. E. *J. Am. Chem. Soc.* **1958**, *80*, 1339.
(61) Marcano, D. C.; Kosynkin, D. V.; Berlin, J. M.; Sinitskii, A.; Sun, Z.; Slesarev, A.; Alemany, L. B.; Lu, W.; Tour, J. M. *ACS Nano* **2010**, *4*, 4806.
(62) Mattevi, C.; Eda, G.; Agnoli, S.; Miller, S.; Mkhoyan, K. A.; Celik, O.; Mastrogiovanni, D.; Granozzi, G.; Garfunkel, E.; Chhowalla, M. *Adv. Funct. Mater.* **2009**, *19*, 2577.
(63) Fernández-Merino, M. J.; Paredes, J. I.; Villar-Rodil, S.; Guardia, L.; Solís-Fernández, P.; Salinas-Torres, D.; Cazorla-Amorós, D.; Morallón, E.; Martínez-Alonso, A.; Tascón, J. M. D. *Carbon* **2012**, *50*, 3184.
(64) Gómez-Navarro, C.; Meyer, J. C.; Sundaram, R. S.; Chuvilin, A.; Kurasch, S.; Burghard, M.; Kern, K.; Kaiser, U. *Nano Lett.* **2010**, *10*, 1144.
(65) Lotya, M.; King, P. J.; Khan, U.; De, S.; Coleman, J. N. *ACS Nano* **2010**, *4*, 3155.
(66) Premkumar, T.; Mezzenga, R.; Geckeler, K. E. *Small* **2012**, *8*, 1299.

(67) Davis, V. A.; Parra-Vasquez, A. N. G.; Green, M. J.; Rai, P. K.; Behabtu, N.; Prieto, V.; Booker, R. D.; Schmidt, J.; Kesselman, E.; Zhou, W.; Fan, H.; Adams, W. W.; Hauge, R. H.; Fischer, J. E.; Cohen, Y.; Talmon, Y.; Smalley, R. E.; Pasquali, M. *Nat. Nanotechnol.* **2009**, *4*, 830.
(68) Fujigaya, T.; Nakashima, N. In *Chemistry of Nanocarbons*; John Wiley & Sons, Ltd: 2010, p 301.
(69) Backes, C.; Mundloch, U.; Ebel, A.; Hauke, F.; Hirsch, A. *Chem. Eur. J.* **2010**, *16*, 3314.
(70) Yurekli, K.; Mitchell, C. A.; Krishnamoorti, R. *J. Am. Chem. Soc.* **2004**, *126*, 9902.
(71) Matarredona, O.; Rhoads, H.; Li, Z.; Harwell, J. H.; Balzano, L.; Resasco, D. E. *J. Phys. Chem. B* **2003**, *107*, 13357.
(72) Richard, C.; Balavoine, F.; Schultz, P.; Ebbesen, T. W.; Mioskowski, C. *Science* **2003**, *300*, 775.
(73) Backes, C.; Hauke, F.; Hirsch, A. *Adv. Mater.* **2011**, *23*, 2588.
(74) Grossiord, N.; Regev, O.; Loos, J.; Meuldijk, J.; Koning, C. E. *Anal. Chem.* **2005**, *77*, 5135.
(75) Clark, M. D.; Subramanian, S.; Krishnamoorti, R. *J. Colloid Interface Sci.* **2011**, *354*, 144.
(76) Vigolo, B.; Pénicaud, A.; Coulon, C.; Sauder, C.; Pailler, R.; Journet, C.; Bernier, P.; Poulin, P. *Science* **2000**, *290*, 1331.
(77) Sun, Z.; Nicolosi, V.; Rickard, D.; Bergin, S. D.; Aherne, D.; Coleman, J. N. *J. Phys. Chem. C* **2008**, *112*, 10692.
(78) Hilding, J.; Grulke, E. A.; George Zhang, Z.; Lockwood, F. *J. Dispersion Sci. Technol.* **2003**, *24*, 1.
(79) Yu, H.; Hermann, S.; Schulz, S. E.; Gessner, T.; Dong, Z.; Li, W. J. *Chem. Phys.* **2012**, *408*, 11.
(80) Wenseleers, W.; Vlasov, I. I.; Goovaerts, E.; Obraztsova, E. D.; Lobach, A. S.; Bouwen, A. *Adv. Funct. Mater.* **2004**, *14*, 1105.
(81) Ghosh, S.; Bachilo, S. M.; Weisman, R. B. *Nat. Nanotechnol.* **2010**, *5*, 443.
(82) Zhao, P.; Einarsson, E.; Xiang, R.; Murakami, Y.; Maruyama, S. *J. Phys. Chem. C* **2010**, *114*, 4831.
(83) O'Connell, M. J.; Bachilo, S. M.; Huffman, C. B.; Moore, V. C.; Strano, M. S.; Haroz, E. H.; Rialon, K. L.; Boul, P. J.; Noon, W. H.; Kittrell, C.; Ma, J.; Hauge, R. H.; Weisman, R. B.; Smalley, R. E. *Science* **2002**, *297*, 593.
(84) Manne, S.; Cleveland, J. P.; Gaub, H. E.; Stucky, G. D.; Hansma, P. K. *Langmuir* **1994**, *10*, 4409.
(85) Glover, A. J.; Adamson, D. H.; Schniepp, H. C. *J. Phys. Chem. C* **2012**, *116*, 20080.
(86) Hsieh, A. G.; Punckt, C.; Korkut, S.; Aksay, I. A. *J. Phys. Chem. B* **2013**, *117*, 7950.
(87) Calvaresi, M.; Dallavalle, M.; Zerbetto, F. *Small* **2009**, *5*, 2191.
(88) Rastogi, R.; Kaushal, R.; Tripathi, S. K.; Sharma, A. L.; Kaur, I.; Bharadwaj, L. M. *J. Colloid Interface Sci.* **2008**, *328*, 421.
(89) Ernst, F.; Heek, T.; Setaro, A.; Haag, R.; Reich, S. *J. Phys. Chem. C* **2012**, *117*, 1157.
(90) Sandanayaka, A. S. D.; Takaguchi, Y.; Uchida, T.; Sako, Y.; Morimoto, Y.; Araki, Y.; Ito, O. *Chem. Lett.* **2006**, *35*, 1188.
(91) Chen, J.; Collier, C. P. *J. Phys. Chem. B* **2005**, *109*, 7605.
(92) Tomonari, Y.; Murakami, H.; Nakashima, N. *Chem. Eur. J.* **2006**, *12*, 4027.
(93) Detriche, S.; Devillers, S.; Seffer, J. F.; Nagy, J. B.; Mekhalif, Z.; Delhalle, J. *Carbon* **2011**, *49*, 2935.
(94) Liu, J.; Bibari, O.; Mailley, P.; Dijon, J.; Rouviere, E.; Sauter-Starace, F.; Caillat, P.; Vinet, F.; Marchand, G. *New J. Chem.* **2009**, *33*, 1017.
(95) Backes, C.; Schmidt, C. D.; Rosenlehner, K.; Hauke, F.; Coleman, J. N.; Hirsch, A. *Adv. Mater.* **2010**, *22*, 788.
(96) Ernst, F.; Heek, T.; Setaro, A.; Haag, R.; Reich, S. *Adv. Funct. Mater.* **2012**, *22*, 3921.
(97) Takaguchi, Y.; Tamura, M.; Sako, Y.; Yanagimoto, Y.; Tsuboi, S.; Uchida, T.; Shimamura, K.; Kimura, S.-i.; Wakahara, T.; Maeda, Y.; Akasaka, T. *Chem. Lett.* **2005**, *34*, 1608.

(98) Hammershøj, P.; Bomans, P. H. H.; Lakshminarayanan, R.; Fock, J.; Jensen, S. H.; Jespersen, T. S.; Brock-Nannestad, T.; Hassenkam, T.; Nygård, J.; Sommerdijk, N. A. J. M.; Kilså, K.; Bjørnholm, T.; Christensen, J. B. *Chem. Eur. J.* **2012**, *18*, 8716.
(99) Romero-Nieto, C.; García, R.; Herranz, M. Á.; Ehli, C.; Ruppert, M.; Hirsch, A.; Guldi, D. M.; Martín, N. *J. Am. Chem. Soc.* **2012**, *134*, 9183.
(100) Maragó, O. M.; Bonaccorso, F.; Saija, R.; Privitera, G.; Gucciardi, P. G.; Iatì, M. A.; Calogero, G.; Jones, P. H.; Borghese, F.; Denti, P.; Nicolosi, V.; Ferrari, A. C. *ACS Nano* **2010**, *4*, 7515.
(101) Hirsch, A.; Englert, J. M.; Hauke, F. *Acc. Chem. Res.* **2012**, *46*, 87.
(102) Guardia, L.; Fernández-Merino, M. J.; Paredes, J. I.; Solís-Fernández, P.; Villar-Rodil, S.; Martínez-Alonso, A.; Tascón, J. M. D. *Carbon* **2011**, *49*, 1653.
(103) Sun, Z.; Masa, J.; Liu, Z.; Schuhmann, W.; Muhler, M. *Chem. Eur. J.* **2012**, *18*, 6972.
(104) Ramalingam, P.; Pusuluri, S. T.; Periasamy, S.; Veerabahu, R.; Kulandaivel, J. *R. Soc. Chem. Adv.* **2013**, *3*, 2369.
(105) Notley, S. M. *Langmuir* **2012**, *28*, 14110.
(106) Sampath, S.; Basuray, A. N.; Hartlieb, K. J.; Aytun, T.; Stupp, S. I.; Stoddart, J. F. *Adv. Mater.* **2013**, *25*, 2740.
(107) Lee, D.-W.; Kim, T.; Lee, M. *Chem. Commun.* **2011**, *47*, 8259.
(108) Hong, C.-Y.; You, Y.-Z.; Pan, C.-Y. *Chem. Mater.* **2005**, *17*, 2247.
(109) Guoyong, X.; Wei-Tai, W.; Yusong, W.; Wenmin, P.; Pinghua, W.; Qingren, Z.; Fei, L. *Nanotechnology* **2006**, *17*, 2458.
(110) Lin, S.-T.; Chiu, C.-W.; Chen, W.-C.; Lin, J.-J. *J. Phys. Chem. C* **2007**, *111*, 13016.
(111) Ren, L.; Huang, S.; Zhang, C.; Wang, R.; Tjiu, W.; Liu, T. *J. Nanopart. Res.* **2012**, *14*, 1.
(112) Bak, J. M.; Lee, T.; Seo, E.; Lee, Y.; Jeong, H. M.; Kim, B.-S.; Lee, H.-I. *Polymer* **2012**, *53*, 316.
(113) Wang, D.; Chen, L. *Nano Lett.* **2007**, *7*, 1480.
(114) Zhang, X.; Ji, J.; Zhang, X.; Yang, B.; Liu, M.; Liu, W.; Tao, L.; Chen, Y.; Wei, Y. *R. Soc. Chem. Adv.* **2013**, *3*, 21817.
(115) Etika, K. C.; Jochum, F. D.; Cox, M. A.; Schattling, P.; Theato, P.; Grunlan, J. C. *Macromolecules* **2010**, *43*, 9447.
(116) Chen, G.; Wright, P. M.; Geng, J.; Mantovani, G.; Haddleton, D. M. *Chem. Commun.* **2008**, 1097.
(117) Soll, S.; Antonietti, M.; Yuan, J. *ACS Macro Letters* **2011**, *1*, 84.
(118) Ikeda, A.; Totsuka, Y.; Nobusawa, K.; Kikuchi, J.-i. *J. Mater. Chem.* **2009**, *19*, 5785.
(119) Iatridi, Z.; Tsitsilianis, C. *Soft Matter* **2013**, *9*, 185.
(120) Bailey, S.; Visontai, D.; Lambert, C. J.; Bryce, M. R.; Frampton, H.; Chappell, D. *J. Chem. Phys* **2014**, *140*.
(121) Newkome, G. R.; Lin, X. *Macromolecules* **1991**, *24*, 1443.
(122) Dupraz, A.; Guy, P.; Dupuy, C. *Tetrahedron Lett.* **1996**, *37*, 1237.
(123) Cardona, C. M.; Gawley, R. E. *J. Org. Chem.* **2002**, *67*, 1411.
(124) Klein, E.; Crump, M. P.; Davis, A. P. *Angew. Chem. Int. Ed.* **2005**, *44*, 298.
(125) Rosenlehner, K.; Schade, B.; Böttcher, C.; Jäger, C. M.; Clark, T.; Heinemann, F. W.; Hirsch, A. *Chem. Eur. J.* **2010**, *16*, 9544.
(126) Ouchetto, H.; Dias, M.; Mornet, R.; Lesuisse, E.; Camadro, J. M. *Biorg. Med. Chem.* **2005**, *13*, 1799.
(127) Sugandhi, E. W.; Macri, R. V.; Williams, A. A.; Kite, B. L.; Slebodnick, C.; Falkinham, J. O.; Esker, A. R.; Gandour, R. D. *J. Med. Chem.* **2007**, *50*, 1645.
(128) Kikkeri, R.; Liu, X.; Adibekian, A.; Tsai, Y.-H.; Seeberger, P. H. *Chem. Commun.* **2010**, *46*, 2197.
(129) Dehuyser, L.; Schaeffer, E.; Chaloin, O.; Mueller, C. G.; Baati, R.; Wagner, A. *Bioconjugate Chem.* **2012**, *23*, 1731.
(130) Cho, T. J.; Zangmeister, R. A.; MacCuspie, R. I.; Patri, A. K.; Hackley, V. A. *Chem. Mater.* **2011**, *23*, 2665.

(131) Newkome, G. R.; Behera, R. K.; Moorefield, C. N.; Baker, G. R. *J. Org. Chem.* **1991**, *56*, 7162.
(132) Cousins, B. G.; Das, A. K.; Sharma, R.; Li, Y.; McNamara, J. P.; Hillier, I. H.; Kinloch, I. A.; Ulijn, R. V. *Small* **2009**, *5*, 587.
(133) Szczepankiewicz, B. G.; Heathcock, C. H. *Tetrahedron* **1997**, *53*, 8853.
(134) Zhang, Y.; Liu, C.; Shi, W.; Wang, Z.; Dai, L.; Zhang, X. *Langmuir* **2007**, *23*, 7911.
(135) Ocak, Ü.; Ocak, M.; Parlayan, S.; Basoglu, A.; Çaglar, Y.; Bahadir, Z. *J. Lumin.* **2011**, *131*, 808.
(136) Wang, X.; Zhang, B.; Wang, D. Z. *J. Am. Chem. Soc.* **2009**, *133*, 5160.
(137) *Nat. Chem.* **2009**, *1*, 585.
(138) Zhou, L.-H.; Yu, X.-Q.; Pu, L. *Tetrahedron Lett.* **2010**, *51*, 475.
(139) Joo, C.; Kang, S.; Kim, S. M.; Han, H.; Yang, J. W. *Tetrahedron Lett.* **2010**, *51*, 6006.
(140) Kang, S.; Joo, C.; Kim, S. M.; Han, H.; Yang, J. W. *Tetrahedron Lett.* **2011**, *52*, 502.
(141) Kang, S.; Lee, S.; Jeon, M.; Kim, S. M.; Kim, Y. S.; Han, H.; Yang, J. W. *Tetrahedron Lett.* **2013**, *54*, 373.
(142) Wang, X.; Wang, D. Z. *Tetrahedron* **2011**, *67*, 3406.
(143) Lewis, G. E. *J. Org. Chem.* **1965**, *30*, 2433.
(144) Wang, J.; Liu, C.; Yuan, J.; Lei, A. *New J. Chem.* **2013**, *37*, 1700.
(145) Jackson, R. W. *Tetrahedron Lett.* **2001**, *42*, 5163.
(146) Strazzolini, P.; Misuri, N.; Polese, P. *Tetrahedron Lett.* **2005**, *46*, 2075.
(147) McDougal, P. G.; Rico, J. G.; Oh, Y. I.; Condon, B. D. *J. Org. Chem.* **1986**, *51*, 3388.
(148) Veronese, F. M.; Pasut, G. *Drug Discovery Today* **2005**, *10*, 1451.
(149) Amela-Cortes, M.; Roullier, V.; Wolpert, C.; Neubauer, S.; Kessler, H.; Bedel, O.; Mignani, S.; Marchi-Artzner, V. *Chem. Commun.* **2011**, *47*, 1246.
(150) Gillich, T.; Acikgöz, C.; Isa, L.; Schlüter, A. D.; Spencer, N. D.; Textor, M. *ACS Nano* **2012**, *7*, 316.
(151) Rahme, K.; Chen, L.; Hobbs, R. G.; Morris, M. A.; O'Driscoll, C.; Holmes, J. D. *R. Soc. Chem. Adv.* **2013**, *3*, 6085.
(152) Ravelli, D.; Merli, D.; Quartarone, E.; Profumo, A.; Mustarelli, P.; Fagnoni, M. *R. Soc. Chem. Adv.* **2013**, *3*, 13569.
(153) Bouzide, A.; Sauvé, G. *Tetrahedron Lett.* **1997**, *38*, 5945.
(154) Bouzide, A.; Sauvé, G. *Org. Lett.* **2002**, *4*, 2329.
(155) Loiseau, F. A.; Hii, K. K.; Hill, A. M. *J. Org. Chem.* **2004**, *69*, 639.
(156) Niculescu-Duvaz, D.; Getaz, J.; Springer, C. J. *Bioconjugate Chem.* **2008**, *19*, 973.
(157) Svedhem, S.; Hollander, C.-Å.; Shi, J.; Konradsson, P.; Liedberg, B.; Svensson, S. C. T. *J. Org. Chem.* **2001**, *66*, 4494.
(158) Samanta, D.; Sawoo, S.; Patra, S.; Ray, M.; Salmain, M.; Sarkar, A. *J. Organomet. Chem.* **2005**, *690*, 5581.
(159) Samanta, D.; Sawoo, S.; Sarkar, A. *Chem. Commun.* **2006**, 3438.
(160) Bertozzi, C. R.; Bednarski, M. D. *J. Org. Chem.* **1991**, *56*, 4326.
(161) Ahmed, S. A.; Tanaka, M. *J. Org. Chem.* **2006**, *71*, 9884.
(162) Javier Munoz, F.; Andre, S.; Gabius, H.-J.; Sinisterra, J. V.; Hernaiz, M. J.; Linhardt, R. J. *Green Chem.* **2009**, *11*, 373.
(163) Heumann, L. V.; Keck, G. E. *Org. Lett.* **2007**, *9*, 1951.
(164) Chen, B.; Baumeister, U.; Pelzl, G.; Das, M. K.; Zeng, X.; Ungar, G.; Tschierske, C. *J. Am. Chem. Soc.* **2005**, *127*, 16578.
(165) Bal, B. S.; Kochhar, K. S.; Pinnick, H. W. *J. Org. Chem.* **1981**, *46*, 1492.
(166) Mart, R. J.; Liem, K. P.; Wang, X.; Webb, S. J. *J. Am. Chem. Soc.* **2006**, *128*, 14462.
(167) Welsh, D. J.; Posocco, P.; Pricl, S.; Smith, D. K. *Org. Biomol. Chem.* **2013**, *11*, 3177.
(168) Rerat, V.; Dive, G.; Cordi, A. A.; Tucker, G. C.; Bareille, R.; Amédée, J. l.; Bordenave, L.; Marchand-Brynaert, J. *J. Med. Chem.* **2009**, *52*, 7029.
(169) Gaunt, M. J.; Yu, J.; Spencer, J. B. *J. Org. Chem.* **1998**, *63*, 4172.

(170) Xia, J.; Abbas, S. A.; Locke, R. D.; Piskorz, C. F.; Alderfer, J. L.; Matta, K. L. *Tetrahedron Lett.* **2000**, *41*, 169.
(171) Wright, J. A.; Yu, J.; Spencer, J. B. *Tetrahedron Lett.* **2001**, *42*, 4033.
(172) Stocks, M. J.; Harrison, R. P.; Teague, S. J. *Tetrahedron Lett.* **1995**, *36*, 6555.
(173) Lampkins, A. J.; O'Neil, E. J.; Smith, B. D. *J. Org. Chem.* **2008**, *73*, 6053.
(174) Fujimoto, K.; Muto, Y.; Inouye, M. *Bioconjugate Chem.* **2008**, *19*, 1132.
(175) Li, Z. F.; Luo, G. H.; Zhou, W. P.; Wei, F.; Xiang, R.; Liu, Y. P. *Nanotechnology* **2006**, *17*, 3692.
(176) Marsh, D. H.; Rance, G. A.; Zaka, M. H.; Whitby, R. J.; Khlobystov, A. N. *Phys. Chem. Chem. Phys.* **2007**, *9*, 5490.
(177) Clark, M. D.; Krishnamoorti, R. *J. Phys. Chem. C* **2009**, *113*, 20861.
(178) Baskaran, D.; Mays, J. W.; Bratcher, M. S. *Chem. Mater.* **2005**, *17*, 3389.
(179) Ansón-Casaos, A.; González-Domínguez, J. M.; Lafragüeta, I.; Carrodeguas, J. A.; Martínez, M. T. *Carbon* **2014**, *66*, 105.
(180) Jeong, S. H.; Kim, K. K.; Jeong, S. J.; An, K. H.; Lee, S. H.; Lee, Y. H. *Synth. Met.* **2007**, *157*, 570.
(181) Skaltsas, T.; Karousis, N.; Yan, H.-J.; Wang, C.-R.; Pispas, S.; Tagmatarchis, N. *J. Mater. Chem.* **2012**, *22*, 21507.
(182) Brahmachari, S.; Das, D.; Das, P. K. *Chem. Commun.* **2010**, *46*, 8386.
(183) Backes, C.; Hauke, F.; Hirsch, A. *Phys. Status Solidi B* **2013**, *250*, 2592.
(184) Moore, V. C.; Strano, M. S.; Haroz, E. H.; Hauge, R. H.; Smalley, R. E.; Schmidt, J.; Talmon, Y. *Nano Lett.* **2003**, *3*, 1379.
(185) Millero, F. J.; Feistel, R.; Wright, D. G.; McDougall, T. J. *Deep Sea Research Part I: Oceanographic Research Papers* **2008**, *55*, 50.
(186) Phillies, G. D. J.; Yambert, J. E. *Langmuir* **1996**, *12*, 3431.
(187) Israelachvili, J. N. *Intermolecular and Surface Forces*; 3rd ed.; Academic Press, 2010.
(188) Davis, K. G.; Gallardo-Jimenez, M. A.; Lilley, T. H. *J. Chem. Soc., Faraday Trans. 1* **1989**, *85*, 2901.
(189) Fernandez, J.; Nieves, G.-L.; H. Lilley, T.; Linsdell, H. *J. Chem. Soc., Faraday Trans.* **1997**, *93*, 407.
(190) Pereira, R. F. P.; Valente, A. J. M.; Fernandes, M.; Burrows, H. D. *Phys. Chem. Chem. Phys.* **2012**, *14*, 7517.
(191) Soontravanich, S.; Lopez, H.; Scamehorn, J.; Sabatini, D.; Scheuing, D. *J. Surfact. Deterg.* **2010**, *13*, 367.
(192) Huibers, P. D. T.; Shah, D. O.; Katritzky, A. R. *J. Colloid Interface Sci.* **1997**, *193*, 132.
(193) Kim, H. C.; Kim, J.-D. *J. Colloid Interface Sci.* **2010**, *352*, 444.
(194) Schott, H. *J. Colloid Interface Sci.* **2003**, *260*, 219.
(195) Work, W. J.; Horie, K.; Hess, M.; Stepto, R. F. T. *Pure Appl. Chem.* **2004**, *76*, 1985.
(196) Sigma-Aldrich. Non-Ionic Detergents http://www.sigmaaldrich.com/life-science/biochemicals/biochemical-products.html?TablePage=14572924 (accessed Mar 11, 2014)
(197) Ward, M. A.; Georgiou, T. K. *Polymers* **2011**, *3*, 1215.
(198) Maeda, Y.; Higuchi, T.; Ikeda, I. *Langmuir* **2000**, *16*, 7503.
(199) Li, S.; Su, Y.; Dan, M.; Zhang, W. *Polym. Chem.* **2014**, *5*, 1219.
(200) Kono, K.; Murakami, E.; Hiranaka, Y.; Yuba, E.; Kojima, C.; Harada, A.; Sakurai, K. *Angew. Chem. Int. Ed.* **2011**, *50*, 6332.
(201) Li, X.; Haba, Y.; Ochi, K.; Yuba, E.; Harada, A.; Kono, K. *Bioconjugate Chem.* **2013**, *24*, 282.
(202) Steed, J. W.; Atwood, J. L. *Supramolecular Chemistry*; Wiley: Chichester, UK, 2009.
(203) Sach, N. W.; Richter, D. T.; Cripps, S.; Tran-Dubé, M.; Zhu, H.; Huang, B.; Cui, J.; Sutton, S. C. *Org. Lett.* **2012**, *14*, 3886.
(204) Yu, C. C.; Lee, Y.-S.; Cheon, B. S.; Lee, S. H. *Bull. Korean Chem. Soc.* **2003**, *24*, 1229.

(205) Batovska, D.; Kishimoto, T.; Bankova, V.; Kamenarska, Z.; Ubukata, M. *Molecules* **2005**, *10*, 552.
(206) Choi, K.-M.; Lee, D.-H.; Jang, W.-D. *Bull. Korean Chem. Soc.* **2010**, *31*, 639.
(207) Krakowiak, K. E.; Bradshaw, J. S.; Zamecka-Krakowiak, D. J. *Chem. Rev.* **1989**, *89*, 929.
(208) Bordunov, A. V.; Hellier, P. C.; Bradshaw, J. S.; Dalley, N. K.; Kou, X.; Zhang, X. X.; Izatt, R. M. *J. Org. Chem.* **1995**, *60*, 6097.
(209) Kokotos, G.; Verger, R.; Chiou, A. *Chem. Eur. J.* **2000**, *6*, 4211.
(210) Hurley, C. A.; Wong, J. B.; Hailes, H. C.; Tabor, A. B. *J. Org. Chem.* **2004**, *69*, 980.
(211) Navas Díaz, A.; García Sánchez, F.; García Pareja, A. *Colloids Surf., A* **1998**, *142*, 27.
(212) Ruiz, F.-J.; Rubio, S.; Pérez-Bendito, D. *Anal. Chem.* **2007**, *79*, 7473.
(213) Mao, H.; Li, C.; Zhang, Y.; Bergbreiter, D. E.; Cremer, P. S. *J. Am. Chem. Soc.* **2003**, *125*, 2850.
(214) Hou, L.; Wu, P. *Soft Matter* **2014**, *10*, 3578.
(215) Xu, Y.; Xie, J.; Chen, L.; Gao, H.; Yuan, C.; Li, C.; Luo, W.; Zeng, B.; Dai, L. *Polym. Adv. Technol.* **2014**, *25*, 613.
(216) López-Pérez, P. M.; da Silva, R. M. P.; Pashkuleva, I.; Parra, F.; Reis, R. L.; San Roman, J. *Langmuir* **2009**, *26*, 5934.
(217) El Malah, T.; Rolf, S.; Weidner, S. M.; Thünemann, A. F.; Hecht, S. *Chem. Eur. J.* **2012**, *18*, 5837.
(218) Luzon, M.; Boyer, C.; Peinado, C.; Corrales, T.; Whittaker, M.; Tao, L.; Davis, T. P. *J. Polym. Sci., Part A: Polym. Chem.* **2010**, *48*, 2783.
(219) Lutz, J.-F.; Weichenhan, K.; Akdemir, Ö.; Hoth, A. *Macromolecules* **2007**, *40*, 2503.
(220) Griffin, W. C. *Journal of the Society of Cosmetic Chemists* **1949**, *1*, 311.
(221) Griffin, W. C. *Journal of the Society of Cosmetic Chemists* **1954**, *5*, 249.
(222) Davies, J. T. In *Gas/Liquid and Liquid/Liquid Interfaces. Proceedings of 2nd International Congress Surface Activity,*; Butterworths: London, 1957, p 426.
(223) AkzoNobel. HLB & Emulsification http://sc.akzonobel.com/en/fabric-cleaning/Documents/AkzoNobel_tb_HlbEmulsions.pdf (accessed Feb 10, 2014)
(224) Berthod, A.; Tomer, S.; Dorsey, J. G. *Talanta* **2001**, *55*, 69.
(225) Hernandez, Y.; Nicolosi, V.; Lotya, M.; Blighe, F. M.; Sun, Z.; De, S.; McGovern, I. T.; Holland, B.; Byrne, M.; Gun'Ko, Y. K.; Boland, J. J.; Niraj, P.; Duesberg, G.; Krishnamurthy, S.; Goodhue, R.; Hutchison, J.; Scardaci, V.; Ferrari, A. C.; Coleman, J. N. *Nat. Nanotechnol.* **2008**, *3*, 563.
(226) Khan, U.; O'Neill, A.; Lotya, M.; De, S.; Coleman, J. N. *Small* **2010**, *6*, 864.
(227) Das, S.; Wajid, A. S.; Shelburne, J. L.; Liao, Y.-C.; Green, M. J. *ACS Appl. Mater. Interfaces* **2011**, *3*, 1844.
(228) Seo, J.-W. T.; Green, A. A.; Antaris, A. L.; Hersam, M. C. *J. Phys. Chem. Lett.* **2011**, *2*, 1004.
(229) Djerassi, C.; Sheehan, M.; Spangler, R. J. *J. Org. Chem.* **1971**, *36*, 3526.
(230) Shozda, R. J.; Depp, E. A.; Stevens, C. M.; Neuworth, M. B. *J. Am. Chem. Soc.* **1956**, *78*, 1716.